



PHD

Studies on subcellular trafficking of glucose transporters-GLUT1 and GLUT4 in 3T3-L1 cells

Yang, Jing

Award date:
1993

Awarding institution:
University of Bath

[Link to publication](#)

Alternative formats

If you require this document in an alternative format, please contact:
openaccess@bath.ac.uk

Copyright of this thesis rests with the author. Access is subject to the above licence, if given. If no licence is specified above, original content in this thesis is licensed under the terms of the Creative Commons Attribution-NonCommercial 4.0 International (CC BY-NC-ND 4.0) Licence (<https://creativecommons.org/licenses/by-nc-nd/4.0/>). Any third-party copyright material present remains the property of its respective owner(s) and is licensed under its existing terms.

Take down policy

If you consider content within Bath's Research Portal to be in breach of UK law, please contact: openaccess@bath.ac.uk with the details. Your claim will be investigated and, where appropriate, the item will be removed from public view as soon as possible.

**STUDIES ON SUBCELLULAR TRAFFICKING OF
GLUCOSE TRANSPORTERS-GLUT1 AND GLUT4
IN 3T3-L1 CELLS**

Submitted by

Jing Yang

for the degree of Ph.D.
of the University of Bath
1993.

Copyright

Attention is drawn to the fact that the copyright of this thesis rests with its author. This copy of the thesis has been supplied on condition that anyone who consults it is understood to recognise that its copyright rests with its author and that no quotation from the thesis and no information derived from it may be published without the prior written consent of the author.

This thesis may be made available for consultation within the University Library and may be photocopied or lent to other libraries for the purpose of consultation.

Signed: *Jing Yang*

UMI Number: U554321

All rights reserved

INFORMATION TO ALL USERS

The quality of this reproduction is dependent upon the quality of the copy submitted.

In the unlikely event that the author did not send a complete manuscript and there are missing pages, these will be noted. Also, if material had to be removed, a note will indicate the deletion.



UMI U554321

Published by ProQuest LLC 2013. Copyright in the Dissertation held by the Author.
Microform Edition © ProQuest LLC.

All rights reserved. This work is protected against
unauthorized copying under Title 17, United States Code.



ProQuest LLC
789 East Eisenhower Parkway
P.O. Box 1346
Ann Arbor, MI 48106-1346

UNIVERSITY OF LATH
LIBRARY
26 17 MAY 1994
PHD
S579898

CONTENTS

	Page
ABSTRACT	i
ACKNOWLEDGEMENTS	iii
ABBREVIATIONS	iv
1.0 INTRODUCTION	
1.1 THE MAMMALIAN GLUCOSE TRANSPORTER FAMILY	1
1.1.1 Structure of the facilitative glucose transporter	2
1.1.2 Mechanisms for facilitative glucose transport	3
1.1.3 Characteristic of the tissue specific glucose transporter isoforms	5
1.1.3.1 The erythrocyte-type glucose transporter-GLUT1	7
1.1.3.2 The liver-type glucose transporter-GLUT2	8
1.1.3.3 The brain-type glucose transporter-GLUT3	9
1.1.3.4 The insulin-responsive glucose transporter-GLUT4	10
1.1.3.5 The small-intestine glucose transporter-GLUT5	12
1.1.3.6 The pseudogene-GLUT6	13
1.1.3.7 The hepatic microsomal glucose transporter-GLUT7	13
1.2 PHOTOAFFINITY LABELLING OF FACILITATIVE GLUCOSE TRANSPORTERS	13
1.3 MURINE 3T3-L1 CELLS-A GOOD MODEL FOR STUDY OF GLUCOSE TRANSPORT	17
1.4 INSULIN STIMULATION OF GLUCOSE TRANSPORT	20
1.4.1 The translocation hypothesis	21
1.4.2 The intrinsic activation hypothesis	27
1.5 REGULATION OF GLUCOSE TRANSPORT	29
1.5.1 Insulin signalling	29

1.5.1.1	The insulin receptor kinase	30
1.5.1.2	Post-receptor signalling	30
1.5.2	Role of protein kinase C in glucose transport	32
1.5.3	Cyclic AMP and phosphorylation	33
1.6	RECEPTOR MEDIATED ENDOCYTOSIS	34
1.6.1	Outline of receptor mediated endocytosis	34
1.6.2	Coated pits and vesicles	37
1.6.3	Early endosomes	37
1.7	FLUID-PHASE ENDOCYTOSIS	38
1.8	SUBCELLULAR TRAFFICKING OF GLUT1 AND GLUT4	39
1.9	EFFECT OF PHENYLARSINE OXIDE ON TRAFFICKING OF GLUT1 AND GLUT4	49
1.10	AIMS	51
2.0	MATERIALS AND METHODS	
2.1	GENERAL REAGENTS	53
2.2	BUFFERS AND SOLUTIONS	53
2.3	MURINE 3T3-L1 CELL CULTURE	55
2.3.1	Culture of 3T3-L1 fibroblasts	55
2.3.2	3T3-L1 cell differentiation	56
2.3.3	Storing 3T3-L1 cells	56
2.4	PROTEIN DETERMINATION	57
2.5	PREPARATION OF ALKALI-STRIPPED ERYTHROCYTE MEMBRANES (PROTEIN DEPLETED)	58
2.6	PREPARATION OF ANTIBODIES	58
2.7	ENZYME LINKED IMMUNOSORBANT ASSAY (ELISA)	60
2.8	MEASUREMENT OF 2-DEOXYGLUCOSE UPTAKE	61

2.8.1	Measurement of insulin stimulation	61
2.8.2	Measurement of reversal of insulin stimulation	62
2.9	MEASUREMENT OF INSULIN BINDING	62
2.10	PHOTOLABELLING WITH ATB-BMPA	63
2.10.1	Preparation of ATB-[2- ³ H]BMPA	63
2.10.2	Cell surface photolabelling	63
2.10.3	Total cellular pool photolabelling	64
2.10.4	Immunoprecipitation of ATB-BMPA labelled proteins	64
2.11	CELL FRACTIONATION	65
2.11.1	Preparation of crude plasma membrane	65
2.11.2	Preparation of purified plasma membrane	66
2.12	SODIUM DODECYL SULPHATE POLYACRYLAMIDE GEL ELECTROPHORESIS (SDS-PAGE)	67
2.13	WESTERN BLOTTING	69
2.13.1	Electrophoretic transfer of proteins to nitrocellulose	69
2.13.2	Staining nitrocellulose filters for total protein	69
2.13.3	Immunoblotting of nitrocellulose-bound protein	70
3.0	RESULTS	
	PART I BACKGROUND STUDIES	72
3.1	MORPHOLOGY OF MURINE 3T3-L1 CELLS	72
3.1.1	3T3-L1 fibroblasts	72
3.1.2	3T3-L1 adipocytes	74
3.2	INSULIN STIMULATION OF GLUCOSE TRANSPORT AND ATB-BMPA LABELLING OF THE CELL SURFACE GLUT1 AND GLUT4	74

3.2.1 Determination of anti-GLUT1 and anti-GLUT4 antibody levels by ELISA	74
3.2.2 Insulin dose-response	77
3.2.3 Basal and insulin stimulated 2-deoxyglucose transport activity	81
3.2.4 Cell surface labelling of GLUT1 and GLUT4 by ATB-BMPA in 3T3-L1 adipocytes	82
PART II DEVELOPMENT OF AN INTRACELLULAR POOL OF GLUCOSE TRANSPORTERS IN 3T3-L1 CELLS	87
3.3 MEASUREMENT OF TRANSPORT ACTIVITY AND ATB-BMPA PHOTOLABELLING IN 3T3-L1 FIBROBLASTS	87
3.3.1 Measurement of 2-deoxyglucose transport activity in 3T3-L1 fibroblasts	87
3.3.2 ATB-BMPA labelling of cell-surface and total-cellular pools of GLUT1 in 3T3-L1 fibroblasts	89
3.4 ATB-BMPA LABELLING OF CELL-SURFACE AND TOTAL CELLULAR POOLS OF GLUT1 AND GLUT4 IN 3T3-L1 ADIPOCYTES	92
3.5 MEASUREMENT OF THE CHANGES OF GLUCOSE TRANSPORT ACTIVITY AND CHANGES OF GLUT1 AND GLUT4 THROUGHOUT THE CELL DIFFERENTIATION	96
PART III TRAFFICKING OF GLUT1 AND GLUT4 IN 3T3-L1 ADIPOCYTES	101
3.6 INSULIN STIMULATION OF GLUCOSE TRANSPORT AND THE AVAILABILITY OF CELL-SURFACE TRANSPORTERS	101

3.6.1	Insulin stimulation of glucose transport and the availability of cell-surface transporters at 37° C	101
3.6.2	Insulin stimulation of glucose transport and the availability of cell-surface transporters at 27° C	105
3.7	REVERSAL OF INSULIN ACTION ON GLUCOSE TRANSPORT AND LOSS OF CELL-SURFACE GLUCOSE TRANSPORTERS	112
3.8	EFFECT OF PHENYLARSINE OXIDE (PAO) ON GLUT1 AND GLUT4 TRAFFICKING	117
3.8.1	Effect of low concentration PAO on basal glucose transport	117
3.8.2	Effect of 20 μ M PAO on transport activity	121
3.8.3	Effect of PAO on the availability of GLUT1 and GLUT4 in insulin-stimulated 3T3-L1 adipocytes	121
3.8.4	Effect of PAO on internalization of GLUT1 and GLUT4	130
3.9	COMPARISON OF GLUT1 AND GLUT4 SUBCELLULAR TRAFFICKING IN BASAL AND INSULIN-STIMULATED 3T3-L1 ADIPOCYTES	133
PART IV INVESTIGATION OF DIFFERENT pH BUFFERS ON INSULIN-STIMULATED TRANSLOCATION OF GLUT1 AND GLUT4		146
3.10	DOSE-RESPONSE OF INSULIN-STIMULATED TRANSLOCATION OF GLUT1 AND GLUT4 AT pH 7.4	146
3.11	DOSE-RESPONSE OF INSULIN-STIMULATED TRANSLOCATION OF GLUT1 AND GLUT4 AT pH 8.0	149
3.12	DOSE-RESPONSE OF INSULIN-STIMULATED TRANSLOCATION OF GLUT1 AND GLUT4 AT pH 6.5	158
3.13	THE EFFECT OF DIFFERENT pH BUFFERS ON INSULIN BINDING	162

4.0 DISCUSSION

4.1	BACKGROUND STUDIES	171
4.2	DEVELOPMENT OF AN INTRACELLULAR POOL OF GLUCOSE TRANSPORTERS IN 3T3-L1 CELLS	173
4.3	DETERMINATION OF THE RATES OF APPEARANCE AND LOSS OF GLUCOSE TRANSPORTERS AT THE CELL SURFACE IN 3T3-L1 ADIPOCYTES	179
4.4	EFFECT OF PHENYLARSINE OXIDE ON GLUT1 AND GLUT4 TRAFFICKING	185
4.5	COMPARISON OF GLUT1 AND GLUT4 SUBCELLULAR TRAFFICKING IN BASAL AND INSULIN-STIMULATED 3T3-L1 ADIPOCYTES	187
4.6	DOSE RESPONSE OF INSULIN-STIMULATED TRANSLOCATION OF GLUT1 AND GLUT4 AT DIFFERENT pH BUFFERS	189

REFERENCES	I-XIII
-------------------	---------------

ABSTRACT

This thesis describes an investigation of the cell surface levels and membrane trafficking of the glucose transporter isoforms GLUT1 and GLUT4. A new method has been developed to compare the cell surface pool of transporters with the total cellular pool. The impermeant bis-mannose photolabel ATB-BMPA was used to photolabel the cell-surface transporters. Digitonin was used to permeabilize the cells and allow ATB-BMPA to label the total cellular pool of GLUT1 and GLUT4. ATB-BMPA labelling showed that only GLUT1 was present in preconfluent fibroblasts and that most of the transporters were distributed to the cell surface. The insulin-responsive reserve pool of transporters developed when the fibroblasts reached confluence. In the insulin-stimulated state approximately half of the total of both GLUT1 and GLUT4 was recruited to the plasma membrane. Measurements of the changes in the distribution of both GLUT1 and GLUT4 throughout the differentiation of confluent fibroblasts into adipocytes showed that both transporters were sequestered in parallel. Basal levels of transport and photolabelling remained low throughout the differentiation period when the total pool of transporters (GLUT1 plus GLUT4) was increased by ≈ 5 fold. These results suggest that the sequestration process was present before new transporters were synthesized.

At 27°C the half times for the appearance of GLUT1 and GLUT4 at the cell-surface were 5.7 min and 5.4 min respectively and were slightly faster than the observed rate of stimulation of transport activity ($t_{1/2} = 8.6$ min). This lag may be due to a slow dissociation of surface transporters from trafficking proteins responsible for translocation. The reversal of insulin action on glucose transport was associated with loss of cell-surface GLUT1 and GLUT4 when reversal was induced by incubation with a low pH buffer. The levels of GLUT1 and GLUT4 decreased with half times of 9.2 and 6.8 min respectively with the low pH treatment. These times correlated well with reduction of transport activity ($t_{1/2} = 6.5$ min). Phenylarsine oxide (PAO)

treatment has been examined. This also reversed the insulin stimulation of transport activity. The cell-surface level of GLUT1 remained high throughout the PAO treatment. But however recycling of GLUT1 and GLUT4 to the light microsome membrane pool occurred when cells were maintained in the presence of insulin for 60 min even with PAO treatment. These results suggest that both transporters are recycled but that PAO may inhibit this recycling at a stage which involves the re-emergence of internalized GLUT4 at the plasma membrane. The redistribution of these ATB-BMPA labelled transporters from the plasma membrane to the low-density microsome membrane fraction has then been followed while cells were maintained at either insulin-stimulated or basal steady states. In both these steady states GLUT1 and GLUT4 were continuously recycled. Calculations of endocytosis and exocytosis rate constants for GLUT1 and GLUT4 in insulin-stimulated and basal states have indicated that the main effect of insulin is to increase glucose transporter exocytosis and that the unique feature of the GLUT4 isoform is the very low rate of exocytosis in the basal state.

The effect of insulin on the translocation of glucose transporters and glucose transport activity has been studied in different pH buffers (pH 7.4, pH 8.0 and pH 6.5) and these stimulations have been correlated with the amount of insulin binding at these pHs. At pH 7.4 and at submaximal insulin concentrations, the levels of GLUT1 and GLUT4 that were detected by Western blotting were higher than the levels detected by ATB-BMPA labelling and these levels were both higher than the 2-deoxy-D-glucose transport activity. At pH 8.0, the levels of transport activity, ATB-BMPA labelling and Western blotting were very similar and were very similar to the levels detected by Western blotting at pH 7.4. The differences in the dose responses in these parameters may indicate the possibility of the presence of occluded or inactive glucose transporters in the cell membrane at pH 7.4.

ACKNOWLEDGEMENTS

I would like to express my appreciation to my supervisor Dr. Geoffrey D. Holman for his guidance, continuous encouragement and endless help during the course of this study. I am also very grateful for his critical reading of the draft of this thesis.

I would like to thank Dr. A.E. Clark, Dr. I. Kozka, Dr. N. Jordan and those working in Dr. G.D. Holman's laboratory for their practical help, advice and friendship.

I am grateful to the Medical Research Council for financial support during this study.

Finally, I would like to thank my mother, my husband and my daughter for their support and encouragement.

ABBREVIATIONS

ACTH	adrenocorticotrophin
AMP	adenosine monophosphate
ASA-BMPA	2-N-(4-azidosalicyl)-1,3-bis-(D-mannos-4-yloxy)-propyl-2-amine
ATB-BMPA	2-N-[4-(1-azi-2,2,2-trifluoroethyl)-benzoyl]-1,3-bis-(D-mannos-4-yloxy)-propyl-2-amine
BB-BMPA	2-N-(4-benzoyl)-benzoyl-1,3-bis-(D-mannos-4-yloxy)-propyl-2-amine
BCA	bicinchonic acid
BSA	Bovine Serum Albumin
C ₁₂ E ₉	Nonaethylene glycol dodecyl ether
CHO	Chinese hamster ovary
cyt B	Cytochalasin B
DMEM	Dulbecco's modified Eagle's medium
DMSO	dimethylsulphoxide
ED ₅₀	half effective dose
EDTA	Ethylenediaminetetraacetic acid
ELISA	Enzyme-linked immunosorbent assay
FCS	Foetal calf serum
GLUT	Glucose transporter isoform
G-proteins	guanine-nucleotide-binding proteins
GTP [γ S]	guanosine 5'-[γ -thio]triphosphate
Hepes	N-2-hydroxyethylpiperazine-N'-2-ethane sulphonic acid
HRP	Horse radish peroxidase
IBMX	isobutylmethylxanthine
IGF-II	Insulin-like growth factor II
IRS-1	Insulin receptor substrate-1
kDa	kilodalton
K _d	Affinity constant

Hepes	N-2-hydroxyethylpiperazine-N'-2-ethane sulphonic acid
HRP	Horse radish peroxidase
IBMX	isobutylmethylxanthine
IGF-II	Insulin-like growth factor II
IRS-1	Insulin receptor substrate-1
kDa	kilodalton
K _d	Affinity constant
KRH buffer	Kreb-Ringer-Hepes buffer
KRM buffer	Kreb-Ringer-Mes buffer
LDCVs	large dense core vesicles
LDL	low-density lipoprotein
LDM	low-density microsomes
NCS	Newborn calf serum
NEM	N-ethyl maleimide
MES	2[N-morpholino]ethanesulfonic acid
NSF	N-ethylmaleimide-sensitive fusion protein
3-O-MG	3-O-methyl-D-glucose
PAO	Phenylarsine oxide
PBS	Phosphate-buffered saline
PEG	Polyethylene glycol
PI3-kinase	phosphatidylinositol 3 kinase
PMA	phorbol 12-myristate 13-acetate
PMSF	Phenylmethylsulphonyl fluoride
SDS-PAGE	Sodium dodecyl sulphate-polyacrylamide gel electrophoresis
SSV	small synaptic vesicles
TBS	Tris-buffered saline
TEMED	N,N',N'-tetramethylethylene diamine
TES	Tris/EDTA/sucrose buffer
TGR	trans-Golgi reticulum

1.0 INTRODUCTION

1.1 THE MAMMALIAN GLUCOSE TRANSPORTER FAMILY

Transport of glucose across the plasma membrane in mammalian cells is a very important cellular nutrient transport event, since glucose plays a central role in cellular homeostasis and metabolism. The defects in glucose transport may be associated with diseases such as diabetes mellitus and this has led to an increased interest in mechanisms involved in glucose transport.

In mammalian cells, glucose is not freely permeable across the lipid bilayer, its uptake requires specific carrier proteins. Two types of glucose transport protein have been described.

The active uptake of glucose from the lumen of the small intestine and proximal tubule of the kidney requires a Na^+ -linked glucose transport protein and transport of glucose is against its concentration gradient (Wright *et al.*, 1991).

The glucose transport across the cell membrane in most cells is via facilitative glucose transporters. Transport is bidirectional, but net transport occurs from a high to a low sugar concentration.

Molecular cloning studies have revealed a family of facilitated diffusion glucose transporter proteins which are structurally related but are encoded by distinct genes that are expressed in tissue specific manner (Mueckler, 1990; Bell *et al.*, 1990). Currently, seven genes for members of the facilitative glucose transporter family have been identified. The proteins they encode have been named GLUT1-GLUT7 (Gould and Bell, 1990; Pilch, 1990). The GLUT6 is a facilitative glucose

transporter pseudogene-like sequence and this sequence cannot encode a functional protein (Kayano *et al.*, 1990).

1.1.1 Structure of the facilitative glucose transporter

Computer analyses of the predicted amino acid sequence of human GLUT1, including hydropathy and secondary-structure determinations have indicated that this protein is an extremely hydrophobic protein and suggested approximately 50% of the protein lies within the lipid bilayer. Based upon this analysis, Mueckler *et al.* (1985) proposed a model for the topology of GLUT1 in the plasma membrane. In this model, the protein spans the plasma membrane 12 times with its NH₂- and COOH termini internally orientated. A large extracellular segment links transmembrane domains M1 and M2 and a very hydrophilic intracellular segment joins M6 and M7. Short regions of 7-14 amino acids connect the remaining membrane-spanning regions.

Infrared spectroscopic analysis indicates that the α -helix is the predominant structure of the native glucose transporter, although an appreciable amount of β -structure and random coil conformation is also present (Lienhard *et al.*, 1992).

Analysis of complementary DNA from human HepG2 hepatoma cells (Mueckler *et al.*, 1985) and rat brain libraries (Birnbaum, 1986) has deduced that the predicted sequence of the 492 amino acid GLUT1 protein is highly conserved, with 98% sequence identity between the human and rat.

It is important to study the conserved regions of the glucose transporters because the regions that are significantly different may be responsible for the presence of distinct catalytic properties of each isoform.

Carruthers, (1990) have reported that homology analyses have indicated that hydrophobic regions M5, M10 and M11 are >90% conserved between transporter isoforms, and M1, M2, M4, M7, M8 and M12 share >80% sequence homology. The hydrophobic regions M6 and M9 share >70% and M3 >60%.

There is 39-65% sequence identity and 50-76% sequence similarity between isoforms; 26% of the residues are invariant in all seven proteins, and another 13% represent conservative amino acid replacements (Gould *et al.*, 1991).

From multiple sequence alignment data, Hodgson, Osguthorpe and Holman (unpublished results) have shown M7, M8, M10 and M11 have a high degree of conservation of certain hydrophilic and aromatic side chains. Membrane-spanning regions M9 and M12 are less conserved and have fewer hydrophilic amino acids. This finding and also the photoaffinity labelling results (see below) all indicate that the C-terminal half of the protein is important in ligand binding.

The basic model of GLUT1 (Fig. 1) is also applicable to the other isoforms. All members of this family have similar size (≈ 500 amino acids) and similar orientation in the plasma membrane, including 12 membrane-spanning segments, intracellularly oriented N and C-termini, a large extracellular loop joining transmembrane segments M1 and M2, which contains a single consensus site for N-linked glycosylation, and a large hydrophilic segment joining transmembrane domains M6 and M7. (Pessin and Bell, 1992). Despite their structural and functional similarity, the amino acid sequence of the mammalian facilitative glucose transporters vary considerably.

1.1.2. Mechanisms for facilitative glucose transport

To account for the accumulated data on sugar transport in cells, a number of

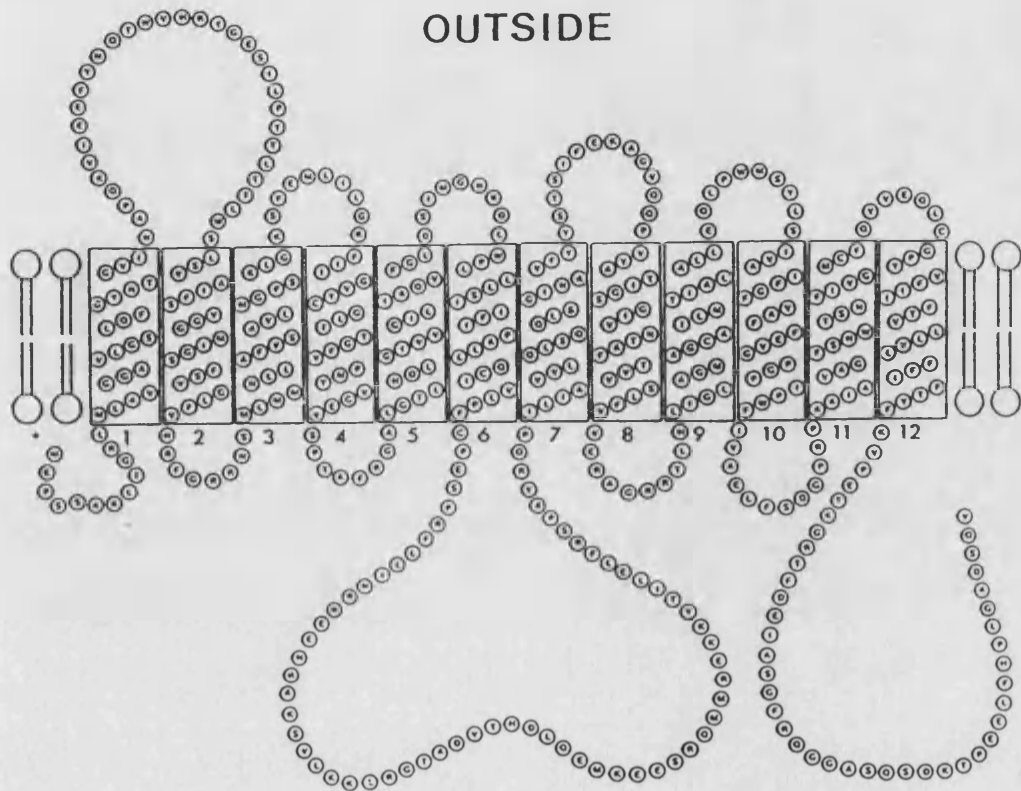


Fig.1 A model for the arrangement of GLUT1 in the membrane.
Numbered rectangles indicate membrane-spanning α -helices.
(From Baldwin and Henderson, 1989)

models have been proposed. An alternating-conformer model is widely accepted as being the best model currently available. This model is also called the mobile carrier, the simple carrier, the cyclic carrier or the one-site carrier.

In this model (Widdas, 1952), the glucose carrier was proposed to contain mutually exclusive saturable sugar influx and efflux sites. Thus at any point in time, a carrier can be available for sugar influx or sugar efflux but not for both simultaneously (Carruthers, 1990). When sugar binds to one of these sites to form the carrier-sugar complex, a conformational change is promoted that results in sugar translocation, dissociation of sugar from the carrier at the opposite side of the membrane, and the exposure of a glucose transport site at the opposite side of the membrane. The carrier is now available for transport in the opposite direction or can isomerize back to its original side of the membrane.

Baker and Widdas (1988), Naftalin *et al.* (1985) proposed a model called a fixed site model. In this model, the glucose carrier is proposed to have saturable sugar influx and efflux sites that exist simultaneously.

Transport in human erythrocytes is asymmetric and transport in rat adipocytes is symmetric. Either model can account for these properties.

1.1.3 Characteristics of the tissue specific glucose transporter isoforms

The facilitative glucose transporters have distinct physiological and biochemical properties that allow them to serve the specific functions in the tissues in which they are expressed. A summary of the glucose transporter isoforms are shown in table 1.

Name	Number of amino acids in human sequence	Calculated M _r from amino acid sequence	Tissue expression	K _m (mM) 3-O-MG for glucose transporters expressed in <i>Xenopus</i> oocytes	Regulatory factors	References
GLUT1 Erythrocyte Hep G2	492	54.1 (Apparent M _r from SDS-PAGE 45-55)	Erythrocyte, Immortal cell lines, Brain. Minor expression in: Placenta, Adipocytes, Muscle	19.4 ± 1.94	Oncogenes, Tumour promoters, Growth factors, Fasting, Refeeding, Obesity, Insulin, Exercise, Glucose deprivation	Mueckler <i>et al.</i> (1985) Gould & Lienhard (1989) Gould <i>et al.</i> (1991) Keller <i>et al.</i> (1989)
GLUT2 Liver Pancreatic	524	57.5 (Apparent M _r from SDS-PAGE 55-61)	Liver, Pancreatic β-cells, Kidney, Intestine	42.3 ± 4.1	Refeeding, Fasting, Diabetes	Thorens <i>et al.</i> (1988) Fukumoto <i>et al.</i> (1988) Gould <i>et al.</i> (1991)
GLUT3 Brain	496	53.9	Brain Minor expression in: Kidney, Gall bladder, Placenta, Foetal skeletal muscle	10.6 ± 1.3	?	Kayano <i>et al.</i> (1988) Gould <i>et al.</i> (1991)
GLUT4 Insulin regulatable	509	54.8 (Apparent M _r from SDS-PAGE 45-55)	Muscle, Adipose tissue, Heart	1.8	Insulin, Fasting, Refeeding, Obesity, Exercise, Diabetes	James <i>et al.</i> (1989) Birnbaum (1989) Fukumoto <i>et al.</i> (1989) Charron <i>et al.</i> (1989) Kaestner <i>et al.</i> (1989) Keller <i>et al.</i> (1989)
GLUT5 Intestine	501	54.9	Small intestine Minor expression in: Kidney, Adipocytes, Brain, Skeletal muscle	Not determined	?	Kayano <i>et al.</i> (1990)
GLUT7 Liver microsome	528 (rat)	53	Liver microsomes	Not determined	?	Waddell <i>et al.</i> (1992)

Table 1 The facilitative glucose transporter family

1.1.3.1 GLUT1 - the erythrocyte-type glucose transporter

The first member of the glucose transporter family is GLUT1. Mueckler and co-workers (1985) screened a cDNA library prepared using RNA from the human hepG2 hepatoma cell line and isolated a cDNA encoding a 492 amino acid glucose transport protein. This perhaps is the best studied glucose transporter (Gould and Holman, 1993).

Utilising both cDNA and antibodies probes, many subsequent studies have demonstrated that both the GLUT1 protein and mRNA is present in many tissues and cells (Mueckler *et al.*, 1990; Flier and Kahn, 1990). It is expressed at highest levels in brain, but is also enriched in the cells of the blood-tissue barriers, such as the blood-brain/nerve barrier, the placenta, the retina etc (Froehner *et al.*, 1988). The mRNA and protein for this transporter have also been demonstrated in muscle and fat tissue. Only very low levels of GLUT2 were found in the liver, the major tissue involved in the whole body glucose homoeostasis (Mueckler *et al.*, 1990).

Gould *et al.* (1991) have investigated the kinetics of isolated GLUT1 by functional expression of the protein in *Xenopus* oocytes. Transport rate is determined by both the V_{max} , maximal velocity, and K_m which inversely reflects the affinity for glucose. Under equilibrium exchange conditions a K_m for 3-O-methyl-D-glucose of about 17 mM has been obtained. This agrees well with the results that Carruthers reported (1990) who studied human erythrocytes. They found the range of K_m values under equilibrium exchange conditions for D-glucose was 17-38 mM.

Low levels of GLUT1 are expressed in adipose, muscle, kidney, colon and liver tissue (Gould and Bell, 1990). This indicates that GLUT1 plays a role in supplying the basal glucose requirements of cells (Mueckler, 1990).

1.1.3.2 GLUT2 - The liver-type glucose transporter

The inability to detect GLUT1 in hepatocyte membranes, and also the observation that the kinetics of glucose transport in hepatocytes were radically different from erythrocytes, indicated that a distinct transporter may be expressed in hepatocytes.

1988, Thorens *et al.* cloned and sequenced GLUT2 from rat. This isoform has been also cloned and sequenced from mouse (Asano *et al.*, 1989) and human liver (Fukumoto *et al.*, 1988).

The rat gene codes for a protein with 522 amino acids which shares 82% sequence identity with the 524 amino acid human protein (Gould and Bell, 1990).

Further analysis of the sites of expression of GLUT2 demonstrated that this isoform is expressed at highest levels in the liver, pancreatic β -cells, kidney and small intestine (Thorens *et al.*, 1988; Fukumoto *et al.*, 1988).

The apparent molecular weight of GLUT2 for different tissue is slightly different. The rat GLUT2 varies from 55-61 kDa, the liver GLUT2 is about 53 kDa, the islet β -cells is about 55 kDa, in kidney it is 57 kDa and in intestine it is 51 kDa (Thorens *et al.*, 1988).

The big different between GLUT2 and other transporter isoforms is that it has a high K_m and V_{max} and therefore it has a much lower affinity but has a higher capacity for transport at high concentrations of substrate. This means that the rate of flux through this transporter will be directly proportional to concentration over a wide range. It has been suggested that this property allows GLUT2 to participate in glucose sensing by the pancreatic β -cell and is favourable for the transepithelial

movement of glucose in the small intestine and kidney, and the regulation of circulating glucose levels by the liver (Okuno and Gliemann, 1986).

1.1.3.3 GLUT3 - The brain-type glucose transporter

The development of the low-stringency hybridization approach to cloning transporter-like cDNAs was subsequently applied to other tissues. Using this approach, Kayano *et al.* (1988) screened a human foetal muscle library for the expression of transporter-proteins and isolated a novel transporter-like cDNA. This protein is GLUT3. Its predominant site of expression is brain, and its lower levels have been found in fat, kidney, liver and muscle tissue (Gould and Holman, 1993).

The human GLUT3 gene codes for a 496 amino acid protein which shares 64% and 52% identity with GLUT1 and GLUT2, respectively, with 83% amino acid sequence identity between the sequences of human and mouse GLUT3 (Nagamatsu *et al.*, 1992).

Gould *et al.* (1991) have reported that under equilibrium exchange conditions a K_m for 3-O-methyl-D-glucose uptake is ≈ 10 mM for GLUT3 expressed in *Xenopus* oocytes.

The expression of GLUT3 in brain indicates that two facilitative glucose transporters, GLUT1 and GLUT3 are involved in the uptake and disposal of glucose in this tissue. GLUT1 is primarily responsible for the transport across the blood-brain barrier, whereas GLUT3 probably controls glucose uptake into neuronal cells (Gerhart *et al.*, 1992; Nagamatsu *et al.*, 1992).

1.1.3.4 GLUT4 - The insulin-responsive glucose transporter

Following the success in utilizing a GLUT1 cDNA probe to obtain the homologous sequence of GLUT2 and GLUT3, the fourth glucose transporter isoform has been cloned by 5 independent groups in 1989 (James *et al.*, 1989; Birnbaum, 1989; Fukumoto *et al.*, 1989; Charron *et al.*, 1989; Kaestner *et al.*, 1989). The putative topology of the rat GLUT4 glucose transporter protein shows in Fig. 2. This isoform is the insulin-responsive glucose transporter isoform. It only occurs in muscle and adipose tissue and it is in these tissues that insulin produces an ≈ 30 fold increase in glucose transport.

James *et al.* (1989) have reported that the rat gene encodes a 509 amino acid protein with an apparent molecular mass of 43 kDa, or when deglycosylated, the molecular mass is 38 kDa. Other groups have reported an apparent molecular mass of 50-55 kDa (Birnbaum, 1989; Fukumoto *et al.*, 1989; Charron *et al.*, 1989).

It has been found that human GLUT4 has 65% sequence identity with human GLUT1, 54% with GLUT2 and 58% with GLUT3. The sequence of GLUT4 is highly conserved, and there is 95 and 96% identity between the sequence of human and rat or mouse GLUT4, respectively. GLUT4 mRNA is found at highest levels in brown and white adipose tissue, and also in cardiac and skeletal muscle (Birnbaum, 1989; James *et al.*, 1989; Kaestner *et al.*, 1989).

Expressing GLUT4 in *Xenopus* oocytes has indicated that a K_m for 3-O-methyl-D-glucose transport is 1.8 mM. This was measured under equilibrium exchange conditions (Keller *et al.*, 1989).

Studies using isoform-specific antibodies have demonstrated that in rat adipocytes 90% of the glucose transporters are GLUT4 and about 3-5% are GLUT1

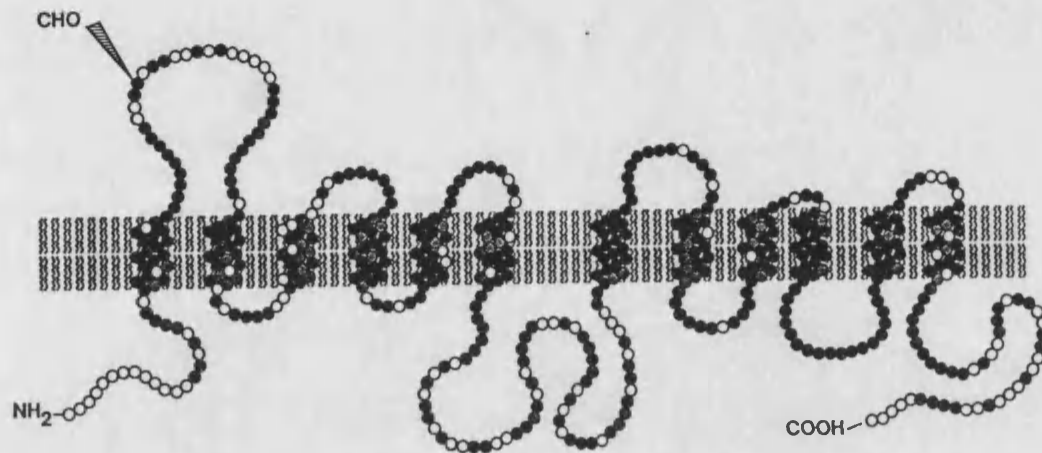


Fig.2 Putative topology of the rat GLUT4 glucose transporter Protein.

The transporter is drawn with the cytoplasmic surface of the plasma membrane facing downward. The probable single site of N-linked glycosylation is indicated (CHO), as are the amino and carboxy termini. Amino acids that are identical in the rat GLUT1 and GLUT4 glucose transporters are represented by black circles and conservative differences are shown as shaded circles. The precise locations of the borders of the transmembrane segments are arbitrary and drawn for convenience of representation. The overall sequence identity between the two transporters is 63.5%. However, the identity between the putative membrane-spanning domains is 73.0%, and the identity between the three large cytoplasmic domains of GLUT1 and GLUT4 is 40.5%. (Form Birnbaum, 1989)

(Oka *et al.*, 1988; Zorzano *et al.*, 1989). Under basal conditions, GLUT4 is predominantly localized to an intracellular vesicle population with little being present in the plasma membrane. In contrast, GLUT1 is distributed approximately equally between plasma membrane and intracellular low density microsomal fractions. In response to insulin, the amount of GLUT4 present at the cell surface increases 15-20 fold, while GLUT1 increases only 3-5 fold (Holman *et al.*, 1990). This indicates that GLUT4 is the major isoform to respond to insulin. The proposed translocation of GLUT4 has become known as the "recruitment hypothesis" (Cushman and Wardzala, 1980; Suzuki and Kono, 1980). This will be introduced later.

In insulin-resistant states such as diabetes mellitus, obesity and fasting, GLUT4 expression is decreased in adipocytes and muscle tissue which results in decreased glucose uptake in response to insulin (Kahn and Flier, 1990).

1.1.3.5 GLUT5 - The small-intestine glucose transporter

Kayano *et al.* (1990) isolated a glucose transporter cDNA from human small intestine. Northern blot analysis has suggested that this isoform is mainly in small intestine, but detectable levels of GLUT 5 mRNA have also been reported in human fat and muscle tissue. The protein appears to be localised exclusively to the apical-brush-border on the luminal side of the epithelial cells. (Davidson *et al.*, 1992).

Human GLUT5 shares 42, 40, 39, and 42% identity with human GLUT1, GLUT2, GLUT3, and GLUT4, respectively (Kayano *et al.*, 1990).

Its role is at present unclear. Since the transport of glucose from the lumen into the epithelial cell is normally mediated predominantly by the unrelated Na⁺-dependent glucose transporter, the presence of a facilitative glucose transporter in the brush-border is not easily explained (Gould and Holman, 1993). Recent evidence

(Burant *et al.*, 1992) suggests GLUT5 is a fructose transporter.

1.1.3.6 The pseudogene-GLUT6

Kayono *et al.* (1990), have sequenced a facilitative glucose transporter-like cDNA and designated this as GLUT6. The gene has been identified in a number of tissues but the sequence cannot encode a functional transporter protein.

1.1.3.7 A hepatic microsomal glucose transporter-GLUT7

GLUT7 is the most recently identified member of the glucose transporter family. It is found in the liver endoplasmic reticulum and nuclear envelope but not in the plasma membrane. GLUT7 codes for a 528 amino acid protein and is 68% identical to GLUT2 (Waddell *et al.*, 1992).

1.2 PHOTOAFFINITY LABELLING OF THE FACILITATIVE GLUCOSE TRANSPORTER

Mueckler *et al.* (1985) have cloned and sequenced a hepatoma cDNA for the facilitative glucose transporter and the molecular weight of this transporter is about 55 kDa. It occurs in the 4.5 band of SDS-polyacrylamide gels of the erythrocyte membrane. The availability of this sequence for the transporter is a major breakthrough in the investigation of glucose transport. To understand which regions of the transporter are involved in glucose transport, photoaffinity labelling of the glucose transporter has been used in such studies.

There are a number of compounds which have been reported to be affinity or photoaffinity labels for the hexose transporter in human erythrocytes. These include D-maltosylisothiocyanate (Mullins and Langdon, 1980) and 6-N-(4-azido-2-hydroxy-

3, 5-diiodobenzoyl-D-glucosamine (Weber and Eichholz, 1985). The most widely used compound is the fungal metabolite, cytochalasin B.

Cytochalasin B is a potent inhibitor of facilitative glucose transport (Jung and Rampal, 1977; Deves and Krupka, 1978; Axelrod and Pilch, 1983) and is thought to bind to an internal site on the transporter (Basketter and Widdas, 1978; Baldwin and Lienhard, 1980). It binds the transporter between membrane spanning regions M10 and M11 (Holman and Rees, 1987). In the presence of high intensity ultraviolet light cytochalasin B can bind covalently to the erythrocyte transporter and rat adipocytes (Carter-Su *et al.*, 1982; Oka and Czech, 1984).

A number of bis (D-mannose) compounds have been reported by Holman and associates (Midgeley *et al.*, 1985; Holman *et al.*, 1986; Holman *et al.*, 1988; Clark and Holman, 1990). They are 1,3-bis-(D-mannos-4'yloxy) propyl-2-amine (BMPA) derivatives. These compounds have been considered as photoaffinity labels for the external site of the transporter. These compounds are synthesized from two D-mannose moieties joined at their C-4' positions by a 2-propylamine bridge. The photolabel substituent is attached through the amino group. They have high affinity for the hexose transporter of both the human erythrocyte and the rat adipocyte. During a period of 90 min time, the compounds have not been found to be taken up into either type of cells.

A 4-azidosalicylate derivative of BMPA (ASA-BMPA) has been shown to successfully label the band 4.5 transporter peptide of erythrocytes (Holman *et al.*, 1986) and binds to the exofacial surface of the transporter, probably between membrane-spanning regions M9 and M10 (Holman and Rees, 1987). It has been shown that it is a good photoaffinity label for the erythrocyte hexose transporter (Holman *et al.*, 1986). But with ASA-BMPA, Holman *et al.* (1986) have observed some labelling (about 10-15% of total) in an additional band at about 75 kDa and also

it was found to be unsuitable for labelling adipocytes in which the transporter was present in low abundance.

The ligands containing precursor groups such as benzophenone or azitrifluoroethyl benzoyl groups, which produce carbenes, on irradiation, were found to be more effective (Holman *et al.*, 1988). The benzophenone derivative of 1,3-bis(D-mannos-4-yloxy)-2-propylamine(BB-BMPA) and 2N-4(1-azi-2,2,2-trifluoroethyl)benzoyl-1,3 bis(D-mannose-4-yloxy)2-propylamine (ATB-BMPA) both label the erythrocyte and adipocyte transporters (Holman *et al.*, 1988; Clark and Holman, 1990; Holman *et al.*, 1990). The structure of ATB-BMPA is shown in Fig.3.

The advantage of ATB-BMPA is that this compound is impermeable and photolabelling can be confined to the discrete plasma membrane pool of glucose transporters. Also ATB-BMPA is very stable in the dark and is soluble in physiological buffers. Using this compound to estimate the levels of glucose transporter on the cell surface is independent of the homogenization protocol. Because microsomal glucose transporters will not be exposed to or bind the exofacial ligand during the photolabelling procedure the problem of contamination of the plasma membrane by microsomal transporters can be avoided by this approach. Thus the cell physiology of insulin's stimulation of glucose transport can be studied directly in the intact adipose cell. This in situ labelling allows cellular processing of the transporter to be followed. Thus the impermeable bis (hexoses) may be a good tool for studying the recruitment hypothesis for transporter activation by insulin (Holman *et al.*, 1990).

Recently, Davies *et al.* (Davies, Preston, Clark, Holman and Baldwin-unpublished work) have shown ATB-BMPA binds to GLUT1 on the exofacial surface of transmembrane regions M8 between Ala301 and Arg 330. The ASA-BMPA binds

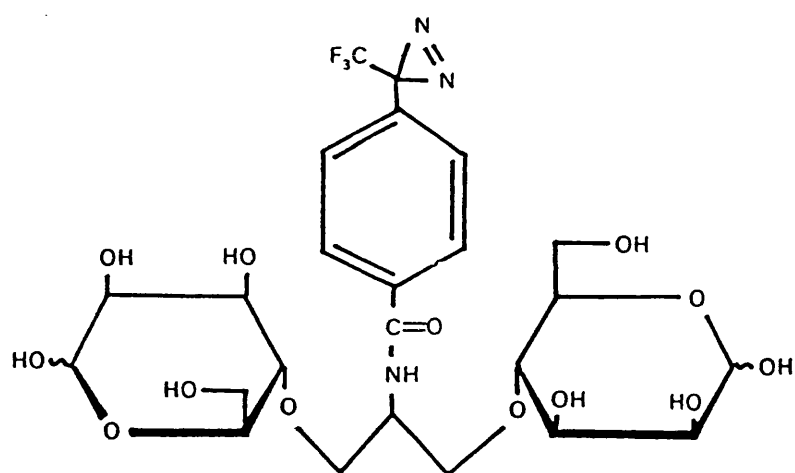


Fig.3 **Structure of ATB-BMPA.** (From Clark and Holman, 1990)

erythrocyte transporter on the exofacial surface of the transmembrane regions M9 and M10 (Holman and Rees, 1987). This suggest that transmembrane segments M7-M10 are involved in ligand binding.

ATB-BMPA has successfully been used as an exofacial probe for the human erythrocyte glucose transport system (Clark *et al.*, 1991) and also has been used for identifying cell surface glucose transporters in isolated rat adipose cells (Holman *et al.*, 1990; Clark *et al.*, 1991; Kozaka *et al.*, 1992) and 3T3-L1 adipocytes (Kozka *et al.*, 1991; Calderhead *et al.*, 1990; Palfreyman *et al.*, 1992 and present studies).

1.3 MURINE 3T3-L1 CELLS-A GOOD MODEL FOR THE STUDY OF GLUCOSE TRANSPORT

Green and colleagues (Green and Kehinde, 1974; 1975; 1976; Green and Meuth, 1974) established a cloned line of murine 3T3-L1 cells. This cell line exhibits fibroblastic characteristics during rapid proliferation. Growth arrest occurs on attaining confluence and the cells undergo a spontaneous morphological change. Although the adipocyte conversion process can occur spontaneously over a period of 2 to 4 weeks following confluence (Green and Meuth, 1974) conversion can be accelerated by treatment of the confluent cells with either 20 to 30 % serum (Green and Meuth, 1974), 0.18 μ M insulin (Green and Kehinde, 1976), 0.5 mM isobutylmethylxanthine (Russell and Ho, 1976), 0.3 μ M prostaglandin F₂ (Russell and Ho, 1976), 33 μ M biotin and combinations of insulin with any of the other agents or with 12.5 μ M indomethacin (Williams and Polakis, 1977).

Initially this cell line was used for testing the effect of drugs on lipid metabolism (Mackall *et al.*, 1976), currently 3T3-L1 cells have been used as a good model to investigate the regulation of glucose transport. This cell type was chosen for several reasons:

These cells can be differentiated to produce a reserve of internal glucose transporters which can be translocated to the cell surface in response to insulin. Like the rat adipocyte, it exhibits a 10-15 fold increase in the rate of hexose transport upon exposure to insulin (Frost and Lane, 1985).

The amount of transporter per 3T3-L1 adipocyte is almost as large as that per rat adipocyte (Schroer *et al.*, 1986).

GLUT1 is more abundant than GLUT4 in these cells. Quantitative immunoblotting studies indicate that there are about 950000 and 280000 molecules of GLUT1 and GLUT4, respectively, per cell (Calderhead *et al.*, 1990).

3T3-L1 cells growth as a monolayer allows a convenient and accurate assay of the rates of endocytosis and exocytosis (Gibbs *et al.*, 1986).

Preadipocyte 3T3-L1 cells transport glucose at low rates but after differentiation into mature adipocytes become insulin responsive and express a markedly elevated transport capacity (Rubin *et al.*, 1978; Rosen *et al.*, 1978; Reed and Lane, 1980). The GLUT4 is expressed in differentiated adipocytes but not in undifferentiated preadipocytes (Kaestner *et al.*, 1989; Garcia de Herreros and Birnbaum, 1989; Tordjman *et al.*, 1990; Weiland *et al.*, 1990), while GLUT1 is expressed in both undifferentiated and differentiated 3T3-L1 adipocytes (Kaestner *et al.*, 1989; James *et al.*, 1989; Kaestner *et al.*, 1989; Garcia de Herreros and Birnbaum, 1989; Tordjman *et al.*, 1990; Reed *et al.*, 1990; Weiland *et al.*, 1990). A study of the subcellular distribution of glucose transporters revealed that the GLUT4 was preferentially inserted into the intracellular compartment of the adipocytes, since 90% of the total GLUT4 was found in the low-density microsomes (Weiland *et al.*, 1990). In the fibroblasts, GLUT1 was almost exclusively located in the plasma membrane, whereas in differentiated cells it appeared to be re-distributed to the

intracellular compartment, since approximately 60% of the total GLUT1 was detected in the low-density microsomes (Weiland *et al.*, 1990 and present study).

It is known that both GLUT1 and GLUT4 mRNA and total cellular protein rise in concentration during differentiation. By days 8-11 days after initiation of differentiation, the concentrations of these transporters within the cells reach a maximum.

The changes in transporter protein expression elicited by differentiation were attributed primarily to increased rates of transporter synthesis, while the disproportionate changes in mRNA and protein expression from chronic insulin treatment and starvation suggested these conditions increase synthesis and decrease turnover rates in regulating transporter protein expression (Reed *et al.*, 1990). Chronic insulin exposure of differentiated adipocytes also increased cellular transporter mRNA and protein concentration (Reed *et al.*, 1990). Glucose starvation increased transporter mRNA and protein levels in both undifferentiated preadipocytes and differentiated adipocytes.

It has been reported that large changes in cell-surface levels of glucose transporters occur in 3T3-L1 cells.

Piper *et al.*, (1991) have reported that the ratio of the GLUT1:GLUT4 ratio was 5:1 in basal state. Using membrane impermeant bis-mannose photolabel ATB-BMPA, Calderhead *et al.*, (1990) and Kozka *et al.*, (1991) have reported that in basal cells the GLUT1:GLUT4 ratio was 3.5:1. Acute insulin treatment increases the cell-surface availability of both GLUT4 and GLUT1, so that both are present at the surface in equal amounts. The GLUT1:GLUT4 ratio is 1:1. Acute insulin treatment increase GLUT4 15-17 fold and GLUT1 3-7 fold.

Chronic insulin treatment (24 hours) on 3T3-L1 adipocytes has been reported to increase GLUT1 by 4-5 fold, GLUT4 is down-regulated by 50%, as measured by surface ATB-BMPA labelling. The GLUT1:GLUT4 ratio increases to 10:1. This large increase in total concentrations of cell-surface transporters (the sum of GLUT1 and GLUT4 concentrations) was not reflected in a large increase in 3-O-methyl-D-glucose transport, this suggesting that, compared to GLUT4, the GLUT1 makes a smaller contribution to transport (Kozka *et al.*, 1991).

To examine the proportion of newly synthesized transporters which become available at the cell surface, both cell surface and the total cellular pool of transporters have been measured with ATB-BMPA in this thesis. Permeabilization of 3T3-L1 cells with digitonin can allow the normally impermeant photolabel access to those transporters that are sequestered within the cell.

1.4 INSULIN STIMULATION OF GLUCOSE TRANSPORT

One important area of insulin action is the stimulation of glucose transport. Insulin's effect to stimulate the transport of glucose into cell was first demonstrated in intact animals over 40 years ago, but the molecular basis of this insulin effect was not understood.

Insulin increase the Vmax of glucose transport in adipocytes without affecting the Km (Whitesell and Gliemann, 1979; Luvigsen and Jarett, 1980; Taylor and Holman, 1981). This could be either by increasing the number of active transporters in the plasma membrane, or by increasing the Vmax of already existing transporters. The former possibility could occur in one of two ways: either by conversion (activation) of a pre-existing, functionally inactive transporter system already in the plasma membrane, or by recruitment of functionally active transport systems to the plasma membrane from a separate, intracellular site.

1.4.1 The translocation hypothesis

In 1980, Cushman, Kono, and their colleagues proposed a novel molecular mechanism by which insulin increased glucose transport in adipocytes (Cushman and Wardzala, 1980; Suzuki and Kono, 1980). These two groups independently demonstrated that the major effect of insulin on isolated rat adipocytes was to induce the translocation of an intracellular pool of glucose transporters to the plasma membrane; i.e. insulin increased the number of functional transport proteins at the surface of the cell.

Cushman and Wardzala (1980) using the cytochalasin B binding assay, found that the number of transporter-specific cytochalasin B binding sites associated with the microsomal fraction decreases in cells stimulated by insulin, by exactly the same amount as the number of sites associated with the plasma membrane fraction increased.

In a separate series of studies, Suzuki and Kono (1980) reconstituted the adipocyte glucose transporter (from plasma membrane and microsomal fractions) into liposomes, and assayed the transport activity directly. In agreement with the results of Cushman and Wardzala (1980), they were able to show directly that glucose transport activity in the subcellular, microsomal fraction decreased when the adipocytes were incubated with insulin, while that in the plasma membrane fraction increased.

Using the specific D-glucose-inhibitable [^3H] cytochalasin B-binding assay, Karnielli *et al.*, (1981a) have studied the time course, reversibility, and insulin concentration dependency of an insulin-induced translocation of glucose transport systems and they proposed a hypothetical mechanism of insulin's stimulation action on glucose transport in the isolated rat epididymal adipose cell (see Fig. 4).

As illustrated, insulin associates with its receptor inducing a signal which is still unknown. In response to this signal, intracellular vesicles containing the glucose transporter are translocated by an exocytic-like mechanism to the plasma membrane in a manner comparable to the various secretory processes (Pollard *et al.*, 1979; Mehler *et al.*, 1980). Following fusion of these vesicles with the plasma membrane, glucose transporters are then exposed to the extracellular medium and the glucose transport activity is increased.

In the reversal of this process (following dissociation of insulin from its receptor) glucose transporters are translocated back to the same intracellular pool by an endocytic-like mechanism similar to receptor-mediated endocytosis (Silverstein *et al.*, 1977). This recycling process could occur continuously if the insulin receptors were occupied.

Since this translocation or so called recruitment hypothesis was proposed there has been considerable evidence to support this hypothesis.

Studies were also carried out on the insulin-resistant states that accompany streptozotocin-induced diabetes and maturity obesity in rats. In these animals, stimulation of adipocyte glucose transport by insulin is impaired, though insulin binding is increased. It now appears that this impairment is due to depletion of intracellular transport systems (Karnielli *et al.*, 1981b) such that full stimulation can not occur.

Studies on isolated rat diaphragm using the cytochalasin B binding technique have shown that glucose transport in this tissue is also stimulated by recruitment of transporters from an intracellular site (Wardzala and Jeanrenaud, 1981, 1983), and the characteristics of the translocation are similar to those observed in adipocytes.

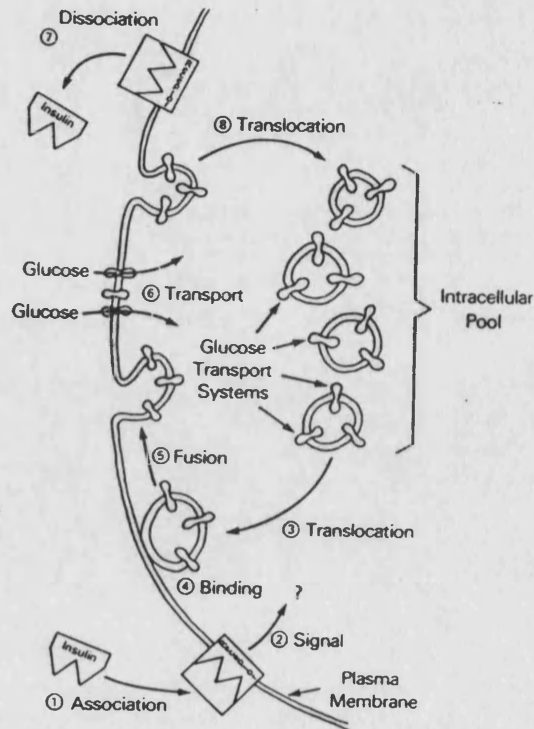


Fig.4 Schematic representation of a hypothetical mechanism of insulin's stimulatory action on glucose transport in the isolated rat epididymal adipose cell.
(From Karnielli *et al.*, 1981)

Watanabe *et al.* (1984) studied the insulin action on glucose transport in cardiac muscle. In this study, rat heart were perfused either in the presence or absence of insulin and then homogenized. The homogenate was fractionated, and the glucose transport activity in subcellular fractions was assayed by the reconstitution method. They found insulin appears to increase the glucose transport activity in rat hearts at least in part, by inducing translocation of the glucose transport mechanism from the unidentified vesicles (in fraction p 6) to the plasma membrane (in fraction p-5).

Klip *et al.* (1987) used glucose-inhibitable cytochalasin B binding to estimate the number of glucose transporters in membrane fractions from insulinized and control muscles. Insulin treatment caused an approx. 2 fold increase in cytochalasin B-binding sites in the plasma membrane fraction and an approx. 70% decrease in cytochalasin B - binding sites in an intracellular membrane fraction.

Although the transport of glucose itself does not need ATP, the translocation of glucose transporters in response to insulin and reversal of this process are ATP-dependent (Klip *et al.*, 1987; Simpson and Cushman, 1986).

The above findings indicate that the mechanism by which insulin stimulates facilitated glucose transport may be similar in both adipose and muscle tissue.

James *et al* 1988 isolated and characterized a monoclonal antibody, 1F8, that recognizes the insulin-regulated glucose transporter of adipocytes. The results using this antibody showed a marked translocation from the LDM to the plasma membrane in response to insulin and they named this protein as insulin regulatable glucose transporter. Subsequently, Zorzano *et al.* (1989) reported that rat adipocytes possess two immunologically distinct glucose-transporters; one recognized by 1F8, now known to be GLUT4 and one reactive with antibody raised against the human

erythrocyte glucose transporter-GLUT1. Immunoabsorption experiments indicate that these glucose transporters reside in different vesicle population and that both transporter isoforms translocate from intracellular sites to the plasma membrane in response to insulin.

Evidence for translocation has also come from use of the membrane impermeant photoaffinity labelling technique. Holman *et al.* (1988) have reported that photoincorporation of cell impermeant, exofacial photoaffinity reagent(BB-BMPA) into a 50-kDa plasma membrane protein of intact insulin treated adipocytes is blocked by cytochalasin B and 3-O-methylglucose. This plasma membrane protein has the characteristics expected of the glucose transporter. The photoincorporation of BB-BMPA into this protein is at least seven fold greater in insulin-treated versus basal intact adipocytes. Approximately 30% of plasma membrane carrier labelled in insulin treated intact cells recycles to the LDM fraction within 40 min. These experiments demonstrate that carrier recruitment is at least seven fold, and turnover (recycling) of carrier in insulin treated cells is much faster than in basal cells. The GLUT1 and GLUT4 antibodies were not available for this study.

Holman *et al.* (1990) synthesised another impermeant photoaffinity label (ATB-BMPA) (see 1:2). They have used this reagent to photolabel the GLUT4 and GLUT1 on the surface of the intact adipose in order to estimate the relative abundance of these two transporters on the cell surface following insulin stimulation. In response to insulin, GLUT4 increases 15-20 fold and GLUT1 increases 5 fold compared to basal state while 3-O-methyl-D-glucose transport is stimulated 20-30 fold. The ≈ 20 fold increase in the recruitment of the GLUT4 glucose transporter isoform can explain most of insulin's stimulation of glucose transport activity.

Calderhead *et al.* (1990) used ATB-BMPA to label the surface transporters GLUT1 and GLUT4 in 3T3-L1 adipocytes. They found the increases in GLUT1 and

GLUT4 averaged 6.5- and 17- fold respectively, whereas there was a 21 fold in hexose transport. These results indicate that the translocation of GLUT4 could largely account for the insulin effect on transport rate, but only if the intrinsic activity of GLUT4 is much higher than that of GLUT1.

Widnell *et al.* (1990) reported using an immunofluorescence technique to localize the glucose transporter protein in BHK cells, they found that hyperthermia, treatment with arsenite, infection with vesicular stomatitis virus or Semliki Forest virus, and treatment with insulin cause the transporter to move from an intracellular site in the perinuclear region to the plasma membrane; the degree of translocation correlates approximately with the increase in glucose uptake. They conclude that stress induces an insulin-like distribution of certain membrane proteins.

Studies investigated by using electron microscopy give direct evidence to support the translocation hypothesis.

Blok *et al.* (1988) used immunocytochemistry and a GLUT1 antibody with a protein A-gold technique to study the effect of insulin on the cellular distribution of the GLUT1 in 3T3-L1 adipocytes. They reported that insulin induced a threefold increase in the number of these transporters in the plasma membrane and that these transporters were recruited from an intracellular compartment located mainly at the trans side of the Golgi complex.

Slot *et al.* (1991a) studied on cardiac myocytes of the rat. The insulin regulated glucose transporter GLUT4 was immunolocalized in rat cardiac muscle under conditions of basal and insulin stimulated states. In basal myocytes there was very little (<1%) GLUT4 in the different domains of the plasma membrane. Upon insulin stimulation about 42% of GLUT4 was found in the plasma membrane.

A very elegant study by Slot *et al.* (1991b), has clearly shown that insulin produces a very large increase in GLUT4 in the plasma membrane of brown adipose tissue as detected by immunogold electron microscopy. The increase in plasma membrane transporter was paralleled by a decrease in glucose transporter in a cytoplasmic pool associated with tubulo-vesicular structures. They conclude that translocation of GLUT4 to the cell surface is the major mechanism by which insulin increases glucose transport.

1.4.2 The intrinsic activation hypothesis

It is believed that translocation of glucose transporters from an intracellular pool to the plasma membrane can account for most of the effect of insulin on glucose transport. In addition to recruitment, glucose uptake may also be regulated by altering the intrinsic activity of the glucose transporter.

Clark *et al.* (1991) have used ATB-BMPA to photolabel the glucose transporter isoform GLUT4 and GLUT1 in rat adipose cells. They labelled both the plasma membrane fractions and light microsome membrane fraction using this reagent. The labelling of GLUT4 in the plasma membrane fraction from insulin treated cells was about 3 fold higher than that of basal cells and corresponded with a decrease in the labelling of the light microsome fraction. The cell surface labelling of GLUT4 from insulin treated intact adipose cells was increased about 15-20 fold above basal levels. Insulin stimulated glucose transport activity increased about 30 fold. Thus the cell surface labelling, but not the labelling of membrane fractions, closely corresponded with the stimulation of transport. The remaining discrepancy may be due to an approx. 2 fold activation of GLUT4 intrinsic transport activity.

The discrepancy between glucose transporter number and activity is even more pronounced when the actions of hormones such as catecholamines, adrenocorticotrophin (ACTH) and glucagon are studied. These hormones are mediated by Gs-coupled receptors (Rs). Adenosine, prostaglandins and nicotinic acid, agents whose actions are mediated by Gi-coupled receptors (Ri), are superimposed upon insulin stimulation (Kuroda *et al.*, 1987; Joost *et al.*, 1987). Rs receptors therefore mediate inhibition and Ri receptors mediate augmentation of insulin-stimulated glucose transport activity and these changes are independent of changes in cAMP-dependent protein kinase activity (Kuroda *et al.*, 1987). The changes in insulin-stimulated glucose transport induced by Rs and Ri receptors occurred without a major change in the subcellular distribution of glucose transporters. This has been detected by cytochalasin B binding (Kuroda *et al.*, 1987) and ATB-BMPA labelling (Vannucci *et al.*, 1992). This had led to the hypothesis that these hormones alter the intrinsic activity of the glucose transporter in the plasma membrane (Kuroda *et al.*, 1987).

The mechanism responsible for modulating the intrinsic activity of the facilitative glucose transporters is still not clear. There is some evidence that both GLUT1 and GLUT4 can be phosphorylated. GLUT1 by protein kinase C (Gibbs *et al.*, 1986) and GLUT4 by protein kinase A (Lawrence *et al.*, 1990a). The site of protein kinase C-mediated phosphorylation of GLUT1 has not been determined. The site of phosphorylation of rat GLUT4 by protein kinase A is restricted to the region of the putative intracellular COOH-terminal domain at Ser⁴⁸⁸ and is conserved in the sequences of rat, human and mouse GLUT4 (Lawrence *et al.*, 1990a).

Czech and co-workers (1980) proposed that an activation of transporters already in the membrane must play a significant role in transport stimulation. Studies on 3T3-L1 cells in their group, have indicated that GLUT1 and GLUT4 present in these cells is already largely present on the cell surface in resting cells. However, its

catalytic activity is markedly suppressed by a mechanism that blocks its binding to extracellular sugar molecules. They propose that in 3T3-L1 cells, the restraint on GLUT1 catalytic activity is released by known glucose transport activators, including insulin itself, cholera toxin, cadmium and protein synthesis inhibitors (Harrison *et al.* 1991a, Clancy *et al.* 1991, Harrison *et al.*, 1991b).

A stimulation of glucose transport by incubation at alkaline pH has been reported in rat adipocytes and an apparent translocation of glucose transporters to the plasma membrane has been suggested as a possible mechanism (Sonne *et al.*, 1981; Toyoda *et al.*, 1986)

To investigate the translocation mechanism, in this thesis, studies on dose response of insulin-stimulated translocation of GLUT1 and GLUT4 have been carried out in 3T3-L1 adipocytes at different pH conditions.

1.5 REGULATION OF GLUCOSE TRANSPORT

1.5.1 Insulin signalling

Stimulation of glucose transport is one of the fundamental responses to insulin. The signals that mediate between insulin binding to stimulation of transport are still not very clear. However, considerable progress in the last few years has suggested that at least two possible routes may be involved in this response. These are from the tyrosine-specific kinase activity of the insulin receptor, and from insulin receptor activation of the serine and threonine-specific kinase which possibly does not involve the tyrosine kinase activity of the receptor (Klip and Douen, 1989).

1.5.1.1 The insulin receptor kinase

The insulin receptor is an integral membrane glycoprotein consisting of two α -subunits ($M_r \approx 135000$) and two β -subunits ($M_r \approx 95000$) linked by disulphide bridges to yield a symmetrical $\beta\alpha\text{-}\alpha\beta$ complex (Massague *et al.*, 1980). The α -subunit contains the insulin binding domain and the β -subunits contains an insulin tyrosine-specific kinase (Ebina *et al.*, 1985; Ullrich *et al.*, 1985).

It is believed that insulin-induced conformational changes of the receptor transfer a signal from the extracellular to the cytoplasmic receptor domains, leading to the activation of the β -subunit associated tyrosine kinase (Ebina *et al.*, 1985; Ullrich *et al.*, 1985).

Insulin induces phosphorylation of several endogenous proteins on tyrosine residues, which differ from tissue to tissue. In 3T3-L1 adipocytes, insulin-induced β -subunit phosphorylation was complete within 1 min ($t_{1/2} = 8$ sec), while a 1 min latency period preceded insulin activation of hexose transport (Kohanski *et al.*, 1986). Removal of insulin from the medium resulted in rapid loss of phosphorylation ($t_{1/2} = 2.5$ min), while hexose transport decreased with a $t_{1/2}$ of 8 min. The observation that the time course of stimulation and reversal of receptor kinase activity precedes effects on glucose transport suggests that tyrosine kinase activation is rapid enough to elicit slower down-stream signalling processes (Klip and Douen, 1989).

1.5.1.2 Post-receptor signalling

White *et al.* (1985, 1987) have reported that insulin stimulates the tyrosyl phosphorylation of a 165-185 kDa protein in intact cells. This phosphoprotein, called pp185, is barely detectable in cells expressing few insulin receptors, strongly detected in cells expressing high levels of receptors and weakly detected in cells expressing

mutant receptors defective in biological signaling (White *et al.*, 1988; Backer *et al.*, 1991; Wilden *et al.*, 1992). Thus, pp185 appears to be a substrate of the insulin receptor which plays a significant role in the early stages of post-receptor insulin signal transduction.

Rothenberg *et al.* (1990) have purified a protein from rat liver in the pp185 band. The complementary DNA sequence encodes a 131 kDa hydrophilic protein called insulin receptor substrate-1 (IRS-1) (Sun *et al.*, 1991). IRS-1 contains a kinase-like ATP-binding site, many potential serine and threonine phosphorylation sites and at least 14 potential tyrosine phosphorylation sites. Six of these tyrosyl residues are located in YMXM motifs and three others are in YXXM motifs. Synthetic peptides based on the sequence of these YXXM motifs are excellent substrates of the insulin receptor, with K_m values between 24 and 100 nM (Shoelson *et al.*, 1992).

Backer *et al.* (1992) have found that during insulin stimulation, the IRS-1 protein undergoes tyrosine phosphorylation and binds phosphatidylinositol 3 kinase (PI3-kinase). Purification of PI-3 kinase has demonstrated that the kinase is a heterodimer consisting of 85-kDa (p85) and 110-kDa (p110) subunits (Carpenter *et al.*, 1990; Morgan *et al.*, 1990; Shibasaki *et al.*, 1991). The amino acid sequence of p85 showed that the protein contains (SH) Src homology regions: two SH-2 domains and one SH-3 domain (Otsu *et al.*, 1991; Escobedo *et al.*, 1991; Skolnik *et al.*, 1991). The SH-2 domains are involved in interactions with tyrosine-phosphorylated proteins (Koch *et al.*, 1991). Binding to IRS-1 increases the specific activity of PI3-kinase in insulin stimulated cells and overexpression of IRS-1 potentiates insulin stimulation of PI3-kinase. This activation occurs both *in vivo* and *in vitro*. These findings suggest that tyrosyl phosphorylation of IRS-1 by the insulin receptor and the subsequent association of IRS-1 with p85 activates PI3-kinase (Backer *et al.*, 1992).

Kelly *et al.* (1992) have reported that upon stimulation of rat adipocytes with insulin, the majority of IRS1 precipitable PI3-kinase is found in the low-density microsomes. The significance of this in terms of coupling to glucose transporter vesicular trafficking is at present unclear.

1.5.2 Role of protein kinase C in glucose transport

Protein kinase C is a Ca^{2+} and phospholipid-dependent enzyme that is activated by diacylglycerol (Kishimoto *et al.*, 1980). There is some evidence to show that protein kinase C plays a role in glucose transport.

The activators of protein kinase C, such as phorbol 12-myristate 13-acetate (PMA) have been shown to increase glucose transport. Saltis *et al.* (1991) found that both insulin and PMA increased GLUT1 in the plasma membranes about 1.5 fold, but the latter effected only about 35% of the six fold stimulation by insulin of GLUT4 translocation. Vogt *et al.* (1991) reported that PMA had no effect on GLUT1 but caused a 2.5 fold stimulation of the redistribution of GLUT4. In both studies, the PMA-dependent change in transport roughly correlated with the translocation of GLUT4 to the cell surface. Using the impermeant glucose transporter photolabel-ATB-BMPA, Holman *et al.* (1990) have reported that PMA stimulated approximately four and five fold increases in cell surface GLUT4 and GLUT1 respectively in rat adipocytes. This is concomitant with an approximate three fold increase in 3-O-MG uptake. Similar results were obtained in 3T3-L1 adipocytes (Gibbs *et al.*, 1991). In any case, the protein kinase C activators are less effective than insulin and this suggests that non-protein kinase C dependent mechanisms may be operative during insulin stimulation.

1.5.3 Cyclic AMP and phosphorylation

In 1986, Joost *et al.* have reported that isoproterenol, in the presence of adenosine deaminase, inhibited the stimulation of glucose transport by insulin (Joost *et al.*, 1986). The inhibitory effect is thought to be due to a decrease in the intrinsic activity of the glucose transporter of the plasma membrane rather than a change in subcellular distribution of the glucose transporter (Joost *et al.*, 1987). There is some evidence that the inhibitory effect of β -adrenergic agents is not mediated by an increase in cyclic AMP, but is related to direct interactions of G-proteins with the transporter or an associated regulatory protein (Kuroda *et al.*, 1987).

James *et al.* (1989) have reported that the inhibitory effects of β -adrenergic agents on glucose transport in rat adipocytes are a result of a cyclic AMP-dependent phosphorylation of GLUT4. In metabolically labelled rat adipocytes, isoproterenol stimulated the incorporation of ^{32}P into GLUT4 by about twofold in both plasma membranes and low-density microsomes. This was mimicked by analogs of cyclic AMP and occurred in broken cells in the presence of the catalytic subunit of cyclic AMP-dependent protein kinase and $[\gamma\text{-}^{32}\text{P}]\text{ATP}$.

The amino acid phosphorylated in response to an elevation in cyclic AMP has been mapped to Ser⁴⁸⁸, located at the carboxyl terminus of GLUT4 (Lawrence *et al.*, 1990a). Because Ser⁴⁸⁸ is unique to GLUT4, they suggest that GLUT4 may be uniquely regulated by phosphorylation. Derivatives of cAMP also stimulated transporter phosphorylation, suggesting that the response to the β -adrenergic agonist occurred via a cAMP-dependent pathway (James *et al.*, 1989).

Okadaic acid, an inhibitor of protein phosphatase-1 and -2A, has been shown to stimulate 2-deoxy-D-glucose uptake in rat adipocytes (Haystead *et al.*, 1989) and this suggested that there is a role for phosphorylation in regulating glucose transport

activity in insulin-responsive cells. Lawrence *et al.* (1990b) reported that okadaic acid was about 50% as potent as insulin in stimulating hexose uptake in adipocytes. When it is present with insulin, it slightly inhibited the stimulation by a maximal concentration of insulin. Measurements of GLUT4 levels in subcellular fractions of adipocytes, indicated that both the stimulatory and inhibitory effects of the phosphatase inhibitor correlated reasonably well with the amount of GLUT4 protein in the plasma membrane and suggested that the inhibition effect on insulin-stimulated glucose transporter translocation by okadaic acid may be due to phosphorylation of GLUT4 which promotes its internalization (Lawrence *et al.*, 1990b).

1.6 RECEPTOR-MEDIATED ENDOCYTOSIS

To better understand the effect of insulin on translocation of GLUT1 and GLUT4 to the cell surface, it is important to study the cellular-trafficking pathways of GLUT1 and GLUT4.

Immunocytochemical studies suggest that glucose transporter trafficking is a regulated process similar to the receptor-mediated endocytosis that occurs in the processing of receptors such as the transferrin, asialoglycoprotein and insulin receptor (Goldstein *et al.*, 1985; Stoorvogel *et al.*, 1987; Tanner and Leinhard, 1987; Sonne, 1988).

1.6.1 Outline of receptor-mediated endocytosis

In most animal cells, clathrin-coated pits and vesicles provide an efficient pathway for taking up specific macromolecules from the extracellular fluid, this process is called receptor-mediated endocytosis.

The studies on the internalisation of low-density lipoproteins (LDL) outlined

some of the early events in the pathway (Anderson *et al.*, 1977). (see Fig. 5).

Ligands bind to specific membrane-spanning receptors located on the cell surface and the receptor/ligand complexes become clustered into coated pits. The major component of the coat is a protein, termed clathrin, which was first identified by Pearse (1975, 1976). The basic structural unit of clathrin is a complex of three molecules of clathrin heavy chain (180 kDa) and three molecules of clathrin light chain (30-40 kDa) in a three-legged structure termed a triskelion (Kirchhausen and Harrison, 1981; Ungewickell and Branton, 1982). Clathrin interacts with the cytoplasmic tail of a receptor probably via adaptor proteins (Pearse, 1988). Clathrin forms lattices on the plasma membrane and growth and rearrangement of this lattice causes invagination of the pit. Scission of the deeply invaginated coated pit results in the release of a coated vesicle from the plasma membrane which carries the ligand into the cell.

Some receptors like the LDL-receptor, are clustered in coated pits and internalized even when unoccupied. Other receptor, for example of some growth factors and hormones, migrate into the pit and are internalized only after binding of their respective ligands (Goldstein *et al.*, 1985). In the latter example, protein kinase C-mediated phosphorylation and auto-phosphorylation events have been proposed as regulatory mechanisms (Carpenter, 1987).

The coated vesicles are rapidly uncoated and these vesicles fuse to form the early endosome system.

In part of the early endosome system the receptor and ligands are sorted for directing to different destinations. They may be targeted to the lysosome for degradation (Stoscheck and Carpenter, 1984) or recycled back to the cell surface.

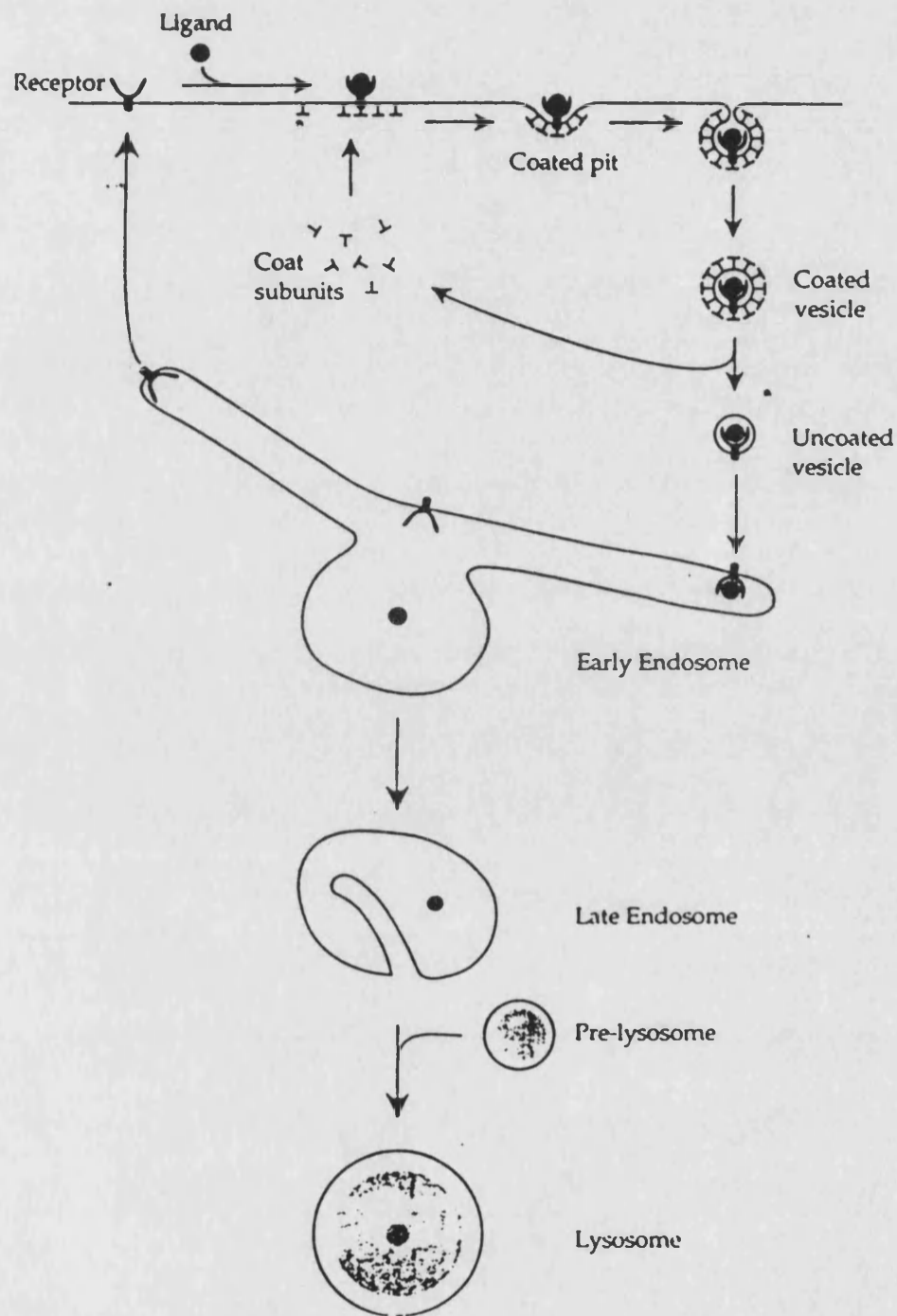


Fig.5 Outline of receptor-mediated endocytosis.

Ligands to be internalised bind to specific receptors on the cell surface. These receptor/ligand complexes become clustered in specialised areas of the plasma membrane, termed coated pits. After invagination and scission to form a coated vesicle, the coat is rapidly removed. Fusion with the early endosome exposes the receptor/ligand complexes to reduced pH which causes dissociation of ligand and receptor. Ligands may be transferred through late endosomes while those receptors which recycle are returned to the cell surface. (From Anderson *et al.*, 1977)

The techniques of site-directed mutagenesis, cell-free assays and cell fractionation have been used to elucidate the endocytic mechanism.

1.6.2 Adaptors in coated pits and vesicles

A family of 100-kDa and 50-kDa proteins termed adaptors have been found which can recognise a signal in the cytoplasmic tail of receptors (Pearse, 1988). Because of their ability to enhance the assembly of clathrin lattices *in vitro* they have also been named assembly proteins (Zaremba and Keen, 1983).

The role of the adaptor proteins is to link clathrin to the membrane (Unanue *et al.*, 1981). The isolated adaptor proteins bind specifically to an integral membrane protein in alkaline-extracted membranes from bovine brain. The binding of clathrin to these membrane was adaptor dependent (Virshup and Bennett, 1988). In order to link the selected components into the clathrin, the adaptors must possess a clathrin binding site. There is some evidence to suggest that it is the β subunit of the adaptor complex which is involved in the interaction with clathrin (Ahle *et al.*, 1988).

1.6.3 Early endosomes

(1). Docking and fusion

Coated vesicles are very rapidly (<1 min) uncoated yielding an endocytic vesicle (Pearse and Brescher, 1981). Once uncoated, the endocytic vesicle docks and fuses with its target in the endosome system. The reconstitution studies *in vitro* have measured the fusion between early endosomal elements (Gruenberg and Howell, 1986). Very recently the cytosol-dependent fusion between purified vesicles and early endosomes has been demonstrated (Woodman and Warren, 1988). From this assay it has been shown that fusion *in vitro* is energy-dependent and requires cytosolic components. One of these cytosolic components is N-ethylmaleimide-sensitive fusion

protein (NSF) (Diaz *et al.*, 1989). This protein has been shown to be required for intra-Golgi (Malhotra *et al.*, 1988; Block *et al.*, 1988) and endoplasmic reticulum to Golgi transport (Beckers *et al.*, 1989). Fusion was inhibited when membranes and cytosol were treated with N-ethylmaleimide (NEM).

(2). Sorting of ligands and receptors

Early endosomes are located close to the plasma membrane and they may become part of a more specialized tubulo-vesicular structure. Early endosomes appear to be the site where those receptor/ligand complexes which recycle to the plasma membrane are sorted. The reduction of pH encountered in this compartment is sufficient for the dissociation of these ligands from their receptors. The receptors are recycled back to the cell plasma membrane (Brown *et al.*, 1982). Reappearance of receptors on the plasma membrane is rapid, the measured half-times for recycling of the asialoglycoprotein and transferrin receptors in HepG2 cells are 4 min and 7 min respectively (Ciechanover *et al.*, 1983)

1.7 FLUID PHASE ENDOCYTOSIS

Fluid phase endocytosis (pinocytosis) is the nonspecific form of endocytosis in which any extracellular material is taken up at a rate proportional to its concentration in the extracellular medium.

In 1986, Gibbs *et al.* studied fluid-phase endocytosis using monolayers of 3T3-L1 adipocytes followed by measuring [^{14}C] sucrose uptake. They found that insulin, at maximal stimulatory concentration, increased the pinocytic rate by 2-fold within 5 min of its addition and this activation persisted for at least 2 hours. The dose-response curve for the enhancement of fluid-phase endocytosis by insulin was identical with that for the stimulation of 2-deoxy-D-glucose. The concentration of insulin eliciting half-maximal effects was 6 nM. Their results suggest that activation

of endocytosis and hexose uptake by insulin are triggered by the same signalling event.

Studied on 3T3-L1 cells by Fan *et al.* (1982); Ronnett, (1983); Reed, (1984) have reported that occupied insulin receptors are rapidly internalized via coated pits and vesicles and then, after dissociation of the bound insulin, rapidly return to the plasma membrane. Marsh *et al.* (1980) and Robinson *et al.* (1983) studied other types of animal cells in culture. They found that a large fraction of fluid-phase endocytosis occurs by the pathway of coated pits and vesicles. So the hypothesis to account for the effect of insulin on fluid-phase endocytosis is that when insulin is bound to its receptor, the receptor possesses a conformation that induces either the more rapid assembly or internalization of coated pits.

1.8. SUBCELLULAR TRAFFICKING OF GLUT1 AND GLUT4

It is well documented that in the basal state, there is a significant intracellular pool of both GLUT1 and GLUT4 glucose transporter. According to these data, there are two questions to ask: whether GLUT1 and GLUT4 reside in the same intracellular compartments and the nature of the compartment(s) in which the transporters exist in unstimulated insulin-responsive cells.

Zorzano *et al.* (1989) have utilized a monoclonal antibody (1F8) directed against GLUT4, to immunopurify transporter-containing vesicles from the low-density microsome fraction of homogenates of isolated rat adipocytes. Vesicles absorbed to 1F8 contained over 90% of GLUT4 but less than 5% of the cellular GLUT1. They concluded that the GLUT1 and GLUT4 are located in distinct cellular compartments and GLUT4 probably resides in a distinct, differentiated organelle.

Piper *et al.* (1991) examined the immunoadsorption of glucose transporter vesicles from 3T3-L1 adipocytes to isoform-specific anti-peptide antisera linked to acrylamide beads. They found that adsorption of low-density microsomes removed 90% of the GLUT4 but only 30% of the immunoreactive GLUT1 from solution. The distribution of vesicles containing each of the transporters was partially overlapping but distinct on equilibrium sucrose density centrifugation. They suggest that GLUT1 and GLUT4 are in different intracellular locations in murine adipocytes.

Calderhead *et al.* (1990) have reported a study in which GLUT4-containing vesicles were immunopurified from 3T3-L1 adipocytes. Adsorption by anti-peptide antisera directed against the carboxyl termini of either GLUT1 or GLUT4 removed almost all of the isoforms from the "low speed" supernatant. They suggest that the GLUT1 and GLUT4 reside in the same intracellular compartment.

These seemingly contradictory results have been explained. One explanation is that there is partial overlap between the distribution of transporters, such that there exists a population of vesicles rich in GLUT1 but containing a few GLUT4 molecules, and vice versa. In addition, the much higher ratio of GLUT1 to GLUT4 in 3T3-L1 adipocytes compared to rat fat cells might alter the apparent colocalization. The other explanation is that the degree of colocalization is dependent on the fragmentation during cell homogenization of a single organelle. A continuous endosomal reticulum with distinct, connected domains has been postulated; the degree of intermixing of proteins in such an organelle during cell disruption might be very dependent on the cell type (Hopkins *et al.*, 1990).

The other strategy for assessing the colocalization of glucose transporter isoforms is morphological studies, but most studies have looked at the separate location of either GLUT1 or GLUT4.

Blok *et al.* (1989) have used the immunogold technique to localize the glucose transporters in basal and insulin-treated 3T3-L1 adipocytes. Using immunoelectron microscopy to determine the cellular distribution of GLUT4 in brown adipose tissue, Slot *et al.* (1991b) demonstrated that in the basal state GLUT4 is localized almost entirely to small tubulo-vesicular (T-V) structures in the Golgi area and elsewhere throughout the cytoplasm, these glucose transporters are often in clusters. Upon insulin treatment, GLUT4 display a marked shift from these sites to the plasma membrane. The amount of GLUT4 at the cell surface increases by at least 40-fold. GLUT4 is seen to enter the coated pit/coated vesicle/early endosome pathway typical of receptor-mediated endocytosis (Slot *et al.*, 1991b). This finding has indicated that the glucose transporter a multispinning membrane protein undergoes recycling by the pathway that has been well established for cell surface receptors.

The effect of insulin is to allow GLUT4 to relocate from tubulo-vesicular (T-V) structures to the plasma membrane and to participate in the recycling pathway. Upon insulin withdrawal the positive signal driving movement of GLUT4 to the cell surface is removed such that GLUT4 appear to be withdrawn from early endosomes and accumulates again in the T-V structures. This proposed mechanism is consistent with the observation that after insulin removal GLUT4 rapidly disappears from the cell surface of adipocytes and reappears in the same subcellular fraction where it was found in basal cells (Karnieli *et al.*, 1981a).

To establish the identity and the location of the sorting factors that determine the intracellular targeting of GLUT4 and GLUT1 it is important to understand the insulin action on glucose transport. The early endosome or the trans-Golgi reticulum (TGR) are the most likely locations for specific sorting (Slot *et al.*, 1991b).

Another strategy to resolve the problem of whether GLUT1 and GLUT4 are targeted to distinct cellular compartments is to express the two transporters in

identical cellular contexts, and define their subcellular distributions. GLUT4 was found to have an intracellular, perinuclear punctate distribution, resembling that visualized in 3T3-L1 adipocytes (Garcia de Herreros and Birnbaum, 1989; Piper *et al.*, 1991; Hudson *et al.*, 1992). In contrast, GLUT1 was present predominantly on the plasma membrane, and to a lesser extent in a juxtanuclear distribution. However expression systems may result in unusual targeting.

There are two models for intracellular trafficking of GLUT1 and GLUT4. One has been referred as the "secretory" model. The other one is referred to as the "receptor" model (see Fig. 6).

In the "secretory" model, GLUT4 resides in a mature storage organelle, and it is actively sorted at the trans-Golgi network into the equivalent of the regulated pathway, whereas GLUT1 follows a default route to the cell surface (Griffiths and Simons, 1986; Burgess and Kelly, 1987). This would account for the difference in relative distribution of the two isoforms between plasma membrane and intracellular compartments.

The small synaptic vesicles (SSVs) of neurons are thought to be first synthesized by a regulated secretory pathway (Cutler and Cramer, 1990; De Camilli and Jahn, 1990). After depolarization-induced release of neuro-transmitter, the integral membrane proteins of SSVs are sorted out of early endosomes and used to reconstruct synaptic vesicles which exist as a mature organelle awaiting another exocytotic event. As is apparently the case with insulin-responsive vesicles, SSVs are capable of undergoing multiple rounds of exocytosis and resynthesis. Calderhead *et al.* (1990); De Camilli and Jahn (1990); Slot *et al.* (1991b) examined immunoadsorption of GLUT4 or its localization by immunoelectron microscopy, they reported that GLUT4 did not appear to reside in vesicles of uniform size resembling classic neuronal SSV. While this may be interpreted as evidence against a secretory

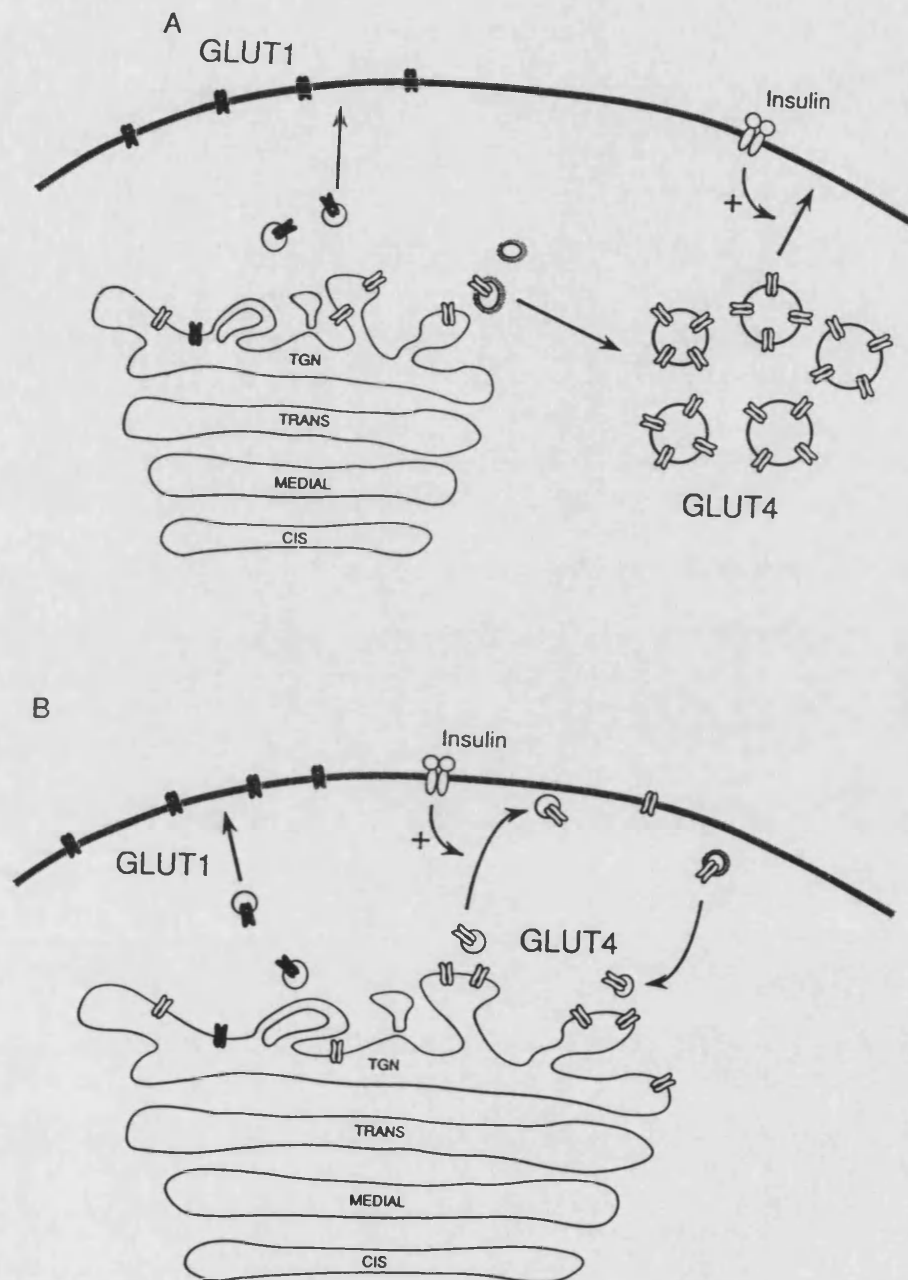


Fig.6 Alternative models for the cellular trafficking of glucose transporters in rat adipocytes.

GLUT1 is represented by closed symbols and GLUT4 by open symbols. (A) The "secretory" model, in which GLUT4 is sorted into a distinct storage organelle. (B) The "receptor" model, in which insulin regulates the rate of GLUT4 recycling through a ubiquitous organelle. (From Birnbaum, 1992)

model, it does not exclude one. Navone *et al.* (1986); Slot *et al.* (1991b) have localized SSV markers in endocrine cells to tubulovesicular structures. These resemble the GLUT4-containing compartment of brown adipose tissue. Thus this "neuronal-like" structure does indeed represent an authentic secretory compartment. A precedent exists for a pleiomorphic tubulovesicular organelle that obeys the rules of regulated secretion. (Reetz *et al.*, 1991).

Recently, there are some experiments in α -toxin-permeabilized rat adipose cells which are consistent with a secretory model. In such cells, nonhydrolyzable analogs of GTP mimicked insulin in inducing the translocation of GLUT4 from low-density microsomes to the plasma membrane (Baldini *et al.*, 1991).

A family of small GTP binding proteins has been shown to have a role in membrane traffic (Bourne, 1988; Balch, 1990) and in the fusion of early endosomes. Mayorga *et al.* (1989) have reported that GTP[γ S] can inhibit fusion of early endosomes at saturating cytosol concentrations. The effect of GTP[γ S] appears to be mediated through the rab family of GTP binding proteins. These proteins are part of the ras superfamily.

There are numerous sites in the insulin signal transduction pathway at which G proteins might influence translocation. There is some evidence to show that nonhydrolyzable GTP analogs stimulate the production of diacylglycerol, which can activate glucose transport via protein kinase C (Farese *et al.*, 1985; Stralfors, 1988; Bader *et al.*, 1989) and that GTP γ S inhibits the fusion of endosomes, which might increase the abundance of GLUT4 in the plasma membrane by slowing its internalization (Chavrier *et al.*, 1990; Gorvel *et al.*, 1991). The simplest and most likely explanation is that a small G protein is associated with the insulin-responsive compartment and is required for fusion to the plasma membrane. Thus this would provide a potential site of regulation that could be modulated by phosphorylation or

dephosphorylation. Bailly *et al.* (1991) have reported that phosphorylation of the endosomal small G protein Rab4 by p34^{cdc2} can cause the inhibition of vesicular fusion during mitosis. It will be interesting to determine where an analogous protein is expressed in insulin-responsive tissues.

Robinson *et al.* 1992 have reported that in streptolysin-O permeabilized adipocytes, insulin, and GTP γ S increased plasma membrane levels of GLUT4 to a similar extent as observed with insulin in intact cells. In the absence of an exogenous ATP source the magnitude of these effects was considerably reduced. Removal of ATP per se caused a significant increase in cell surface levels of GLUT4 suggesting that ATP may be required for intracellular sequestration of these transporters. When insulin and GTP γ S were added together, in the presence of ATP, plasma membrane GLUT4 levels were similar to levels observed when either insulin or GTP γ S was added individually. Addition of GTP γ S was able to overcome this ATP dependence of insulin-stimulated GLUT4 movement. GTP γ S had no effect on constitutive secretion of adiponectin in permeabilized cells. There was no effect of insulin or GTP γ S on GLUT4 movement to the plasma membrane in noninsulin sensitive streptolysin-O-permeabilized 3T3-L1 fibroblasts overexpressing GLUT4. This indicated that insulin-stimulated movement of GLUT4 to the cell surface in adipocytes may require ATP early in the insulin signaling pathway and a GTP-binding protein at a later step.

In the "receptor" model, GLUT4 constitutively recycles through the endocytotic pathway, in the basal state residing predominantly in an intracellular location. At all times GLUT4 is located in nonspecialized cellular compartments. It will be either in the plasma membrane or components of the endosomal system. Insulin would alter the distribution by increasing the rate constant determining extraction of GLUT4 from the endosome to the cell surface.

In 1987, Tanner and Lienhard studied transferrin receptor in 3T3-L1

adipocytes upon insulin treatment. They found that incubation of 3T3-L1 adipocytes with insulin at 37°C resulted in a 2 fold increase in specific binding of transferrin to cell-surface receptors, as measured by a subsequent incubation of cells at 4°C with ¹²⁵I-transferrin. The results they have got are similar to results obtained in rat adipocytes (Davis *et al.*, 1986). They showed that the increased number of transferrin receptors is due to translocation of the receptor from an intracellular location to the plasma membrane. Insulin increased the rate constant for externalization of transferrin receptors and had no significant effect upon the rate constant for receptor internalization. The insulin-like growth factor II (IGF-II) receptor, like the transferrin receptor, continuously recycles. Insulin has no effect on the rate constant for internalization of photoaffinity-labelled IGF-II receptor (Oka *et al.*, 1985; Oka and Czech, 1986).

It is clear that insulin also elicits a redistribution of transferrin receptors in both rat adipocytes (Davis *et al.*, 1986) and 3T3-L1 adipocytes (Tanner and Lienhard, 1987).

In 1989, Tanner and Lienhard studied the effect of insulin on the subcellular distributions of the glucose transporter, transferrin receptor and IGF-II receptor in 3T3-L1 adipocytes using a binding assay. They demonstrate that the insulin-responsive pools of GLUT1, transferrin receptor and IGF-II receptor reside largely in the same intracellular membranes. Insulin stimulated a 2-3 fold increase in the level of each protein at the cell surface and in each case the decrease in the content of the protein in the microsomal membranes can account for the increase at the cell surface.

Although 85-100% of these three membrane proteins in the microsomal fraction are contained in the glucose transporter vesicles, insulin's effect on the content of the proteins in this fraction was not uniform. In response to insulin, a 50% decrease in GLUT1 content occurred while only a 16% decrease in the IGF-II

receptor content occurred (Tanner and Lienhard, 1989). The GLUT1 may have a higher probability of being incorporated into plasma-membrane targetted vesicles than does the IGF-II receptor.

As discussed by Piper *et al.* (1991), the sequestration of GLUT4 could be due either to a very rapid removal of this protein from the plasma membrane or to a very slow rate of exocytosis in the basal state. This could lead us to find out if the GLUT4 protein sequence results in a unique cellular processing by vesicle trafficking and sequestration machinery. If endocytosis is unusual, then the unique cellular processing may occur in the plasma membrane, if exocytosis is slow, the targeting recognition events may occur intracellularly. In the insulin-stimulated state the proportion of GLUT4 associated with coated pits increased 3 fold in early endosomes it increased 4 fold, and in the plasma membrane it increased 40 times that of the basal state (Slot *et al.*, 1991b). This result indicated that the main insulin effect was to increase exocytosis of GLUT4 from tubulo-vesicular structures to the plasma membrane and thence into the endosome pathway. The studies on the steady-state level of the glucose transporters cannot clearly distinguish between an increased exocytosis or decreased endocytosis or show a modification of both these steps in cycling.

Kinetic studies rather than steady-state distribution studies of transporter cycling can directly determine and quantify the site of insulin action on trafficking. Using a photoreactive probe (B3-GL) to study insulin's effect on GLUT4 translocation kinetics in rat adipocytes, Jhun *et al.* (1992) have reported that insulin has equal effects on endocytosis and exocytosis. The former is reduced and the latter increased by 3 fold. They suggested that the insulin dependent phosphorylation influenced internalization as it has been shown to regulate the internalization of many cell surface receptors, including epidermal growth receptor (Chen *et al.*, 1989), insulin receptor (McClain *et al.*, 1988) and IGF-II receptor (Covera and Czech,

1985). They suggested phosphorylation may also regulate internalization of GLUT4. They interpreted the results of James *et al.* (1989) as showing that GLUT4 in basal adipocytes is more phosphorylated in the plasma membrane than in the intracellular compartment and insulin reduces the GLUT4 phosphorylation in the plasma membrane. So they propose that this insulin-induced dephosphorylation of GLUT4 at the plasma membrane may prevent the association of GLUT4 to the clathrin-coated pits, resulting in reduced GLUT4 internalization rate.

This finding is different from the previous studies of GLUT4 trafficking kinetics in rat adipocytes (Clark *et al.*, 1991; Satoh *et al.*, 1991) and the hypothesis (Karnielli *et al.*, 1981a; Piper *et al.*, 1992; Robinson *et al.*, 1992) that the main effect of insulin is to increase exocytosis of GLUT4.

To resolve the site of insulin action on GLUT1 and GLUT4 trafficking, in part of this thesis, a study similar to that described by Jhun *et al.* (1992) was carried out. GLUT1 and GLUT4 present in 3T3-L1 cells were labelled in the insulin-stimulated and the basal states with ATB-BMPA. The redistributions of these labelled transporters from the plasma membrane to the low density microsome membrane fraction were followed while cells were maintained at either insulin-stimulated or basal steady states.

Very recently, Piper *et al.* (1992) have shown that the GLUT4 NH₂ terminus contains important targeting information. Replacement of the GLUT4 NH₂ terminus with that from GLUT1 resulted in an increase in cell surface expression whereas replacement of the GLUT1 NH₂ terminus with that from GLUT4 resulted in an increase accumulation of the chimera in an intracellular compartment. In contrast, Asano *et al.* (1992) reported that replacement of the GLUT4 NH₂ terminus with that from GLUT1 did not alter the subcellular distribution of the protein. In these studies the dominant targeting domains were localized to a region spanning *trans*-membrane

domains 7 and 8. This discrepancy emphasizes the potential pitfalls in studying the targeting of a complex protein such as the glucose transporter which is thought to have 12 membrane spanning domains and three hydrophilic cytosolic domains (Mueckler *et al.*, 1985).

Piper *et al.* (1993) have used a different strategy to further study the targeting role of the GLUT4 NH₂ terminus. The amino acid constituents of the GLUT4 NH₂ terminal targeting domain have been identified. GLUT4 constructs containing NH₂-terminal deletions or alanine substitutions within the NH₂ terminus were expressed in CHO cells using a Sindbis virus expression system. Deletion of eight amino acids from the GLUT4 NH₂ terminus or substituting alanine for phenylalanine at position 5 in GLUT4 resulted in a marked accumulation of the transporter at the plasma membrane. Mutation at other amino acids surrounding Phe5 also caused increased cell surface expression of GLUT4 but not to the same extent as the Phe5 mutation. GLUT4 was also localized to clathrin lattices and this colocalization was abolished when either the first 13 amino acids were deleted or when Phe5 was changed to alanine. They concluded that NH₂ terminus of GLUT4 contains a phenylalanine-based targeting motif that mediates intracellular sequestration at least in part by facilitating interaction of the transporter with endocytic machinery located at the cell surface.

1.9 EFFECT OF PAO ON TRAFFICKING OF GLUT1 AND GLUT4

Kinetic and immunocytochemical studies suggest that some trafficking of GLUT1 and GLUT4 occurs via a common pathway, but that GLUT4 can be excluded from the common pathway in the absence of insulin and is sequestered in a distinct vesicle pool. An approach to examining the possible separate processing of the two transporters is to inhibit their trafficking.

Phenylarsine oxide (PAO) is known to inhibit receptor endocytosis (Knutson *et al.*, 1986; Wiley *et al.*, 1982) and fluid-phase endocytosis in 3T3-L1 cells (Frost *et al.*, 1985). 1983, Knutson *et al.* have observed that phenylarsine oxide was an effective inhibitor of rapid insulin-induced internalization of cell-surface insulin receptors to a trypsin-resistant cell compartment. It was also found that this inhibitor has no effect on the recycling of internalized receptor to the cell surface when insulin was withdrawn. In contrast to these inhibitors of internalization, PAO has been shown to inhibit the insulin stimulation of glucose transport in 3T3-L1 cells and in adipocytes (Frost and Lane, 1985) and as discussed in section 1.8 this is probably an exocytotic process (Sato *et al.*, 1991).

1985, Frost and Lane have shown that insulin-activated deoxyglucose uptake by 3T3-L1 adipocytes is inhibited by phenylarsine oxide (20 μM) but the basal transport was not inhibited and this blocking is reversed by 2,3 -dimercaptopropanol but not mercaptoethanol. The inhibitory site is postreceptor because neither insulin binding to the receptor nor tyrosine kinase activity of the receptor (Frost and Lane, 1987; Bernier *et al.*, 1987) are affected by PAO. They have also shown that in the absence of insulin, low levels of PAO actually activated basal deoxyglucose uptake.

Douen and Jones (1988) have reported that PAO concentration from 1-10 μM can inhibit the stereospecific uptake of D-glucose in basal and insulin-stimulated rat adipocytes. The inhibition they observed was dose dependent and was partially reversed by dithiothreitol. At 1 and 5 μM PAO, recovery of transport activity is of the order of 90% after 20 min. At 10 μM PAO treatment, little or no recovery is observed.

1989, Gould *et al.* reported that at 10 μM PAO activates transport threefold, but at higher concentration an inhibition of transport is observed. Quantitative immunoblotting showed that the GLUT1 content of the plasma membrane fraction

increased with increasing PAO concentrations. The GLUT4 antibody was not available at this time.

1989, Frost *et al.*, using (^{14}C) sucrose as an endocytotic marker, found that phenylarsine oxide immediately blocked insulin-stimulated fluid phase endocytosis and exocytosis. Unlike the selective effect of PAO on insulin-stimulated glucose transport, PAO blocked both basal and insulin-stimulated endocytosis in an identical, concentration-dependent manner ($\text{Ki-}6\ \mu\text{M}$). PAO inhibited all of the specific endocytosis immediately upon addition to cells, even with prior exposure to insulin. This immediate effect contrasts with PAO-induced inhibition of insulin stimulated glucose transport, which is time dependent. They also studied the effect of PAO on exocytosis, and they reported that PAO reduced fluid efflux from both basal and insulin-treated cells by 50%. Thus while endocytosis was completely inhibited, exocytosis was only partially inhibited.

1.10 AIMS

The major aims of this thesis are listed below:

- 1) To determine the development of an intracellular pool of glucose transporters in 3T3-L1 cells by measuring 2-deoxy-D-glucose transport and to photolabel the cell surface and digitonin-permeabilized total cellular pool of glucose transporters.
- 2) To investigate the insulin-stimulation of glucose transport in 3T3-L1 adipocytes by measuring the glucose transport activity. To study the glucose transporters GLUT1 and GLUT4 trafficking by using the cell-impermeant, glucose transporter-specific, photoaffinity ligand 2-N-[4-(1-azitrifluoroethyl) benzoyl]-1,3-bis-(D-mannos-4-yloxy)-2-propylamine (ATB-BMPA). To examine the possibly separate processing of GLUT1 and GLUT4 by treating the cells with Phenylarsine oxide (PAO) and to determine the site of action by PAO by monitoring the appearance (exocytosis) and

loss (endocytosis) of these transporters.

3) To determine the dose response of insulin-stimulated translocation of GLUT1 and GLUT4 from different pH treated 3T3-L1 adipocytes by measuring 2-deoxy-D-glucose, using Western blotting and the ATB-BMPA photolabelling technique.

2.0 MATERIALS AND METHODS

2.1 GENERAL REAGENTS

Unless otherwise stated all standard laboratory reagents were obtained from BDH laboratory supplies (Poole, Dorset, UK), Sigma Chemical Co. (Poole, Dorset, UK) or Aldrich Chemical Co. Ltd (Gillingham, Kent, UK). All radioactive compounds were from Amersham International.

2.2 BUFFERS AND SOLUTIONS

Krebs Ringer Hepes Buffers (KRH) pH 7.4

136 mM NaCl

4.7 mM KCl

1.25 mM CaCl_2

1.25 mM MgSO_4

10 mM Hepes

Buffer stock solutions were prepared as 10x concentrated. Stored at 4°C and were replaced every 14 days.

Krebs Ringer Mes Buffers (KRM) pH 6.0

136 mM NaCl

4.7 mM KCl

1.25 mM CaCl_2

1.25 mM MgSO_4

10 mM MES

Phosphate buffered saline (PBS) pH 7.2

140 mM NaCl

2.7 mM KCl

1.5 mM KH_2HPO_4

8.1 mM Na_2HPO_4

Sodium phosphate buffer pH 7.2

5 mM Na_2HPO_4

TRIS-buffered saline (TBS) pH 7.4

154 mM NaCl (0.9%)

10 mM TRIS

TRIS/EDTA/sucrose buffer (TES) pH 7.2

10 mM TRIS

0.5 mM EDTA
255 mM sucrose

Continuous transfer buffer pH 8.8
39 mM glycine
48 mM TRIS
0.0375% (w/v) SDS
20% (v/v) methanol
In double distilled water

Electrophoresis stock reagents

30% (w/v) Acrylamide Stock
60 g acrylamide
1.6 g N'N methylene bis acrylamide
60 g sucrose
adjust volume to 200 ml with double distilled water

Resolving gel buffer pH 8.8
1.5 M TRIS
0.4% (w/v) SDS

Stacking gel buffer pH 6.8
0.5 M TRIS
0.4% (w/v) SDS

Electrophoresis buffer pH 8.3
25 mM TRIS
192 mM glycine
0.1% (w/v) SDS

Electrophoresis sample buffer
6 M urea
10% (w/v) SDS
10% (v/v) mercaptoethanol (added before use)

Preparation of Insulin Solution

Porcine monocomponent insulin was a gift from Dr. Ronald Eli Lilly's laboratories. A stock was prepared at 0.5 mg/ml. The final concentration is 100 μ M. 5 mg of insulin was first dissolved in 1 ml of 0.3 M hydrochloric acid (sterile) and the solution was then diluted to 10 ml with PBS (pH 7.2) and gently hand mixed to try to avoid air bubbles. The final concentration was 0.5 mg/ml (0.03 M hydrochloric acid) and the resulting insulin solution (100 μ M) was aliquoted into sterile eppendorf tubes and stored at -20°C until required. The solution was not refrozen if it had been thawed.

2.3 MURINE 3T3-L1 CELL CULTURE

2.3.1 Culture of 3T3-L1 fibroblasts

The cells used in these studies were Murine 3T3-L1 cell and these were obtained from the American tissue culture association. All cell culture was performed under sterile conditions. The 3T3-L1 cells were grown in Dulbecco Modified Eagle's medium (DMEM) (from Flow Labs) supplemented with 10% Newborn calf serum (NCS) - heat inactivated at 56°C for 30 Minutes, 100 U/ml penicillin, 100 µg/ml streptomycin and 2 mM glutamine (from Sterilin). Cultures were maintained in a humidified incubator at 37°C in an atmosphere of 10% CO₂ /90% air.

Cells were routinely seeded at a density of 0.1-0.2x10⁶ cells /175 cm² plastic flask and fed every 48 hours. The cells were allowed to reach 80-90% confluent. The cells were never allowed to become too confluent. Subconfluence was reached after 4-5 days and the cells were washed with phosphate buffered saline (PBS - NaCl 0.14 M, KCl 2.7 mM KH₂PO₄ 1.5 mM, Na₂HPO₄ 8.1 mM at pH 7.2). Cells were detached by incubation with 0.05% trypsin/0.02% EDTA (Flow labs) for 1 min at room temperature. When the cells started to detach the trypsin was taken off and 20 ml of medium was added to the flask. After washing by centrifugation (3 min. 1500 rpm) the cells were gently mixed using a 21 G needle attached to a 5 ml syringe. Cell counts were made using a Neubauer haemocytometer and using the viability indicating dye, trypan blue. The cells were then seeded in 0.03-0.08x10⁶/35 mm petri dishes with routine changes of the medium every 48 hours. The cells reached confluence at 5-7 days depending on cell density. If seeded at a high density the cells reached confluence more quickly.

2.3.2 3T3-L1 cell differentiation

The differentiation procedure was carried out after the fibroblast 3T3-L1 cells attained full confluence for 2 days. To induce differentiation, monolayers were maintained in DMEM + 10% fetal calf serum, 100 unit/ml penicillin, 100 mg/ml streptomycin, 2 mM glutamine and were treated for 48 hours with isobutylmethylxanthine (IBMX) (0.55 mM), dexamethasone (0.25 μ M), insulin (0.2 μ M) and then insulin (0.2 μ M) alone for another 48 hours. The medium then was replaced with fresh medium every 48 hours. The cells reached full differentiation on day 8 and during days 8-12 the glucose transport response to insulin reached a steady state so usually experiments were carried out at this time.

The insulin stock was 0.5 mg/ml and was diluted 500 times to 1.0 μ g/ml. (100 ml medium plus 200 μ l stock). The dexamethasone stock was 2.5 mM in ethanol and was then diluted 20 times with medium (200 μ l of solution were diluted into 100 ml medium). The isobutylmethylxanthine was prepared freshly each time. 10-20 mg was dissolved first in 3.5 mM KOH (24 mg IBMX /50 μ l KOH) and then diluted 8 times with medium (200 μ l were diluted in 100 ml medium).

2.3.3 Storing 3T3-L1 cells

Cells from early passages were trypsinised, washed and resuspended at a density of 0.5×10^6 cells/ml in culture medium with 10% NCS and 10% Dimethylsulphoxide (DMSO). After slow cooling overnight at -70°C in sterile Cryotubes (NUNC), the cells were transferred to liquid nitrogen for storage.

High passages number cells have less ability to differentiate, so in the studies described in this thesis, cell passage number was always kept under Passage 10. When required, the low passage cells were rapidly defrosted at 37°C and washed

immediately in 20 ml culture medium before plating out as usual.

2.4 PROTEIN DETERMINATION

Protein was either estimated using the protein-dye (BIO-RAD) assay based on the Coomassie Brilliant Blue dye-binding method of Bradford (1976) or the bicinchonic acid (BCA) protein assay according to the manufacturer's instruction.

The Bio-rad protein assay used a standard curve of 0-15 μg BSA in 775 μl 5 mM sodium phosphate buffer, pH 7.2. Membrane proteins were solubilized by the addition of 25 μl sodium hydroxide (0.1 M) and the colour was developed by 10 minutes incubation at room temperature with 200 μl Biorad solution. Absorbance was measured at 595 nm in a spectrophotometer.

The BCA protein assay was carried out in microtitre plates. 10 ml of reagent A {containing 1% BCA detection reagent (bicinchoninc acid, sodium salt, pierce); 2% disodium carbonate; 0.16% sodium tartrate; 0.4% sodium hydroxide; 0.95% hydroxide and filtered through a 0.7 μm filter (Millipore)} was mixed with 200 μl of reagent B {containing 4% copper sulphate, filtered through a 0.7 μm filter (Millipore)}. 100 μl of standard bovine serum albumin (BSA) solution (2 mg/ml in double-distilled water) was mixed with 100 μl of 0.2 M sodium hydroxide. For the standard protein curve, 0, 2, 4, 6, 8, and 10 μl of this solution was made to 10 μl with 0.1 M sodium hydroxide. 200 μl of reagent A and B solution (containing reagent A 10 ml and reagent B 200 μl) was added to the standard protein and samples and incubated in 37°C for 30 minutes. The absorbance was measured at 450 nm and 540 nm in a microtitre plate reader.

2.5 PREPARATION OF ALKALI-STRIPPED ERYTHROCYTE MEMBRANES (PROTEIN DEPLETED)

Erythrocytes from 1-3 week old transfusion blood were washed four times in PBS (154 mM NaCl, 12.5 mM sodium phosphate, pH 7.2) at 0-4°C. When aspirating off the supernatant care was taken to remove the white cells and platelets. To obtain erythrocyte membranes ghosts, the cells were lysed for 20 minutes at 0-4°C in haemolysis buffer (5 mM sodium phosphate, 1 mM EDTA, 1 µg/ml PMSF, pH 7.8). The membranes were centrifuged at 16000 g_{av} (11000 revs GSA Rotor) for 20 minutes. The pellets were resuspended and washed once in haemolysis buffer then once in 5 mM sodium phosphate buffer pH 7.2. The ghosts were then washed once in 5 mM sodium phosphate buffer pH 7.8 at 16000 g for 20 minutes and resuspended in this buffer to give a protein concentration about 4 mg/ml (BCA protein assay). The membranes then treated with 5 volumes of freshly prepared solution containing 15.4 mM NaOH, 2 mM EDTA, 0.2 mM DTT for 15 minutes at 4°. The membranes were harvested at 16000 g_{av} for 20 minutes at 4°C and resuspended in Tris-HCL buffer (pH 6.8), then spun again once. The protein concentration was determined by BCA protein assay and the membranes stored at 4 mg/ml in aliquots at -70°C (Gorga and Lienhard, 1981).

2.6 PREPARATION OF ANTIBODIES

Anti-GLUT1 and GLUT4 antibodies were kindly prepared by Dr. Avril, E. Clark (University of Bath, Department of Biochemistry).

Antisera against the GLUT1 and GLUT4 glucose transporter isoforms were prepared using synthetic C-terminal peptides. EELFHPLGADSQV and STELEYLGPDEND, respectively, as described by Davies *et al.* (1987). The anti-GLUT1 antibody was affinity purified using alkali-stripped erythrocyte membranes

(Schroer *et al.*, 1986). Human erythrocyte membranes were stripped of peripheral proteins by alkaline treatment. Antiserum (4 ml) was mixed with the membranes (32 ml at 2 mg/ml protein) in 10 mM NaCl (pH 7.4). After incubation for 1 hour, the membranes were pelleted at 48000 g_{max} for 10 min. The membranes were resuspended by homogenization in 40 ml of 10 mM sodium phosphate/800 mM NaCl (pH 7.4) and pelleted again. After a second wash in the same buffer, the membranes were resuspended in 32 ml of 200 mM glycine/82 mM HCl (pH 2.4) in order to release the bound antibodies. The membranes were pelleted, and the supernatant was quickly neutralized with 2 M Tris. The yield of affinity-purified antibodies was about 3.5 mg per ml of serum. These antibodies then were aliquoted and stored at -80°C .

The anti-GLUT4 antibody was affinity purified using a peptide column in a manner similar to that described by Oka *et al.* 1988. 2 ml of Reacti-gel (6x) (1,1-carbonyldiimidazole activated 6% cross-linked beaded agarose, Pierce) was filtered through Whatman 1 filter paper on a Buchner funnel under gentle suction and washed thoroughly with double-distilled water at $0-4^{\circ}\text{C}$ to remove any acetone. 5 mg of peptide (CSTELEYLGPDEND) was coupled to Reactigel-6x by rotation at $0-4^{\circ}\text{C}$ for 48 hours with 2 ml of gel matrix in 0.1 M sodium borate buffer, pH 8.5. (stirring was avoided as this would damage the beads).

The mixture was then filtered and the beads were added to 2 ml of 1.0 M ethanolamine in sodium borate buffer, pH 8.5 and mixed for 3 hours at room temperature. The beads were then added to the column (8 mm diameter x 50 mm length) and washed with 1 M sodium chloride, then double-distilled water and then PBS pH 7.2. 5 ml of antiserum was circulated three times through the column. The column was then successively washed in PBS, pH 7.2 and 2 M sodium chloride in 5 mM phosphate buffer pH 7.2. The antibody was eluted with 3.5 M sodium thiocyanate in 10 mM phosphate buffer, pH 6.6 and immediately dialyzed against phosphate-buffered saline for 18 hours. Finally, the sample was concentrated with

polyethylene glycol 4000 (PEG) then aliquoted and stored at -80°C. An ELISA was used to test the presence of specific antipeptide antibodies for both GLUT1 and GLUT4 at every stage of the purification.

2.7 ENZYME LINKED IMMUNOSORBANT ASSAY (ELISA)

An ELISA was used to confirm the presence of anti-GLUT1 and anti-GLUT4 peptide antibodies in serum samples from immunized rabbits.

96 well ELISA plates (Titertek-Flow) were used. For assaying anti-GLUT1 antibodies, wells were coated with erythrocyte protein depleted membranes (1 μ g in 100 μ l of 50 mM sodium hydrogen carbonate buffer, pH 9.6 per well) overnight at 4°C. For assaying anti-GLUT4 antibodies, wells were coated in GLUT4 peptide (20 ng in 100 μ l of 50 mM sodium hydrogen carbonate buffer pH 9.6 per well) overnight at 4°C.

Unoccupied protein binding sites were blocked by washing three times with 100 μ l of blocking buffer (1% casein, 0.05% tween 20 [polyoxyethylene-sorbitan monolaurate, Sigma] in PBS pH 7.2). Each incubation was for 10 minutes at room temperature. Antiserum was diluted 1:100 in blocking buffer. 100 μ l of antiserum was added to each incubation well for 2 hours at 37°C. Unbound antisera was removed by washing three times with 100 μ l of blocking buffer for 10 min each time.

100 μ l of a 1:2000 dilution of Goat anti-rabbit peroxidase conjugate (Sigma) in blocking buffer was incubated in the wells for 2 hours at 37°C. All horse radish peroxidase conjugated antibodies (Sigma) were diluted 1:2 with glycerol on receipt, to allow prolonged storage at -20°C without freezing. Excess conjugate was removed by three times 10 min washes with a substrate containing 100 μ l PBS, 0.05% Tween 20, pH 7.2 and then 1% 35'55 tetramethyl benzene (TMB) in DMSO which was

diluted 1:100 in 100nM acetate citrate buffer (pH 6.0). Hydrogen peroxide was added at $>3 \mu\text{l}/20 \text{ ml}$. $100 \mu\text{l}$ of this freshly prepared substrate was added to each well. After 15-20 min a bright blue colour developed. $100 \mu\text{l}$ of 2 M H_2SO_4 were added and the resulting bright yellow colour was read on a Titertex multiscan plate reader, using a dual beam. Substrate absorbance was measured at 450 nm. A reading was made at 695 nm and was used to correct for any optical differences in the polystyrene wells. Absorbance values were corrected for the non-specific binding of conjugates to the plastic wells, by including a control to which no antiserum was added.

2.8 MEASUREMENT OF 2-DEOXYGLUCOSE UPTAKE IN 3T3-L1 CELLS

2.8.1 Measurement of insulin stimulation

2-deoxy-D-glucose was used to measure glucose transport activity. The cold 2-deoxy-D-glucose was prepared in 2 mM stock and kept at -20°C . The final concentration for each assay was $50 \mu\text{M}$. The 2-deoxy-(2,6- ^3H)-D-glucose activity was $0.3 \mu\text{Ci}/\text{sample}$ [$25 \mu\text{l}$ of cold 2-deoxy-D-glucose (2 mM stock) plus $0.3 \mu\text{l}$ ($1 \mu\text{Ci}=1 \mu\text{l}$) of 2-deoxy-(2,6- ^3H)-D-glucose plus $24.7 \mu\text{l}$ KRH buffer]. The monolayer fibroblasts or fully differentiated 3T3-L1 cells were washed twice with warm PBS, seeded in serum free DMEM medium for 2 hours and then washed three times with 2 ml KRH buffer pH 7.4 (or pH 8.0, pH 6.5, for detail see figure legends) at 37°C or 27°C (for detail see figure legends). Incubation was with or without insulin (usually 100 nM) for 30 minutes or the indicated time in 1 ml of KRH buffer at 37°C or 27°C . $50 \mu\text{l}$ of labelled 2-deoxy-D-glucose was added in the 1 ml buffer for 5 minutes and then the cells were rapidly washed four times in 2 ml of KRH buffer at room temperature or in some experiments at 4°C . Monolayers were then solubilized with 1 ml of 0.1 M NaOH. In some experiments a small aliquot was removed for a protein assay. The radioactivity was counted in an LKB counter. The

results were expressed in terms of pmoles/min/35 mm dish or pmoles/min/ 10^6 cells.

2.8.2 Measurement of reversal of insulin stimulation

Cell monolayers were stimulated with 100 nM insulin at 37°C for 30 min. The insulin stimulation was then reversed by washing cell monolayers twice with a MES buffer (136 mM NaCl, 4.7 mM KCl, 1.25 mM MgSO₄, 1.25 mM CaCl₂, 10 mM MES pH 6.0) and then maintaining them in this buffer at 37°C. At the times indicated in the figure legends the dishes were washed twice in KRH at 18°C and then either used for 2-deoxy-D-glucose uptake determinations (as above) or in cell-surface photolabelling experiments.

2.9 MEASUREMENT OF INSULIN BINDING

3T3-L1 adipocytes in 35 mm dishes were incubated in serum-free DMEM for 2 hours, washed three times in KRH buffer and incubated at 20°C in 1 ml of KRH buffer containing 30 fmol of mono-A14-¹²⁵I-insulin, 2% serum albumin, bacitracin (10 mg/ml), 5 μM of unlabelled insulin were added to 2 control dishes. 0.025, 0.05, 0.1, 1 and 100 nM unlabelled insulin were added to the other dishes. The dishes were shaken (65 oscillations/min) for 3 hours. After washing three times in KRH buffer, 1 ml of ice-cold 10% trichloroacetic acid was added and the insoluble protein was precipitated and counted for radioactivity. Specific ¹²⁵I-insulin binding was calculated as the difference between the samples with 5 μM unlabelled insulin added and the other different concentrations of insulin.

2.10 PHOTOLABELLING WITH ATB-BMPA

2.10.1 Preparation of ATB-[2-³H]-BMPA

The ATB-[2-³H]-BMPA was prepared from (2-³H) BMPA and 1-azi-2.2.2-trifluoroethyl-benzoic acid by Dr.G.D.Holman as previously described (Clark and Holman, 1990).

ATB-(2-³H) BMPA had a specific activity of 10 Ci/mmol and was stored at -20°C in PBS in the dark at a concentration of 0.5 mM (5 mCi/ml).

2.10.2 Cell surface photolabelling

Plates of the 3T3-L1 cells (35 mm) were washed in KRH buffer pH 7.4 (some experiments used pH 8.0 or pH 6.5 buffer, see Figure legends) and incubated in 1 ml of this buffer at 37°C in the presence or absence of insulin (100 nM) for 30 minutes. Under these conditions the full stimulation of hexose transport occurs. Following this stimulation, the cells were washed quickly with KRH buffer at 18°C and then incubated with 250 μ l of KRH buffer contain 100 μ Ci of (2-³H) ATB-BMPA (about 160 μ M) and 100 nM of insulin for 3 minutes at 18°C. The dishes were then irradiated at 18°C for 1 min in the presence of 100 μ Ci of ATB-[2-³H]-BMPA on a wire shelf placed 5 cm from the bottom in a Rayonet RPR-100 reactor with RPR-3000A lamps turned on its side (most experiments used 300 nm lights. In the studies of comparison of GLUT1 and GLUT4 subcellular trafficking in basal and insulin-stimulated 3T3-L1 cells the irradiation was used half 300 nm and half 350 nm lights. The irradiated cells were washed four times in KRH buffer.

2.10.3 Total cellular pool photolabelling

To photolabel the total cellular transport pool, cells were permeabilized by treatment with 0.025 % (wt/vol) digitonin for 8 minutes at 18°C in the presence of 100 μ Ci of ATB-(2-³H)BMPA. The digitonin used (Sigma D1407 and suitable for use in aqueous solution) was 50% pure and an allowance for this was made in preparing the digitonin solution. The digitonin was dissolved in KRH buffer. The other procedures were the same as cell surface labelling.

2.10.4 Immunoprecipitation of ATB-BMPA labelled proteins

Photolabelled proteins, either from solubilized cells or from crude plasma membranes, or crude light-microsome fractions (see 2.11), were immunoprecipitated with rabbit antisera raised against GLUT1 or GLUT4 antibodies. Preimmune rabbit serum was used in some experiments for a control.

The pellets of washed photolabelled cells, crude plasma membrane or light-microsome fractions were solubilized for 20 min on ice in 1.5 ml of 5 mM sodium phosphate buffer (pH 7.2) containing 2% nonaethylene glycol dodecyl ether (C₁₂E₉) detergent (Boehringer Mannheim) and the proteinase inhibitors pepstain A, leupeptin, antipain and aprotinin each at 1 μ g/ml. Following centrifugation at 20,000 g_{max} for 20 min the supernatant was carefully separated from unsolubilized pellet and the insoluble fat-cake and the supernatant were subjected to immunoprecipitation to determine the amounts of photolabelled GLUT1 and GLUT4 transporter.

For each immunoprecipitation, 7 mg of protein A-Sepharose (Sigma) were coupled with 100 μ l of anti-GLUT1 and 5 mg of protein A-Sepharose were coupled with 50 μ l of anti-GLUT4 antiserum. The solubilized material from the supernatants was incubated with the protein A-sepharose antibody-complex (GLUT4) for 1½

hours by rotation at 4°C. The protein A-sepharose immunoprecipitates were pelleted by low speed centrifugation. The supernatant from this low speed centrifugation was then incubated with the protein A-sepharose antibody-complex (GLUT1) for one 1½ hours by rotation at 4°C (in some experiments, the GLUT1 was immunoprecipitation first).

The protein A-sepharose immunoprecipitates were washed three times with 1.0% and once in 0.1% C₁₂E₉ detergent buffer (5 mM Sodium phosphate buffer pH 7.2 with proteinase inhibitors pepstain A, leupeptin, antipain and aprotinin each at 1 µg/ml). In studies of the comparison of GLUT1 and GLUT4 subcellular trafficking in basal and insulin-stimulated 3T3-L1 adipocytes (see results 3.6), the immunoprecipitates from tracer-tagged GLUT1 and GLUT4 in the basal state were washed five times with 1.0% and once in 0.1% C₁₂E₉ detergent buffer and in insulin-stimulated states were washed four times with 1.0% and once in 0.1% C₁₂E₉ detergent buffer.

The labelled glucose transporters were released from the antibody complexes with 10% SDS, 6 M Urea, 10% mercaptoethanol electrophoresis sample buffer and subjected to electrophoresis.

2.11 CELL FRACTIONATION

2.11.1 Preparation of crude plasma membrane

The procedures used for the preparation of the fraction by homogenization with TES buffer were described by McKeel *et al.*, (1970). For each condition two 35 mm dishes of fully insulin-stimulated or basal state 3T3-L1 adipocytes were photolabelled with 100 µCi each of ATB-[2-³H]-BMPA. In the studies of comparison of GLUT1 and GLUT4 subcellular trafficking 500 µCi were used in the basal state,

and in the insulin stimulated state 250 μCi was used. The labelling was carried out with the lids on the 35 mm dishes so that radiation damage of the cells was minimized. Some experiments used half 300 nm and half 350 nm lights and with 2 mm glass plates to protect the cells. Following four washes of the dishes in KRH buffer to remove excess label, the cells were incubated at 37°C for the indicated times. The cells from each dish were scraped into 0.5 ml for each dish of TES buffer (255 mM sucrose, 10 mM Tris hydrochloride and 0.5 mM EDTA, pH 7.2). The pooled material from the two dishes was then homogenised at 900 rpm in a 2 ml tight-fitting teflon homogeniser (clearance ≈ 0.15 mm) with 10-15 complete strokes. The homogenate was then centrifuged at 20,000 g_{max} for 20 min (in studies of comparison of GLUT1 and GLUT4 subcellular trafficking in basal and insulin-stimulated 3T3-L1 cells, the samples was centrifuged at 12,500 g_{max} for 20 min). The pellet, containing the crude plasma membrane fraction, was dissolved in 0.5 ml of 6% C₁₂E₉ detergent buffer and diluted with 1 ml 5 mM sodium phosphate buffer. The 20,000 g_{max} supernatant from above, containing the crude light microsome fraction, was mixed with 0.5 ml of 6% C₁₂E₉ detergent buffer. Both detergent solubilized samples were kept at 0-4°C for 30 min and then re-centrifuged at 20,000 g_{max} for 20 min. The supernatants were then subjected to immunoprecipitation with anti-GLUT1 and anti-GLUT4 antibodies. In some experiments cells were homogenised in a KCl buffer (150 mM KCl, 2 mM MgCl₂, 20 mM Hepes, pH 7.4) and 16,000 g_{max} plasma membrane and supernatant fractions were isolated as described by Brown *et al.*, (1988). The results obtained were the same as those obtained using the TES buffer.

2.11.2 Preparation of purified plasma membrane

To prepare purified plasma membrane of 3T3-L1 adipocytes, four 35 mm dishes of cells were washed and incubated in different pHs (pH 7.4, pH 8.0 and pH 6.5) KRH buffer and treated with zero, 0.025, 0.05, 0.1, 1 and 100 nM insulin at

37°C for 30 min. The cells from each dish were scraped into 0.5 ml for each dish of TES buffer (255 mM sucrose, 10 mM Tris hydrochloride 0.5 mM EDTA, pH 7.2). The pooled material from the four dishes were then homogenised at 900 rpm in a 2 ml tight-fitting teflon homogeniser (clearance \approx 0.15 mm) with 10 complete strokes. The homogenate was then centrifuged at 15,000 rpm for 20 min. The pellet, containing the crude plasma membrane fraction, was re-homogenized in 300 μ l of TES buffer and then centrifuged at 15,000 rpm for 20 min. The pellet was re-homogenized in 150 μ l of TES buffer and then layered on top of the sucrose cushion (0.6 ml, containing 1.12 M sucrose, 20 mM TRIS, 1 mM EDTA, pH 7.2) and then centrifuged at 35,000 rpm for 20 min. The supernatant was gently taken off, made up to 3ml volume with TES buffer and then centrifuged in 37,000 rpm for 9 min. The pellet was re-homogenized in 300 μ l of TES buffer, made up to 3ml with TES buffer and centrifuged at 37,000 rpm for 9 min. The 100 μ l of TES buffer was added to the pellet (containing the purified plasma membrane) and protein was measured by the BCA method.

2.12 SODIUM DODECYL SULPHATE-POLYACRYLAMIDE GEL ELECTROPHORESIS (SDS-PAGE)

Proteins either from membrane preparations or immunoprecipitates were analysed by SDS-PAGE using the protean II gel system (Bio-Rad).

SDS-PAGE was carried out as described by Laemmli (1970). The gel were run in the Laemmli discontinuous buffer system. Gels were prepared from stock solutions. 10% acrylamide resolving gels (Tris 1.5 M, SDS 0.4%, pH 8.8) were used, with stacking gels containing 3.7% acrylamide (Tris 0.5 M, SDS 0.4%, pH 6.8). The gel was polymerised chemically by the addition of 0.6 μ l/ml N, N, N'.N',tetramethylethylene-diamine (TEMED) and 6 μ l/ml of a 10% solution of ammonium persulphate. The poured gel was overlaid with a layer of water-saturated

butanol and left to polymerize (\approx 1 hour). Following removal of the butanol, the resolving gel was overlaid with a stacking gel and allowed to polymerize for about half hour.

Electrophoresis was generally carried out overnight at 25 mA for a 3 mm gel or at 12.5 mA for a 1.5 mm gel in buffer containing 25 mM TRIS, 192 mM glycine and 0.1% SDS (pH 8.3).

The protein samples were solubilized at room temperature for 20 minutes in 6 M urea sample buffer (10% SDS, 6 M urea, 5% 5-bromophenyl-1% blue) 180 μ l sample buffer were added to each sample and subjected to electrophoresis using 16 cm x 3 mm gels with 2.5 cm wide sample wells in the stacking gel.

The gels were stained with 0.2% Coomassie Blue in destain and then destained in 10% acetic acid, 30% methanol, 60% distilled water for 2 hours and then sliced. The slices (in scintillation vials) where dried at 80°C for 2-3 hours and were then dissolved in 0.5 ml of alkaline hydrogen peroxide at 80°C for a further 2 hours. Scintillant was added and the radioactivity counted. The positions of the photolabelled peaks were compared with the positions of molecular weight markers (Sigma) in adjacent lanes. Molecular weight marker proteins (Sigma): Myosin 205 kDa, β -galactosidase 116 kDa, Phosphorylase 97 kDa, Bovine serum albumin 66 kDa, Ovalbumin 45 kDa and Carbonic anhydrase 29 kDa. The variations of labelled peak positions relative to the slice numbers, which are shown in the figures, occurs because of variations in the total migration distance allowed. The levels of radioactivity associated with each peak were obtained by summing the radioactivity in all the slices under the peak and subtracting a background radioactivity based on the average radioactivity of the slices on either side of the peak.

2.13 WESTERN BLOTTING

2.13.1 Electrophoretic transfer of proteins to nitrocellulose

For analysis of proteins by Western blotting, samples were subjected to electrophoresis on 1.5 mm thick gels with 10-50 μg of protein per lane and transferred to nitrocellulose paper (Gelman Sciences pore size 0.4 μm) using semi-dry transfer methods.

The 1.5 mm thick SDS-polyacrylamide stacking gel was removed and the resolving gel was put in continuous transfer buffer (39 mM glycine, 48 mM Tris, 0.0375% w/v SDS, 20% methanol, pH 8.8). Proteins were transferred using a Multiphor II NovaBlot electrophoretic transfer method which involved soaking sheets of filter paper, nitrocellulose sheets and the gel in the continuous transfer buffer and then layering them on the anode electrode (presoaked in distilled water).

1 transfer unit consisted of 9 sheets of filter paper, the nitrocellulose (Biotrace, Gelman Sciences), the resolving gel and then an additional 9 sheets of filter paper. The cathode electrode (presoaked in distilled water) was then placed on the top and a current applied (0.8 x trans unit area, mA) for 1 hour and 45 minutes.

Care was taken to cut all the sheets to the same size, to soak the sheets evenly and to remove all the trapped air bubbles when layering the sheets together.

2.13.2 Staining nitrocellulose filters for total protein

When the transfer was finished, the nitrocellulose was washed in distilled water and the protein was temporarily stained in Ponceau S (0.1 Ponceau S in 3% trichloroacetic acid). If the protein had transferred well the band could be seen very

clearly. Then, the sheets were cut to the required size. The nitrocellulose was washed twice in blocking buffer containing 3% bovine serum albumin (BSA), 0.2% Tween 20, in TBS buffer (10 mM Tris, 0.9% sodium chloride, pH 7.4) to remove the Ponceau S and then was incubated in blocking buffer overnight at 0-4°C.

Pre-stained molecular weight marker proteins with weights of about 116 and 29 kDa were included on the polyacrylamide gel. When the temporary stain was removed, these could be seen as blue bands on the nitrocellulose paper. The position of transferred protein can thus also be identified by pre-stained molecular weight marker proteins.

2.13.3 Immunoblotting of nitrocellulose-bound protein

This method was based on the protocol used by Dr. S. Cushman and co-workers (personal communication). Nitrocellulose filters were blocked for 1 hour with TBS containing 3% (w/v) BSA in shaker. The nitrocellulose filters were incubated with antisera (1:200 dilution in 1% BSA, 0.2% Tween 20, TBS buffer) for 2 hours at room temperature in shaker, then washed for 5 minutes three times and once for 15 minutes with 50 ml of this buffer.

^{125}I -labelled Protein A (Amersham) was then added at 0.1 $\mu\text{Ci/ml}$ in TBS/Tween for 2 hours at room temperature in a shaker. Then the nitrocellulose was washed at least six times. Every wash was 5 minutes in 50 ml TBS/Tween. The nitrocellulose was air-dried and wrapped in cling-film and then exposed to x-ray film (from Amersham International) for 24-72 hours at -70°C. The glucose transporter band was then cut out of the nitrocellulose using the prestained standards as a reference as these always gave a band with ^{125}I -Protein A and counted in a Gamma counter (see "Results" part III). A background count was obtained from nitrocellulose which was the same size and was cut from above and below the glucose

transporter band. This was subtracted to get the glucose transporter-specific counts.

3.0 RESULTS

PART I BACKGROUND STUDIES

3.1 MORPHOLOGY OF MURINE 3T3-L1 CELLS

Unlike most other cell lines the mammalian fibroblast line 3T3 stop growing when they reach a confluent monolayer and remain viable in a resting state for long periods (Todaro and Green, 1963).

The murine 3T3 fibroblasts convert to adipose cells under defined culture conditions. This conversion is a cellular differentiation which occurs after the cells stop growing, at which time there is an increased incorporation of fatty acid precursors into triglycerides (Russell and Ho, 1976). The mature adipocytes do not divide (Russell and Ho, 1976).

3.1.1 3T3-L1 fibroblasts

Fig.7a shows the picture of pre-confluent 3T3-L1 fibroblasts. The cells were seeded at 0.1×10^6 per 175 cm² flask. Most cells are elongated in shape and at this stage the cells are almost unresponsive to insulin. After about one week from seeding, the cells in the flask became subconfluent and were reseeded at $0.03\text{-}0.05 \times 10^6$ cells per 35 mm dishes. In about 5 days the cells became fully confluent and reached a monolayer. More than 90% of the cells were round at this stage and the cells remained viable in a resting state for long periods (Fig.7b). If cells stay as a confluent monolayer for a long time (more than about 3 weeks), some fibroblasts will start to differentiate to adipocytes even without treating the cells with IBMX, insulin and dexamethasone.

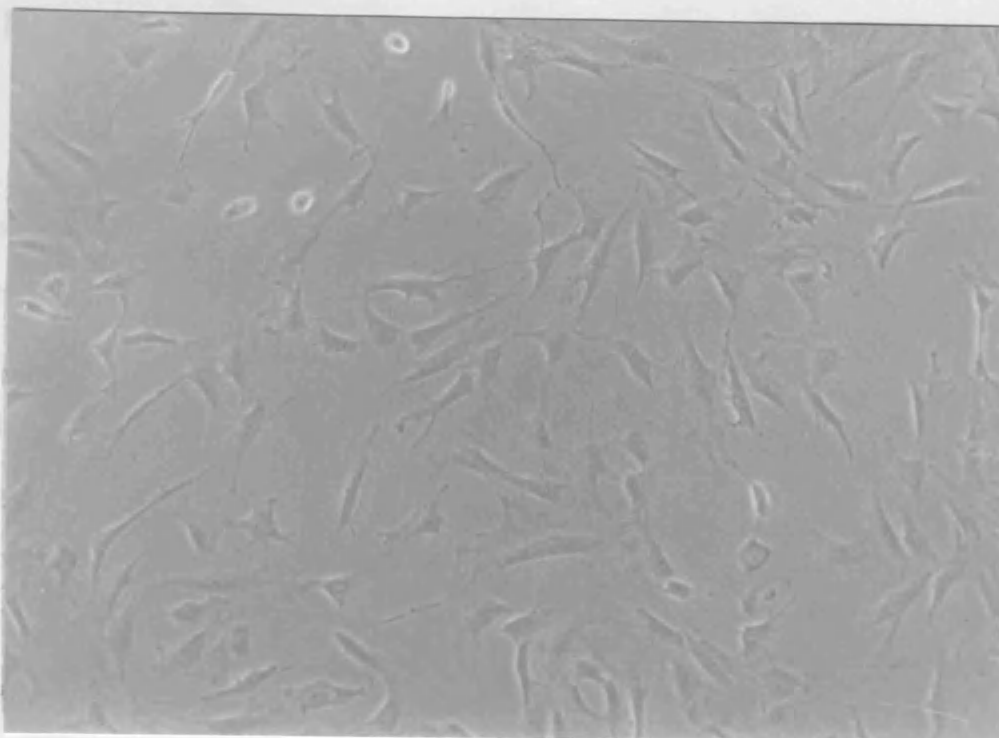


Fig.7a Light micrographs of preconfluent 3T3-L1 fibroblasts
Most cells are isolated and elongated in shape. Magnification x1000.

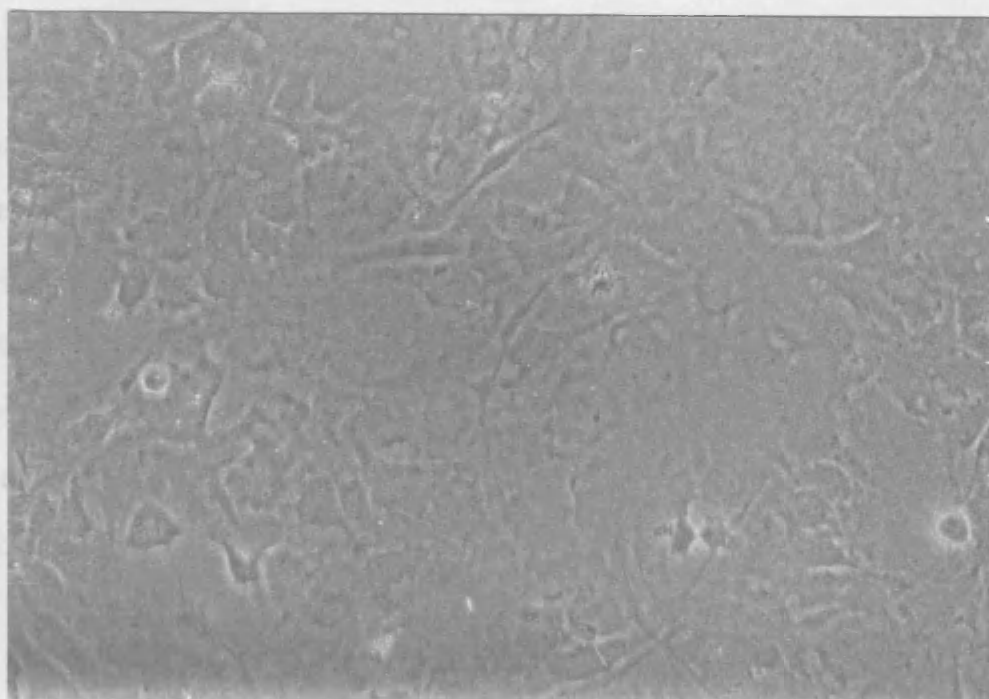


Fig.7b Light micrographs of fully confluent fibroblasts.
The majority of cells are rounded or triangular in shape. The cells are firmly attached to each other. Magnification x3000.

3.1.2 3T3-L1 adipocytes

The fibroblasts are fully confluent after about 2-4 days. In most studies cells were left for 10 days before differentiation. The IBMX, insulin and dexamethasone were added for 48 hours and insulin alone was then added for a further 48 hours. At this stage a dramatic change occurred (Fig. 8a and 8b). Numerous clusters of adipose cells develop. Cells begin to accumulate multiple fat droplets and the cells come to resemble brown adipose cells; later, the droplets fuse to make a single large central droplet surrounded by a thin rim of cytoplasm and an eccentric nucleus, giving the cells a typical signet ring appearance resembling that of white adipose cells. (Fig.9).

3.2 INSULIN STIMULATION OF GLUCOSE TRANSPORT AND ATB-BMPA LABELLING THE CELL SURFACE GLUT1 AND GLUT4

3.2.1. Determination of anti-GLUT1 and GLUT4 antibody levels by ELISA

The rabbit antiserum to the purified human erythrocyte glucose transporter has been described by Lienhard *et al.* (1982). This serum has previously been shown to contain antibodies against the erythrocyte transporter by two criteria (Lienhard *et al.*, 1984). First, these antibodies bind to a polypeptide of average Mr 55000 on immunoblots of erythrocyte proteins. Second, they immunoprecipitate the transporter polypeptide from a detergent-solubilized mixture of erythrocyte membrane proteins, as determined by assay for the removal of a specific transporter function (D-glucose-inhibitable cytochalasin B binding).

To determine if anti-GLUT1 and anti-GLUT4 antibody were present in antiserum, an enzyme linked immunosorbent assay (ELISA) was carried out as described in Materials and Methods.

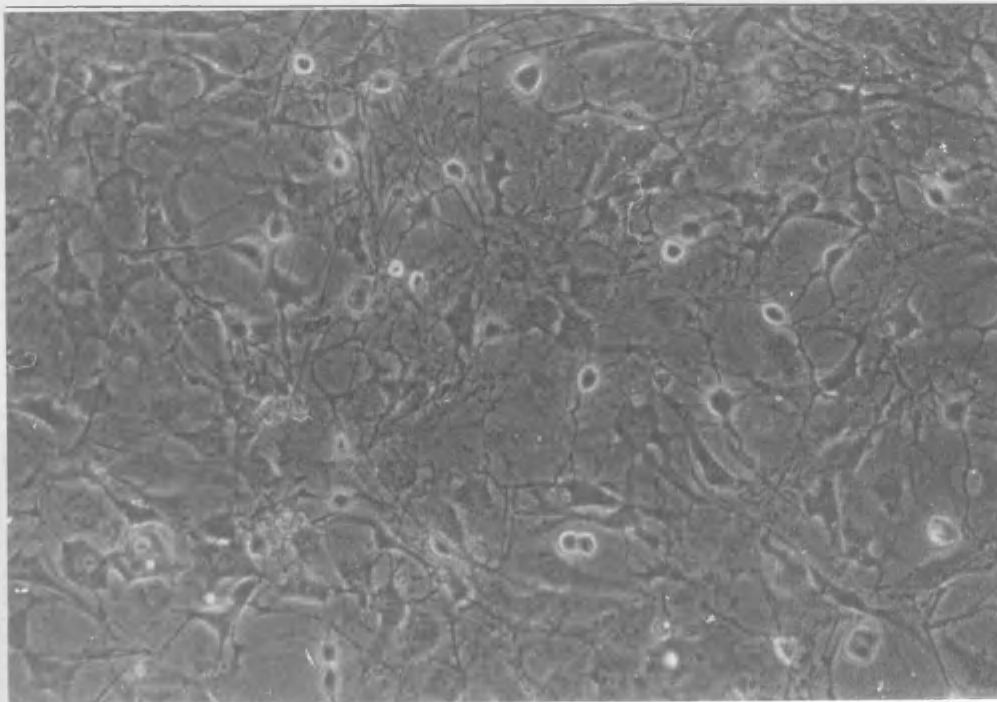


Fig. 8a Light micrographs of day 2 differentiated 3T3-L1 cells.
Some fat droplets developed. Magnification x3000.

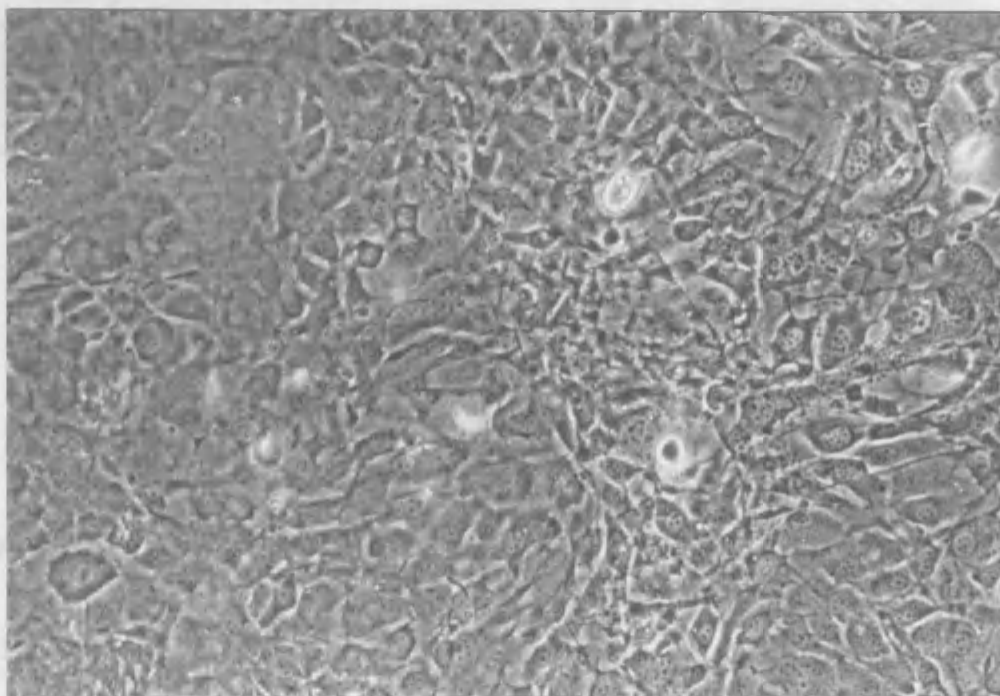


Fig. 8b Light micrographs of day 4 differentiated 3T3-L1 cells.
Numerous clusters of adipose cells developed. Magnification x3000.

Rabbit serum samples (rabbits were immunized with the carboxy-terminal peptide) were assayed using an ELISA. Antiserum from rabbit 17 (as record number), obtained 9 weeks after immunization, was assayed in an ELISA using erythrocyte protein depleted membranes as an antigen and as shown in Fig 10. At a 1:100 dilution the anti-peptide serum showed about a 75% increase in binding over that detected in the preimmune serum.

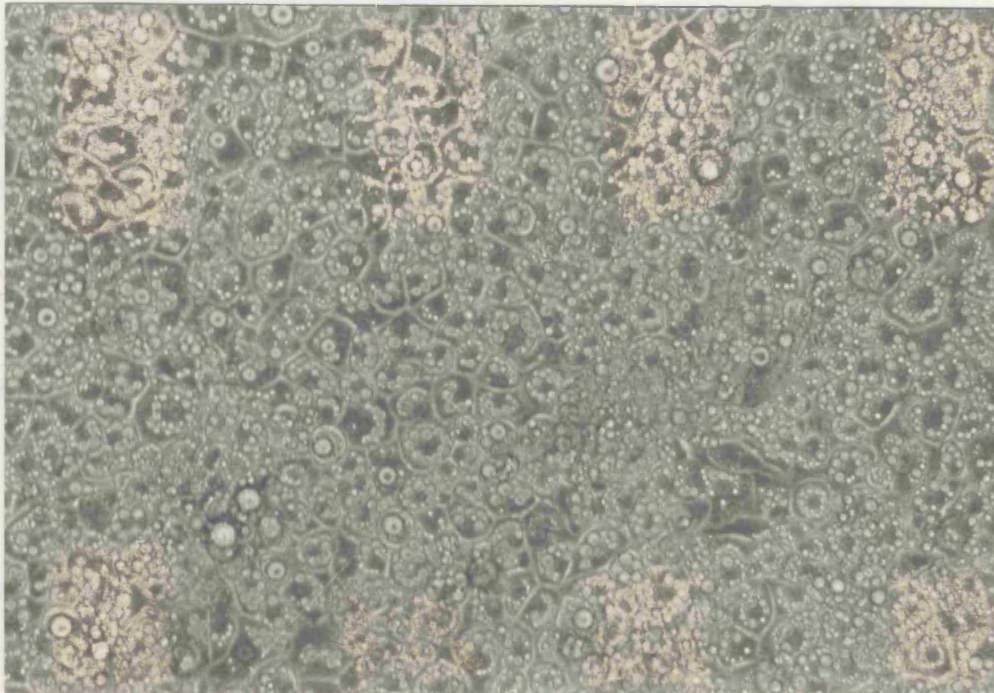


Fig. 9 Light micrographs of fully differentiated (day 10) 3T3-L1 adipocytes.

Most fat droplets fuse to become a single large droplet. Magnification x3000.

Rabbit serum samples (rabbits were immunized with the carboxy-terminal peptide) were assayed using an ELISA. Antiserum from rabbit 17 (as record number), obtained 9 weeks after immunization, was assayed in an ELISA using erythrocyte protein depleted membranes as an antigen and as shown in Fig.10. At a 1:100 dilution the anti-peptide serum showed about a 75% increase in binding over that detected in the preimmune serum.

A comparison of the binding of serum from rabbit 16 taken at week 9 is also shown at Fig.10. At a 1:100 dilution the anti-peptide serum showed about a 60% increase in binding over that detected in the preimmune serum.

The anti-serum from rabbit 17 taken at week 9 was chosen for experiments because this rabbit produced good anti-GLUT1 antibody.

Fig.11. shows antiserum from rabbit 13 which was taken at week 9 after immunization and was assayed in an ELISA using a synthetic C-terminal peptide as an antigen for GLUT4. At a 1:100 dilution the anti-peptide serum showed an about 90% increase in binding over that detected in the preimmune serum. This indicated that rabbit 13 after immunization for 9 weeks produced very good anti-GLUT4 antibody.

3.2.2. Insulin dose-response.

To obtain the maximal transport rate after 3T3-L1 adipocytes were exposed to insulin (i.e. the ability of the 3T3-L1 adipocytes to respond to a maximal dose of insulin), the uptake of 2-deoxy-D-glucose was carried out at 37°C using different concentrations of insulin. Fig.12 shows that after 3T3-L1 adipocytes were incubated with different concentration of insulin for 30 minutes at 37°C, 50 μ M 2-deoxy-D-glucose was taken up at 37°C for 5 minutes (the radioactivity 0.3 μ Ci/dish). The

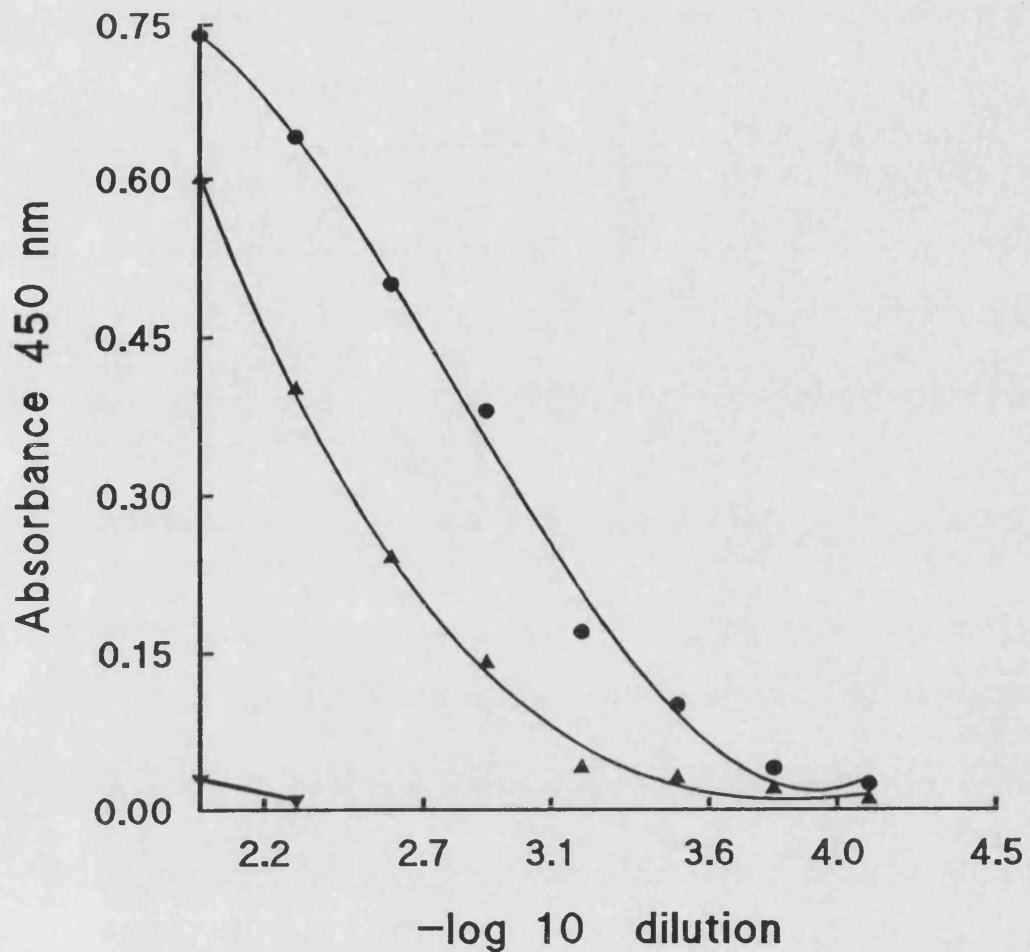


Fig.10 Testing the anti-GLUT1 antiserum with ELISA.

ELISA 96 well plates were coated with erythrocyte protein depleted membrane at $1 \mu\text{g}/\text{well}$. Unoccupied protein binding sites were blocked. The plates were incubated with anti-GLUT1 antiserum (1:100 dilution) from week 9 immunized rabbit 16 (▲), rabbit 17 (●) or preimmune serum (▼) for two hours in blocking buffer and were incubated with the goat anti-rabbit peroxidase conjugate (1:2000 dilution) for another two hours in blocking buffer. The excess conjugate was washed and the colour was developed (see Materials and Method). Substrate absorbance was measured at 450 nm.

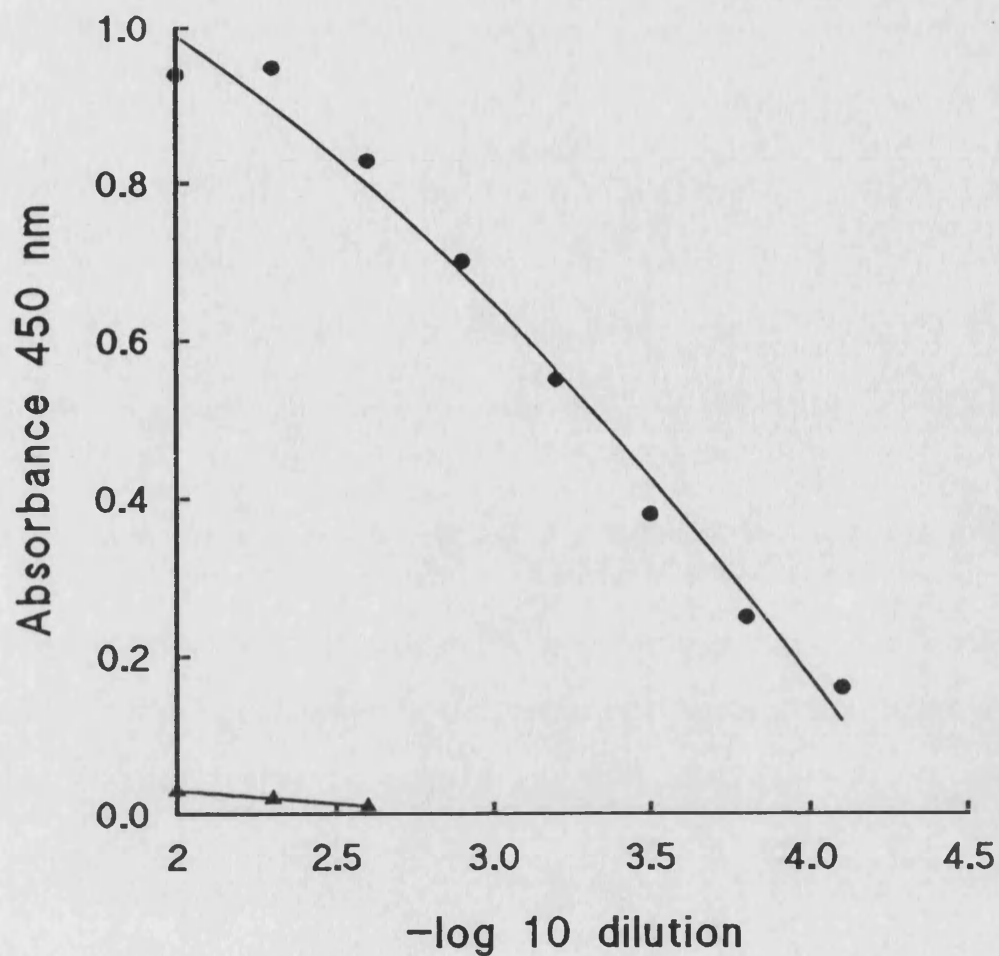


Fig.11 Testing the anti-GLUT4 antiserum with ELISA.

ELISA 96 well plates were coated with anti-C-terminal peptide 20 ng/well. Unoccupied protein binding sites were blocked. The plates were incubated with anti-GLUT4 antiserum (1:100 dilution) from week 9 immunized rabbit (●) or preimmune serum (▲) for two hours in blocking buffer and were incubated with the goat anti-rabbit peroxidase conjugate (1:2000 dilution) for another two hours in blocking buffer. The excess conjugate was washed and the colour was developed (see Materials and Method). Substrate absorbance was measured at 450 nm.

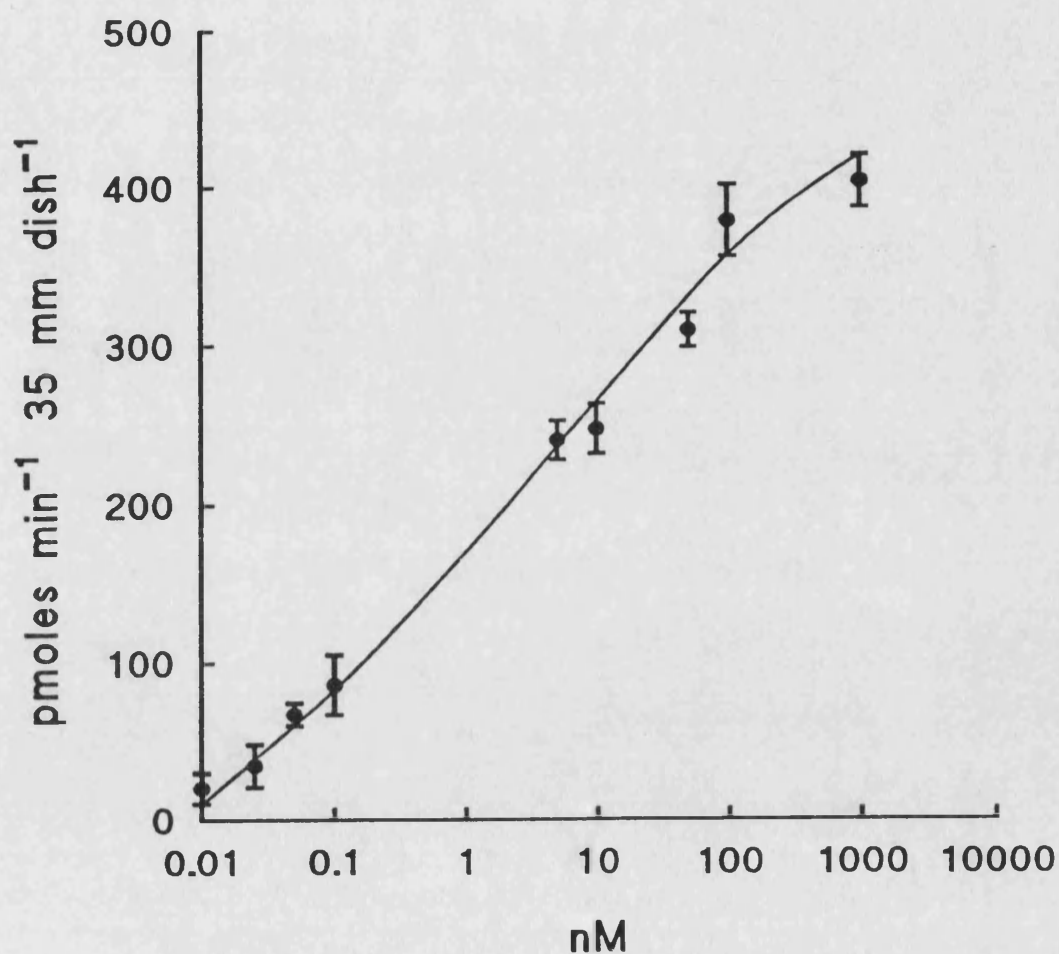


Fig.12 **Insulin stimulation of 2-deoxy-D-glucose uptake in 3T3-L1 adipocytes.**

3T3-L1 adipocytes in 35 mm-diameter dishes were treated with insulin at 37°C at the indicated concentration for 30 min. 2-deoxy [2,6-³H]-D-glucose uptake (50 μ M) was measured over 5 min at 37°C. After washing four times with KRH buffer at 4°C, the cells were dissolved in 0.1 M NaOH and the radioactivity was counted.

dose response curve shows that maximal stimulation at 37°C was seen in cells incubated with 100 nM insulin and no effect of higher insulin concentration was noted. 2-deoxy-D-glucose uptake was half-maximally stimulated by insulin at approximately 1.9 nM. In this thesis, the studies of acute insulin treatment were all performed at this concentration (100 nM).

The rate of uptake 2-deoxy-D-glucose was calculated as below:

$$\frac{\text{Concentration of sugar } (\mu\text{M})}{\text{Total radioactivity (cpm)}} \times 1000 \times \text{cpm at 5 min} = \text{Pmol/5min}$$

Then above values divided by 5 min will gave the rate of pmol/min.

For example: If the counts of a sample are 892 cpm, and the total radioactivity is 144560, the rate will be 61.7 pmol/min.

$$\frac{50 \mu\text{M}}{144560 \text{ (cpm)}} \times \frac{1000}{5} \times 892 \text{ (cpm)} = 61.7 \text{ pmol/min}$$

3.2.3 Basal and insulin stimulated 2-deoxy-D-glucose transport activity

The 2-deoxy-D-glucose has been used in the study of glucose transport in adipocytes. This glucose analogue is supposed to be transported and subsequently phosphorylated by hexokinase, but is not further metabolised (Wick *et al.*, 1951), Hence, the total rate of labelled 2-deoxy-D-glucose glucose uptake can be taken as a measure of the rate of hexose transport.

The 2-deoxy-D-glucose-[1-³H]D-glucose uptake rate in control (basal state)

and in the acute insulin stimulated state is shown in Fig.13. The classical inhibitor of facilitated glucose transport in animal cells, cytochalasin B, was studied. This compound at 30 μ M inhibited both basal and insulin-stimulated 2-deoxy-D-glucose uptake. Basal, insulin stimulated cells and cytochalasin B treated cells were all incubated at 37°C for 30 min. Fig.13 shows that the uptake rate of 2-deoxy-D-glucose in the basal state was 31.85 ± 2.57 pmol/min/35 mm dish, in the insulin stimulated cells it was 502.87 ± 19.42 pmol/min/35 mm dish, and in the cytochalasin B treated cells it was 6.85 ± 0.22 pmol/min/35 mm dish. After correcting for the rate of uptake in the presence of cytochalasin B, the acute insulin treatment was calculated to increase transport by 20 fold compared with the basal state.

After stimulation with a 100 nM insulin for 30 min at 37°C, the transport activity in 3T3-L1 adipocytes measured by 2-deoxy-D-glucose (where the increase was about 20 fold compared with the basal state), was very similar to the transport activity in rat adipocytes measured by 3-O-methyl-D-glucose. This indicates that the 3T3-L1 adipocytes have a good response to insulin stimulation.

3.2.4 Cell surface labelling of GLUT1 and GLUT4 by ATB-BMPA 3T3-L1 adipocytes.

Holman *et al.* (1990) have used a membrane impermanent photoaffinity label ATB-BMPA to identify the cell surface glucose transporters in isolated rat adipose cells. A primary advantage is the rapidity of its activation (Holman *et al.*, 1988). The maximum incorporation of label can be achieved within 45 sec. During 90 sec of uv irradiation, the cells did not appear to lyse and the insulin-stimulated glucose transport activity was found to be unimpaired (Holman *et al.*, 1990). The photolabelled glucose transporters run as a peak at about 50 kDa and the peak is clearly separated from another labelled peak at 75 kDa. The labelling in the 75 kDa

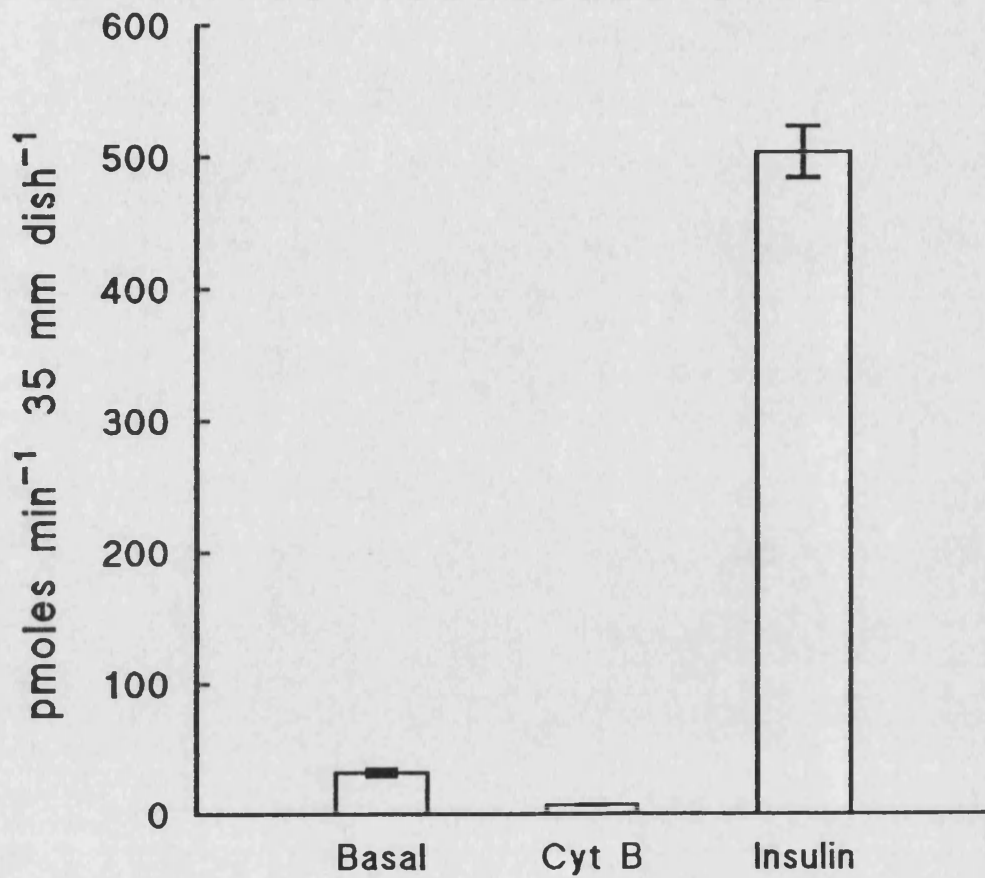


Fig.13 Uptake of 2-deoxy-D-glucose in 3T3-L1 adipocytes.

(All experiment in this thesis used 35 mm-diameter dishes). 3T3-L1 adipocytes in 35 mm-diameter dishes were incubated with (Insulin) or without (Basal) 100 nM insulin, or with 30 μ M of cytochalasin B (Cyt B) for 30 min at 37°C. 2-deoxy [2,6-³H]-D-glucose uptake (50 μ M) was measured over 5 min at 37°C. After washing four times with KRH buffer at 4°C, the cells were dissolved in 0.1 M NaOH and the radioactivity was counted.

region of the SDS gel is unrelated to the presence of glucose transporters because it is not immunoprecipitated by either anti-GLUT1 or anti-GLUT4 antibodies (Holman *et al.*, 1990).

Using the membrane impermanent photolabel ATB-BMPA, the cell surface glucose transporter isoforms GLUT1 and GLUT4 in the basal and acute insulin stimulated state were labelled in the 3T3-L1 adipocytes. Fig.14 shows the GLUT1 cell surface labelling result from basal (control) and 100 nM insulin stimulated 3T3-L1 adipocytes. In the glucose transporter region of the gel there is a slight peak above the normal gel background for cells labelled in the basal state. The calculated dpm for basal is 332 and for the insulin stimulated cells it is 2204. Acute insulin stimulation increased labelling by about 6 fold. Over seven individual experiments the labelling was increased 5 fold compared to the basal state. Fig.15 shows the GLUT4 cell surface labelling results from basal and acute insulin stimulated 3T3-L1 adipocytes. The calculated dpm for basal state is 143 and in the insulin stimulated state it is 2083. Insulin increased the labelling about 14 fold. Over seven experiments the fold increase is about 11 fold. In basal state, the GLUT4 cell surface labelling is about one-third of the GLUT1. These results are consistent with the results reported by Holman *et al.*, (1990); Calderhead *et al.* (1990).

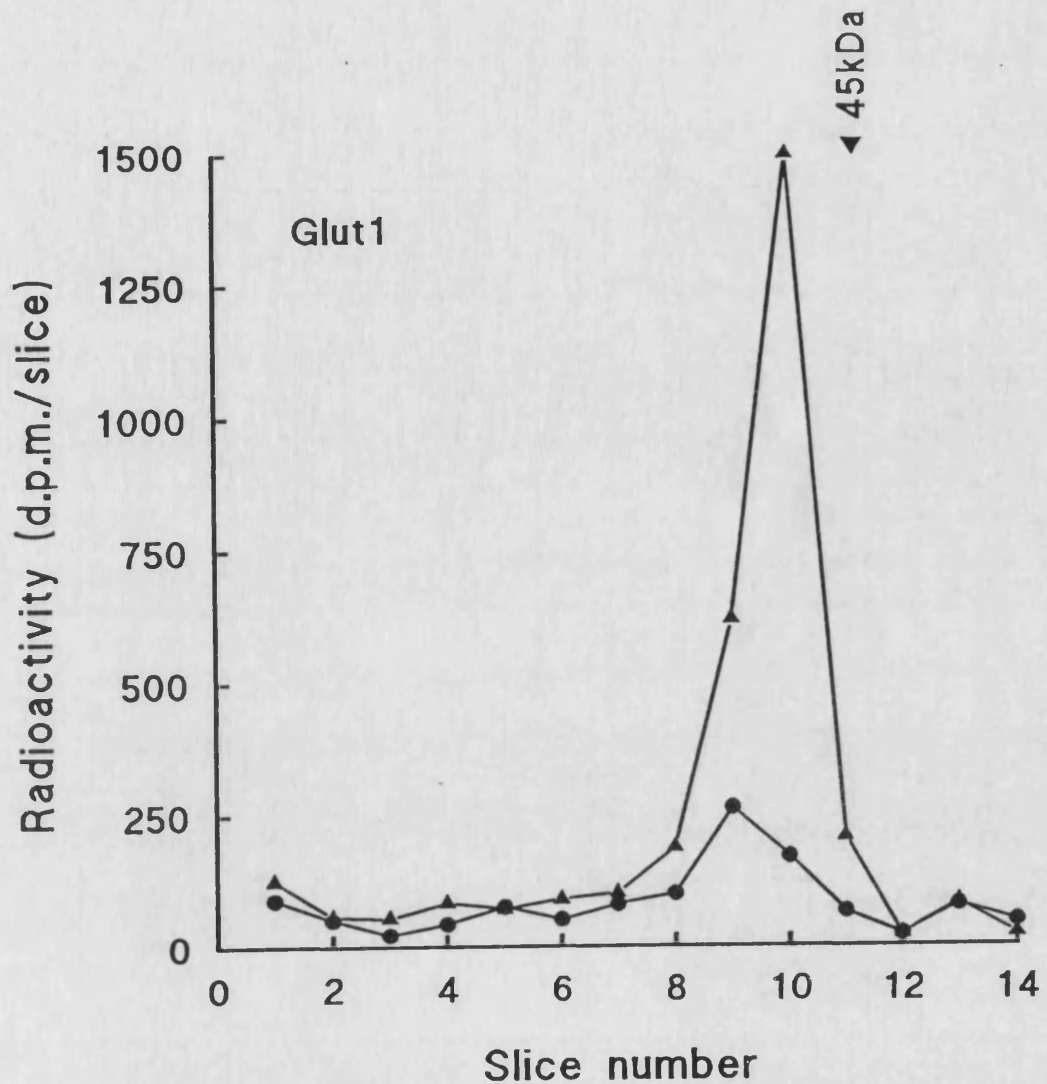


Fig.14 ATB-BMPA cell-surface labelling GLUT1 in 3T3-L1 adipocytes.

3T3-L1 adipocytes were incubated with (▲) or without (●) 100 nM insulin at 37°C and then insulin was removed. The cells were labelled at 18°C with 100 μ Ci of ATB-BMPA in 250 μ l of KRH buffer. After labelling, the cells were washed four times in KRH buffer and then directly solubilized in C₁₂E₉ detergent buffer. GLUT1 was then immunoprecipitated with anti-(C-terminal peptide) antibodies. The protein was then subjected to electrophoresis and the radioactivity was estimated by cutting out and counting the gel slices. The radioactivity in the transporter peaks was corrected for background radioactivity which was based on the average radioactivity of the slices on either side of the peak (the following experiments in this thesis were all calculated in this way).

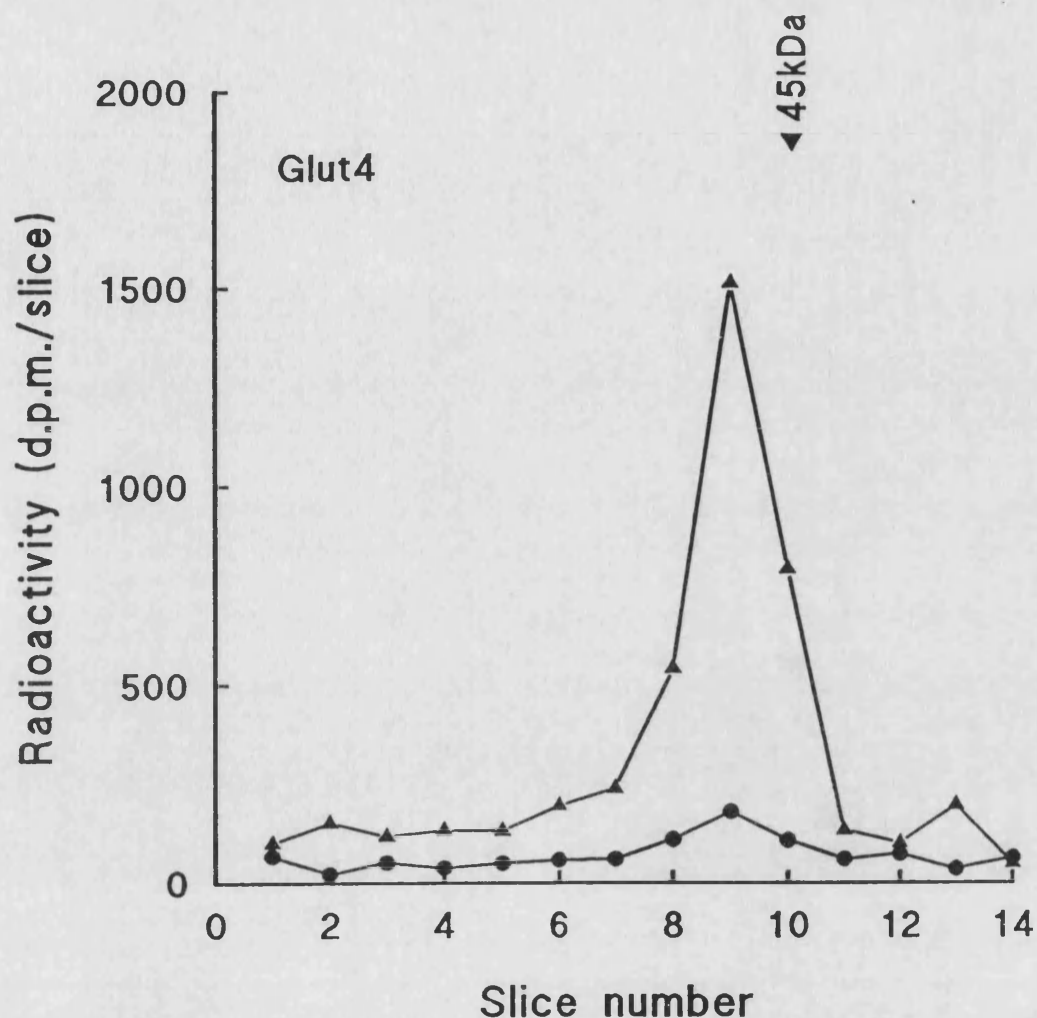


Fig.15 ATB-BMPA cell-surface labelling GLUT4 in 3T3-L1 adipocytes.

3T3-L1 adipocytes were incubated with (▲) or without (●) 100 nM insulin at 37°C and then insulin was removed. The cells were labelled at 18°C with 100 μ Ci of ATB-BMPA in 250 μ l of KRH buffer. After labelling the cells were washed four times in KRH buffer and then directly solubilized in C₁₂E₉ detergent buffer. GLUT4 was then immunoprecipitated with anti-(C-terminal peptide) antibodies. The protein was then subjected to electrophoresis and the radioactivity was estimated by cutting out and counting the gel slices.

PART II DEVELOPMENT OF AN INTRACELLULAR POOL OF GLUCOSE TRANSPORTERS IN 3T3-L1 CELLS

This part of the thesis describes experiments designed to further characterize the development of the insulin-sensitive glucose transport system in 3T3-L1 cells upon differentiation. The two glucose transporter isoforms GLUT1 and GLUT4 have been studied at different stages of this development.

3.3 MEASUREMENT TRANSPORT ACTIVITY AND ATB-BMPA PHOTOLABELLING IN 3T3-L1 FIBROBLASTS

3.3.1 Measurement of 2-deoxy-D-glucose transport activity in 3T3-L1 fibroblasts

To examine the rate of 2-deoxy-D-glucose transport in fibroblasts, the transport activity from initial seeding of dishes to the development of a confluent cell monolayer (which occurs at about Day 5 after seeding) has been studied (Fig. 16). One day after initial seeding of the dishes the transport rate was 0.13 nmoles/ 10^6 cells/min (with 0.026×10^6 cells/ 35 mm dish). This gradually fell over 7 days to 0.025 nmoles/ 10^6 cells/min (with 0.3×10^6 cells/ 35 mm dish) and stayed at this low level for at least a further 6 days. In preconfluent fibroblasts (one day after initial seeding) the 2-deoxy-D-glucose transport activity was about 5 times higher than in confluent fibroblasts. This result is similar to that observed by Ziehm *et al.* (1993). They have measured 2-deoxy-D-glucose transport activity at 4 days after plating and 3 days before confluence and they found the glucose transport rates in preconfluent cells were approximately 5-fold higher than those in the confluent cells.

Insulin failed to stimulate glucose transport in preconfluent cells and from about 7 days after seeding the 2-deoxy-D-glucose transport rate was increased by acute-insulin stimulation to ≈ 2.5 -times above the basal level. This is consistent with

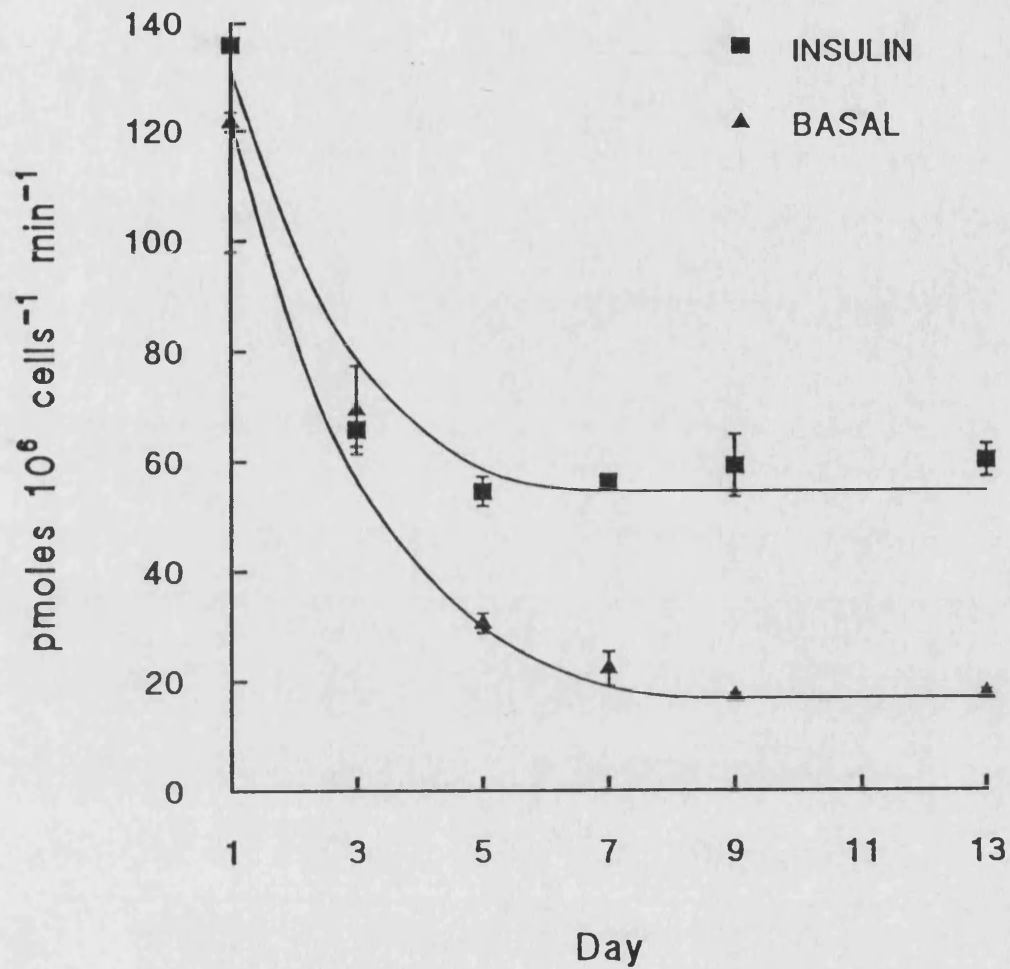


Fig.16 2-deoxy-D-glucose transport activity in 3T3-L1 fibroblasts.

3T3-L1 fibroblasts were seeded at a density of 0.03×10^6 cells per 35 mm dish and maintained in culture in DMEM with 10% newborn-calf serum for up to 13 days. On the indicated days the cells were incubated in the presence of serum-free medium for 2 hours and then maintained at 37°C for 30 min in either the absence (\blacktriangle) or presence of 100 nM insulin (\blacksquare) in 1 ml KRH buffer. The transport of 50 μ M 2-deoxy-[2,6- 3 H]-D-glucose was then measured and cell number determined. Results are mean and S.E.M. from 4 independent determinations.

the results of Ziehm *et al.* (1993), who found insulin did not stimulate glucose transport in preconfluent cells, but gave rise to an approximately 2-fold stimulation of the glucose transport rate in confluent cells (from 10 experiments). However, even in the presence of insulin the transport rate ($0.06 \text{ nmoles}/10^6 \text{ cells/min}$) was approximately half the rate which was observed in preconfluent fibroblasts.

3.3.2. ATB-BMPA labelling of cell-surface and total-cellular pools of GLUT1 in 3T3-L1 fibroblasts

In order to determine the subcellular distribution of transporters, the cell-surface availability of transporters has been measured using the impermeant photolabel ATB-BMPA and this labelling has been compared with that obtained in digitonin-permeabilized cells. When fibroblasts are treated with digitonin the cells detach very easily, so great care should be taken during the washing procedure. The subcellular distribution of GLUT1 in confluent cells was shown in Fig. 17. No GLUT4 was detected in the fibroblasts. There was an ≈ 4 -fold increase in labelling in permeabilized cells compared with untreated cells. Insulin only increased the cell-surface labelling by ≈ 2 -fold and did not increase the total pool of cellular GLUT1. The data from 3 experiments are shown in Fig. 18. The ATB-BMPA photolabelling experiment was also carried out on preconfluent cells. These results are also shown in Fig. 18. From this result it is clearly shown that in preconfluent cells there is no significant increase in labelling in the presence of digitonin indicating that most of the cells transporters were at the cell surface.

Together with the transport data in Fig. 16 and Fig. 18, the labelling data show that in preconfluent 3T3-L1 fibroblasts the high transport rate is associated with the presence of most of the transporters at the cell-surface. As the cells reach confluence, transporters are sequestered from the cell surface and an intracellular reserve pool of transporters develops. Associated with this sequestration is a fall in

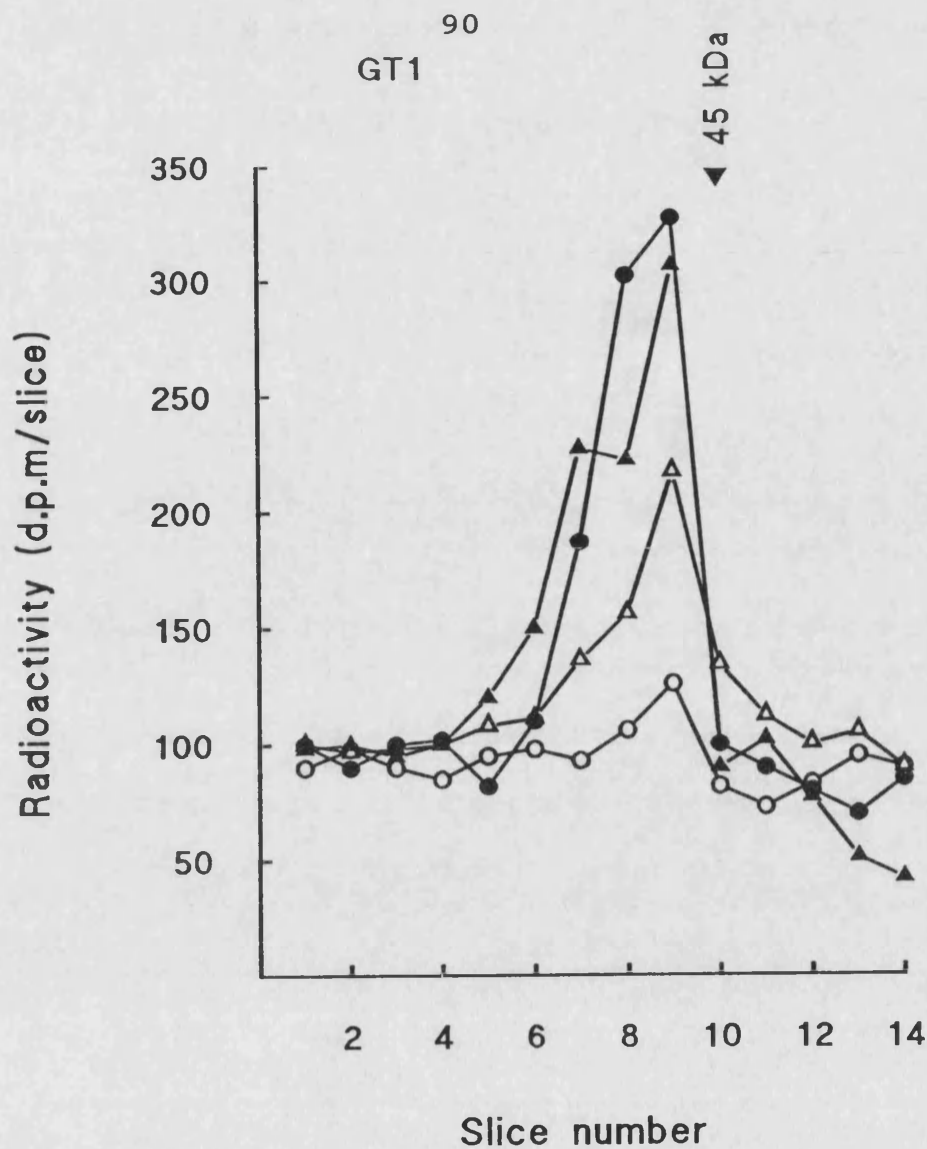


Fig.17 ATB-BMPA labelling of cell-surface and total-cellular pools of GLUT1 in confluent 3T3-L1 fibroblasts.

Cells were maintained in culture for 11 days in DMEM with 10 % newborn-calf serum and then incubated in serum-free medium for 2 hours. Cells were then maintained at 37°C for 30 min either in the absence (○) or in the presence (Δ) of 100 nM insulin in 1 ml of KRH buffer. Cells were then labelled with 100 μ Ci of ATB-[2- 3 H]-BMPA in 250 μ l KRH buffer at 18°C either without (open symbols) or with (closed symbols) of 0.025 % digitonin. Labelled cells were immediately solubilized in C₁₂E₉ detergent buffer and the labelled proteins were subjected to immunoprecipitation with GLUT1 C-terminal-peptide antibody and then analyzed by electrophoresis.

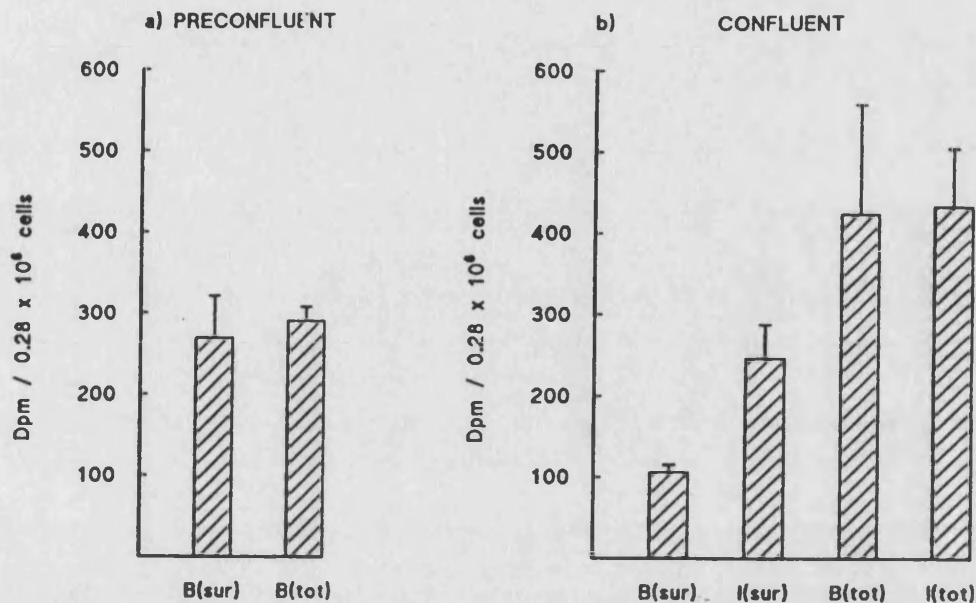


Fig.18 Comparison of GLUT1 cellular distribution in preconfluent and confluent 3T3-L1 fibroblasts.

a) 3T3-L1 fibroblasts were harvested and plated into two 35 mm dishes to give a total of 0.28×10^6 subconfluent cells after 1 day in culture. Cells in each dish were incubated in serum-free medium for 2 hours and then labelled with 100 μ Ci of ATB-[2-³H]-BMPA in 250 μ l of KRH buffer at 18°C either in the absence, B(sur), or presence B(tot) of 0.025 % digitonin. Labelled cells from the 2 dishes were then immediately solubilized in C₁₂E₉ detergent buffer and labelled proteins were subjected to immunoprecipitation with GLUT1 C-terminal-peptide antiserum followed by electrophoresis. Results are the mean and S.E.M. from 4 experiments.

b) 3T3-L1 fibroblasts were maintained in culture for 11 days and at confluence reached a density of 0.28×10^6 cells / 35mm dish. The cells were incubated for 2 hours in serum-free medium and then maintained at 37°C for 30 min either without (B) or with (I) 100 nM insulin in 1 ml KRH buffer. Cells were then labelled with 100 μ Ci of ATB-[2-³H]-BMPA in 250 μ l of KRH buffer at 18°C either in the absence (sur) or presence (tot) of 0.025 % digitonin and GLUT1 immunoprecipitated as described in the Fig. 17 legend. Results are the mean and S.E.M. of 3 experiments.

the transport activity which can then be partially restored by acute-insulin treatment which redistributes approximately half of the available transporters to the cell surface. A similar result was achieved by Ziehm *et al.* (1993) who used a western blotting technique to show that in preconfluent fibroblasts GLUT1 was almost exclusively located in plasma membranes. In confluent fibroblasts, the abundance of GLUT1 in the plasma membranes was moderately decreased, and the relative amount of GLUT1 in the low-density microsomes appeared higher than in the preconfluent cells. No GLUT4 was detected in fibroblasts.

3.4 ATB-BMPA LABELLING OF CELL-SURFACE AND TOTAL-CELLULAR POOLS OF GLUT1 AND GLUT4 IN 3T3-L1 ADIPOCYTES

The technique for comparing cell-surface and total-cellular transporters has also been used to examine the distribution of GLUT1 and GLUT4 in differentiated 3T3-L1 adipocytes. Fig. 19 and Fig. 20 shows an SDS polyacrylamide gel of ATB-BMPA labelled and immunoprecipitated GLUT1 and GLUT4. As shown in previous studies in this thesis {and also by Calderhead *et al.* (1990); Kozka *et al.* (1991)}, there was very little GLUT4 at the cell-surface in the basal state. Upon insulin stimulation the GLUT4 labelling increased by ≈ 12 -fold in this experiment, while the GLUT1 increased about 5 fold. However, as is the case with GLUT1 in confluent fibroblasts only about half of the total available transporters were returned to the cell surface upon insulin treatment. In the digitonin-permeabilized cells there was only a slight difference between the amount of GLUT1 and GLUT4 labelled in the basal compared with the insulin-treated condition. The small difference observed in this experiment and others (see Fig. 21) (from 7 experiments) was possibly due to a difference in efficiency of labelling of the intracellular pool compared with the cell-surface GLUT1 and GLUT4. This small difference was not observed in all experiments and over 7 experiments the mean was only slightly lower than that observed with insulin-treated cells. However, Fig. 21 also shows that the S.E.M. was

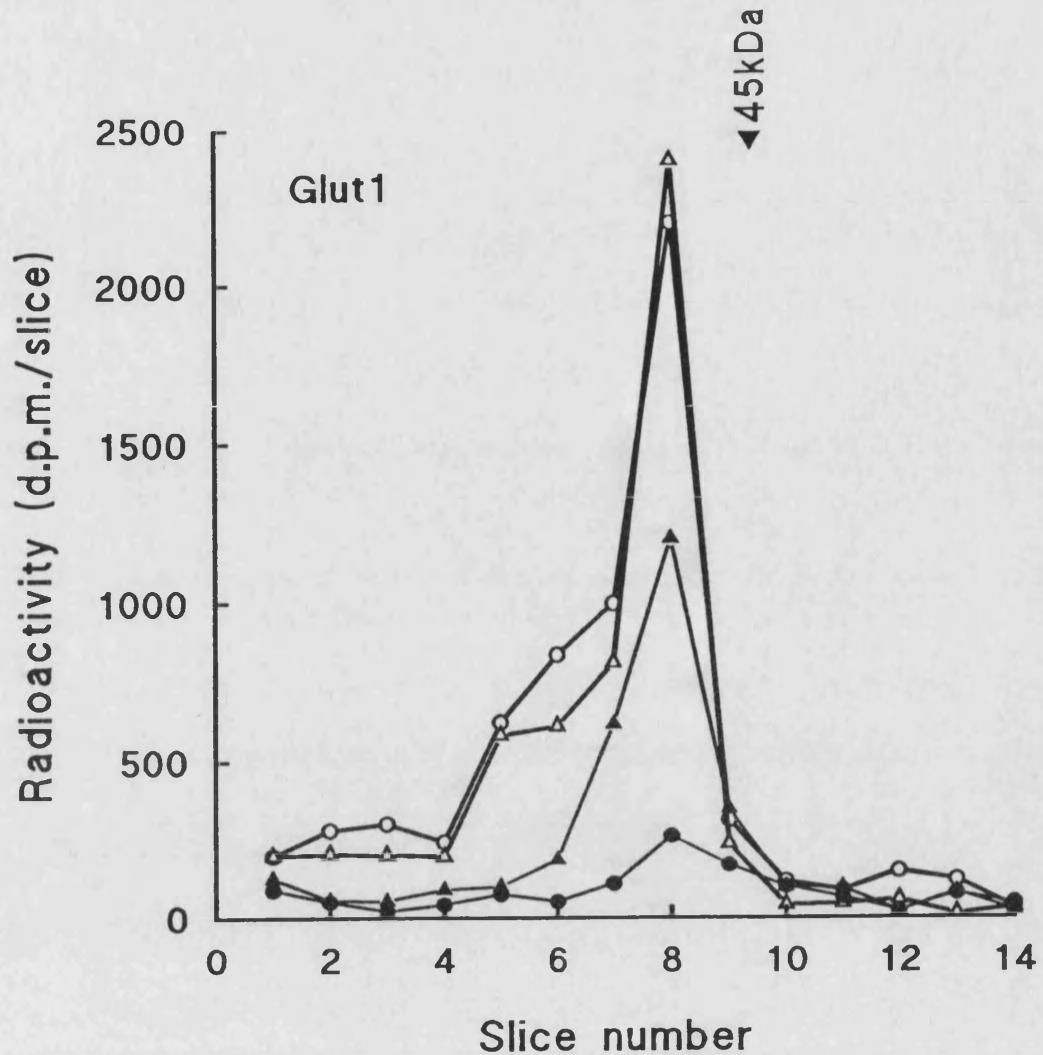


Fig.19 ATB-BMPA labelling of cell-surface and total cellular pools of GLUT1 in 3T3-L1 adipocytes.

Fully differentiated 3T3-L1 adipocytes in 35 mm dishes were incubated in serum-free medium for 2 hours and were then maintained at 37°C for 30 min either in the absence (O) or presence (Δ) of 100 nM insulin in 1 ml KRH buffer. Cells were then labelled with 100 μ Ci of ATB-[2-³H]-BMPA in 250 μ l of KRH buffer at 18° either without (closed symbols) or with (open symbols) 0.025 % digitonin. Cells were then washed twice in KRH buffer and then solubilized in C₁₂E₉ detergent buffer and the labelled proteins were subjected to immunoprecipitation with GLUT1 C-terminal-peptide antiserum and then analyzed by electrophoresis.

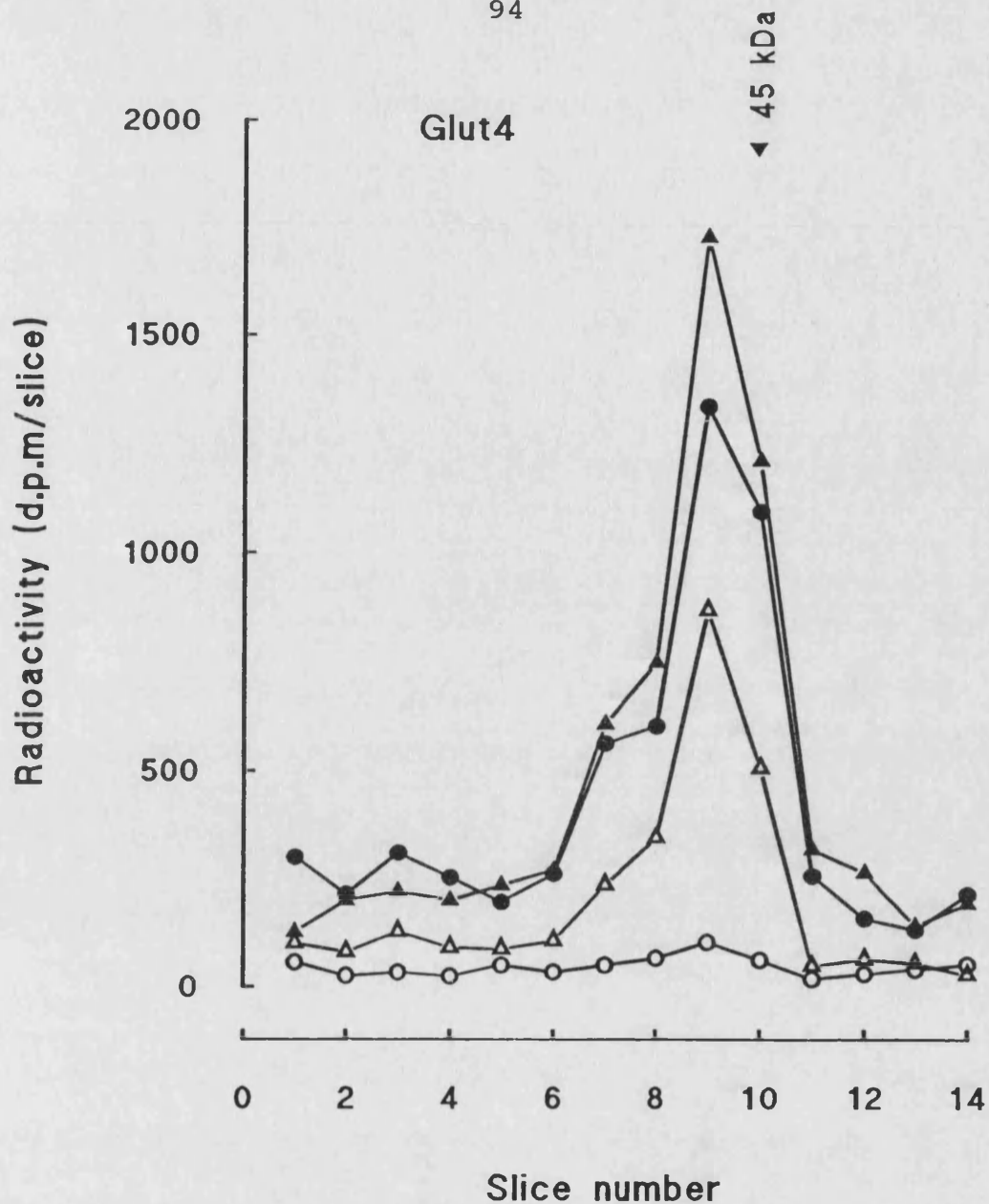


Fig.20 ATB-BMPA labelling of cell-surface and total cellular pools of GLUT4 in 3T3-L1 adipocytes.

Fully differentiated 3T3-L1 adipocytes in 35 mm dishes were incubated in serum-free medium for 2 hours and were then maintained at 37°C for 30 min either in the absence (○) or presence (△) of 100 nM insulin in 1 ml KRH buffer. Cells were then labelled with 100 μ Ci of ATB-[2- 3 H]-BMPA in 250 μ l of KRH buffer at 18° either without (open symbols) or with (closed symbols) 0.025 % digitonin. Cells were then washed twice in KRH buffer and then solubilized in C₁₂E₉ detergent buffer and the labelled proteins were subjected to immunoprecipitation with GLUT4 C-terminal-peptide antiserum and then analyzed by electrophoresis.

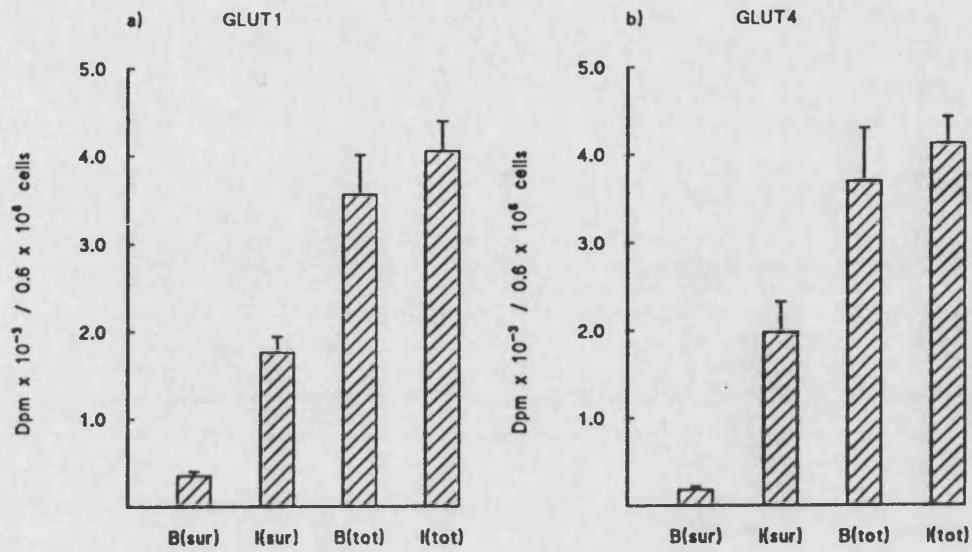


Fig.21 GLUT1 and GLUT4 cellular distribution in 3T3-L1 adipocytes.

Cells were fully differentiated in 35 mm dishes and then subjected to the labelling procedure described in the Fig.19 and 20. The total dpm under the gel peaks were calculated for GLUT1 (Fig.19) and GLUT4 (Fig.20) either without or with 0.025 % digitonin to obtain cell-surface (sur) or total-cellular (tot) levels of labelling for basal cells (B) or cells treated with 100 nM insulin (I). The results are the mean and S.E.M. from 7 experiments.

larger for the labelling of the total-cellular pool of both GLUT1 and GLUT4 in the basal cells. The greater variability of labelling the intracellular pool (which constitutes a greater proportion of the total in the basal state) was probably a consequence of variations between cell-batches in the susceptibility to digitonin permeabilization or the efficiency with which the uv. light could penetrate to intracellular sites of transporter localization. Fig. 21 also shows that in the insulin-stimulated state approximately half of the total of both GLUT1 and GLUT4 was recruited to the plasma membrane. However, as previously shown by Calderhead *et al.* (1990) and also from other studies in this thesis, the GLUT4 has a greater tendency to be internalized in the absence of insulin and the cell-surface labelling of GLUT4 is about a third of the GLUT1 level in this basal state.

3.5 MEASUREMENTS OF THE CHANGES OF GLUCOSE TRANSPORT ACTIVITY AND THE CHANGES OF GLUT1 AND GLUT4 THROUGHOUT THE CELL DIFFERENTIATION

The time-course for changes in the glucose transport activity and subcellular transporter distribution during the transition from confluent fibroblasts to fully differentiated adipocytes have been examined. The experiment was started when the fibroblasts was fully confluent (as day 0). The experiment was then carried out on every other day. Fig. 22 shows that the basal level of 2-deoxy-D-glucose transport remained low throughout the differentiation period. The transport rate in basal cells was ≈ 8 pmoles/ dish/ min in confluent fibroblasts (with 0.3×10^6 cells/ dish) and increased to ≈ 25 pmoles/ dish/ min in fully differentiated cells, where the cell number had also increased to 0.6×10^6 cells/ dish. During the differentiation the amount of protein per 35 mm dish increased enormously from 88 μ g/ dish to 1.1 mg/ dish. The insulin-stimulated rate of transport was approximately double the basal rate for about 4 days after the initiation of differentiation. By 6 days there was a very marked increase in the insulin-stimulated rate of transport which reached by 11 days a

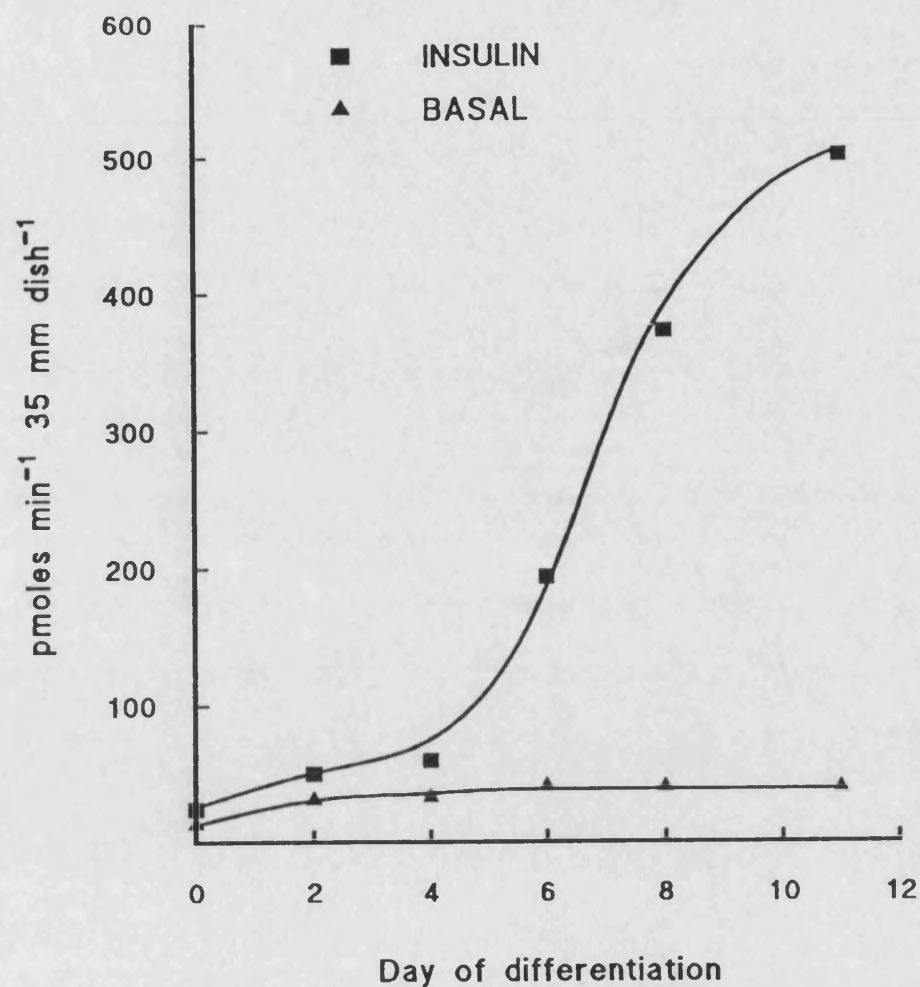


Fig.22 Time course for differentiation of highly insulin-responsive glucose transport in 3T3-L1 cells.

Confluent 3T3-L1 fibroblasts in 35 mm dishes were treated with dexamethasone, IBMX and insulin in DMEM with 10% foetal-bovine serum to initiate differentiation. On the indicated days cells were incubated in serum-free medium for 2 hours and then maintained at 37°C for 30 min in the absence (▲) or presence (■) of 100 nM insulin in 1 ml of KRH buffer. This was followed by determination of the rate of uptake of 50 μ M 2-deoxy-[2,6-³H]-D-glucose. Results are the mean of 2 experiments.

rate which was ≈ 20 -times the basal rate.

Fig.23. shows the distribution of GLUT1 throughout this differentiation period. During the first 4 days the cells behaved in a manner similar to that observed in confluent fibroblasts. The basal level of labelling was approximately 2.5-fold lower than the insulin-stimulated level. The total-cellular levels were approximately double the level found at the cell-surface in the insulin-stimulated state. Between 6 and 11 days there was a marked rise in the total-cellular GLUT1. The cell-surface GLUT1 in the basal cells rose slightly throughout this period and this may have been a consequence of the increased cellular level of this transporter. The GLUT4 was produced in parallel with the rise in GLUT1 (Fig. 24). Thus there was little detectable GLUT4 over the first 2 days of differentiation and then this rose steeply between days 6 and 11.

In contrast with the rise in the basal level of labelled GLUT1, labelling showed that the GLUT4 that was newly synthesized was very effectively sequestered inside the cell. The basal GLUT4 labelling remained consistently low from days 4-11 after the initiation of differentiation while the total cellular GLUT4 rose by > 10 -fold over this period.

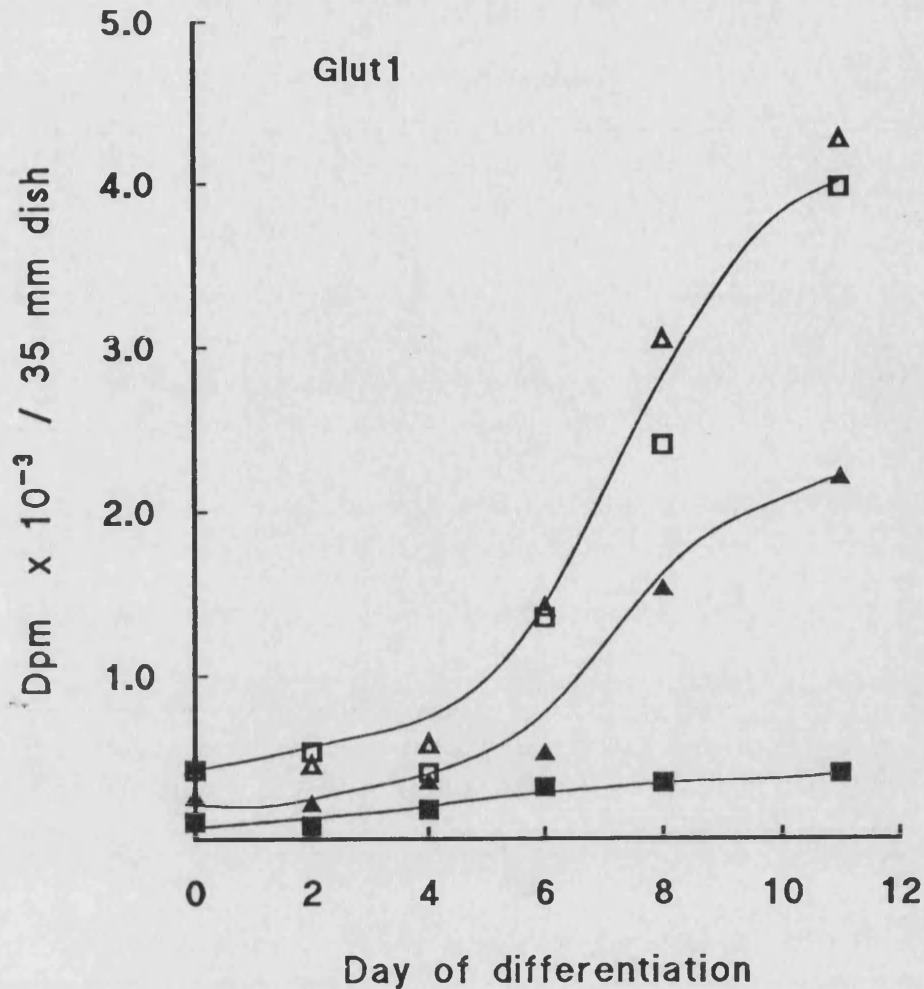


Fig.23 Time course for the increase in cell-surface and total cellular pools of GLUT1 in 3T3-L1 cells.

3T3-L1 fibroblasts in 35 mm dishes were treated with dexamethasone, IBMX and insulin in DMEM with 10% foetal-bovine serum to initiate differentiation. On the indicated days cells were incubated in serum-free medium for 2 hours and were then maintained at 37°C for 30 min either in the absence (\square) or presence (Δ) of 100 nM insulin in 1 ml KRH buffer. GLUT1 distribution was determined by labelling with 100 μ Ci of ATB-[2- 3 H]-BMPA in 250 μ l of KRH buffer at 18°C to obtain either cell-surface levels (closed symbols) or total-cellular levels in cells permeabilized with 0.025 % digitonin (open symbols). Cells were washed twice in KRH buffer and then solubilized in C₁₂E₉ detergent buffer except Day-0 cells which were immediately solubilized in detergent buffer. The isoforms were then immunoprecipitated with anti-C-terminal-peptide antibodies and analyzed by electrophoresis to obtain the total dpm under the gel peaks. Results are the mean from 2 experiments.

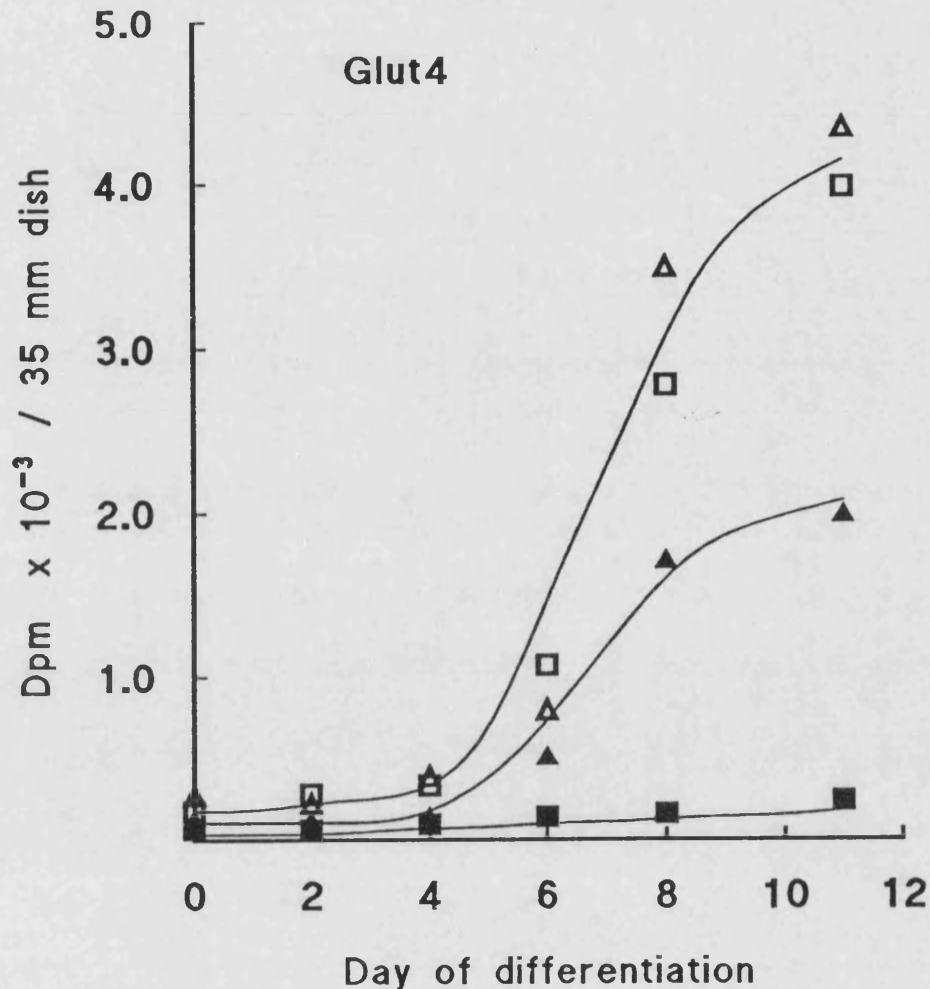


Fig.24 Time course for the increase in cell-surface and total cellular pools of GLUT4 in 3T3-L1 cells.

3T3-L1 fibroblasts in 35 mm dishes were treated with dexamethasone, IBMX and insulin in DMEM with 10% foetal-bovine serum to initiate differentiation. On the indicated days cells were incubated in serum-free medium for 2 h. and were then maintained at 37°C for 30 min either in the absence (□) or presence (Δ) of 100 nM insulin in 1 ml KRH buffer. GLUT1 distribution was determined by labelling with 100 μ Ci of ATB-[2-³H]-BMPA in 250 μ l of KRH buffer at 18°C to obtain either cell-surface levels (closed symbols) or total-cellular levels in cells permeabilized with 0.025 % digitonin (open symbols). Cells were washed twice in KRH buffer and then solubilized in C₁₂E₉ detergent buffer except Day-0 cells which were immediately solubilized in detergent buffer. The isoforms were then immunoprecipitated with anti-C-terminal-peptide antibodies and analyzed by electrophoresis to obtain the total dpm under the gel peaks. Results are the mean from 2 experiments.

PART III TRAFFICKING OF GLUT1 AND GLUT4 IN 3T3-L1 ADIPOCYTES

3.6 INSULIN STIMULATION OF GLUCOSE TRANSPORT AND THE AVAILABILITY OF CELL-SURFACE TRANSPORTERS

3.6.1 Insulin stimulation of glucose transport and the availability of cell-surface transporters at 37°C.

Karnielli *et al.* (1981a) have studied the time course of insulin's action on glucose transport activity in intact cells, measured using 3-O-methylglucose. The maximal response to insulin is achieved within 12 min, with a half-time of approximately 4.0 min. A similar result was obtained in intact rat adipocytes by Clark *et al.* (1991) who found the maximal response to insulin (10 nM) is obtained with 9.2 min with half time of about 3.0 min. To study the insulin's action on 3T3-L1 adipocytes, the time course of 2-deoxy-D-glucose transport activity was measured and cell surface glucose transporters were labelled by ATB-BMPA at 37°C.

Fig.25. shows the time course of insulin stimulated glucose transport at 37°C. The monolayers of fully differentiated 3T3-L1 adipocytes were incubated with insulin at 0, 3, 5, 7, 10, 20, 30 min. When the cells were exposed to insulin for 3.8 min, half maximal rate was achieved. In about 12 min of stimulation, the 2-deoxy-D-glucose uptake rate reached a maximum level and maintained this level until 30 min.

Using the cell-impermeant photoaffinity label ATB-BMPA, the time course of insulin-stimulated appearance of cell surface glucose transporters was examined at 37°C. Fig.26 shows the result from GLUT1, Fig.27 shows the result from GLUT4. The basal level for GLUT1 was 321 dpm, GLUT4 was 108 dpm. The counts of maximum insulin stimulation (30 min) of GLUT1 was 1296 dpm, for GLUT4 it was 1742 dpm. Insulin-stimulated appearance of the cell surface glucose transporter

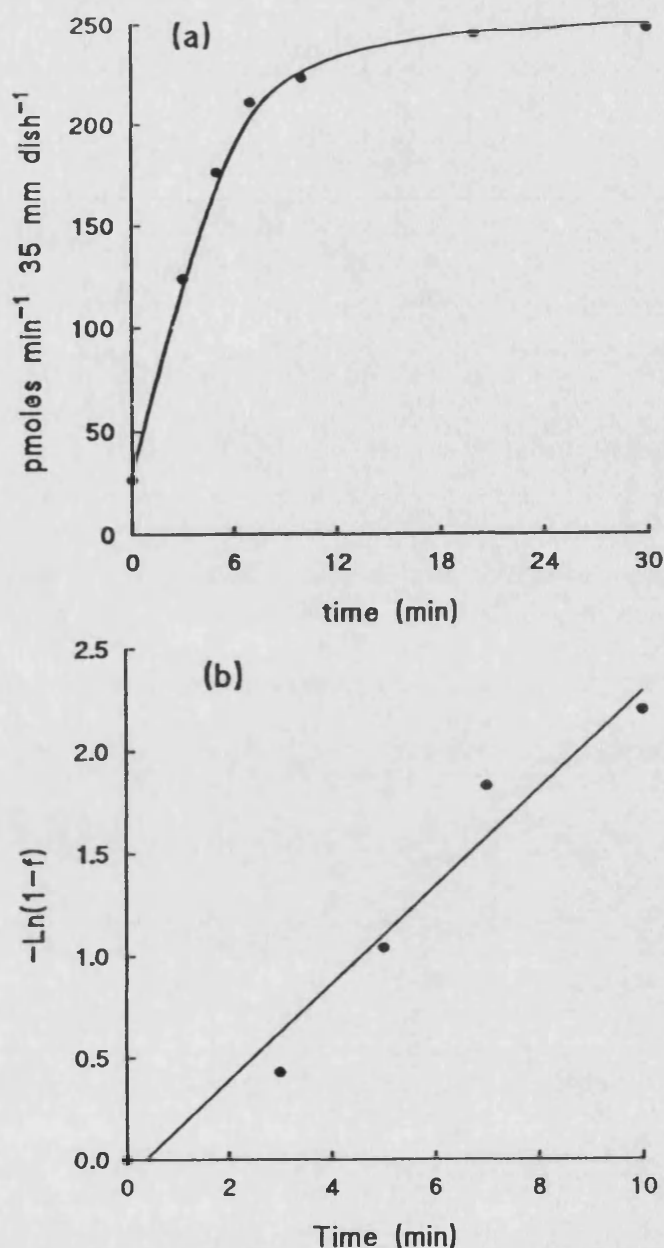


Fig.25 Insulin stimulation of 2-deoxy-D-glucose transport in 3T3-L1 adipocytes at 37°C.

(a) 3T3-L1 adipocytes stimulated with 100 nM-insulin at 37°C and then at zero, 3 min, 5 min, 7 min, 10 min, 20 min, 30 min, the 2-deoxy [2,6-³H]-D-glucose uptake (50 μM) was measured over 5 min at 37°C. The cells were washed four times with KRH buffer at 4°C and then dissolved in 0.1 M NaOH and the radioactivity was counted. The results are from 2 experiments.

(b) Semi-log plots of $-\ln(1-f)$ against time, f is the fraction of the maximum stimulation. The $t_{1/2}$ values were calculated according to the equation: $t_{1/2} = (\ln 2 - a)/b$ where a is the intercept on the $-\ln(1-f)$ axis and b is the slope. The $t_{1/2} = 3.87$ min.

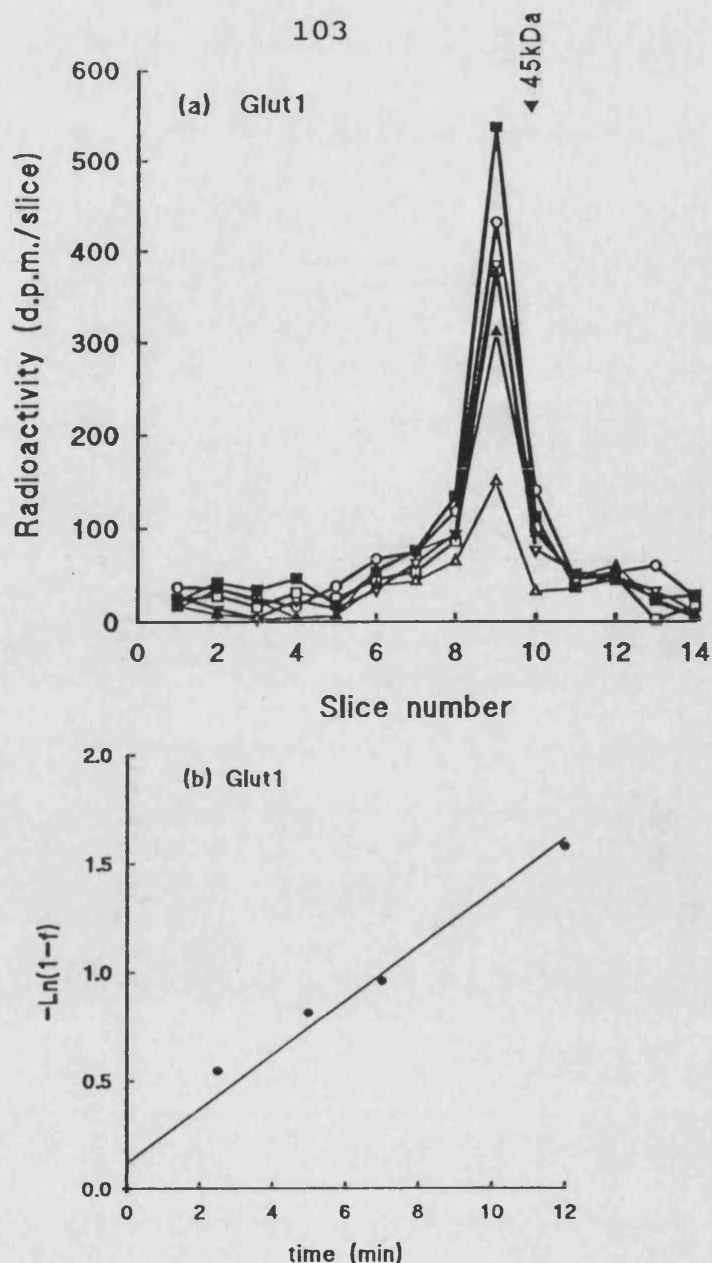


Fig.26 Insulin stimulation of the cell-surface appearance of GLUT1 in 3T3-L1 adipocytes at 37°C.

(a) 3T3-L1 adipocytes were stimulated with 100 nM insulin at 37°C and then at zero time (Δ), 2.5 min (\blacktriangle), 5 min (∇), 7 min (\square), 12 min (\circ) and 30 min (\blacksquare) the insulin was removed by washing twice in KRH buffer at 18°C. The cells were then labelled at 18°C with 100 μ Ci of ATB-BMPA in 250 μ l of KRH buffer. After labelling the cells were washed four times in KRH buffer and then directly solubilized in C₁₂E₉ detergent buffer. GLUT1 was then immunoprecipitated with anti-(C-terminal peptide) antibodies. The protein was then subjected to electrophoresis and the radioactivity was estimated by cutting out and counting the gel slices.

(b) Semi-log plots of $-\ln(1-f)$ against time, f is the fraction of the maximum stimulation. The $t_{1/2}$ values were calculated according to the equation: $t_{1/2} = (\ln 2 - a)/b$ where a is the intercept on the $-\ln(1-f)$ axis and b is the slope. The $t_{1/2} = 3.2$ min. The results from 2 experiments.

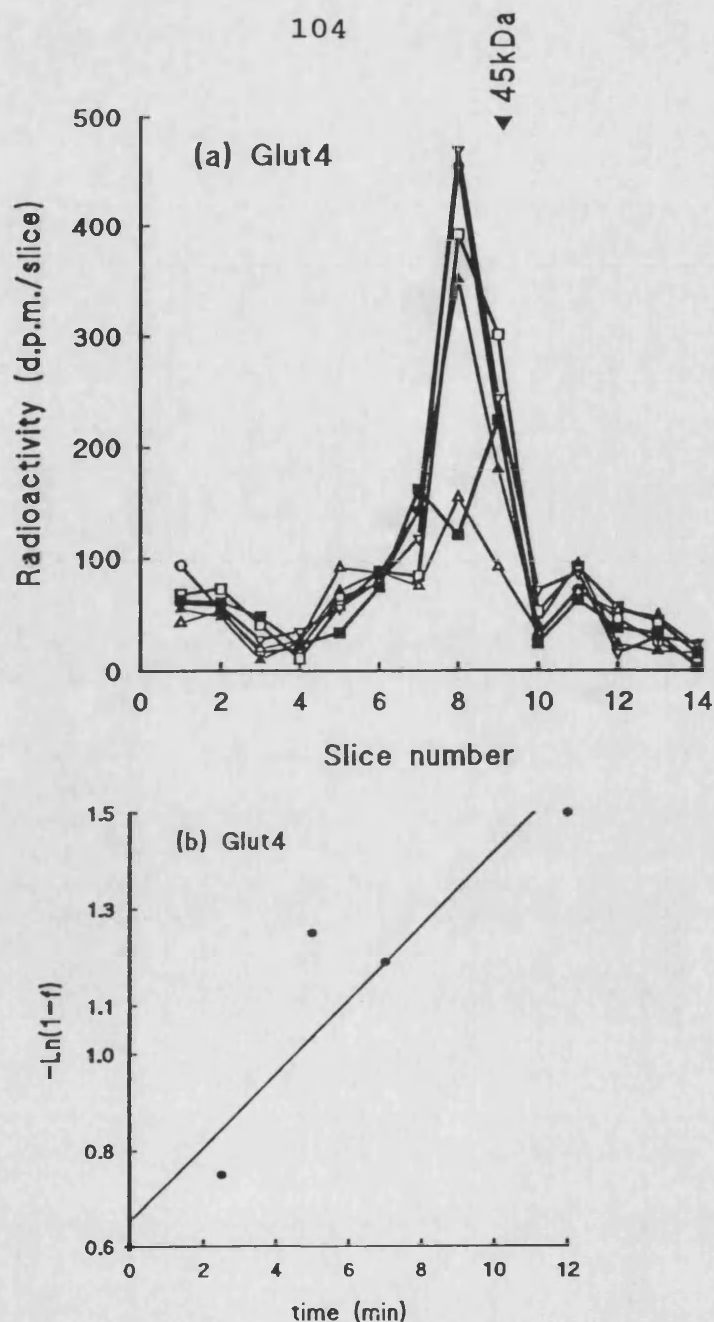


Fig.27 Insulin stimulation of the cell-surface appearance of GLUT4 in 3T3-L1 adipocytes at 37°C.

(a) 3T3-L1 adipocytes were stimulated with 100 nM insulin at 37°C and then at zero time (Δ), 2.5 min (\blacktriangle), 5 min (∇), 7 min (\square), 12 min (\circ) and 30 min (\blacksquare) the insulin was removed by washing twice in KRH buffer at 18°C. The cells were then labelled at 18°C with 100 μ Ci of ATB-BMPA in 250 μ l of KRH buffer. After labelling the cells were washed four times in KRH buffer and then directly solubilized in C₁₂E₉ detergent buffer. GLUT4 was then immunoprecipitated with anti-(C-terminal peptide) antibodies. The protein was then subjected to electrophoresis and the radioactivity was estimated by cutting out and counting the gel slices.

(b) Semi-log plots of $-\ln(1-f)$ against time, f is the fraction of the maximum stimulation. The $t_{1/2}$ values were calculated according to the equation: $t_{1/2} = (\ln 2 - a)/b$ where a is the intercept on the $-\ln(1-f)$ axis and b is the slope. The $t_{1/2} = 2.4$ min. The results from 2 experiments.

GLUT1 measured by impermeant photoaffinity label ATB-BMPA was increased about 4 fold compared to the basal state and GLUT4 was increased about 16 fold. After the cells were stimulated with insulin for 3.2 min, the counts for GLUT1 were 732 dpm, and after the cells were stimulated with insulin 2.4 min, the counts for GLUT4 were 1056 cpm. The half time of appearance of GLUT1 at the cell surface was 3.2 min and GLUT4 was 2.4 min.

The rate of stimulation was determined from semi-log plots of $-\ln(1-f)$ against time, where f is the fraction of the maximum stimulation.

Normally the slope of such a plot gives the activation rate constant, but because a lag phase occurred before the transport activation, the $t_{1/2}$ values for the transport activation were calculated according to the equation:

$$t_{1/2} = (\ln 2 - a) / b \quad (\text{Eq. 1})$$

where a is the intercept on the $-\ln(1-f)$ axis and b is the slope.

3.6.2 Insulin stimulation of glucose transport and the availability of cell-surface transporters at 27°C

The insulin stimulation of the cell-surface availability of glucose transporters at 37°C was found to be very rapid ($t_{1/2} \approx 2$ min). This was considered to be too rapid for comparison with the stimulation of 2-deoxy-D-glucose transport activity at this temperature ($t_{1/2} \approx 3$ min). In rat adipocytes it was possible to measure the time course for stimulation at 37°C because the stimulation of these cells could be blocked at short time points by the addition of KCN. However, that the stimulation of transport in 3T3-L1 cells was not blocked by KCN. Instead, the approach of Gibbs *et al.* (1988) was used. These investigators studied the time-course for insulin

stimulation at 27°C. In Fig.28 3T3-L1 adipocytes were incubated with insulin for 0, 2.5, 5, 7.5, 10, 20, 30 min at 27°C. The 2-deoxy-D-glucose transport activity was measured in 1-5 min at 18°C. The counts for basal state was 42.52 ± 3.16 pmol/min/35 mm dish, the maximal insulin stimulation counts was 201.44 ± 36.95 pmol/min/35 mm dish, the half maximum time was 8.6 ± 0.5 min and the fully activated cells exhibited an 5-8 fold increase in uptake rate. This correlates well with the results that Gibbs obtained, they found the half time for stimulation at 27°C was 9.5 min and the activated cells give an 8.3 fold increase in transport rate.

No further insulin stimulation occurs once insulin is removed and the dishes were washed at 18°C. Fig.29 shows the 3T3-L1 dishes which were first stimulated with 100 nM insulin for 5 min and the insulin was then removed and replaced 1 ml KRH buffer at 18°C for 1, 3, 5, 7, 15 min. Then uptake of 2-deoxy-D-glucose was measured for 1 min at 18°C. The dishes were washed four times with KRH buffer at 18°C. The data shows no further insulin stimulation occurs once insulin is removed and the cells were incubated at 18°C for further 15 min. This indicates that the transport stimulation can be blocked by an 18°C buffer.

At 27°C the increase in cell-surface GLUT1 and GLUT4 occurred in parallel. Fig.30 and Fig.31 show that a large increase above basal levels ($\approx 45\%$ of maximum) in cell-surface labelling of these two isoforms occurred with only 5 min of stimulation by 100 nM insulin. The cell-surface levels of both isoforms then rose progressively and reached a maximum level of stimulation in ≈ 12 min. The cell-surface GLUT1 increases with a $t_{1/2}$ of 5.7 ± 1.5 min (from two experiments) which was similar to the rate of increase in cell-surface GLUT4 ($t_{1/2} = 5.4 \pm 0.7$ min; from two experiments). In Fig.32 the time-course for this stimulation of the cell-surface availability of transporters is shown to slightly precede the time-course for insulin stimulation of 2-deoxy-D-glucose transport activity ($t_{1/2} = 8.6 \pm 1.5$ min ; from three experiments). The observed lag between transporter appearance at the cell surface

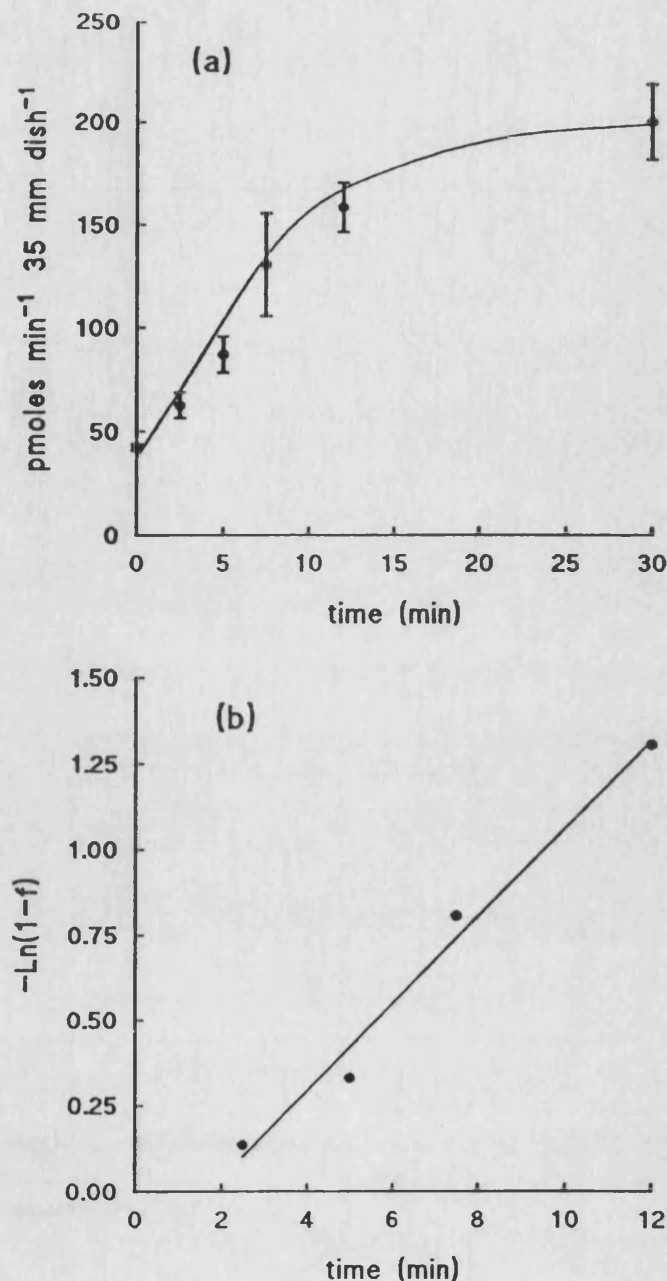


Fig.28 Insulin stimulation of 2-deoxy-D-glucose transport in 3T3-L1 adipocytes at 27°C.

(a) 3T3-L1 adipocytes were stimulated with 100 nM insulin at 27°C and then at zero time, 2.5 min, 5 min, 7.5 min, 12 min, 30 min; the 2-deoxy [2,6-³H]-D-glucose uptake was measured over 1-5 min at 18°C. The cells were washed four times with KRH buffer and dissolved in 0.1 M NaOH and the radioactivity was counted.

(b) Semi-log plots of $-\ln(1-f)$ against time, f is the fraction of the maximum stimulation. The $t_{1/2} = 8.6 \pm 1.5$ min. The results are from 3 experiments. The $t_{1/2}$ values were calculated according to the equation: $t_{1/2} = (\ln 2 - a)/b$ where a is the intercept on the $-\ln(1-f)$ axis and b is the slope.

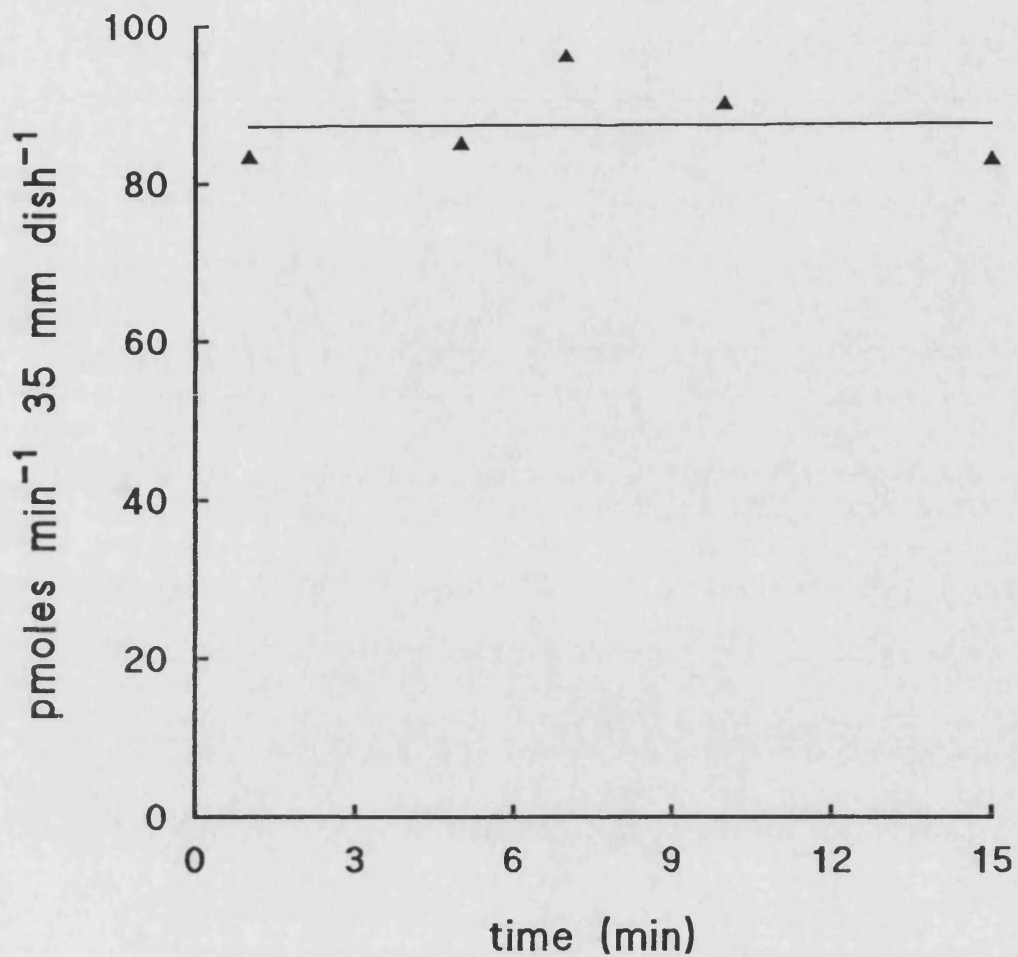


Fig.29 The effect of 18°C to stop further insulin stimulation at 2-deoxy-D-glucose transport in 3T3-L1 adipocytes.

3T3-L1 adipocytes were stimulated with 100 nM insulin at 27°C for 5 min and then insulin was removed. The cells were washed four times with KRH buffer at 18°C and the cells were kept in KRH buffer at 18°C for 1-10 min. Then 2-deoxy [2,6-³H]-D-glucose (50 μM) was measured over 1 min at 18°C.

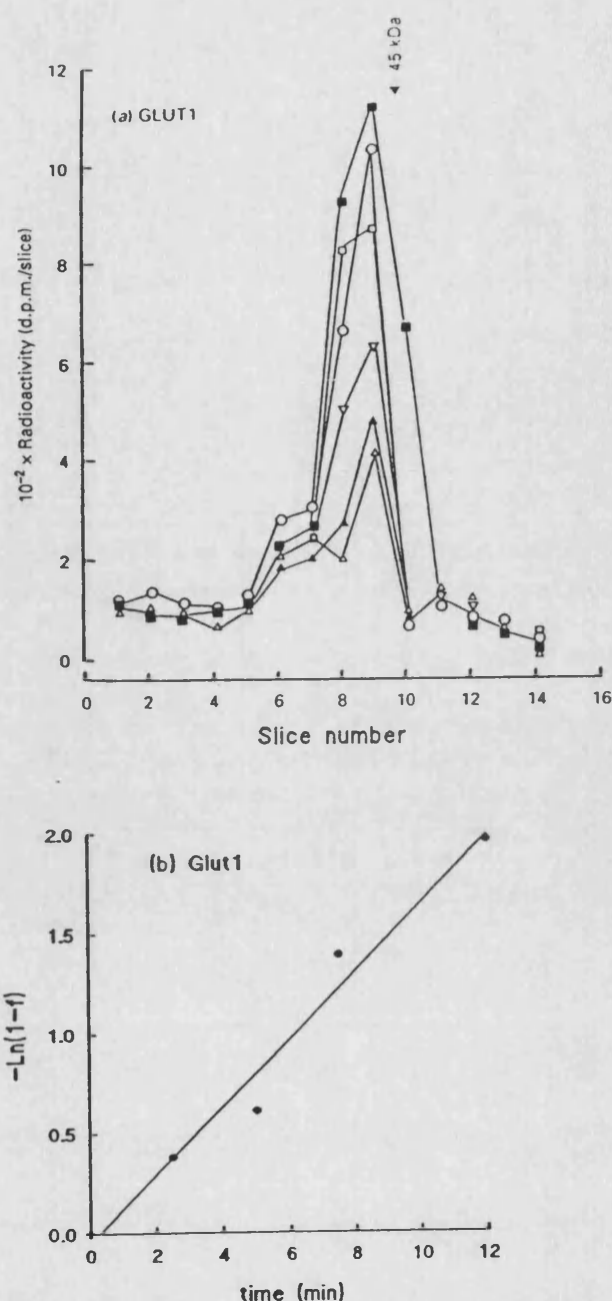


Fig.30 Insulin stimulation of the cell-surface appearance of GLUT1 in 3T3-L1 adipocytes at 27°C.

(a) 3T3-L1 adipocytes were stimulated with 100 nM insulin at 27°C and then at zero time (Δ), 2.5 min (\blacktriangle), 5 min (∇), 7 min (\square), 12 min (\circ) and 30 min (\blacksquare). The insulin was removed by washing twice in KRH buffer at 18°C. The cells were then labelled at 18°C with 100 μCi of ATB-BMPA in 250 μl of KRH buffer. Following labelling the cells were washed four times in KRH buffer and then directly solubilized in C_{12}E_9 detergent buffer. The GLUT1 was then immunoprecipitated with anti-C-terminal peptide antibodies. The protein was then subjected to electrophoresis and the radioactivity was estimated by cutting and counting gel slices.

(b) Semi-log plots of $-\ln(1-f)$ against time, f is the fraction of the maximum stimulation. The $t_{1/2} = 5.7 \pm 1.5$ min. The results are from 2 experiments. The $t_{1/2}$ values were calculated according to the equation: $t_{1/2} = (\ln 2 - a)/b$ where a is the intercept on the $-\ln(1-f)$ axis and b is the slope.

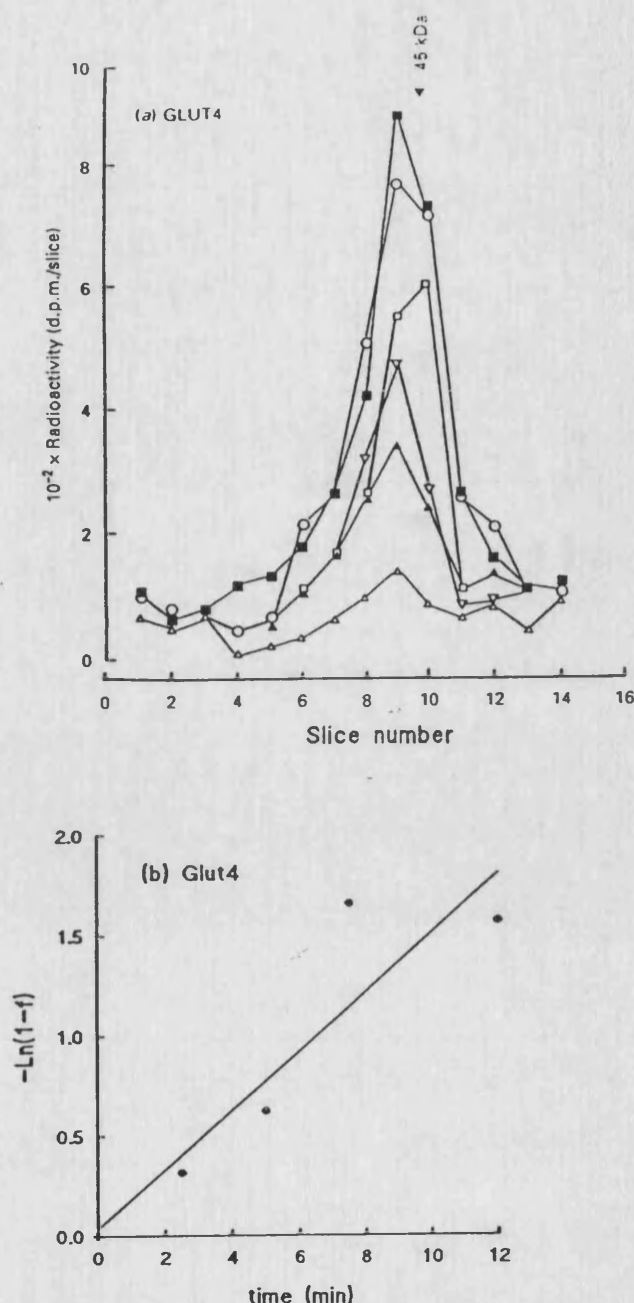


Fig.31 Insulin stimulation of the cell-surface appearance of GLUT4 in 3T3-L1 adipocytes at 27°C.

(a) 3T3-L1 adipocytes were stimulated with 100 nM insulin at 27°C and then at zero time (Δ), 2.5 min (\blacktriangle), 5 min (∇), 7 min (\square), 12 min (\circ) and 30 min (\blacksquare) the insulin was removed by washing twice in KRH buffer at 18°C. The cells were then labelled at 18°C with 100 μCi of ATB-BMPA in 250 μl of KRH buffer. Following labelling the cells were washed four times in KRH buffer and then directly solubilized in C_{12}E_9 detergent buffer. The GLUT4 was then immunoprecipitated with anti-C-terminal peptide antibodies. The protein was then subjected to electrophoresis and the radioactivity was estimated by cutting and counting gel slices.

(b) Semi-log plots of $-\ln(1-f)$ against time, f is the fraction of the maximum stimulation. The $t_{1/2} = 5.4 \pm 0.7$ min. The results are from 2 experiments. The $t_{1/2}$ values were calculated according to the equation: $t_{1/2} = (\ln 2 - a)/b$ where a is the intercept on the $-\ln(1-f)$ axis and b is the slope.

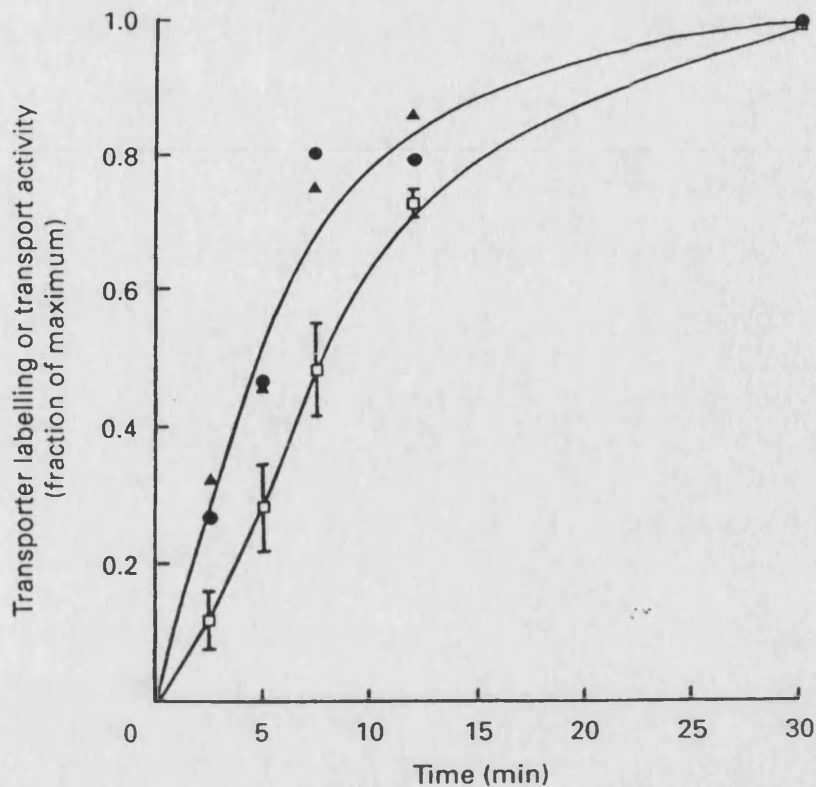


Fig.32 Time course for insulin stimulation of cell-surface availability of glucose transporters and for stimulation of 2-deoxy-D-glucose transport

Compares the time-course for insulin stimulation of cell-surface availability of glucose transporters GLUT1 (Fig.30) (●), GLUT4 (Fig.31) (▲) and for stimulation of 2-deoxy-D-glucose transport (Fig.28) (□) at 27°C. The levels of transporter labelling and transport activity at the indicated times were calculated as a fraction of the maximum determined from the samples which were stimulated with insulin for 30 min. Results shown are from 3 experiments and the average half-time for stimulation was calculated according to the equation: $t_{1/2} = (\ln 2 - a)/b$.

and the full stimulation of transport was also reported by Gibbs *et al.* 1988, Karnielli *et al.*, Clark *et al.* 1991, Satoh *et al.* 1991.

3.7 REVERSAL OF INSULIN ACTION ON GLUCOSE TRANSPORT AND LOSS OF CELL-SURFACE GLUCOSE TRANSPORTERS

The reversal of insulin stimulation might result in glucose transport phosphorylation and this modification could serve as the signal for glucose transport internalization. The binding of insulin to its receptor is known to be weaker at lower pH (Posner *et al.*, 1978), and it was found that the insulin-stimulation of transport was reversed by washing and incubating cells in buffer at pH 6.0 (Gibbs *et al.*, 1986). The time-course for the reduction of 2-deoxy-D-glucose transport activity has been examined (Fig. 33). The cells were fully stimulated by treatment with 100 nM insulin for 30 min at 37°C and then the insulin was removed by washing and incubation was carried out with MES buffer (KRM buffer) at pH 6.0 for the indicated times. The 2-deoxy-D-glucose uptake was carried out at 37°C for 5 min. The fully insulin stimulated rates were 441.27 ± 54.3 pmol/min/35 mm dish, after removal of insulin with MES buffer (KRM buffer) for 30 min the rate reached was 79 ± 1.9 pmol/min/35 mm dish and these low levels were maintained until 60 min. The half time of loss of cell-surface glucose transport activity was calculated as 6.5 ± 0.4 min. This procedure was developed by Gibbs *et al.* (1986) who showed that this low pH buffer resulted in insulin dissociation and a consequent reduction in transport activity. In Fig. 34 and Fig. 35, the cells were treated in the same way as above. Cells were insulin stimulated for 30 min and then insulin was removed with MES buffer (KRM buffer) at the indicated time. The cells were exposed to 100 μ Ci of ATB-BMPA for 3 min at 18°C and then irradiated for 1 min in the uv lamp . The cells were solubilized with detergent buffer and the immunoprecipitation was carried out to determine the loss of from the cell surface of GLUT1 and GLUT4. The calculated half-time for loss of cell surface GLUT1 was 9.2 ± 0.8 min and for

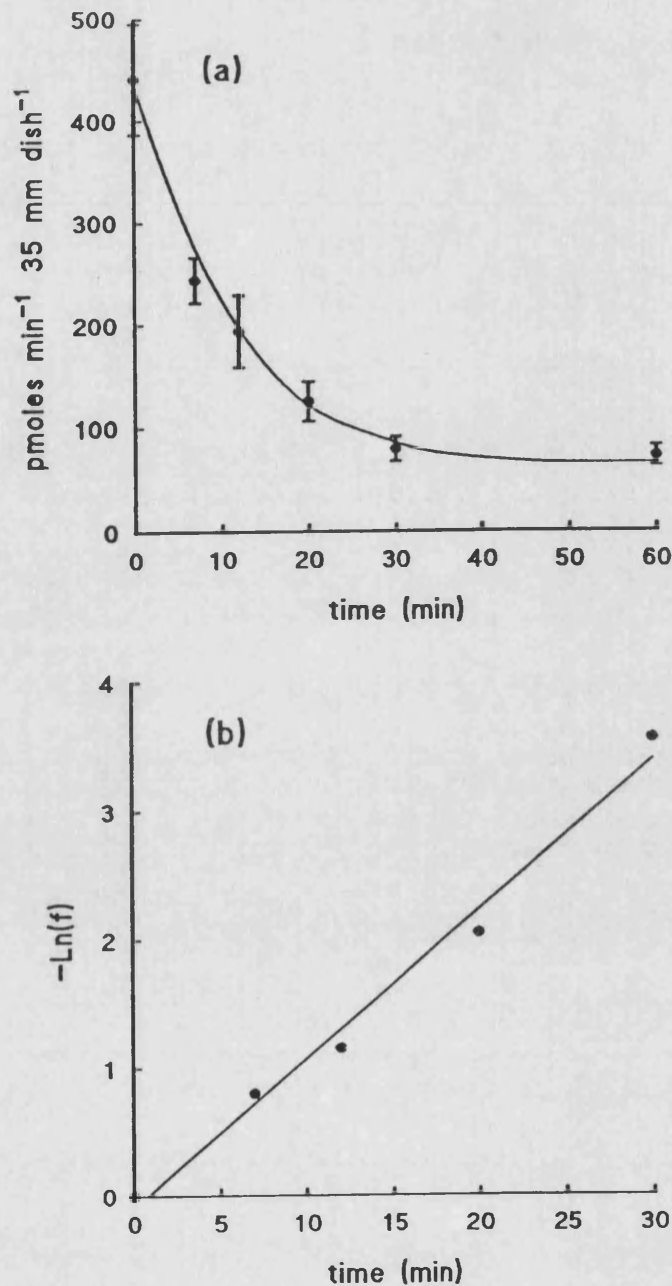


Fig.33 Time course of 2-deoxy-D-glucose transport activity for the reversal of insulin stimulation.

(a) 3T3-L1 adipocytes were stimulated with 100 nM insulin for 30 min at 37°C and then insulin was removed by washing twice with MES buffer and by maintaining the cells in this buffer for the indicated times. The cells were washed in KRH buffer at 18°C and then 2-deoxy [2,6- ^3H]-D- glucose (50 μM) uptake was measured over 2.5 min. The cells were washed four times with KRH buffer and dissolved in 0.1 M NaOH and the radioactivity was counted.

(b) Semi-log plots of $-\text{Ln}(f)$ against time, f is the fraction of the maximum stimulation. The $t_{1/2}$ for reversal insulin stimulation at glucose transport was 6.5 ± 0.4 min. The results were from 3 experiments. The $t_{1/2}$ values were calculated according to the equation: $t_{1/2} = (\ln 2 - a)/b$ where a is the intercept on the $-\text{Ln}(f)$ axis and b is the slope.

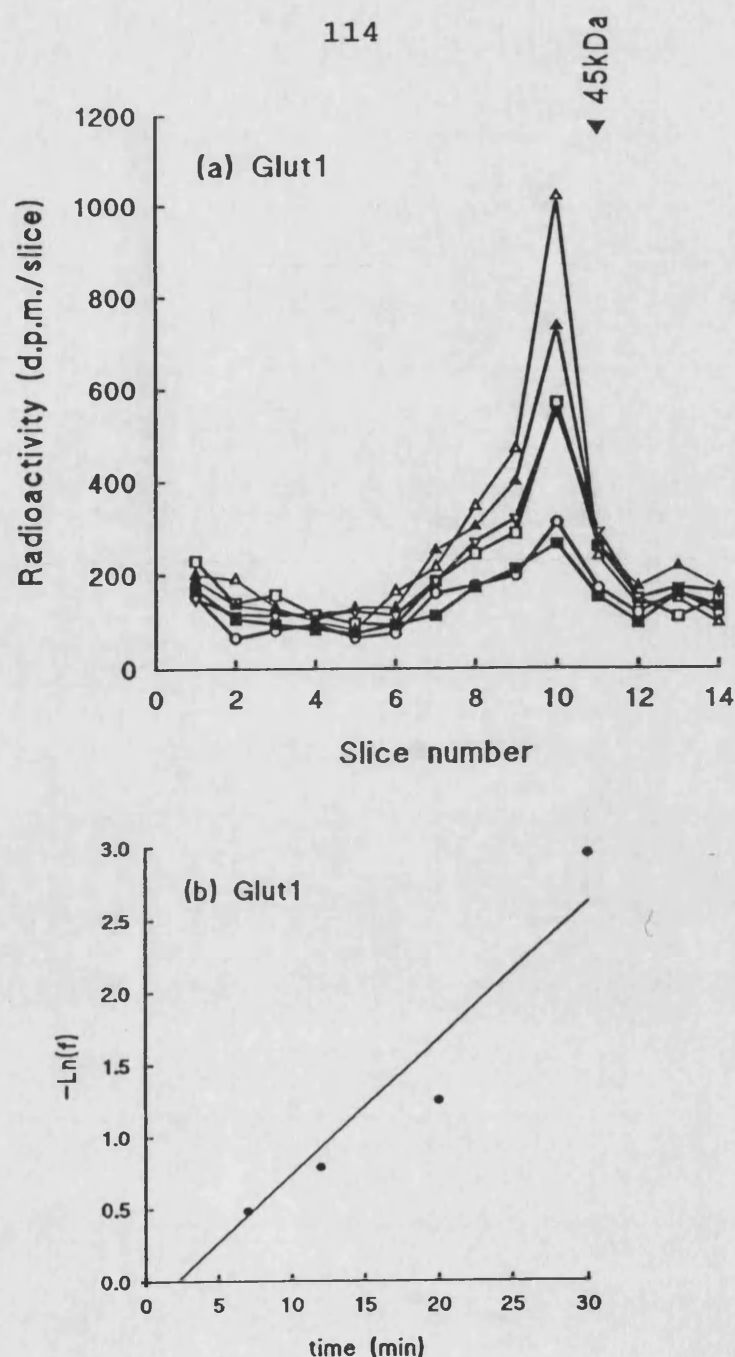


Fig.34 Time course of ATB-BMPA labelled cell-surface GLUT1 for the reversal of insulin stimulation in 3T3-L1 adipocytes.

(a) 3T3-L1 adipocytes were stimulated with insulin for 30 min at 37°C and then insulin was removed by washing twice with MES buffer and by maintaining this buffer for zero time (Δ), 7 min (▲), 12 min (▽), 20 min (□), 30 min (○) and 60 min (■). The cells were washed twice in KRH buffer at 18°C and then photolabelled with 100 μ Ci of ATB-BMPA. Following labelling the cells were washed four times with KRH buffer and then directly solubilized in C₁₂E₉ detergent buffer. The levels of the GLUT1 transporters were determined by immunoprecipitation and electrophoresis.

(b) Semi-log plots of $-\ln(f)$ against time, f is the fraction of the maximum stimulation. The $t_{1/2} = 9.2 \pm 0.8$ min. The results were from 2 experiments. The $t_{1/2}$ values were calculated according to the equation: $t_{1/2} = (\ln 2 - a)/b$ where a is the intercept on the $-\ln(f)$ axis and b is the slope.

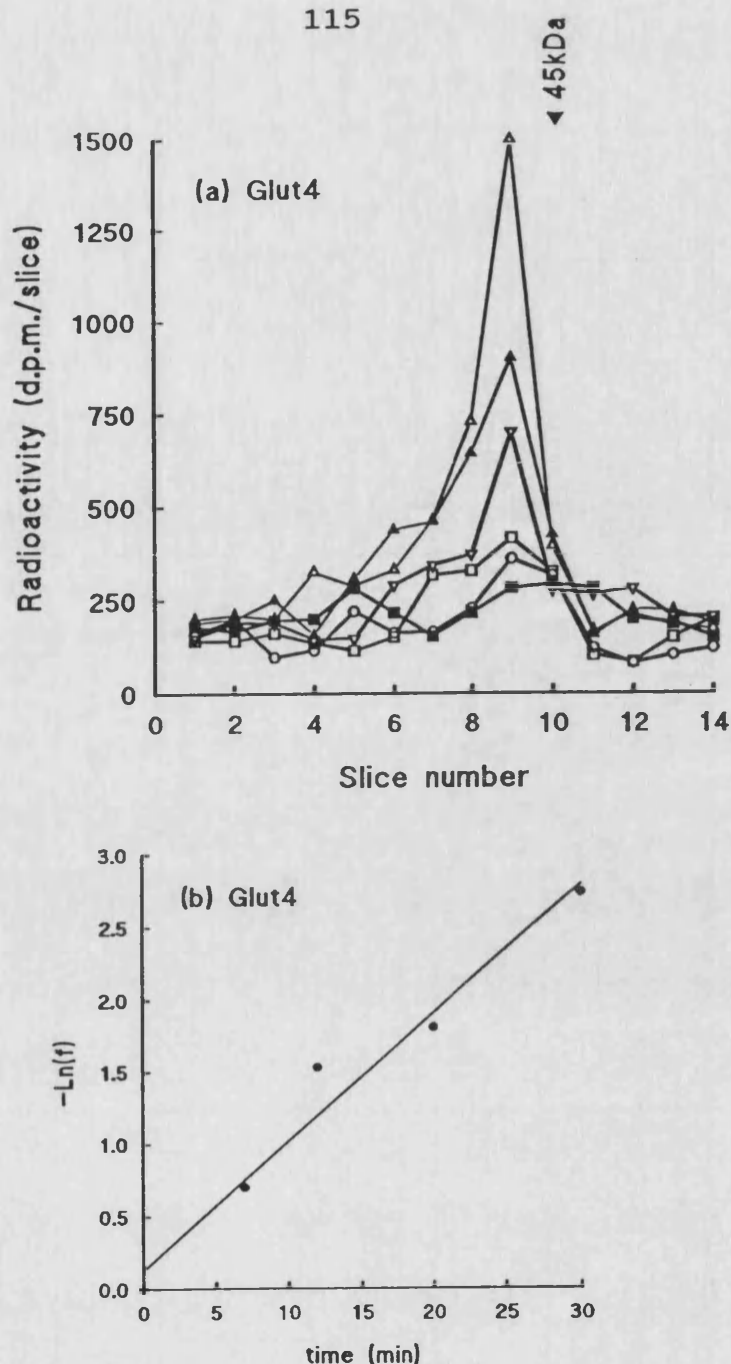


Fig.35 Time course of ATB-BMPA labelled cell-surface GLUT4 for the reversal of insulin stimulation in 3T3-L1 adipocytes.

(a) 3T3-L1 adipocytes were stimulated with insulin for 30 min at 37°C and then insulin was removed by washing twice with MES buffer and by maintaining this buffer for zero time (Δ), 7 min (\blacktriangle), 12 min (∇), 20 min (\square), 30 min (\circ) and 60 min (\blacksquare). The cells were washed twice in KRH buffer at 18°C and the photolabelled with 100 μ Ci of ATB-BMPA. Following labelling the cells were washed four times in KRH buffer and then directly solubilized in $C_{12}E_9$ detergent buffer. The levels of the GLUT4 transporters were determined by immunoprecipitation and electrophoresis.

(b) Semi-log plots of $-\ln(f)$ against time, f is the fraction of the maximum stimulation. The $t_{1/2} = 6.8 \pm 1.7$ min. The results were from 2 experiments. The $t_{1/2}$ values were calculated according to the equation: $t_{1/2} = (\ln 2 - a)/b$ where a is the intercept on the $-\ln(f)$ axis and b is the slope.

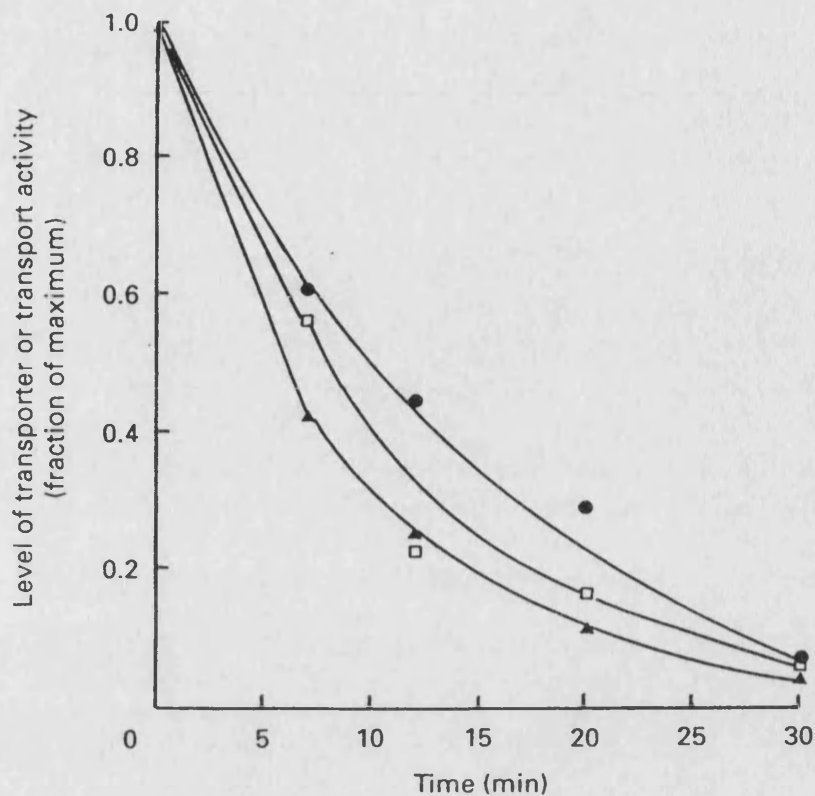


Fig.36 Time course for the reversal of insulin stimulation.

The time course for the reversal of insulin stimulation on labelling the levels of the GLUT1 (Fig.34) (●) and GLUT4 (Fig.35) (□) transporters and 2-deoxy-D-glucose transport activity (Fig.33) (▲) were compared in 3T3-L1 adipocytes. The levels of transporter labelling and transport activity at the indicated times were calculated as a fraction of the maximum determined. The results shown are the mean of two photolabelling experiments and three experiments to determine transport activity.

GLUT4 it was 6.8 ± 1.7 min (both results were from two experiments). This correlates well with the decrease in 2-deoxy-D-glucose-transport activity of 6.5 ± 0.4 min (three experiments). The comparison of glucose transport activity and the cell surface labelling of GLUT1 and GLUT4 is shown in Fig. 36. The decrease in cell-surface GLUT4 was slightly more extensive than for GLUT1, possibly reflecting the greater tendency of GLUT1 to be re-exocytosed in the absence of insulin.

3.8 EFFECT OF PHENYLARSINE OXIDE ON GLUT1 AND GLUT4 TRAFFICKING

3.8.1 The effect of low concentration PAO on basal glucose transport

A number of effects of phenylarsine oxide on the glucose transport activity in basal 3T3-L1 cells have been noted. Frost and Lane (1985) reported that PAO reduced the insulin stimulation of transport activity but had no effect on the transport activity of basal cells. However, Gould *et al.* (1988) reported that at low concentrations of PAO (of $< 20 \mu\text{M}$) a stimulation of the basal rate of transport occurred. Surprisingly, at concentrations of PAO where a transport stimulation was noted they found a decrease in cell-surface transporters (as detected by cell-surface labelling with sodium borotritide of galactose oxidase treated cells) and a rise in plasma-membrane associated GLUT1 as detected by western blotting. Therefore the transport activity after treatment with 1-20 μM PAO in the basal state was examined. The Fig. 37 shows the transport rate after 1-20 μM PAO treatment. A maximum rate was achieved at 10 μM and this gave a ≈ 1.5 -fold increase in 2-deoxy-D-glucose transport activity. To determine the changes on cell surface glucose transporter after 10 μM PAO treatment, the cells were labelled with 100 μCi ATB-BMPA. As shown in Fig. 38 and Fig. 39. 10 μM PAO gave no detectable rise in either the concentration of GLUT1 or GLUT4. It is clear from this result, however, that any effect of PAO on basal levels of transporters is very small in comparison with the

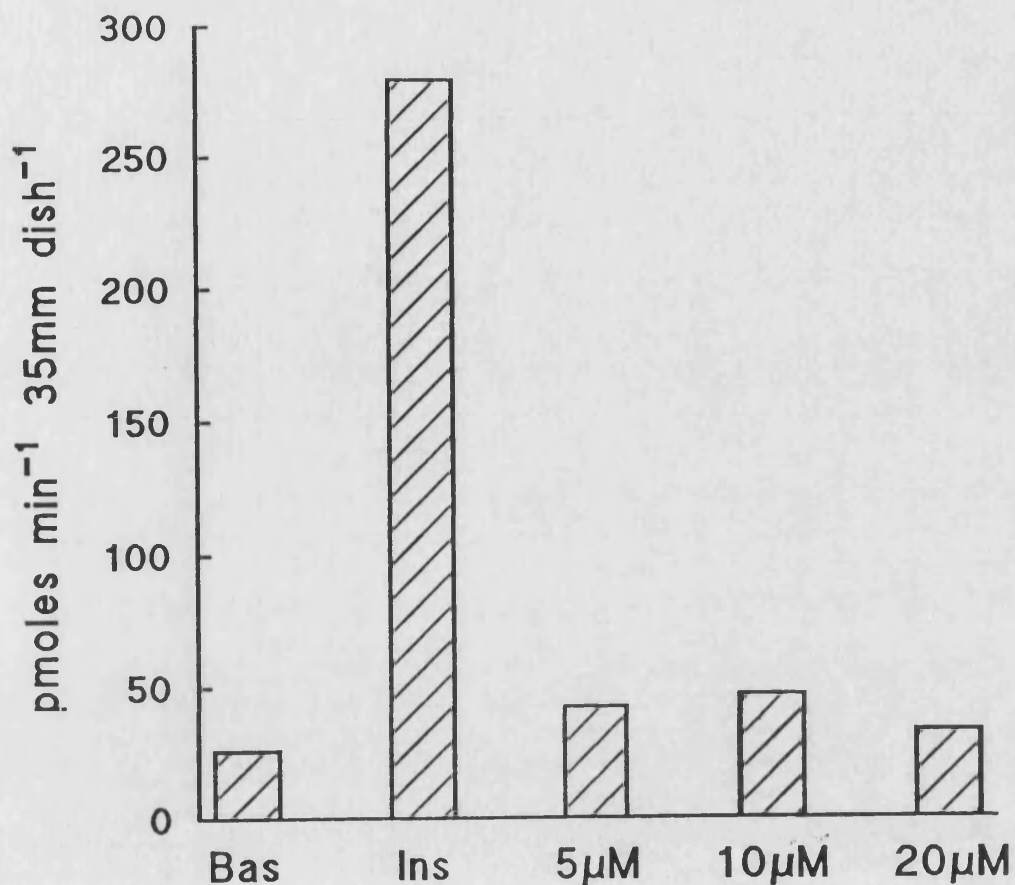


Fig.37 Effect of different concentration of PAO on 2-deoxy-D-glucose transport activity.

3T3-L1 adipocytes were incubated with 5 μ M, 10 μ M and 20 μ M of PAO, or without PAO for 30 min at 37°C. The 2-deoxy [2,6-³H]-D-glucose (50 μ M) uptake was measured over 5 min. The cells were dissolved in 0.1 M NaOH and the radioactivity was counted.

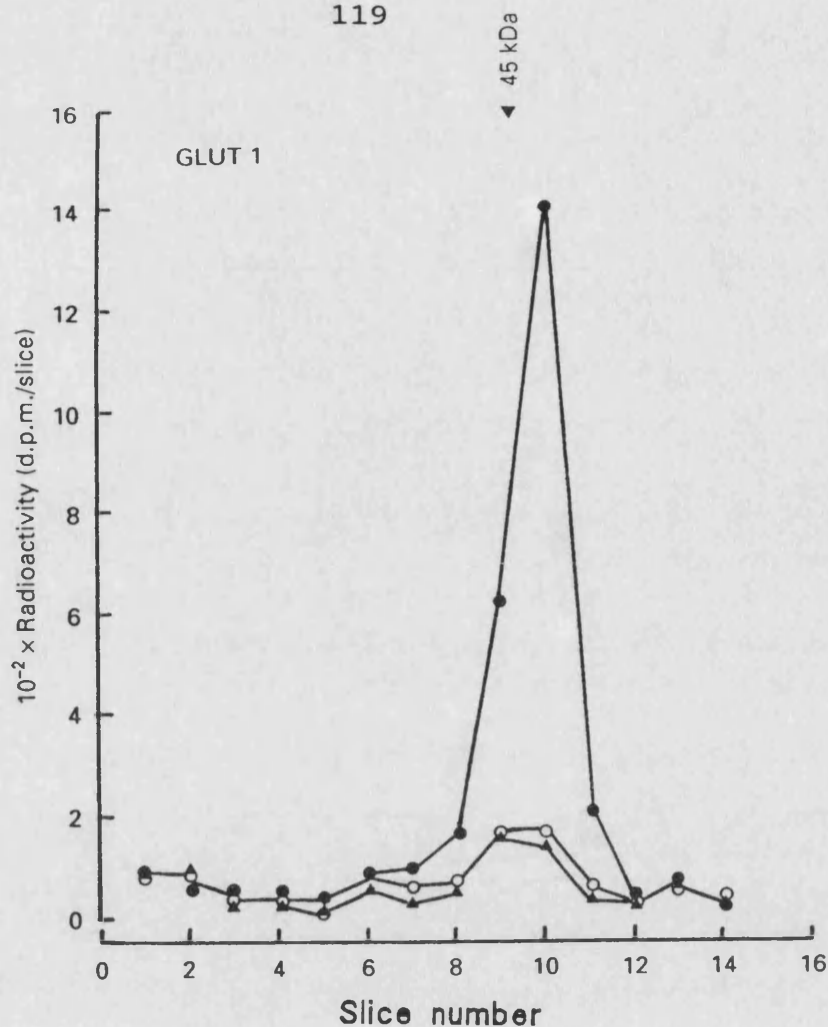


Fig.38 Effect of PAO and insulin on the cell-surface photolabelling of GLUT1.

3T3-L1 adipocytes cells were maintained either with no additions (○) , with 100 nM insulin (●) , or with 10 μ M phenylarsine oxide (▲) for 30 min at 37°C. The cells were then labelled with 150 μ Ci of ATB-BMPA. Following labelling the cells were washed four times in KRH buffer and then directly solubilized in C₁₂E₉ detergent buffer. The GLUT1 was immunoprecipitated with anti-C-terminal peptide antibodies. The protein was then subjected to electrophoresis and the radioactivity was estimated by cutting and counting gel slices.

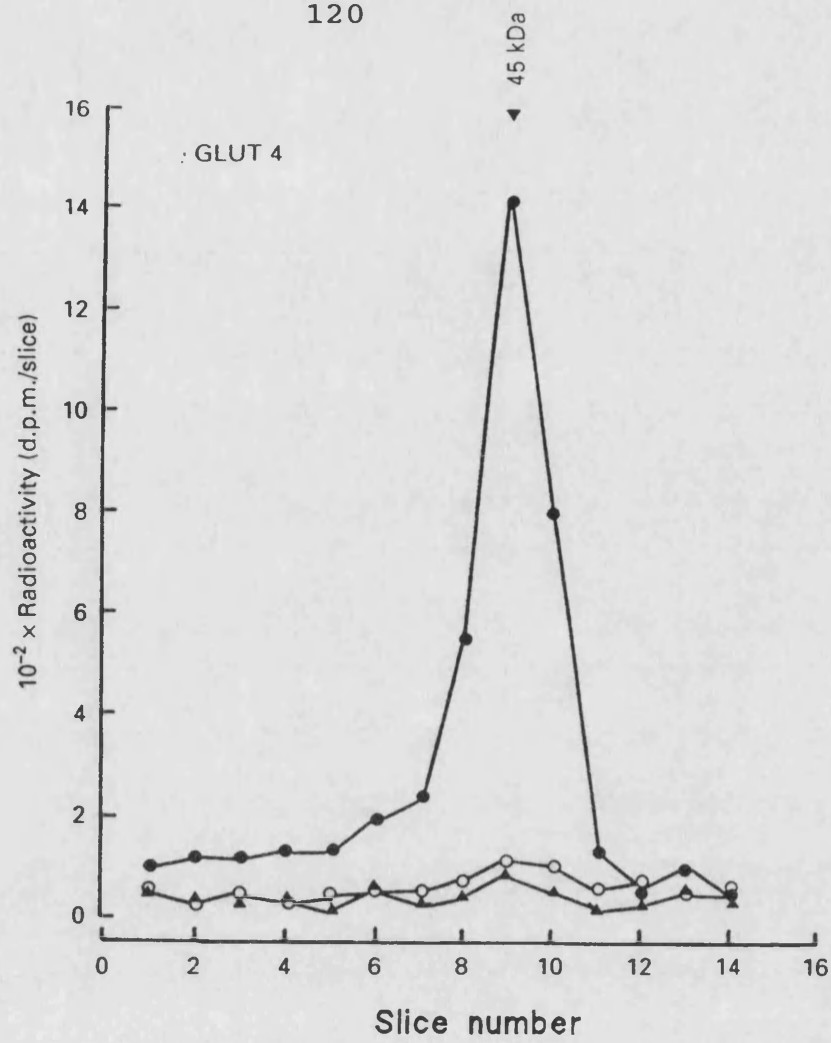


Fig.39 Effect of PAO and insulin on the cell-surface photolabelling of GLUT4.

3T3-L1 adipocytes cells were maintained either with no additions (O) , with 100 nM insulin (●), or with 10 μ M phenylarsine oxide (▲) for 30 min at 37°C. The cells were then labelled with 150 μ Ci of ATB-BMPA. Following labelling the cells were washed four times in KRH buffer and then directly solubilized in C₁₂E₉ detergent buffer. The GLUT4 was immunoprecipitated with anti-C-terminal peptide antibodies. The protein was then subjected to electrophoresis and the radioactivity was estimated by cutting and counting gel slices.

stimulating effect of insulin.

3.8.2 The effect of 20 μ M PAO on glucose transport activity

Frost and Lane have reported in 1985 that maximal inhibition of insulin-activated sugar uptake was achieved at 20 μ M PAO, so this concentration was used in this studies. Fully insulin-stimulated 3T3-L1 cells (30 min) were treated with 20 μ M phenylarsine oxide for 7.5, 12.5, 22.5, 32.5, and 57.5 min at 37°C and then the 2-deoxy-D-glucose uptake was measured for 2.5 min at 37°C. When PAO was added to fully insulin stimulated cells, the transport activity declined slowly toward the basal rate ($t_{1/2}$ = 9.8 min. The result is shown in Fig.40). This correlates well with the results of Frost and Lane in which they found the half maximal time is 10 min. This result suggest that phenylarsine oxide blocks the movement of transporters from one compartment to another, specifically from the intracellular location to the plasma membrane. However, in the "activated" state when most of the glucose transporters are already at the plasma membrane as monitored by transport rate in Fig. 40, phenylarsine oxide dose not block the re-entry of the transporter back to its internal "inactive" site. This is in contrast to the effects of other thiol-reactive reagents which block not only activation but also reversion to the basal state (Czech, 1976).

3.8.3 The effect of PAO on the availability of GLUT1 and GLUT4 in insulin stimulated 3T3-L1 adipocytes

The time course of changes in the uptake of 2-deoxy-D-glucose from 20 μ M PAO treated 3T3-L1 cells after full insulin stimulation have show that the maximum effect of inhibitor occurs before 60 min. Therefore, treatment of fully insulin-stimulated 3T3-L1 cells with 20 μ M PAO was for 60 min followed by labelling with ATB-BMPA (100 μ Ci). This markedly reduced the cell-surface level of the GLUT4 isoform. However, the level of the GLUT1 isoform was only slightly reduced (see

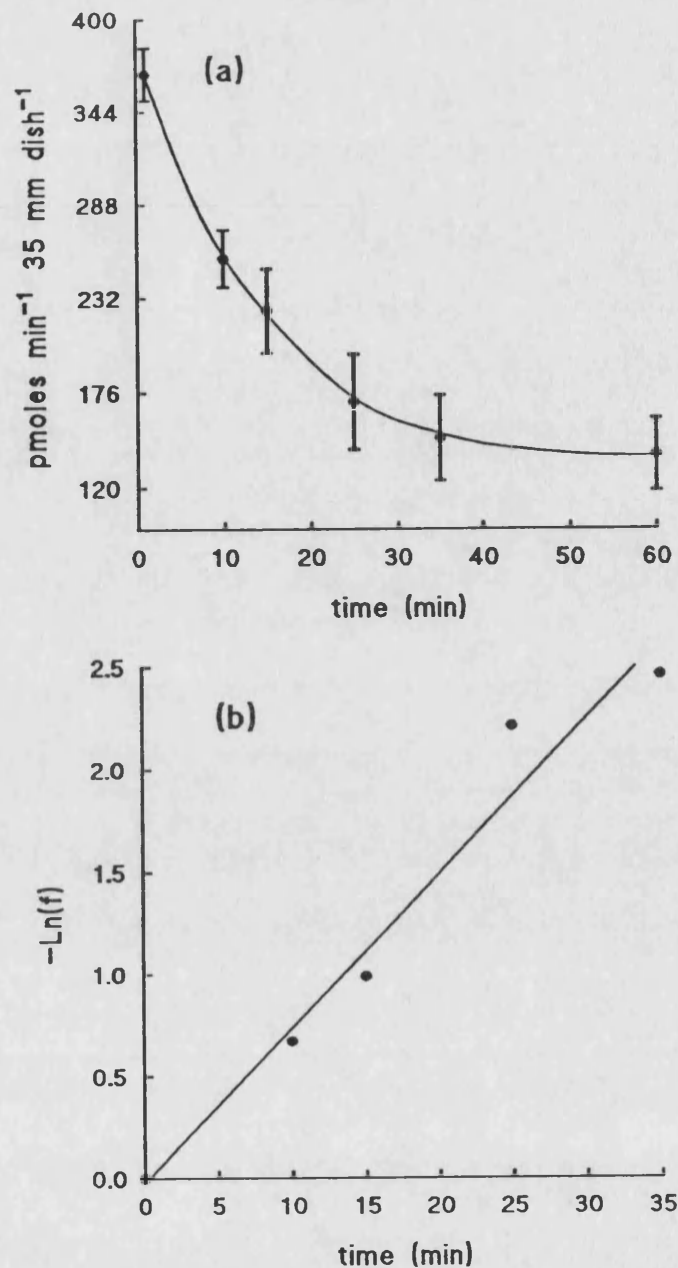


Fig.40 Time course for the PAO-induced loss of 2-deoxy-D-glucose transport activity in 3T3-L1 adipocytes.

(a) 3T3-L1 adipocytes were stimulated with 100 nM insulin for 30 min at 37°C. At zero time insulin was removed and 20 μ M PAO was added for 7.25 min, 12.5 min, 22.5 min, 32.5 min and 57.5 min and at indicated time the 2-deoxy-[2,6-³H] glucose (50 μ M) was measured for 2.5 min. The cells were dissolved in 0.1 M NaOH and the radioactivity was counted.

(b) Semi-log plots of $-\ln(f)$ against time, f is the fraction of the maximum stimulation. The $t_{1/2} = 9.8 \pm 1.6$ min. The results from 3 experiments. The $t_{1/2}$ values were calculated according to the equation: $t_{1/2} = (\ln 2 - a)/b$ where a is the intercept on the $-\ln(f)$ axis and b is the slope.

Fig. 41). To further examine the kinetics of trafficking in insulin stimulated 3T3-L1 adipocytes which were treated with PAO, the time-course for the PAO induced loss of cell-surface transporters was determined by labelling with 100 μ Ci ATB-BMPA. Again, the cells were first stimulated with insulin for 30 min at 37°C and then 20 μ M PAO was added at the indicated times. The cells were then labelled and subjected to immunoprecipitation. The ATB-BMPA labelled cell surface GLUT1 is shown in Fig. 42 and GLUT4 is shown in Fig. 43. The time course for the PAO induced loss of the cell-surface transporters was also compared with the reduction in 2-deoxy-D-glucose transport activity in Fig. 44. The loss of transport activity and GLUT4 occurred with half-times of 9.8 ± 1.6 and 7.8 ± 0.8 min respectively (from two experiments) which were similar to the half-time for the reduction of transport activity that occurred when insulin was removed by the low pH washing procedure (Fig.33). In contrast to this, the level of cell-surface GLUT1 remained high during the PAO treatment. During the PAO treatment the half-time for the reduction in cell-surface GLUT1 was greater than 60 min and was much slower than the half-time for the loss of GLUT1 which occurred when insulin was removed by the low pH washing procedure and which was only ≈ 9 min. To confirm that the reduction in GLUT4 was due to a redistribution of these transporters within the cell and not to an irreversible inhibition of transport (Douen and Jones, 1988), the binding of ATB-BMPA to the transporters in permeabilized cells has been measured. The cells were permeabilized by treatment with 0.025% digitonin. This treatment can allow the membrane impermeant label to enter the inside of the cell and the total intracellular pool of glucose transporter can then be labelled. Fig. 45 shows that the total concentration of available GLUT4 was only slightly reduced (by $\approx 30\%$). This slight reduction may have occurred because the efficiency of labelling transporters present inside the cell may have been slightly less than for surface labelling. To further confirm this finding, Western blotting was carried out in 3T3-L1 cells. The γ -count results are shown in Fig.46. This indicated that neither GLUT1 nor GLUT4 was lost from the cells by Western blotting crude membrane fractions obtained from cells treated with

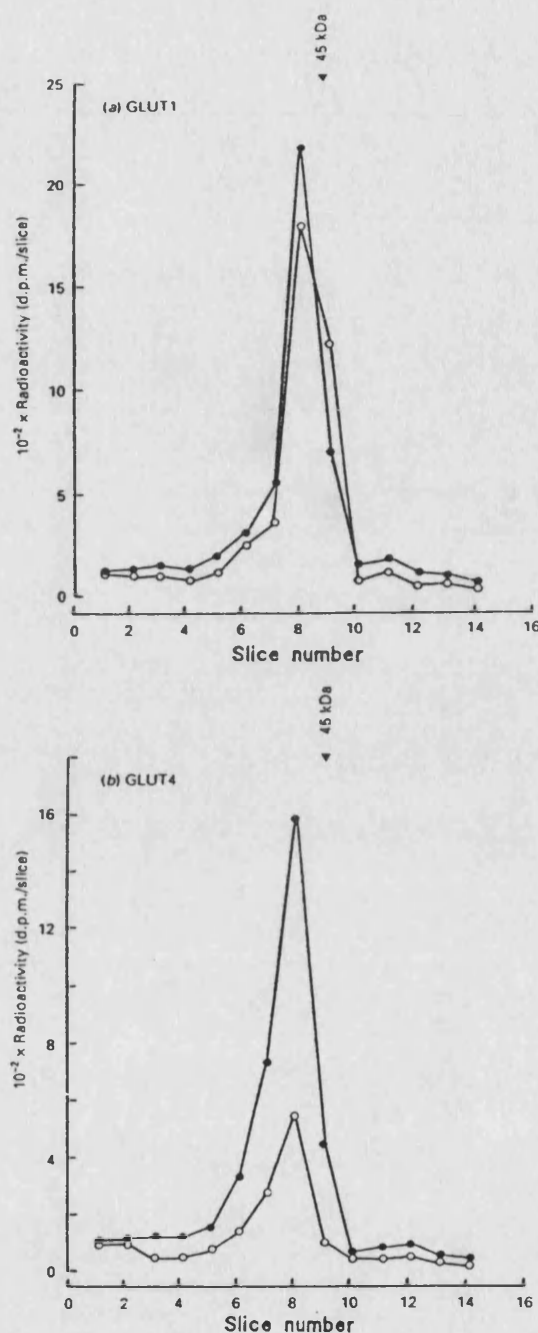


Fig.41 Comparison of the effect of 20 μ M PAO on the availability of GLUT1 and GLUT4 in insulin-treated 3T3-L1 adipocytes.

3T3-L1 cells in 35 mm dishes were fully stimulated by treatment with 100 nM insulin for 30 min at 37°C. The cells were then maintained at 37°C for a further 60 min in the presence (○) and the absence (●) of 20 μ M phenylarsine oxide. The cells were then photolabelled with 100 μ Ci of ATB-BMPA and then the GLUT1 (a) and GLUT4 (b) were immunoprecipitated with anti-C-terminal peptide antibodies. The protein was then subjected to electrophoresis and the radioactivity was estimated by cutting and counting gel slices.

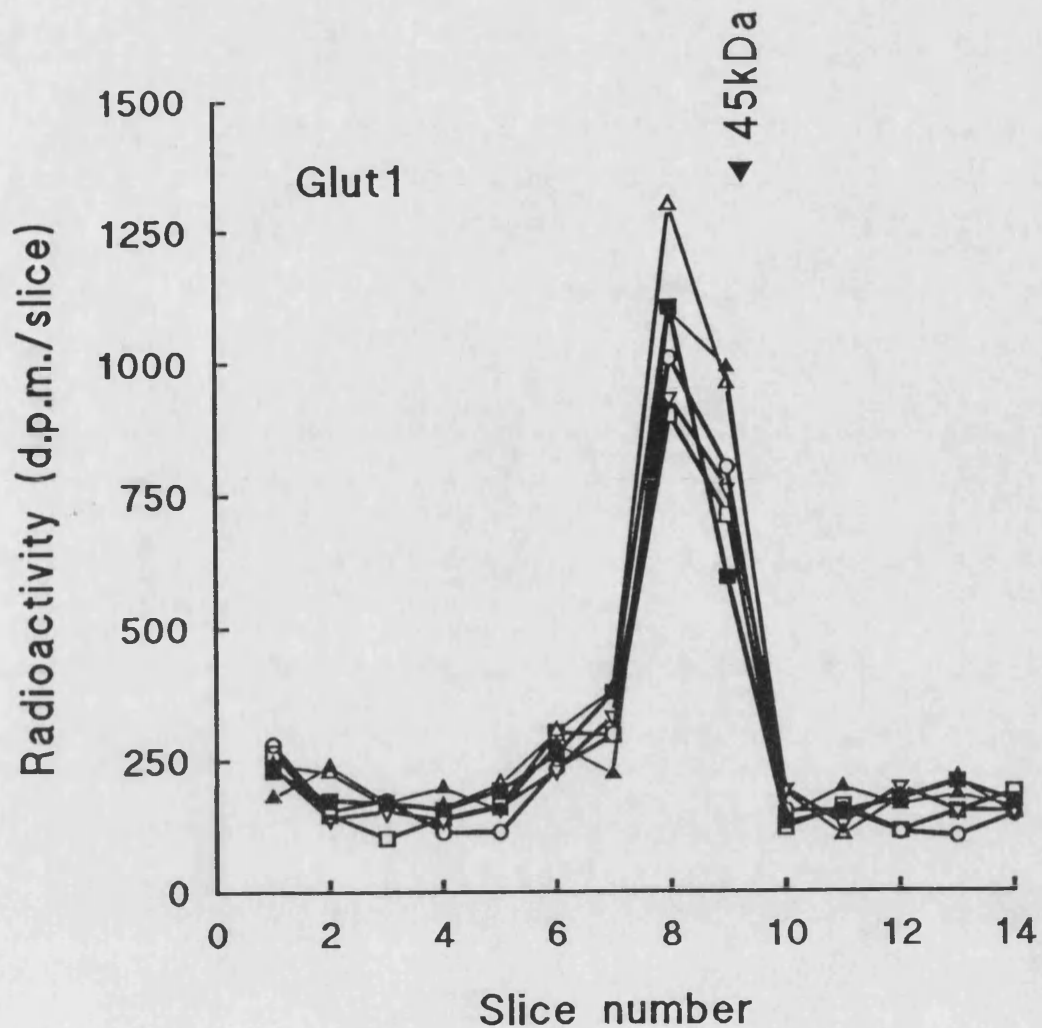


Fig.42 Time course of the PAO-induced loss of cell-surface GLUT1 in 3T3-L1 adipocytes.

3T3-L1 adipocytes were stimulated with 100 nM insulin for 30 min at 37°C. At zero time (Δ) insulin was removed and 20 μM PAO was added for 10 min (▲), 15 min (▽), 25 min (□), 35 min (○) and 60 min (■). At indicated time the 20 μM PAO was removed and the cells were photolabelled with 100 μCi of ATB-BMPA. Following labelling the cells were washed four times in KRH buffer and then directly solubilized in C₁₂E₉ detergent buffer. The GLUT1 were immunoprecipitated with anti-(C-terminal peptide) antibodies. The protein was then subjected to electrophoresis and the radioactivity was estimated by cutting out and counting gel slices.

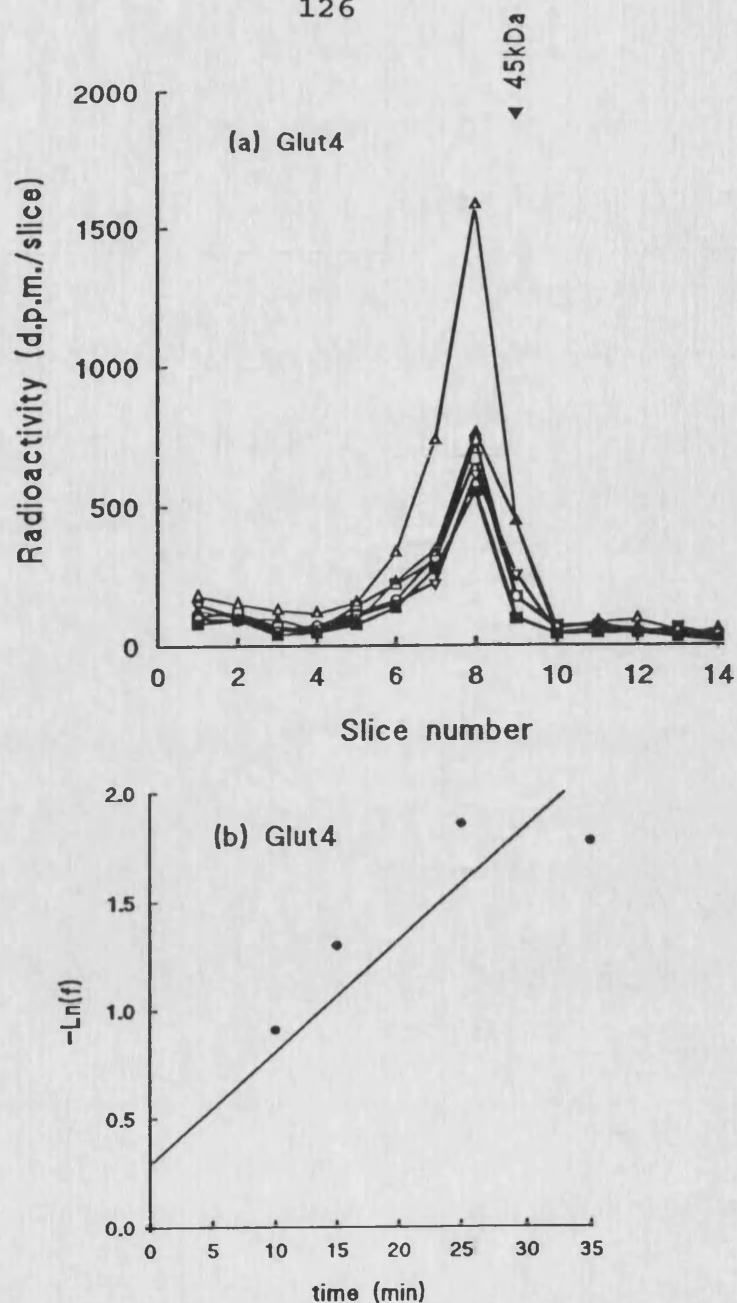


Fig.43 Time course of the PAO-induced loss of cell-surface GLUT4 in 3T3-L1 adipocytes.

3T3-L1 adipocytes were stimulated with 100 nM insulin for 30 min at 37°C. At zero time (Δ) insulin was removed and 20 μ M PAO was added for 10 min (\blacktriangle), 15 min (∇), 25 min (\square), 35 min (\circ) and 60 min (\blacksquare). At indicated time the 20 μ M PAO was removed and the cells were photolabelled with 100 μ Ci of ATB-BMPA. Following labelling the cells were washed four times in KRH buffer and then directly solubilized in $C_{12}E_9$ detergent buffer. The GLUT4 were immunoprecipitated with anti-(C-terminal peptide) antibodies. The protein was then subjected to electrophoresis and the radioactivity was estimated by cutting out and counting gel slices.

(b) Semi-log plots of $-\ln(f)$ against time, f is the fraction of the maximum stimulation. The $t_{1/2} = 7.8 \pm 0.8$ min. The results were from 2 experiments. The $t_{1/2}$ values were calculated according to the equation: $t_{1/2} = (\ln 2 - a)/b$ where a is the intercept on the $-\ln(f)$ axis and b is the slope.

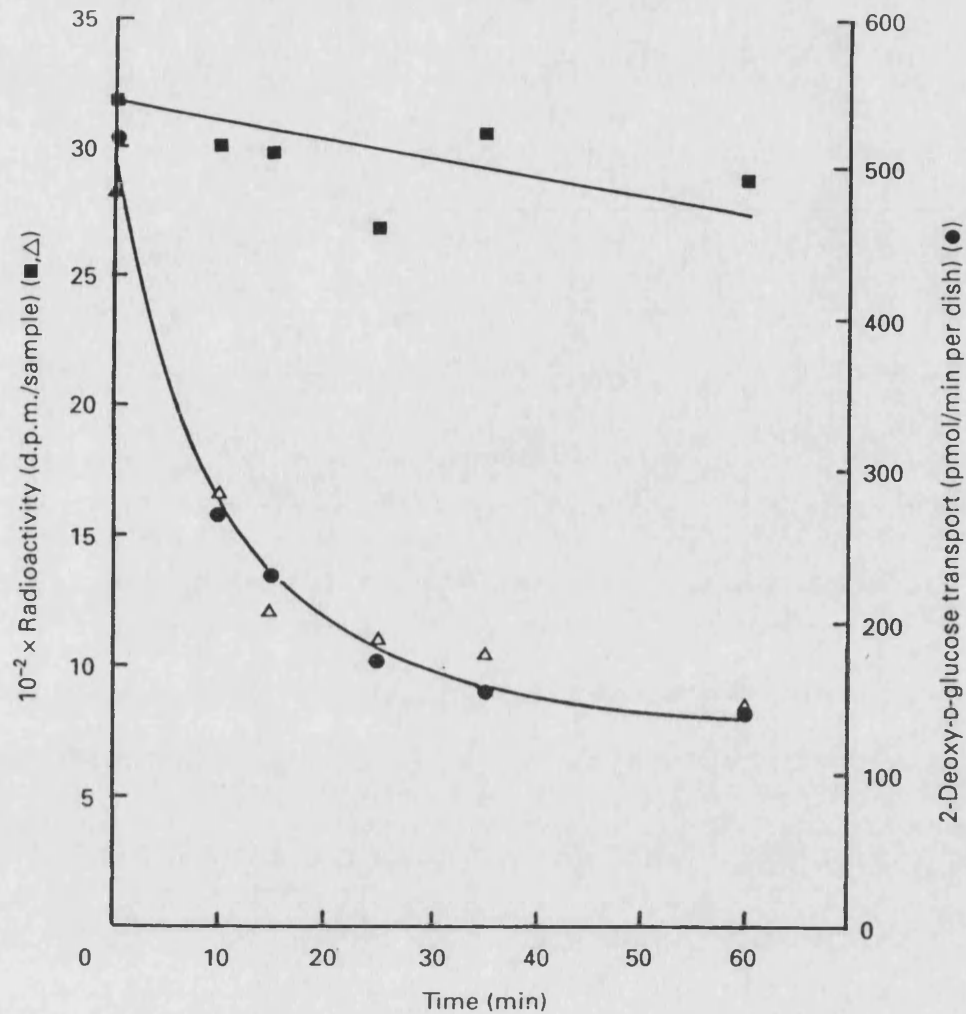


Fig.44 Time course for the PAO-induced loss of cell-surface transporters and transport activity.

20 μ M PAO treatment of fully insulin-stimulated 3T3-L1 cells was carried out as described in Fig.42 and Fig. 43. The total radioactivity associated with photolabelled GLUT1 (■) in Fig.42 and GLUT4 (Δ) in Fig.43 was compared with the loss of 2-deoxy-D-glucose transport activity (●) in Fig.40. The results are the mean of two photolabelling experiments and three experiments to determine transport activity.

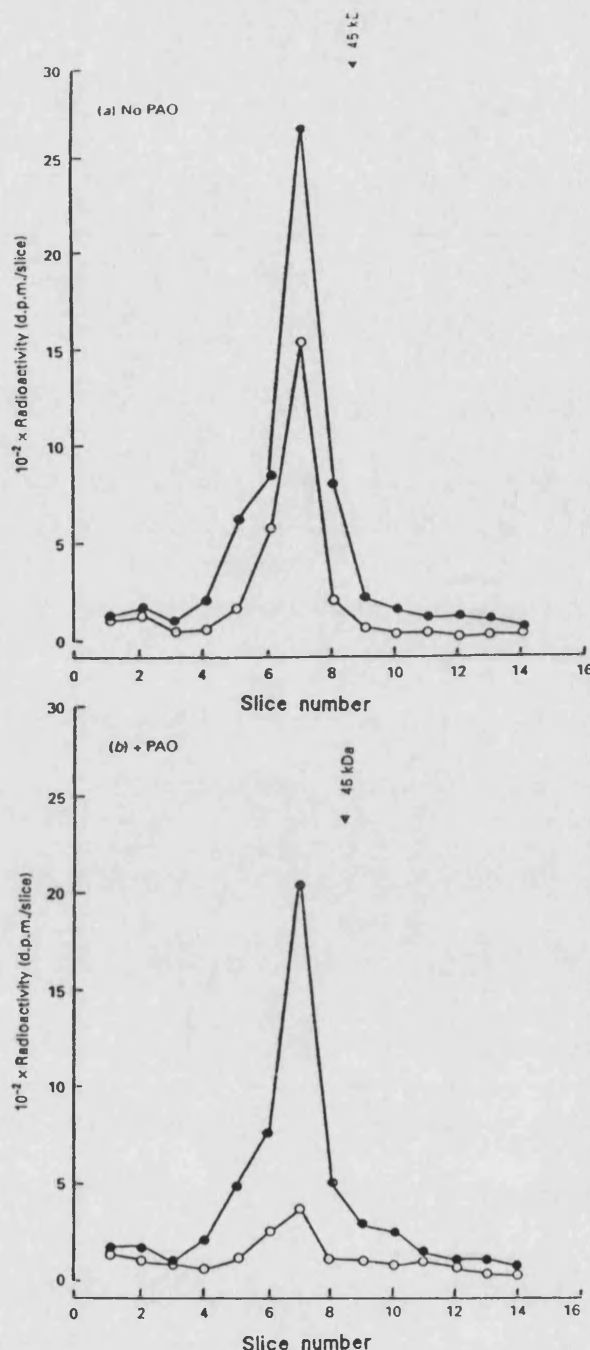


Fig.45 Experiment to determine whether the PAO-induced decrease in cell-surface GLUT4 is due to a redistribution to the cell interior.

3T3-L1 adipocytes cells were fully stimulated by treatment with 100 nM insulin for 30 min at 37°C. The cells were then maintained at this temperature for a further 50 min in the absence (a) or in the presence (b) of 20 μ M PAO. The cells were then either photolabelled directly with 100 μ Ci of ATB-BMPA (○) or were permeabilized in the presence of 100 μ Ci of ATB-BMPA by treatment with 0.025% digitonin for 8 min at 18°C (●). GLUT4 was then immunoprecipitated with anti-C-terminal antibody. The protein was then subjected to electrophoresis and the radioactivity was estimated by cutting and counting gel slices.

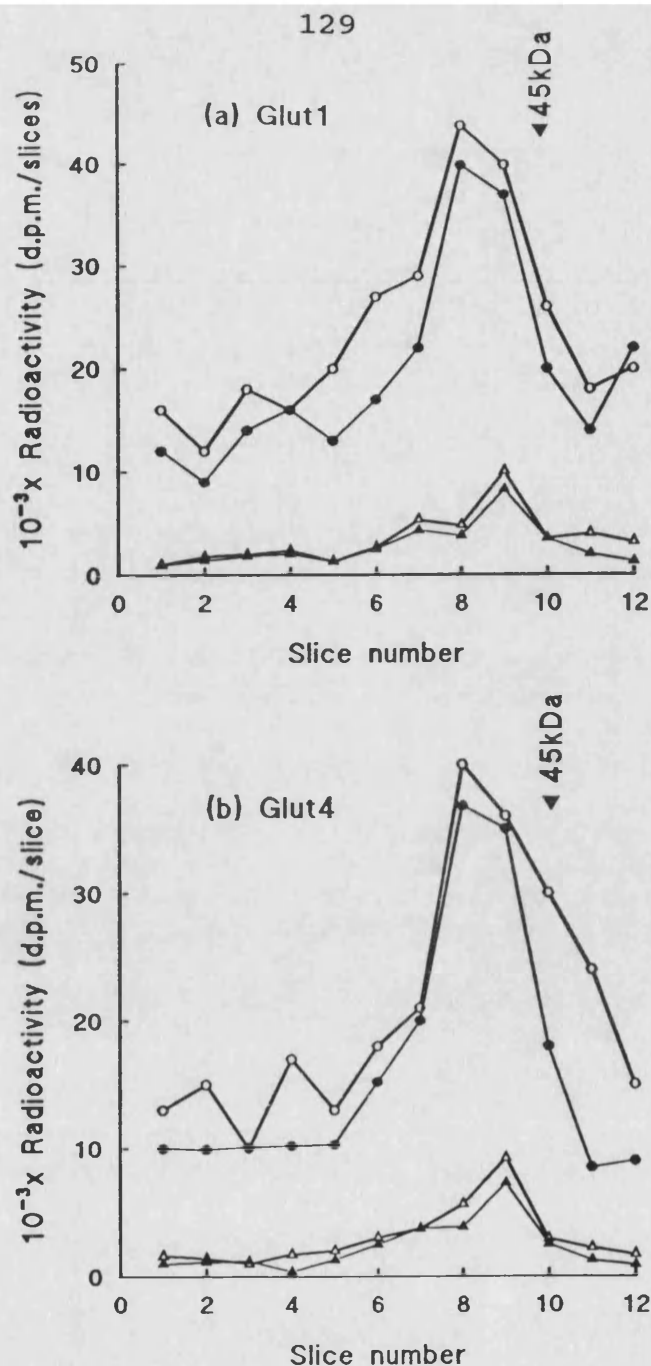


Fig.46 To test if GLUT1 and GLUT4 internalization to the light-microsome fraction was increased by the PAO treatment compared with insulin alone.

3T3-L1 adipocytes were fully stimulated with 100 nM insulin for 30 min at 37°C. The cells were then maintained at 37°C for a further 60 min in the presence (open symbols) or absence (closed symbols) of 20 μ M PAO. 50 μ g protein from Crude plasma membrane (O) and microsome (Δ) were subjected to SDS-PAGE. Proteins were transferred to nitrocellulose paper and incubated with a 1:500 dilution of anti-GLUT1 and anti-GLUT4 antibody. Blots were developed with 125 I labelled protein A and quantified by gamma counting.

insulin and then 20 μ M PAO. The more striking effect of PAO treatment was to reduce just the GLUT4 at the cell-surface. In the cells treated with insulin alone $\approx 60\%$ of the available transporter was at the cell surface. In the cells treated with PAO $\approx 20\%$ of the available transporters were at the surface. In addition, by measuring ATB-BMPA photolabelling in permeabilized cells, it was found that the total available GLUT1 concentration was only slightly reduced following PAO treatment. Approximately 60% of the available GLUT1 transporters were at the surface both in the presence and in the absence of PAO.

A possible interpretation of this differential effect on GLUT1 and GLUT4 cell-surface availability is that in the presence of PAO both transporters are removed from the cell-surface at the same rate but their recycling is differentially perturbed. Thus both GLUT1 and GLUT4 could be endocytosed even in the presence of PAO but inhibition of GLUT4, but not GLUT1, re-emergence and re-exposure to the photolabel at the cell-surface could then have resulted in the observed fall in its detected surface concentration.

3.8.4. Effect of PAO on internalization of GLUT1 and GLUT4

To examine the possibility that both transporters were internalized in the presence of PAO, the cell-surface transporters in fully insulin-stimulated cells was labelled with ATB-BMPA and then treated with PAO and insulin for a further 60 min. The cells then were homogenised and a crude plasma membrane fraction was separated from the light-microsome fraction. After 60 min in the continuous presence of insulin the light-microsome level of photolabelled GLUT1 and GLUT4 was increased above that observed at zero time (Fig. 47 and Fig. 48). This indicates that internalization of transporters occurred even in the continuous presence of insulin (Table 2). The percentages of photolabelled transporter found in the light microsome fraction are consistent with the results of Calderhead *et al.* (1990) who determined by

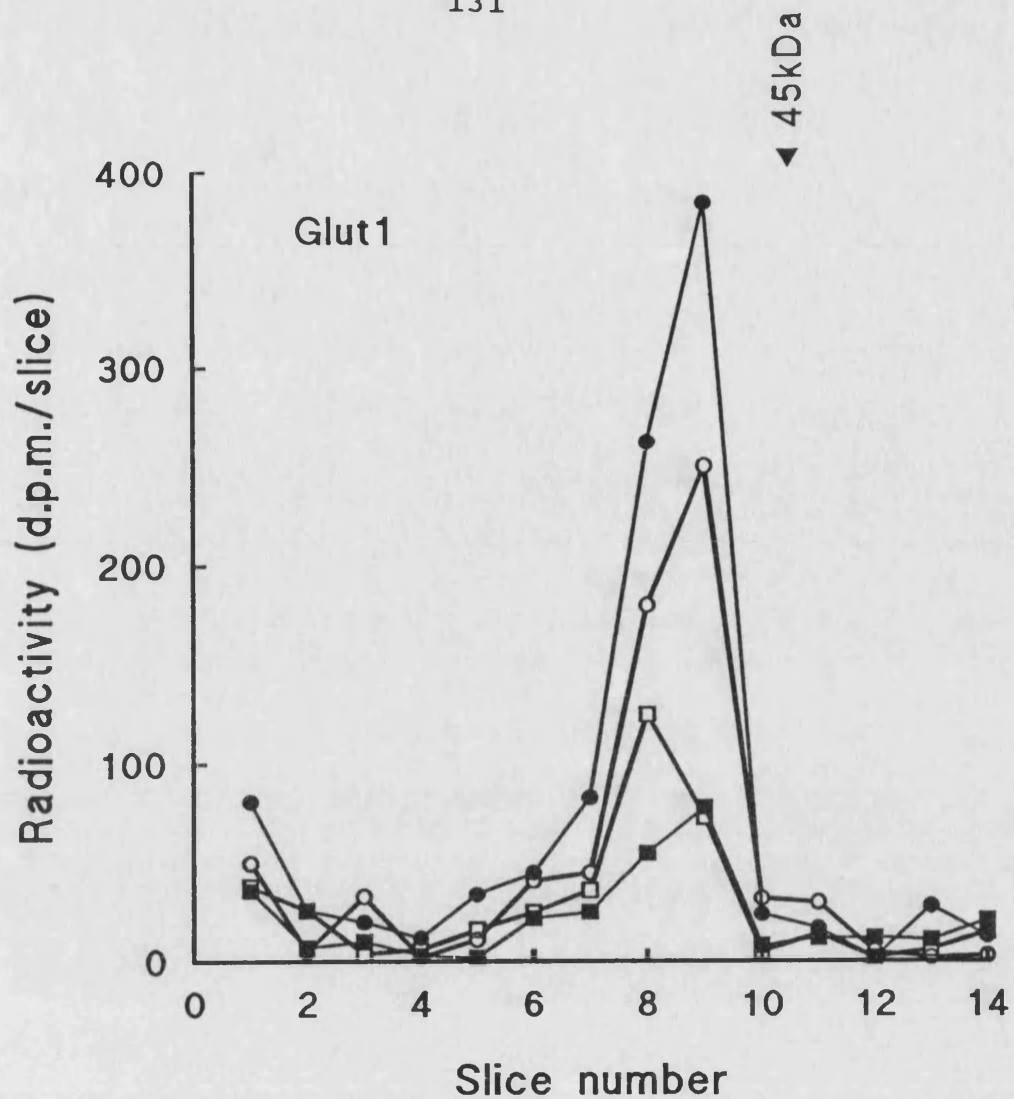


Fig.47 **Redistribution of photolabelled GLUT1 to subcellular membrane fractions of 3T3-L1 adipocytes.**

3T3-L1 adipocytes were fully insulin stimulated by treatment with 100 nM insulin for 30 min at 37°C. They were then photolabelled with 100 μ Ci of ATB-BMPA and then maintained with (○) and without (□) 100 nM insulin for a further 60 min. Crude plasma membrane (closed symbols) and light-microsome membranes (open symbols) were prepared from 2 dishes for each condition. These fractions were solubilized in C₁₂E₉ detergent buffer. GLUT1 was then immunoprecipitated with anti-C-terminal peptide antibody and subjected to electrophoresis and the radioactivity was estimated by cutting and counting gel slices.

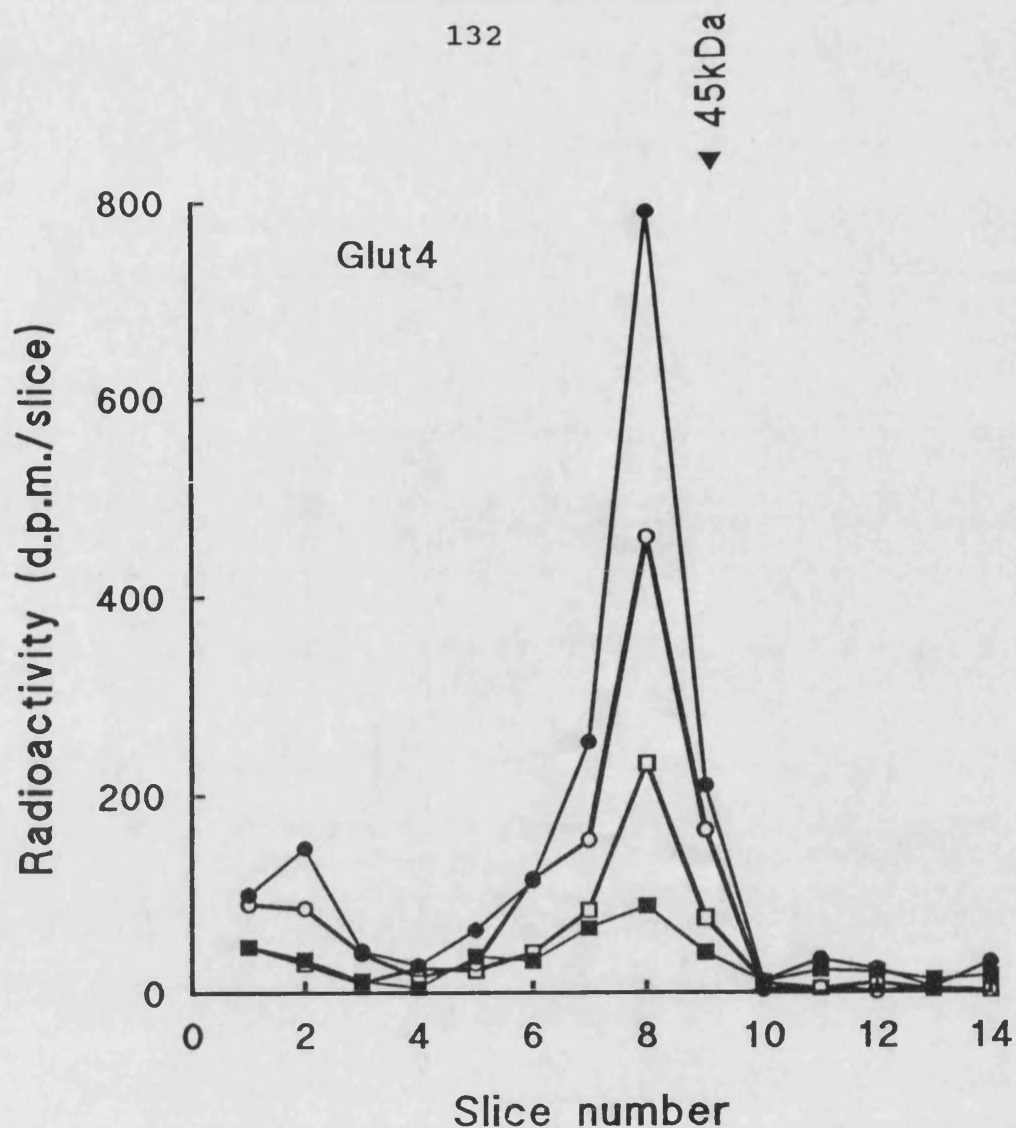


Fig.48 **Redistribution of photolabelled GLUT4 to subcellular membrane fractions of 3T3-L1 adipocytes.**

3T3-L1 adipocytes were fully insulin stimulated by treatment with 100 nM insulin for 30 min at 37°C. They were then photolabelled with 100 μ Ci of ATB-BMPA and then maintained with (○) and without (□) 100 nM insulin for a further 60 min. Crude plasma membrane (closed symbols) and light-microsome membranes (open symbols) were prepared from 2 dishes for each condition. These fractions were solubilized in C₁₂E₉ detergent buffer. GLUT4 was then immunoprecipitated with anti-C-terminal peptide antibody and subjected to electrophoresis and the radioactivity was estimated by cutting and counting gel slices.

western blotting that $\approx 50\%$ of the total recovered GLUT1 and GLUT4 were present in the light microsome pool of basal cells and that this was reduced to $\approx 25\%$ in insulin treated cells. However results from digitonin-permeabilized cells suggest different results and that in the presence of insulin $\approx 50\%$ of the transporters are at the surface and 50% are in the light microsome pool. The light microsome association of GLUT1 was slightly less than that which occurred for the GLUT4 isoform. This probably reflects the greater tendency of GLUT1 to be re-exocytosed under these conditions.

Table 2. also shows that the internalization of GLUT1 and GLUT4 also occurred in cells treated with PAO. However, in PAO-treated cells the additional GLUT4, above that found with insulin alone, that was lost from the cell-surface was not recovered in the light-microsomes but partitioned with the plasma membrane fraction during homogenization. The total recovered photolabel was unaltered by the PAO treatment. Western blotting confirmed that neither GLUT4 nor GLUT1 internalization to the light microsome fraction was increased by the PAO treatment compared with insulin alone (Fig. 46). This result was consistent with the result from cell fractionation experiments (see Fig. 49). This result shows that $\approx 35\%$ of GLUT4 transporters that were photolabelled in the insulin-stimulated state were transferred to the light-microsome fraction after 60 min. This proportion was not altered by the PAO treatment.

3.9 COMPARISON OF GLUT1 AND GLUT4 SUBCELLULAR TRAFFICKING IN BASAL AND INSULIN-STIMULATED 3T3-L1 ADIPOCYTES

Kinetic, rather than steady-state distribution, studies of transporter cycling should be able to directly determine and quantify the site of insulin action on trafficking.

Addition	Time (min)	Expt.	Percentage of radioactivity in light-microsome fraction			
			Transporter ...			
			GLUT1		GLUT4	
			Individual results	Mean \pm S.E.M.	Individual results	Mean \pm S.E.M.
Insulin	0	1	13.7	11.0 \pm 0.5	17.1	14.0 \pm 0.8
		2	9.8		10.9	
		3	13.1		14.4	
		4	11.0		13.2	
Insulin	60	1	38.1	27.9 \pm 4.5	39.0	35.6 \pm 5.3
		2	29.8		31.1	
		3	27.5		42.0	
		4	16.2		18.2	
Insulin + PAO	60	1	21.9	23.2 \pm 1.8	33.3	32.0 \pm 1.2
		2	29.3		35.4	
		3	20.6		29.8	
		4	20.9		29.5	

Table 2 Internalization of glucose transporters in 3T3-L1 cells

Fully-insulin-stimulated 3T3-L1 cells were photolabelled with ATB-BMPA and then either homogenized immediately (0 min) or maintained at 37°C with insulin (60 min) or insulin + 20 μ M-PAO (60 min) before homogenization. Crude plasma-membrane and light-microsome fractions were prepared and solubilized in C₁₂E₉ detergent buffer. GLUT1 and GLUT4 were then immunoprecipitated and subjected to electrophoresis. The radioactivity in the transporter peaks was estimated, and the results are expressed as a percentage of radioactivity recovered in the light-microsome fraction compared with the sum of the radioactivity recovered in the plasma-membrane and light-microsome fractions.

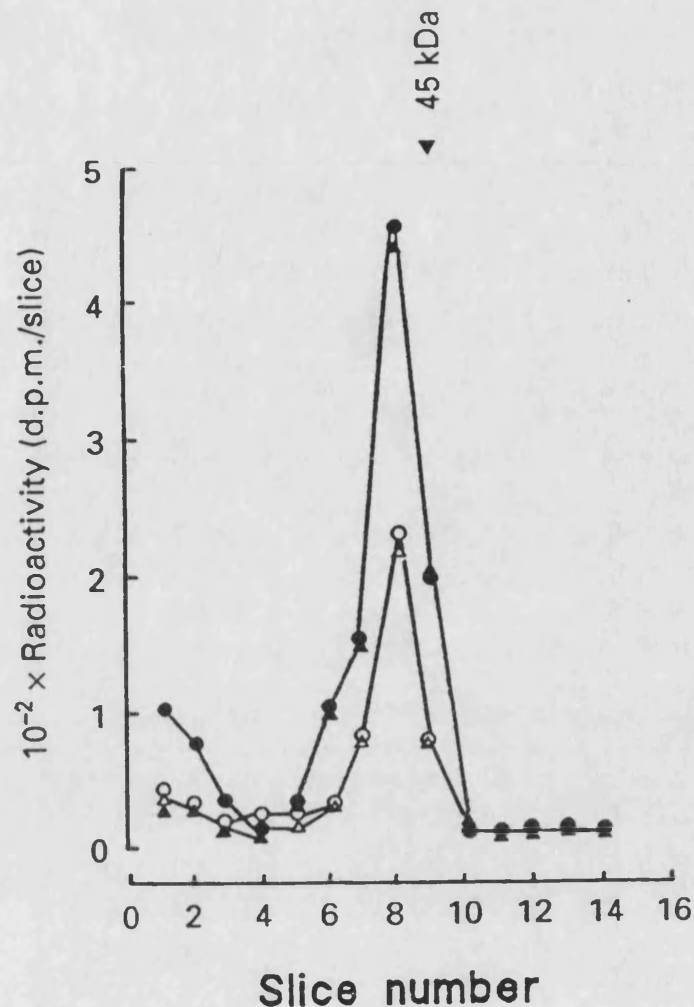


Fig.49 **Redistribution of photolabelled GLUT4 to subcellular membrane fractions of 3T3-L1 adipocytes.**

3T3-L1 adipocytes were fully insulin stimulated by treatment with 100 nM insulin for 30 min at 37°C. They were then photolabelled with 100 μ Ci of ATB-BMPA and then maintained with (Δ) and without (\circ) 20 μ M PAO for a further 60 min. Crude plasma membrane (closed symbols) and light-microsome membranes (open symbols) were prepared from 2 dishes for each condition. These fractions were solubilized in C₁₂E₉ detergent buffer. GLUT4 was then immunoprecipitated with anti-C-terminal peptide antibody and subjected to electrophoresis and the radioactivity was estimated by cutting and counting gel slices

The impermeant glucose transporter photolabel-ATB-BMPA has been used to tracer-tag cell-surface GLUT1 and GLUT4 in 3T3-L1 cells. The removal of these transporters from the plasma membrane of cells maintained in either basal or insulin-stimulated states has then been followed. The maintenance of a steady state of non-labelled transporter distribution was confirmed by comparing the amounts of immunodetectable GLUT1 and GLUT4 at the initial labelling time and following a further 40 min of incubation at 37°C. Fig. 50 shows an SDS-PAGE profile obtained by labelling and immunoprecipitating GLUT4 in insulin-treated 3T3-L1 cells. The label recovered in the post plasma membrane fraction of cells which were homogenized immediately was very low. This is an improvement over the results from the PAO study described above because of an improvement in the homogenization procedure. This suggests that tracer-tagged GLUT4 was not significantly transferred to the low-density microsomes during the processing period. This results contrast with those of Jhun *et al.* (1992) who have reported that in rat adipose cells approximately one third of the labelled GLUT4 was recovered in the post plasma membrane fraction in samples which were processed immediately after labelling.

Following 40 min of incubation of the cells at 37°C the label in the plasma membrane was reduced to approximately one-half its initial value. The label that was lost from the plasma membrane was recovered in the low-density microsome fraction. The material transferred to the low-density microsome fraction was not routinely analyzed because of the need to simultaneously process multiple immunoprecipitated samples obtained for estimating GLUT1 and GLUT4 in the plasma membrane. Previous studies have demonstrated that constitutive turnover of transporters occurs (Satoh., *et al.* unpublication results; Holman *et al.*, 1988;) and that label which is lost from the plasma membrane is recovered in the low-density microsome fraction.

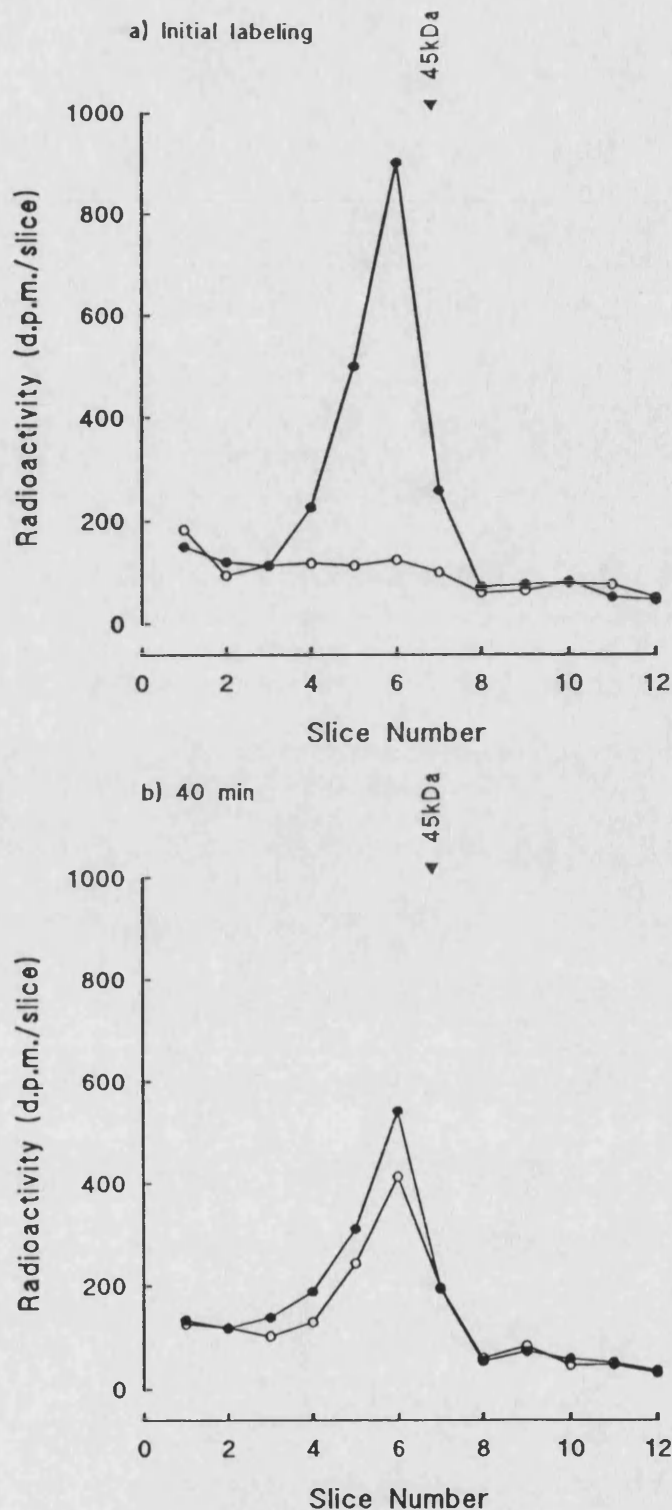


Fig. 50 **Equilibration of tracer-tagged GLUT4 with the intracellular membrane pool in 3T3-L1 adipocytes.**

3T3-L1 cells (two 35mm dishes) were stimulated for 30 min with 100 nM insulin and then labelled with 500 μ Ci of ATB-[2- 3 H]-BMPA. Following labelling, the dishes were either homogenized immediately (*a*) or were maintained at 37°C in the continuous presence of insulin for a further 40 min and then homogenized (*b*). GLUT4 was immunoprecipitated from either the plasma membrane (●) or the post plasma membrane supernatant (low-density microsomes) (○) and was then analyzed by electrophoresis.

In basal cells, the labelling of GLUT1 and GLUT4 was low (Fig. 51 and Fig. 52) and following 40 min of incubation of the labelled cells at 37°C the level of tracer-tagged transporter in the plasma membrane was reduced to background levels.

The least squares curve fitting to directly estimate exocytosis and endocytosis rate constants from time courses of loss of tracer-tagged GLUT1 (Fig. 53) and GLUT4 (Fig. 54) from the plasma membrane has been used. For analytical purposes the rate of loss of label from the plasma membrane is assumed to be dependent on just two rate constants; one describing the exocytosis (k_{ex}) and one the endocytosis (k_{en}). The rate of loss of labelled transporters is then:

$$\frac{dL_p}{dt} = k_{ex} \cdot (1 - L_p) - k_{en} \cdot L_p \quad (\text{Eq. 2})$$

where L_p is the fraction of the label in the plasma membrane.

Integration of Eq. 2 with $l_p = 1.0$ at $t=0$ gives:

$$L_p = \frac{k_{ex} + k_{en} \exp(-t \cdot (k_{ex} + k_{en}))}{(k_{ex} + k_{en})} \quad (\text{Eq. 3})$$

In the experiments described here this equation has been used to analyze the redistribution of label under steady-state conditions but (Eq. 3) is equally applicable to an analysis of label equilibration under non-steady-state conditions. All that is required is that the total pool of transporters is conserved. It is only necessary to consider the concentration of unlabelled transporters if there are saturation steps in the flux pathway as would be the case if one were analyzing equilibrium exchange by a carrier protein.

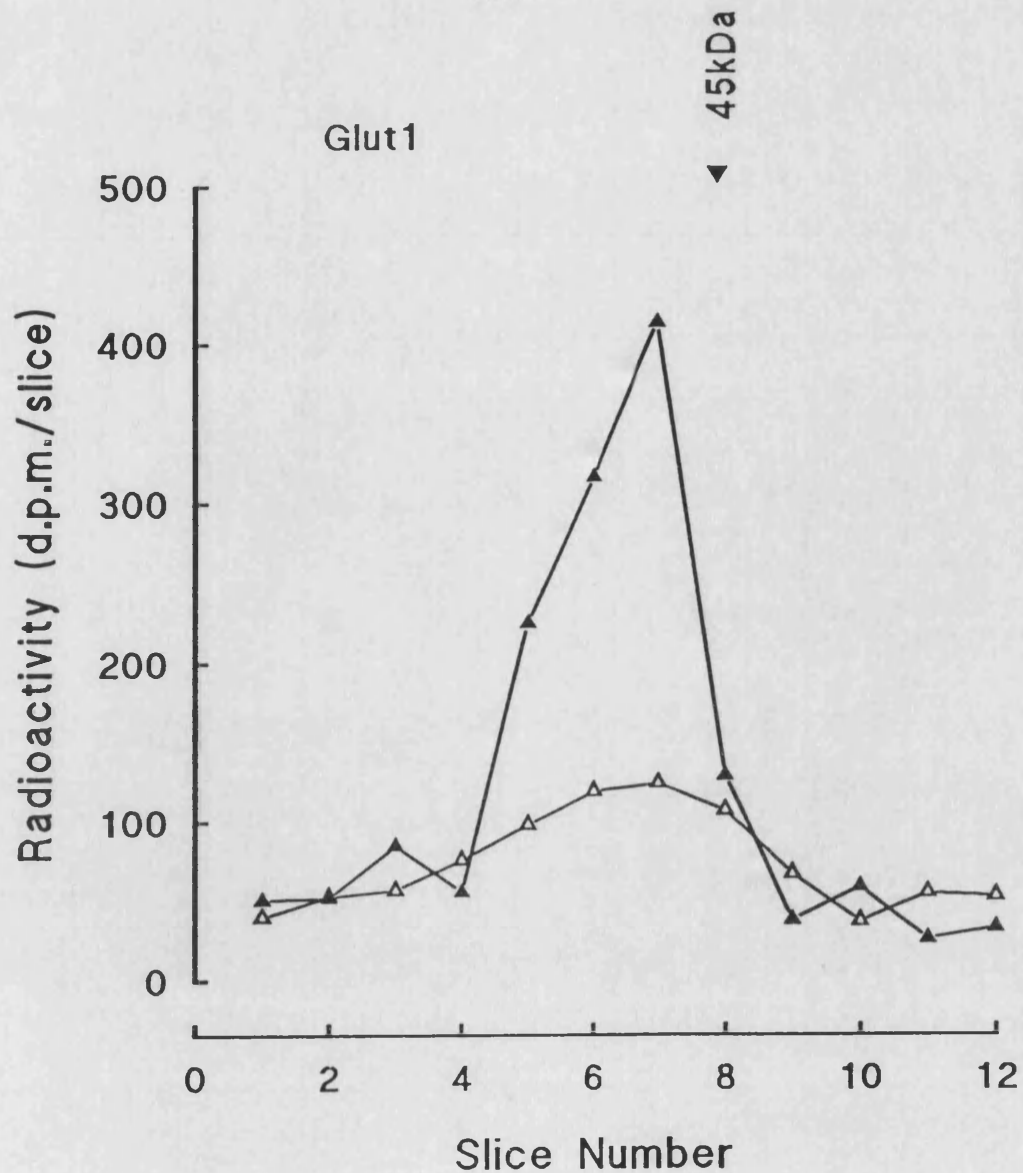


Fig. 51 **Equilibration of tracer-tagged GLUT1 in basal 3T3-L1 adipocytes.**

3T3-L1 cells (two 35 mm dishes) were labelled in the basal state with 500 μ Ci of ATB-[2- 3 H]-BMPA. Following labelling the dishes were either homogenized immediately (Δ) or were maintained at 37°C for a further 40 min and then homogenized (Δ). GLUT1 was then immunoprecipitated from the plasma membrane fractions and analyzed by electrophoresis.

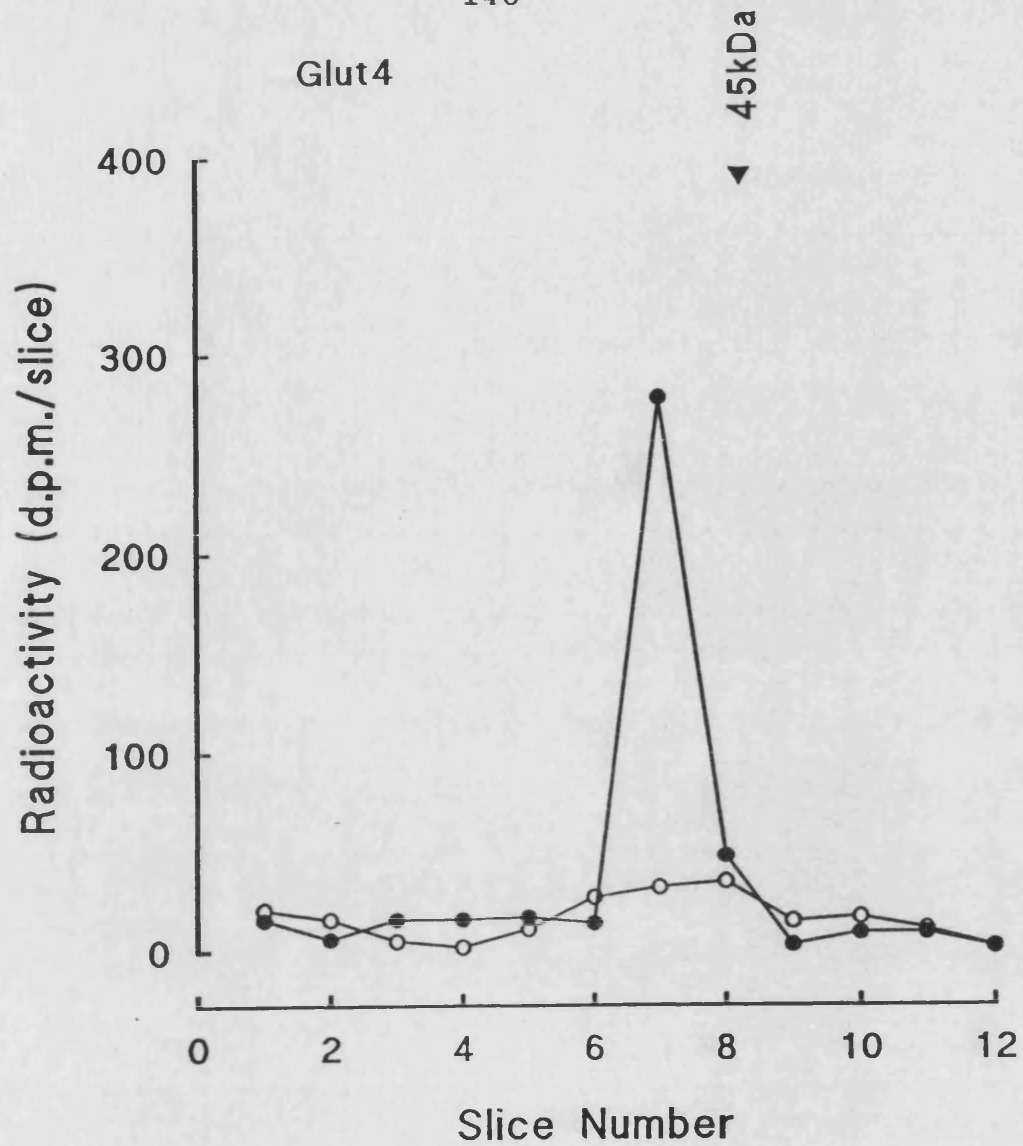


Fig. 52 **Equilibration of tracer-tagged GLUT4 basal 3T3-L1 adipocytes.**

3T3-L1 cells (two 35 mm dishes) were labelled in the basal state with 500 μCi of ATB-[2- ^3H]-BMPA. Following labelling the dishes were either homogenized immediately (●) or were maintained at 37°C for a further 40 min and then homogenized (○). GLUT4 was then immunoprecipitated from the plasma membrane fractions and were then analyzed by electrophoresis.

In the continuous presence of insulin both tracer-tagged GLUT1 and GLUT4 were rapidly removed from the plasma membrane. The values of *k_{ex}* and *k_{en}* derived from the mean results of 3 separate experiments are shown in Table 3. The estimated rate constants were similar for both GLUT1 and GLUT4. In addition, the end points of the equilibration of the tracer-tagged transporters were not significantly different. At 40 min the levels of tracer-tagged GLUT1 and GLUT4 remaining in the plasma membrane were $53 \pm 1.2\%$ ($n = 3$) and $51.1 \pm 1.7\%$ ($n = 3$) respectively, of the initial values. The maintenance of the insulin steady-state in which approximately one-half of the total transporter pool is at the surface thus occurs because the exocytosis of transporters (dependent on *k_{ex}*) matches an equal rate of endocytosis (dependent on *k_{en}*).

In the basal state, tracer-tagged GLUT4 was more extensively removed from the plasma membrane than in the insulin-stimulated state. At 40 min the fraction of the tracer-tagged GLUT4 remaining in the plasma membrane was only $8.4 \pm 2.0\%$ ($n = 4$) of the initial value. In contrast, the fraction of the tracer-tagged GLUT1 remaining in the plasma membrane was $20.8 \pm 1.3\%$ ($n = 3$) of the initial value. Analysis of the time course of tracer-tagged GLUT1 and GLUT4 redistribution in the basal state (Table 3) showed that the endocytosis rate constants were only $\approx 40\%$ faster than in the insulin-stimulated state. However, the GLUT4 exocytosis rate constant was 8.6 times lower. In contrast to the low exocytosis rate constant of GLUT4, exocytosis of GLUT1 was only 3-times lower in the basal compared with the insulin-stimulated state (Table 3).

Although the curve fitting to directly obtain the rate constants *k_{ex}* and *k_{en}* has been used, the half-time for label equilibration can also be easily calculated from least squares curve fitting using Eq.3. The half-time is only dependent on the exponential term so that:

	k_{ex}	k_{en}	$t_{1/2}$
	min^{-1}	min^{-1}	min
Basal			
GLUT4	0.010 ± 0.001	0.116 ± 0.006	5.6 ± 0.3
GLUT1	0.035 ± 0.009	0.121 ± 0.020	4.4 ± 0.6
Insulin			
GLUT4	0.086 ± 0.011	0.080 ± 0.007	4.2 ± 0.3
GLUT1	0.096 ± 0.023	0.093 ± 0.017	3.7 ± 0.6

Table 3 Kinetic parameters for glucose transporter trafficking in 3T3-L1 cells

Kinetic parameters were calculated from the mean data shown in Fig. 44 and Fig. 45. These data were from three separate experiments (insulin) and three separate experiments (basal) except in the case of GLUT4 in basal cells where the results were from four separate experiments. The data were fitted to Equation 5 using least squares analysis (weighted for relative error)

$$t_{1/2} = \ln 2 / (k_{ex} + k_{en}) \quad (\text{Eq. 4})$$

The values for the half-times for equilibration of tracer-tagged transporter were therefore calculated from summing the rate constants *k_{ex}* and *k_{en}* as in (Eq. 4) and are shown in Table 3. The half-times for GLUT1 and GLUT4 equilibration in basal cells were 4.4 and 5.6 min respectively. These values are similar to, but slightly faster than, the half-times (6.5 min) for the decrease in glucose transport activity in 3T3-L1 cells following removal of insulin. The calculated half-times for loss of tracer-tagged transporters in the continuous presence of insulin were slightly faster than in its absence because of the greater contribution of the re-exocytosis, the *k_{ex}* term in (Eq. 4), to the equilibration rate.

Kinetic parameters were calculated from the mean data shown in Fig.53 and 54. These data were from three separate experiments (Insulin) and three separate experiments (Basal) except in the case of GLUT4 in basal cells where the results were from four separate experiments. The data were fitted to (Eq. 3) using least squares analysis (weighted for relative error).

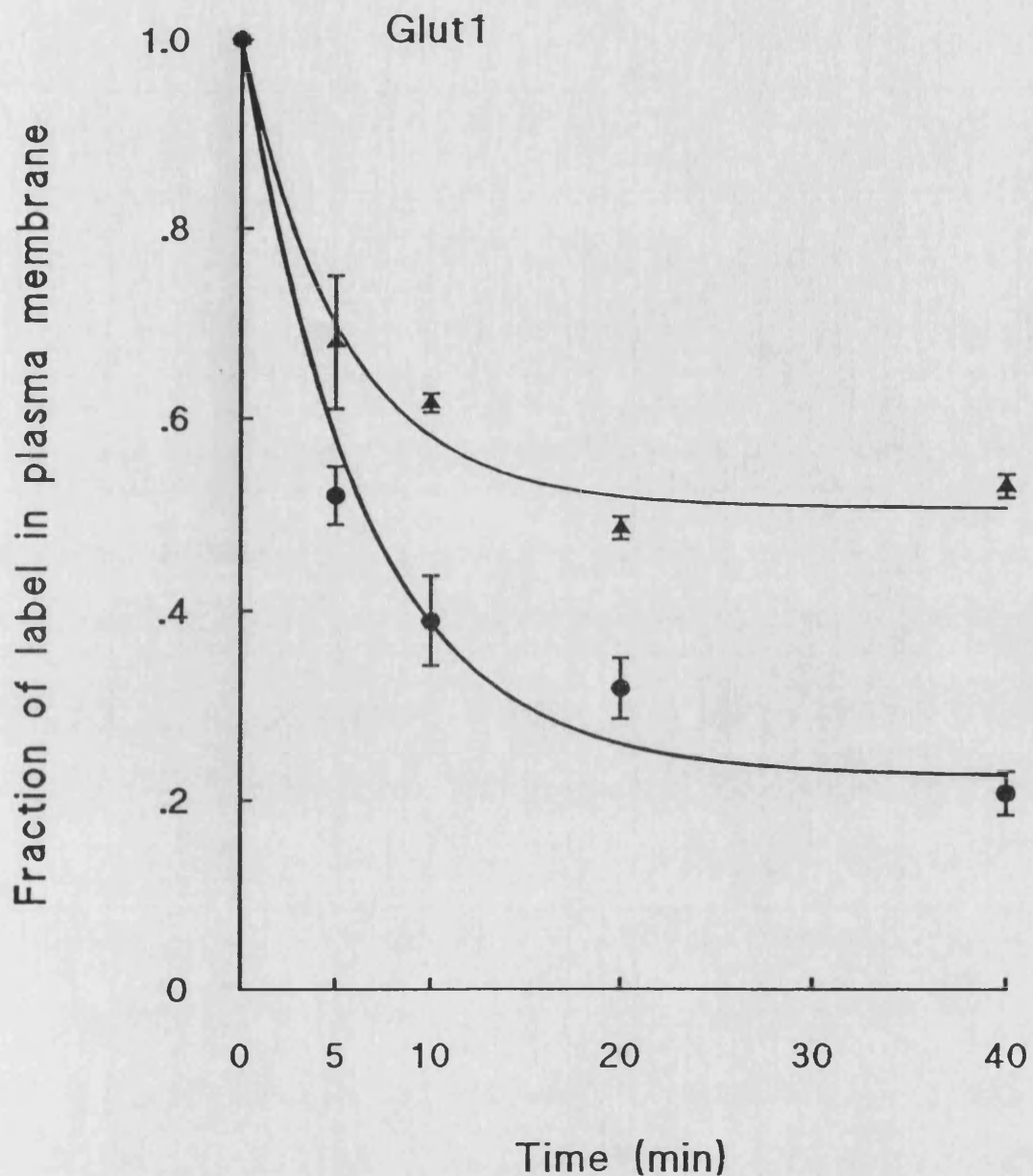


Fig.53 Time courses for equilibration of tracer-tagged GLUT1 in 3T3-L1 adipocytes.

3T3-L1 cells were labelled either in the basal (●) or insulin-stimulated (▲) states and were then maintained in these steady states for the indicated times before homogenization to obtain the plasma membrane fraction. GLUT1 was then immunoprecipitated and analyzed by electrophoresis. The lines through the data were derived from least squares fitting to Eqn. 5. (see "Results" 3.6). The results are the mean and S.E.M. from 3 separate experiments.

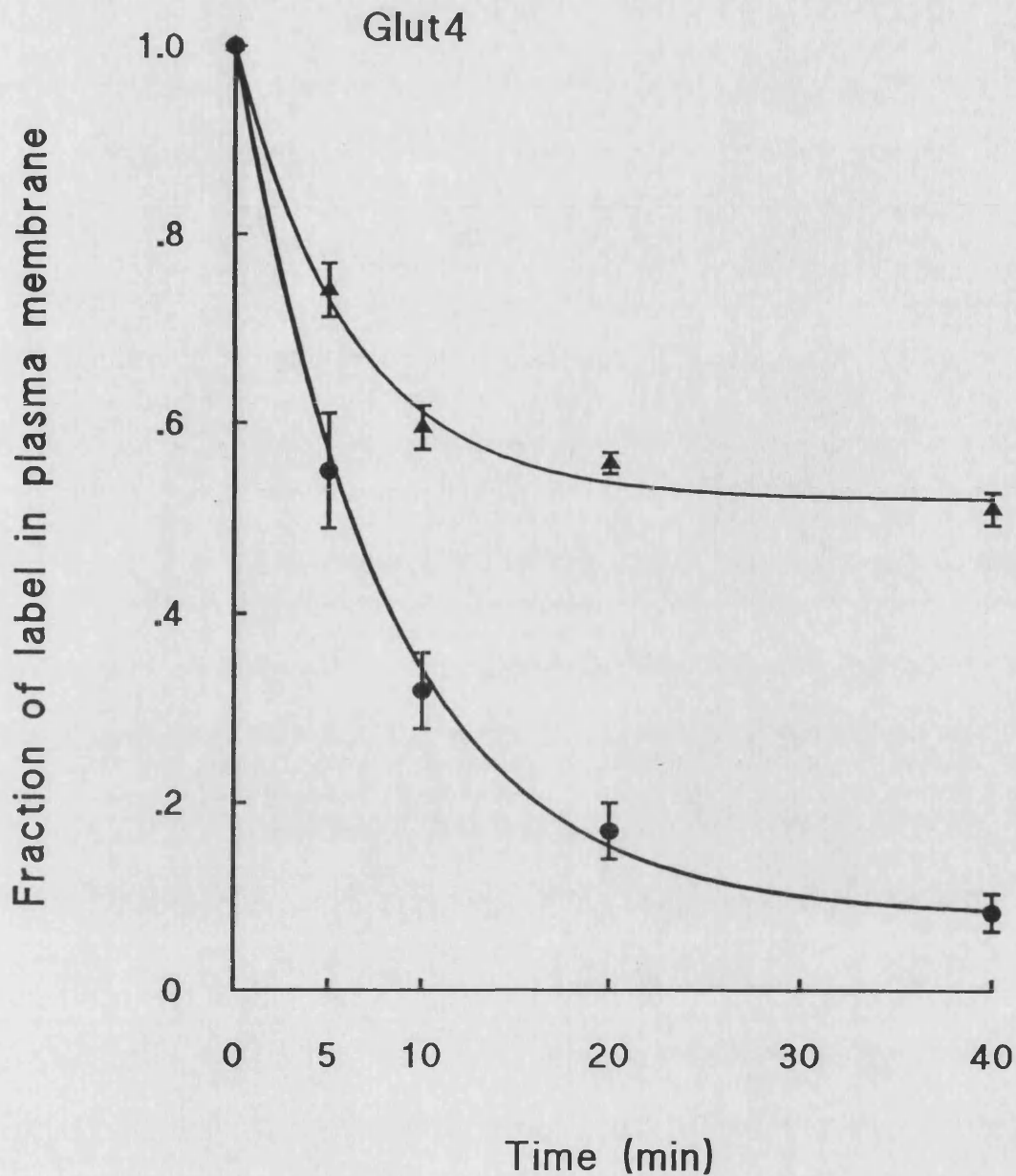


Fig.54 Time courses for equilibration of tracer-tagged GLUT4 in 3T3-L1 adipocytes.

3T3-L1 cells were labelled either in the basal (●) or insulin-stimulated (▲) states and were then maintained in these steady states for the indicated times before homogenization to obtain the plasma membrane fraction. GLUT4 was then immunoprecipitated and analyzed by electrophoresis. The lines through the data were derived from least squares fitting to Eqn.5. (see "Results" 3.6). The results are the mean and S.E.M. from 3 separate experiments in insulin treated cells and 4 experiments in basal cells.

PART IV INVESTIGATION OF DIFFERENT pH ON INSULIN-STIMULATED TRANSLOCATION OF GLUT1 AND GLUT4

3.10 DOSE-RESPONSE OF INSULIN-STIMULATED TRANSLOCATION OF GLUT1 AND GLUT4 AT pH 7.4

Using the ATB-BMPA photolabeling technique, the time course for translocation was determined by incubating cells in the presence of a maximal insulin concentration (100 nM) for variable times at 27 °C and it has been shown that the half-times for the appearance of GLUT1 and GLUT4 at the cell surface were 5.7 and 5.4 min respectively. To compare with this result, the effect of different concentration of insulin has been examined in 3T3-L1 adipocytes. At the same time, the GLUT1 and GLUT4 in purified plasma membrane was determined by quantitative immunoblotting.

The 3T3-L1 adipocytes were treated with zero, 0.025, 0.05, 0.1, 1, and 100 nM insulin and incubated in pH 7.4 KRH buffer for 30 min at 37°C. The 2-deoxy-D-glucose transport activity were measured (see Fig. 12) and the cell-surface glucose transporter were labelled with 100 μ Ci ATB-BMPA at pH 7.4 KRH buffer. The ATB-BMPA labelled GLUT1 is shown in Fig. 55, the GLUT4 is shown in Fig. 56. The half effective dose (ED₅₀) for GLUT1 was 0.12 nM, for GLUT4 was 0.3 nM.

Using the Western blotting technique to examine the dose response of insulin-stimulated glucose transporter levels in plasma membrane, the cells were treated with same concentration of insulin and incubated in pH 7.4 KRH buffer and then the cells were homogenized and the purified plasma membrane was assessed by SDS-PAGE, gel transfer, and Western blotting using an anti-GLUT1 and anti-GLUT4 C-terminal peptide antiserum and [¹²⁵I]-protein A. The amount of purified plasma membrane was measured by the BCA protein assay and the protein was loaded onto a 1.5 mm

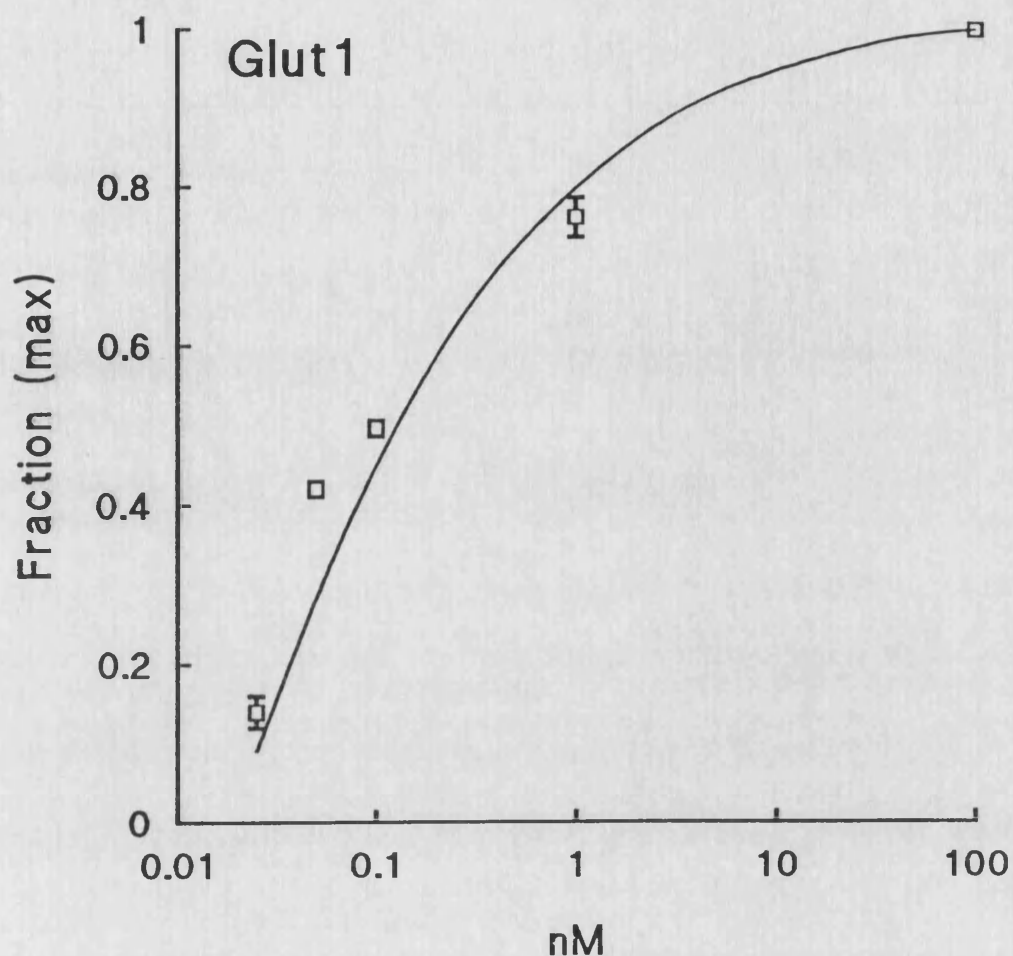


Fig.55 Dose response of translocation of GLUT1 at pH 7.4 by ATB-BMPA photolabelling in 3T3-L1 adipocytes.

3T3-L1 adipocytes were incubated with 0, 0.025, 0.05, 0.1, 1 and 100 nM of insulin in KRH buffer (pH 7.4) at 37°C for 30 min. The cells then were labelled with 100 μ Ci of ATB-[2- 3 H]-BMPA in 250 μ l of KRH buffer at 18°C. Following labelling the cells were washed four times in KRH buffer (pH 7.4) and solubilized in C₁₂E₉ detergent buffer. GLUT1 was then immunoprecipitated with anti-(C-terminal peptide) antibodies. The protein was then subjected to electrophoresis and the radioactivity was estimated by cutting out and counting the gel slices.

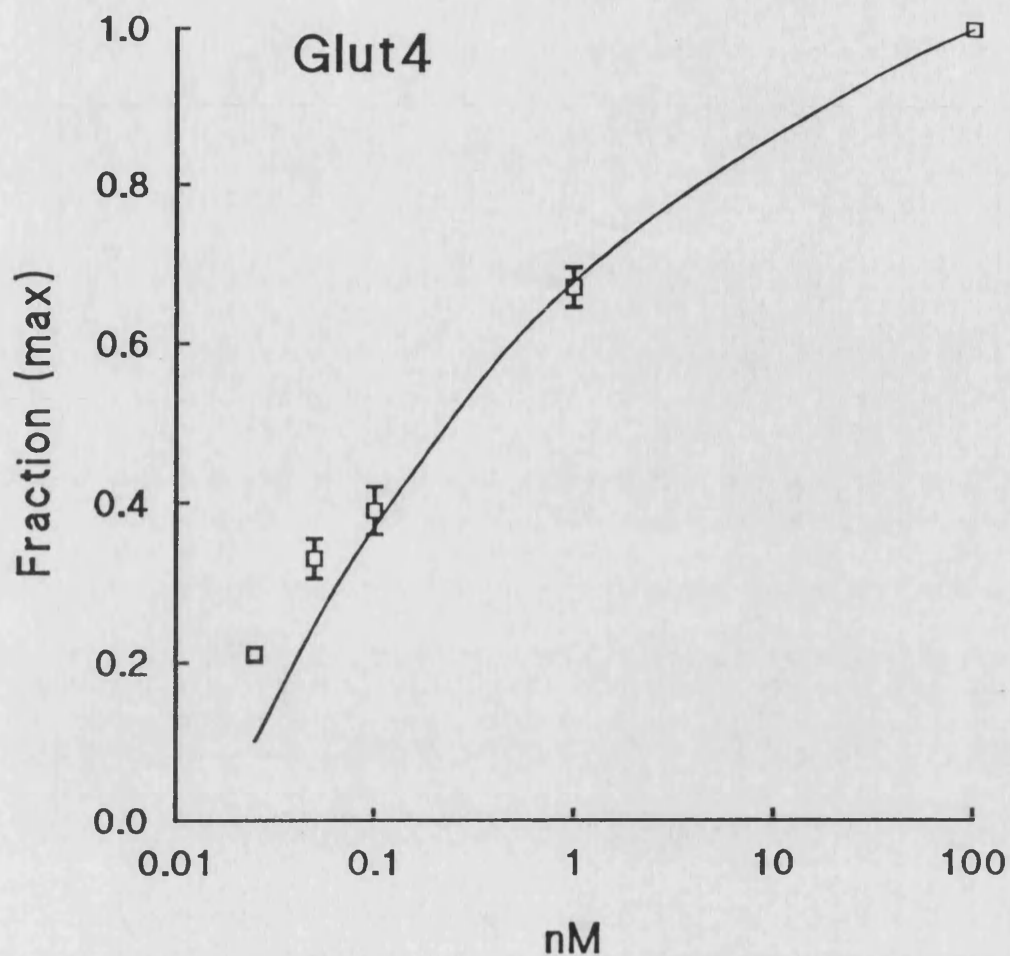


Fig.56 Dose response of translocation of GLUT4 at pH 7.4 by ATB-BMPA photolabelling in 3T3-L1 adipocytes.

3T3-L1 adipocytes were incubated with 0, 0.025, 0.05, 0.1, 1 and 100 nM of insulin in KRH buffer (pH 7.4) at 37°C for 30 min. The cells then were labelled with 100 μ Ci of ATB-[2-³H]-BMPA in 250 μ l of KRH buffer at 18°C. Following labelling the cells were washed four times in KRH buffer (pH 7.4) and solubilized in C₁₂E₉ detergent buffer. GLUT4 was then immunoprecipitated with anti-(C-terminal peptide) antibodies. The protein was then subjected to electrophoresis and the radioactivity was estimated by cutting out and counting the gel slices.

gel at 30 μg protein/lane. Fig. 57 shows the Western blotting result of GLUT1 and GLUT4. The γ -counts result of GLUT1 in the basal state was 4311 cpm and in the insulin (100 nM) stimulated state it was 12546 cpm. The insulin increase the counts about 3 fold compared to the basal level. The γ -counts result of GLUT4 in basal state was 1901 cpm and in insulin (100 nM) stimulated state it was 8221 cpm. The insulin increase the counts about 4 fold compared to the basal level. The half effective dose (ED_{50}) is 0.041 nM for GLUT1 and 0.046 nM for GLUT4. The comparison of the cell surface ATB-BMPA results, the Western blotting results and the 2-deoxy-D-glucose transport activity of GLUT1 is shown in Fig. 58, GLUT4 in Fig. 59. These results clearly indicated that the plasma membrane glucose transporter detected by Western blotting was higher than the ATB-BMPA labelled cell surface glucose transporter levels and these were both higher than the 2-deoxy-D-glucose transport activity.

3.11 DOSE-RESPONSE OF INSULIN-STIMULATED TRANSLOCATION OF GLUT1 AND GLUT4 AT pH 8.0

Ismail-Beigi *et al.* (1990) have reported that the rate of carrier-mediated glucose transport in a nontransformed rat liver cell line (Clone 9) is markedly stimulated by incubation at pH 8.5. A stimulation of glucose transport by incubation at alkaline pH has also been reported in rat adipocytes and an apparent translocation of glucose transporters to plasma membranes has been suggested as a possible mechanism (Sonne *et al.*, 1981; Toyoda *et al.*, 1986).

To examine the effect of alkaline pH on insulin-stimulated translocation of glucose transporter, the 3T3-L1 adipocytes were treated at zero, 0.025, 0.05, 0.1, 1 and 100 nM of insulin and incubated at pH 8.0 KRH buffer for 30 min at 37 °C. The 2-deoxy-D-glucose transport activity was measured, and was compared with results from the cell surface ATB-BMPA labelling and Western blotting technique. The 2-

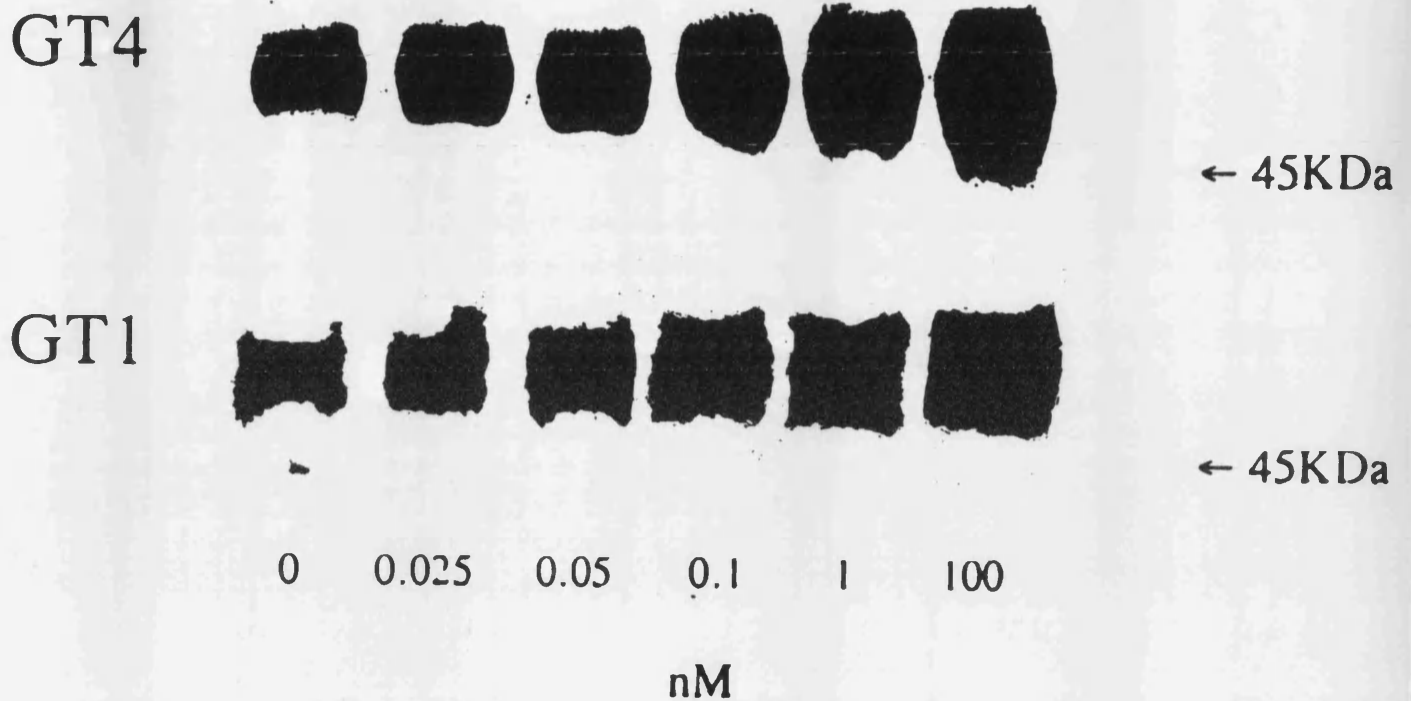


Fig.57 To test the dose response of translocation of GLUT1 and GLUT4 at pH 7.4 by Western blotting.

3T3-L1 adipocytes were incubated with 0, 0.025, 0.05, 0.1, 1 and 100 nM of insulin and KRH buffer (pH 7.4) at 37°C. The cells then were homogenized and purified plasma membrane (30 μ g) was subjected to SDS-PAGE. Proteins were transferred to nitrocellulose paper and incubated with a 1:500 dilution of anti-GLUT1 (a) and anti-GLUT4 (b) antibody. Blots were developed with 125 I labelled protein A and this photo was taken from x-ray films.

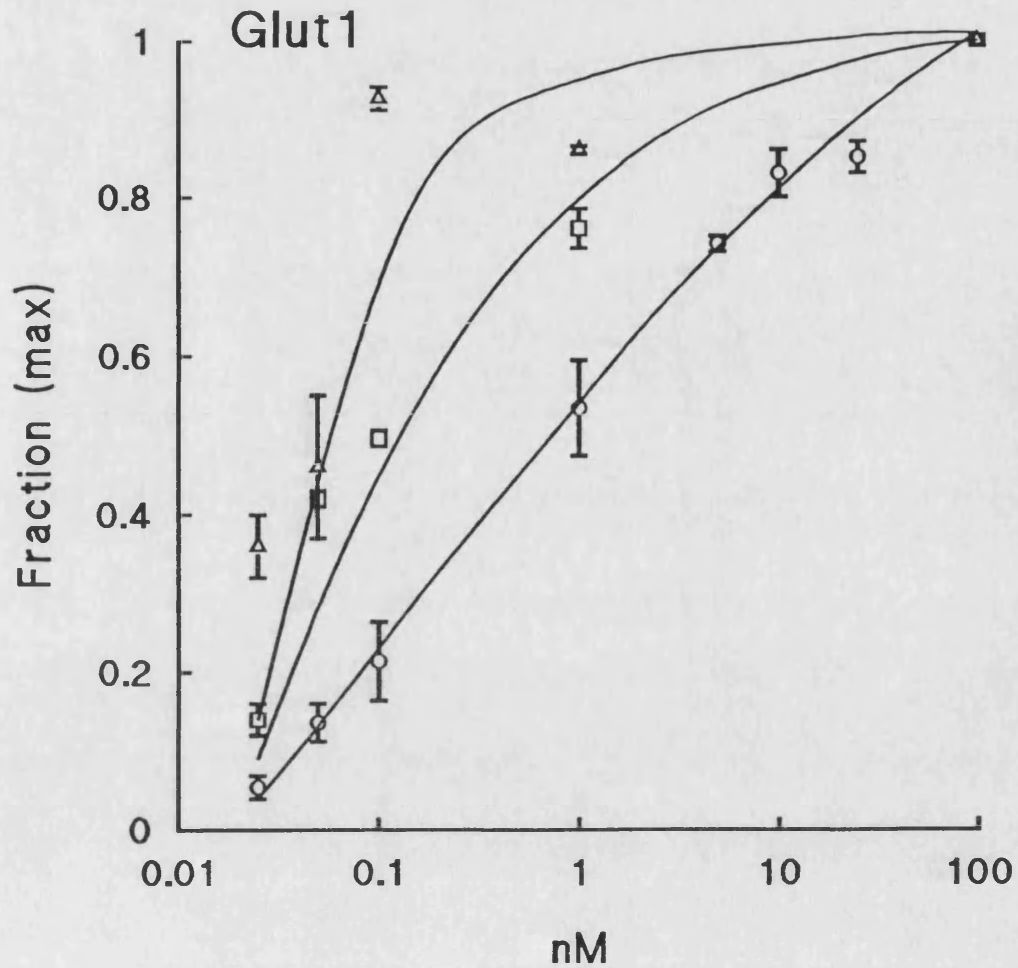


Fig.58 Comparison the dose response of translocation of GLUT1 and 2-deoxy-D-glucose transport activity at pH 7.4.

3T3-L1 adipocytes were incubated with 0, 0.025, 0.05, 0.1, 1 and 100 nM of insulin in KRH buffer (pH 7.4) at 37°C for 30 min. The fractions of maximum 2-deoxy-D-glucose transport Fig. 12 (○), ATB-BMPA labelling Fig.55 (□) and immunoblotting Fig. 57 (Δ) of GLUT1 were compared.

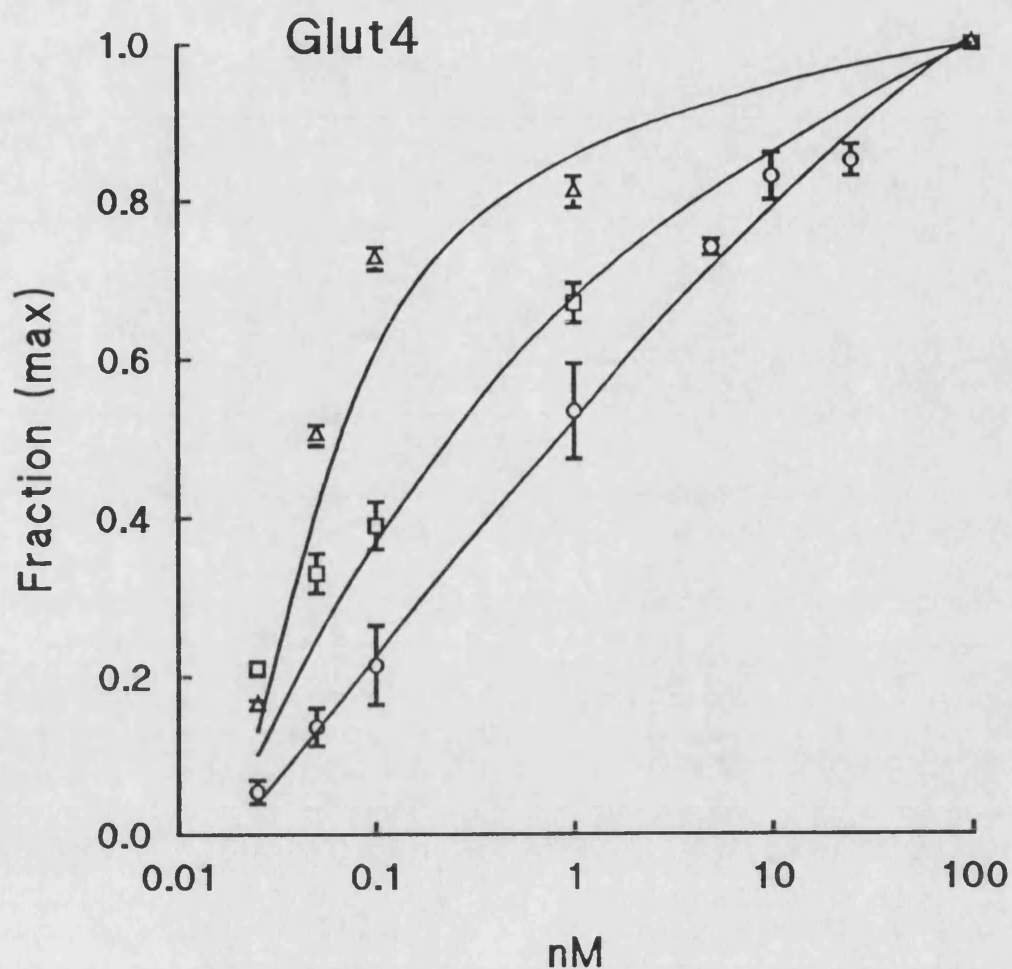


Fig.59 Comparison the dose response of translocation of GLUT4 and 2-deoxy-D-glucose transport activity at pH 7.4.

3T3-L1 adipocytes were incubated with 0, 0.025, 0.05, 0.1, 1 and 100 nM of insulin in KRH buffer (pH 7.4) at 37°C for 30 min. The fractions of maximum 2-deoxy-D-glucose transport Fig. 12 (○), ATB-BMPA labelling Fig.56 (□) and immunoblotting Fig. 57 (Δ) of GLUT4 were compared.

deoxy-D-glucose transport activity is shown in Fig.60. At this pH, the basal transport rate is 39.1 pmole/min/35 mm dish. The transport rate of insulin (100 nM) stimulated cells was increase to 542.3 pmole/min/35 mm dish. The insulin increased transport activity about 17 fold compared with the basal state. The half effective dose (ED₅₀) is 0.077 nM. This is compared with the ED₅₀ at pH 7.4 which is 1.9 nM. The transport activity at pH 8.0 is stimulated by lower insulin concentrations than the transport activity at pH 7.4.

This result indicates that the pH 8.0 markedly activated the insulin stimulated glucose transport activity.

In the same pH condition and the same insulin concentration, 100 μ Ci of ATB-BMPA was used to detect the changes in the cell-surface glucose transporter levels. The ATB-BMPA labelled cell surface glucose transporter levels of GLUT1 are shown in Fig. 61. The half effective dose (ED₅₀) for GLUT1 is 0.09 nM. The GLUT4 ATB-BMPA labelling result is shown in Fig. 62. The half effective dose (ED₅₀) for GLUT4 is 0.16 nM. The ATB-BMPA labelling results have shown that the half effective doses (ED₅₀) for stimulation of GLUT1, GLUT4 and 2-deoxy-D-glucose transport activity are very close. This indicates that the transport activity and cell-surface glucose transporter levels are very similar.

Fig. 63 demonstrates Western blotting results of GLUT1 and GLUT4. The purified plasma membranes were loaded at 10 μ g protein per well (1.5 mm gel). The half effective dose (ED₅₀) for GLUT1 is 0.09 nM, and for GLUT4 it is 0.05 nM. The basal level γ -counts of GLUT1 is 4720 cpm and insulin (100 nM) stimulated state is 7980 cpm (the increase is about 2 fold). The basal level γ -counts of GLUT4 is 992 cpm and insulin (100 nM) stimulated state is 4228 cpm. (The increase is about 4 fold). In contrast with the pH 7.4 results, at pH 8.0 both stimulation of cell surface ATB-BMPA labelled glucose transporter and purified plasma membrane Western

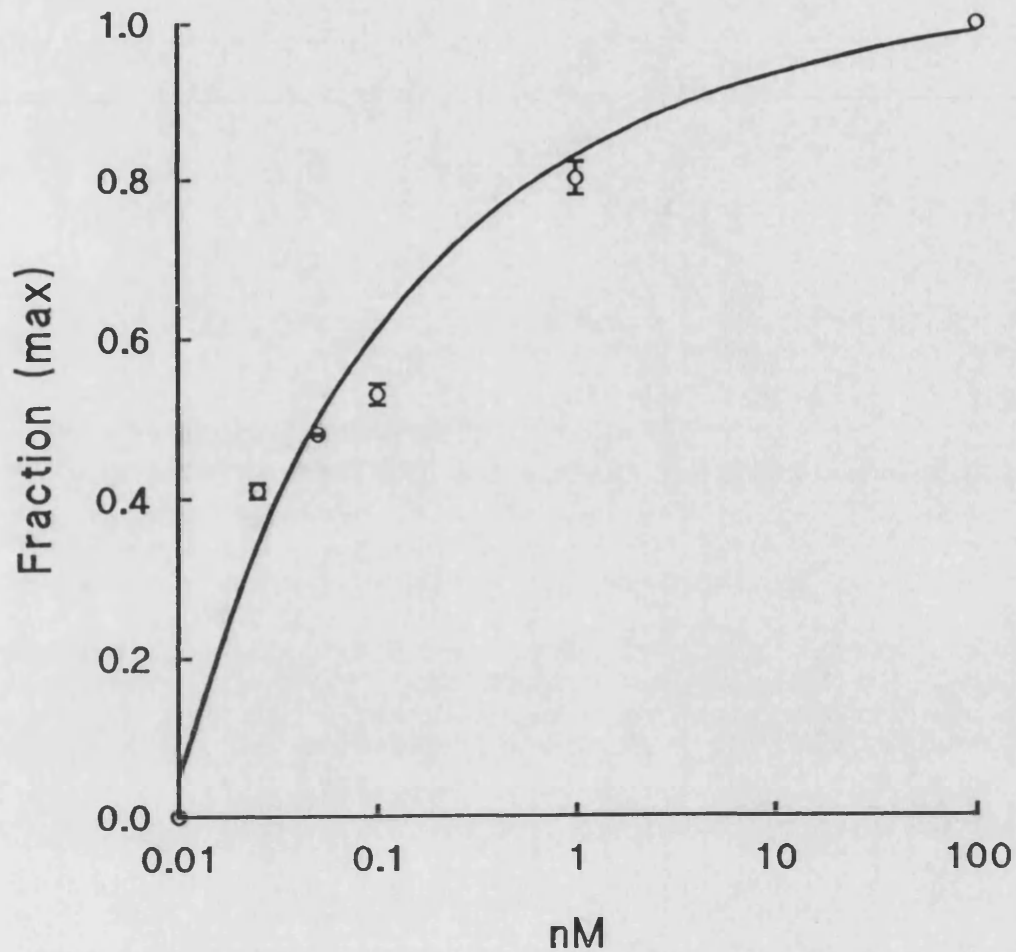


Fig.60 Dose response of translocation of 2-deoxy-D-glucose transport activity at pH 8.0.

3T3-L1 adipocytes were treated with 0, 0.025, 0.05, 0.1, 1, and 100 nM of insulin in KRH buffer (pH 8.0) for 30 min at 37°C. The 50 μ M 2-deoxy-[2,6- 3 H]-D-glucose was then measured over 5 min. After washing four times with KRH buffer (pH 8.0), the cells were dissolved in 0.1 M NaOH and the radioactivity was counted.

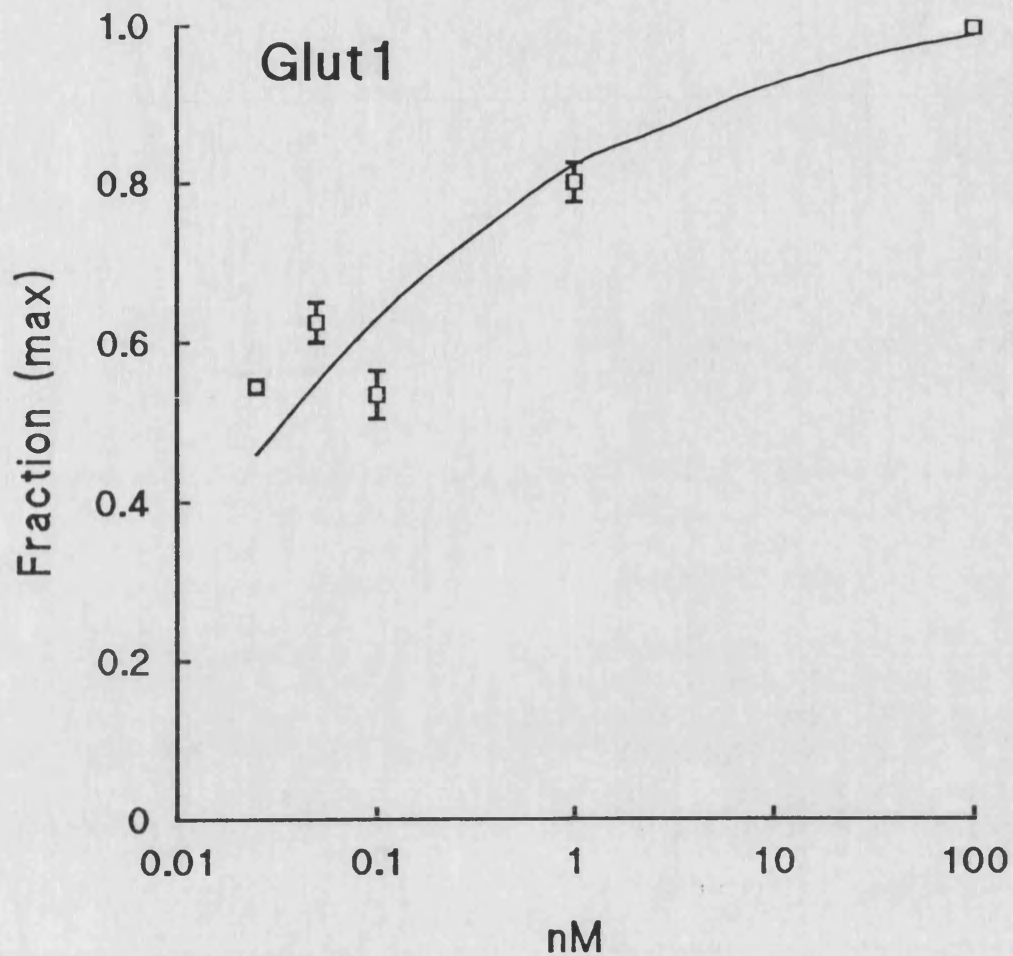


Fig.61 Dose response of translocation of GLUT1 at pH 8.0 by ATB-BMPA photolabelling in 3T3-L1 adipocytes.

3T3-L1 adipocytes were incubated with 0, 0.025, 0.05, 0.1, 1 and 100 nM of insulin in KRH buffer (pH 8.0) at 37°C for 30 min. The cells then were labelled with 100 μ Ci of ATB-[2- 3 H]-BMPA in 250 μ l of KRH buffer at 18°C. Following labelling the cells were washed four times in KRH buffer (pH 7.4) and solubilized in C₁₂E₉ detergent buffer. GLUT1 was then immunoprecipitated with anti-(C-terminal peptide) antibodies. The protein was then subjected to electrophoresis and the radioactivity was estimated by cutting out and counting the gel slices.

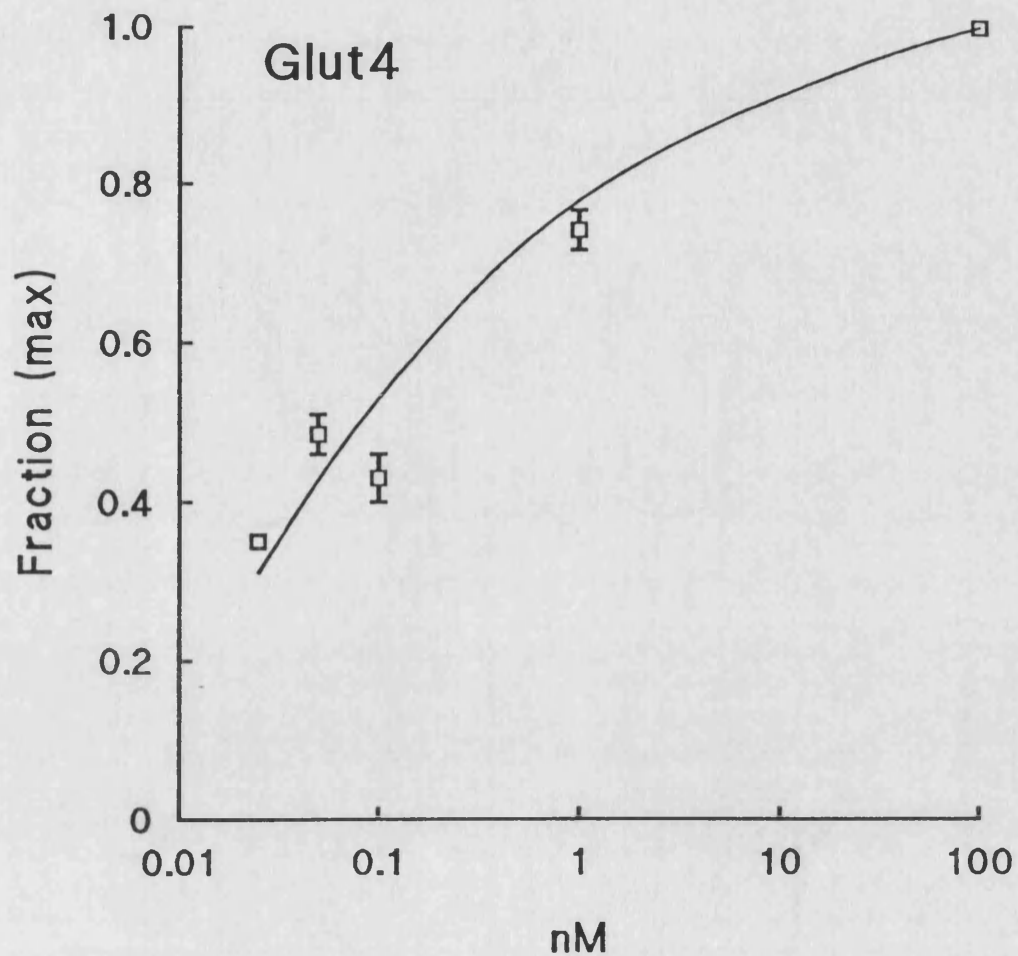


Fig.62 Dose response of translocation of GLUT4 at pH 8.0 by ATB-BMPA photolabelling in 3T3-L1 adipocytes.

3T3-L1 adipocytes were incubated with 0, 0.025, 0.05, 0.1, 1 and 100 nM of insulin in KRH buffer (pH 8.0) at 37°C for 30 min. The cells then were labelled with 100 μ Ci of ATB-[2- 3 H]-BMPA in 250 μ l of KRH buffer at 18°C. Following labelling the cells were washed four times in KRH buffer (pH 7.4) and solubilized in C₁₂E₉ detergent buffer. GLUT4 was then immunoprecipitated with anti-(C-terminal peptide) antibodies. The protein was then subjected to electrophoresis and the radioactivity was estimated by cutting out and counting the gel slices.

binding results of GLUT1 and GLUT4 show no difference from the 2-deoxy-D-glucose transport activity (Fig. 64 for GLUT1 and Fig. 65 for GLUT4).

3.12 DOSE-RESPONSE OF INSULIN STIMULATED TRANSLOCATION OF GLUT1 AND GLUT4 AT pH 8.5

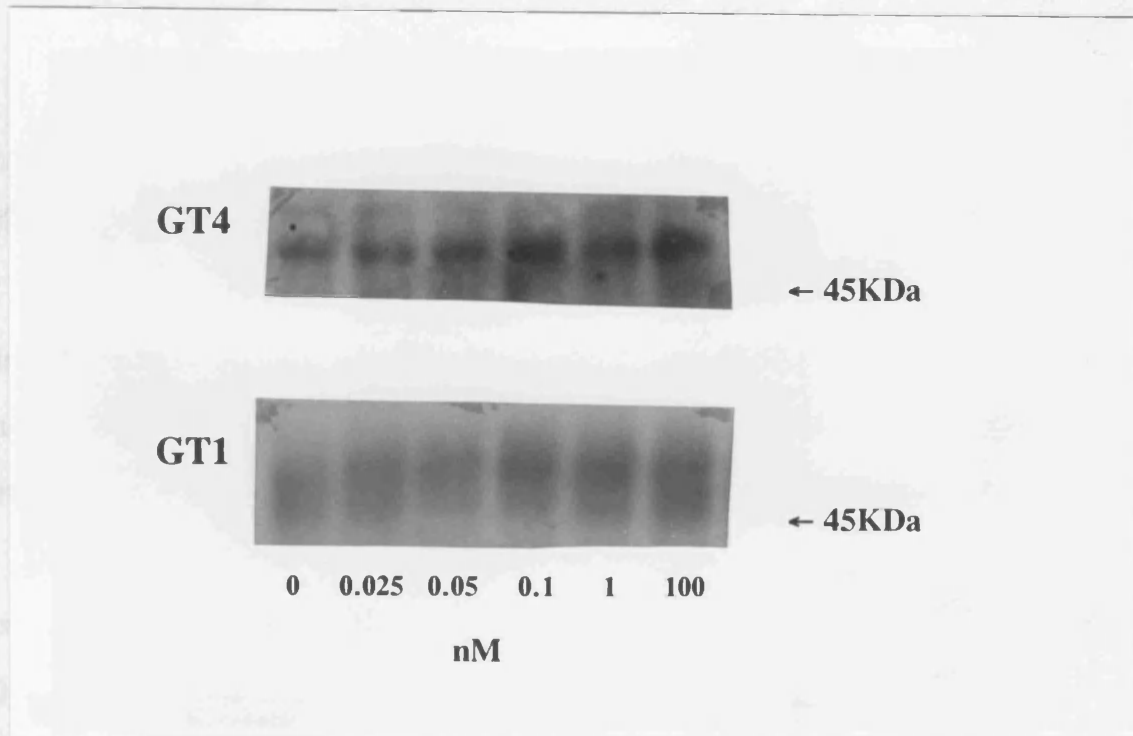


Fig.63 To test the dose response of translocation of GLUT1 and GLUT4 at pH 8.0 by Western blotting.

3T3-L1 adipocytes were incubated with 0, 0.025, 0.05, 0.1, 1 and 100 nM of insulin and KRH buffer (pH 8.0) at 37°C. The cells then were homogenized and purified plasma membrane 10 μ g were subjected to SDS-PAGE. Proteins were transferred to nitrocellulose paper and incubated with a 1:500 dilution of anti-GLUT1 (a) and anti-GLUT4 (b) antibody. Blots were developed with 125 I labelled protein A and this photo was taken from x-ray films.

blotting results of GLUT1 and GLUT4 show no difference from the 2-deoxy-D-glucose transport activity (Fig. 64 for GLUT1 and Fig. 65 for GLUT4).

3.12 DOSE-RESPONSE OF INSULIN STIMULATED TRANSLOCATION OF GLUT1 AND GLUT4 AT pH 6.5

At pH 6.5, the insulin concentration dependency on 2-deoxy-D-glucose transport activity has been studied. At this pH, the glucose transport rate is much lower than in the pH 7.4 and pH 8.0 buffer. When the cells were treated with 100 nM insulin, the transport rate at pH 6.5 is 357.9 pmole/min/35 mm dish. When the cells were treated at pH 7.4 with the same insulin concentration (100 nM), the transport rate is 509.5 pmole/min/35 mm dish. When the insulin concentration was increased to 500 nM the transport rate was 465.4 pmole/min/35 mm dish. Increasing the insulin concentration to 10 μ M increased the transport activity very little. The maximum insulin concentration in the follow investigation at pH 6.5 was chosen as 500 nM. The transport assay result on pH 6.5 is shown in Fig. 66. The half effective dose (ED₅₀) is 140.6 nM.

Using ATB-BMPA labelling and Western blotting techniques, the 3T3-L1 adipocytes were studied at this low pH condition. The cells were incubated with 0, 0.025, 0.1, 1, 10 and 500 nM of insulin at pH 6.5 for 30 min at 37°C. 100 μ Ci of ATB-BMPA was used for labelling the cell-surface GLUT1 and GLUT4. ATB-BMPA labelled GLUT1 is shown in Fig. 67 and GLUT4 is shown in Fig. 68. The half effective dose (ED₅₀) for GLUT1 is 16.36 nM and for GLUT4 it is 64.66 nM. Both GLUT1 and GLUT4 ATB-BMPA labelling were stimulated more effectively than the transport activity.

At same concentrations and pH condition, the Western blotting result of GLUT1 and GLUT4 is shown in Fig. 69. The purified plasma membrane was loaded

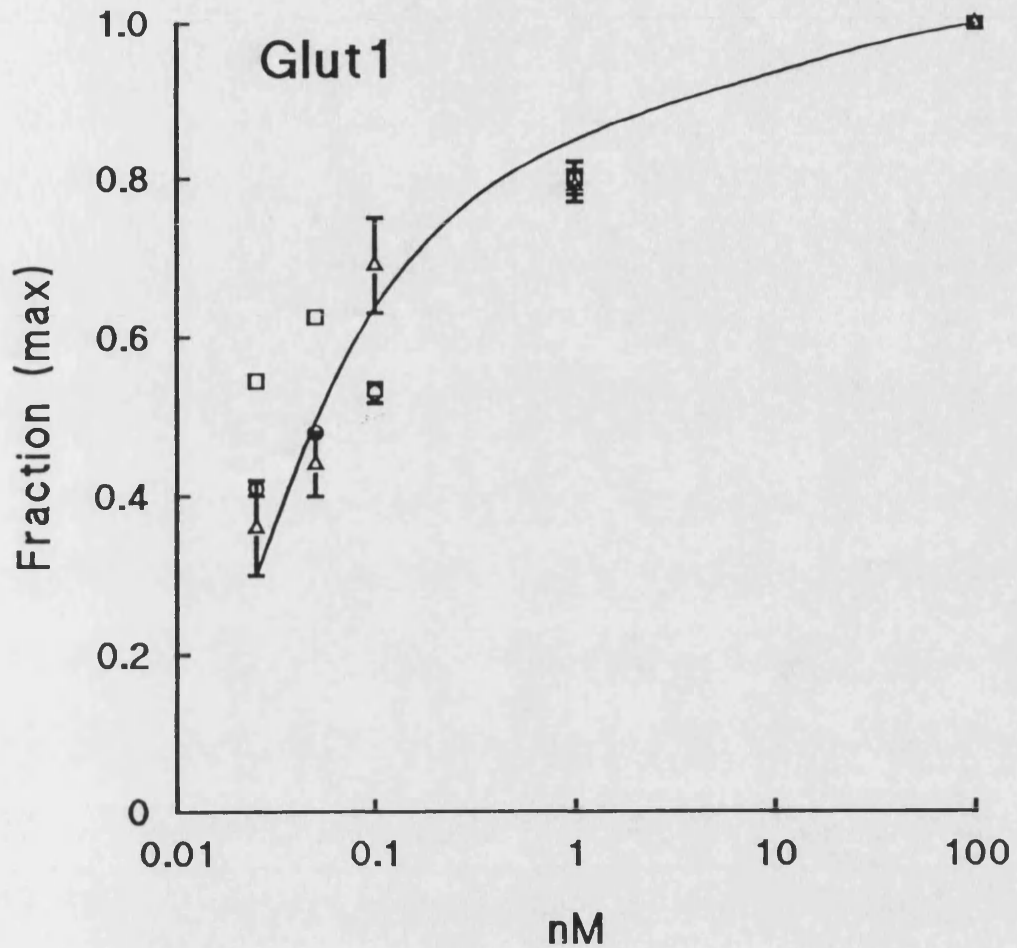


Fig.64 Comparison the dose response of translocation of GLUT1 and 2-deoxy-D-glucose transport activity at pH 8.0.

3T3-L1 adipocytes were incubated with 0, 0.025, 0.05, 0.1, 1 and 100 nM of insulin in KRH buffer (pH 8.0) at 37°C for 30 min. The fractions of maximum 2-deoxy-D-glucose transport Fig. 60 (○), the ATB-BMPA labelling Fig.61 (□) and immunoblotting Fig. 63 (Δ) of GLUT1 were compared.

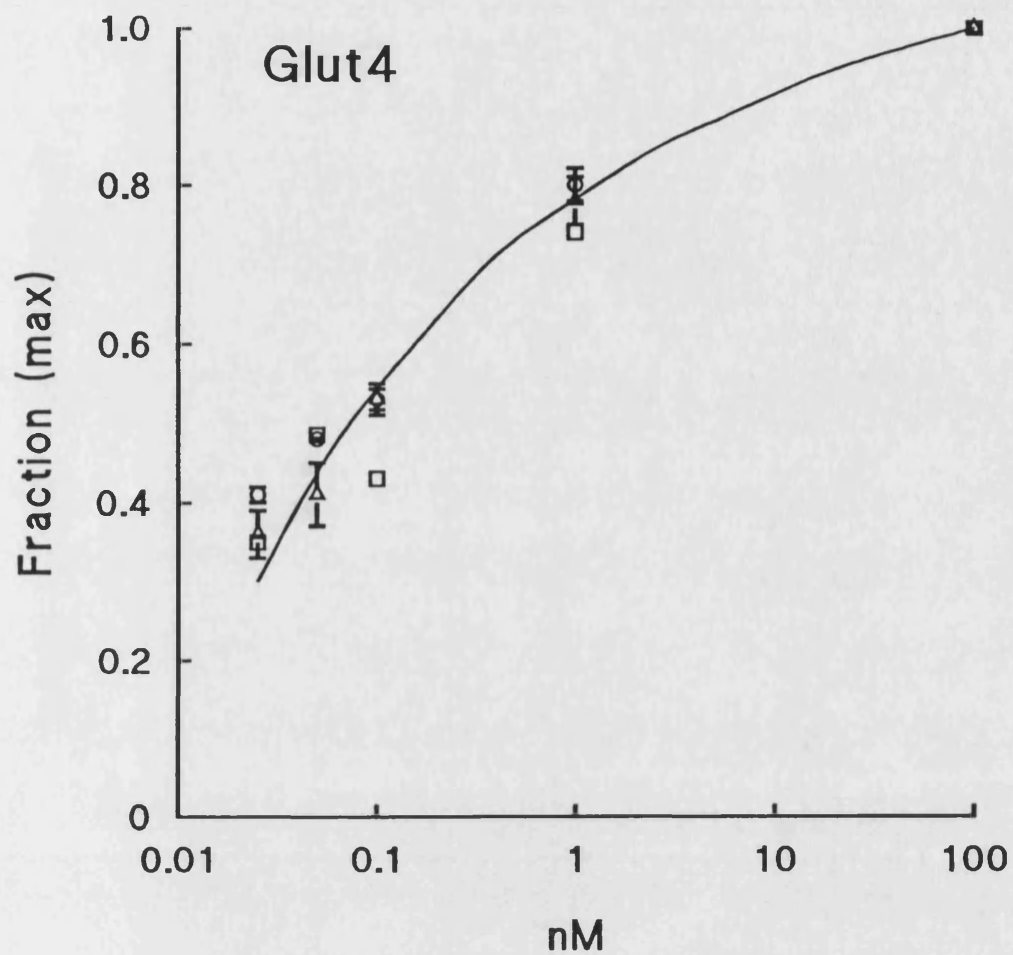


Fig.65 Comparison the dose response of translocation of GLUT4 and 2-deoxy-D-glucose transport activity at pH 8.0.

3T3-L1 adipocytes were incubated with 0, 0.025, 0.05, 0.1, 1 and 100 nM of insulin in KRH buffer (pH 8.0) at 37°C for 30 min. The fractions of maximum 2-deoxy-D-glucose transport Fig. 60 (○), the ATB-BMPA labelling Fig.62 (□) and immunoblotting Fig. 63 (Δ) of GLUT1 were compared.

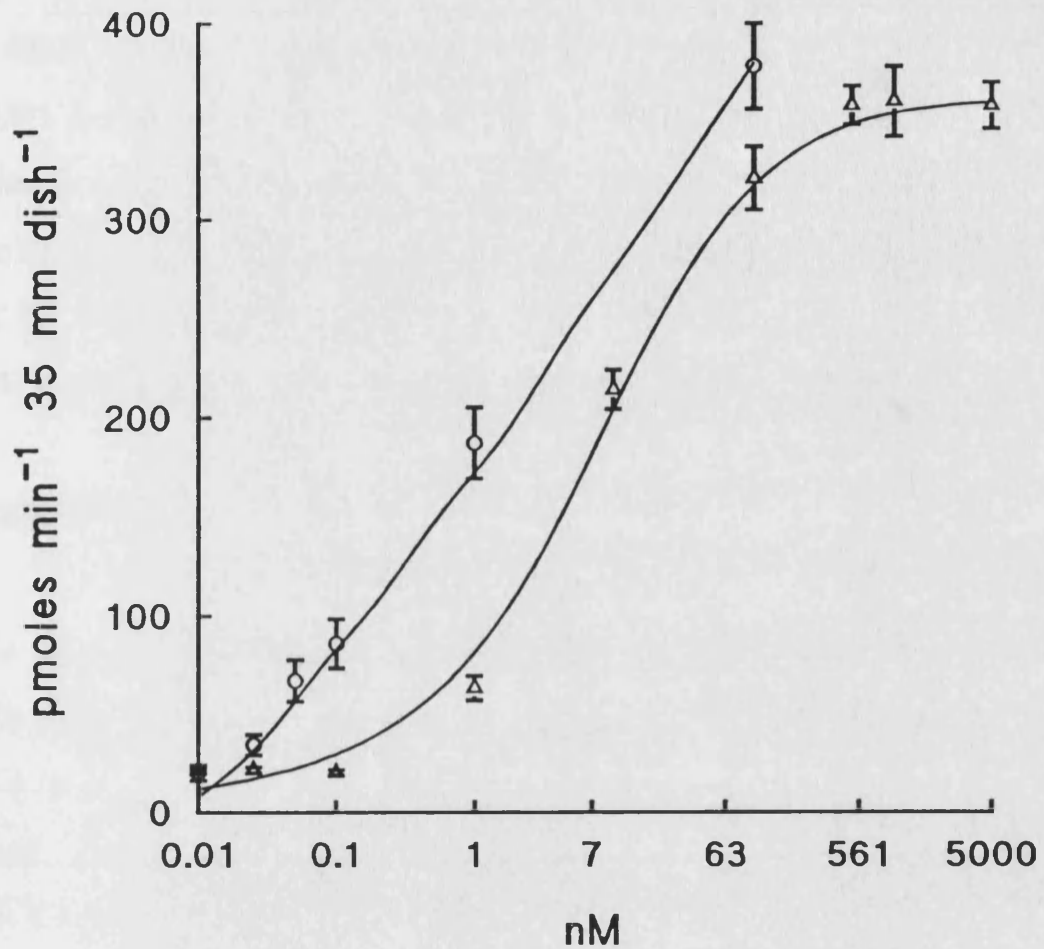


Fig.66 Dose response of translocation of 2-deoxy-D-glucose transport activity at pH 6.5.

3T3-L1 adipocytes were treated with 0, 0.025, 0.1, 1, 10, 100, 500 nM, 1 μ M and 10 μ M insulin in KRH buffer (pH 6.5) for 30 min at 37°C. The transport of 50 μ M 2-deoxy-[2,6-³H]-D-glucose was measured over 5 min. The cells were washed four times with KRH buffer (pH 6.5) and then dissolved in 0.1 M NaOH. The radioactivity was counted (Δ).

The 2-deoxy-D-glucose transport at pH 7.4 (O) was compared with pH 6.5.

at 10 $\mu\text{g}/\text{well}$ onto 1.5 mm gel. At basal state the γ -counts for GLUT1 was 2837 cpm and for GLUT4 it was 741 cpm. At 500 nM insulin concentration, the γ -counts result for GLUT1 was 8506 cpm, for GLUT4 it was 2189 cpm. Insulin increased both the basal state for GLUT1 and GLUT4 by about 3 fold. The half effective dose (ED_{50}) for GLUT1 was 1.04 nM and for GLUT4 was 4.22 nM. The comparison of transport activity, the ATB-BMPA labelling and Western blotting results are shown in Fig. 70 (GLUT1) and Fig. 71 (GLUT4).

3.13 THE EFFECT OF DIFFERENT pH ON INSULIN BINDING

It is well known that binding of [^{125}I]iodoinsulin to several cell types is markedly dependent on pH with a maximum in the range 7.5 to 8.2 (Cuatrecasas, 1971; Gavin *et al.*, 1973; Pederson and Beck-Nielsen, 1976; Ginsberg *et al.* 1976; Sonne and Gliemann, 1980). Sonne *et al.* (1981) reported that the amount of tracer bound at steady state at pH 7.8 was 6 times that at pH 6.8, the fractional degradation of receptor-bound iodoinsulin remained the same. The decreased binding at acidic pH could be accounted for by a decrease in the affinity.

De Meyts *et al.* (1976) have studied insulin binding in cultured human lymphocytes(IM-9) at 15°C and have shown that the dissociation rate constant at low receptor occupancy is markedly increased at acidic pH as compared to pH 7.8. In addition, these studies suggested that a high concentration of unlabelled insulin in the wash out medium had a more pronounced effect at pH 7.8 than at pH 7.0. It is therefore inferred from the work of De Meyts *et al.* that the receptors are in a low affinity state at acidic pH mainly because the dissociation rate constant is increased.

By contrast, Van Putten *et al.* (1985) reported that lowering of physiologic pH (pH 7.4) to pH 6.9 induced a decrease in insulin binding (50%) in cultured 3T3 adipocytes, which was due to a decrease in the rate of association.

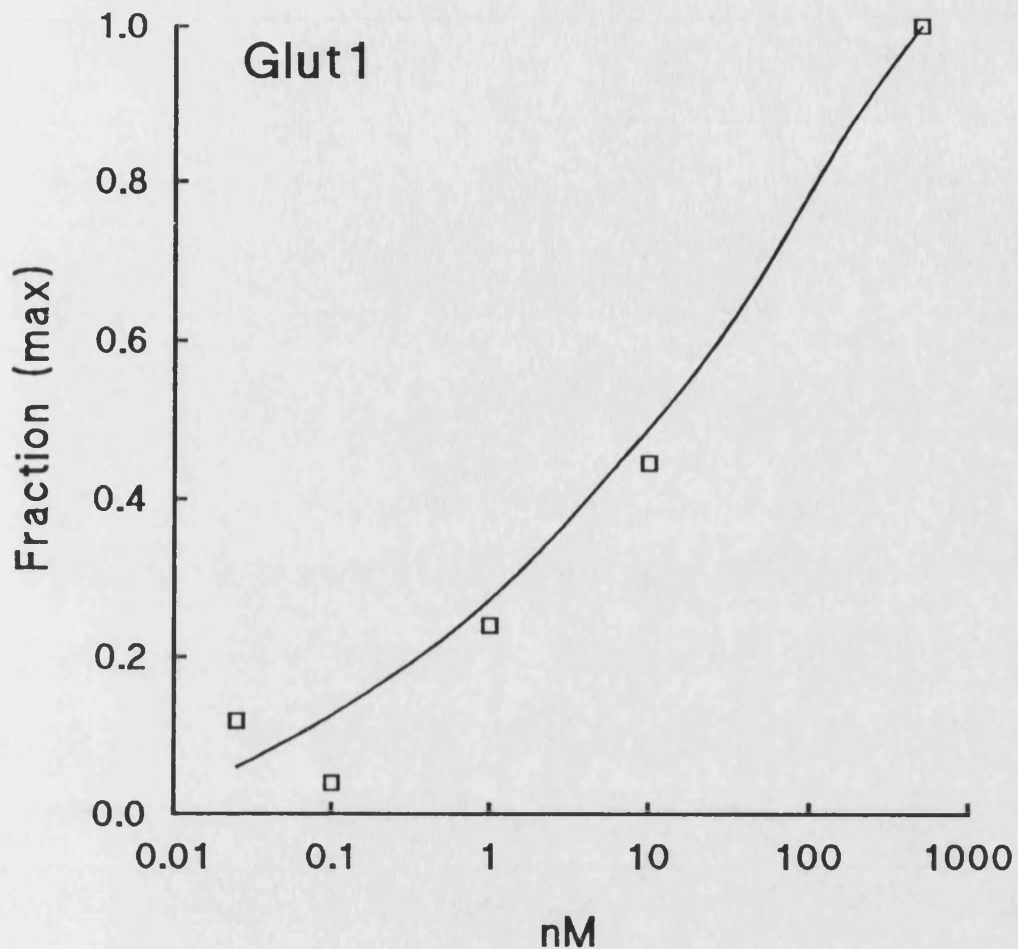


Fig.67 Dose response of translocation of GLUT1 at pH 6.5 by ATB-BMPA photolabelling in 3T3-L1 adipocytes.

3T3-L1 adipocytes were incubated with 0, 0.025, 0.1, 1, 10 and 500 nM of insulin in KRH buffer (pH 6.5) at 37°C for 30 min. The cells then were labelled with 100 μ Ci of ATB-[2-³H]-BMPA in 250 μ l of KRH buffer at 18°C. Following labelling the cells were washed four times in KRH buffer (pH 7.4) and solubilized in C₁₂E₉ detergent buffer. GLUT1 was then immunoprecipitated with anti-(C-terminal peptide) antibodies. The protein was then subjected to electrophoresis and the radioactivity was estimated by cutting out and counting the gel slices.

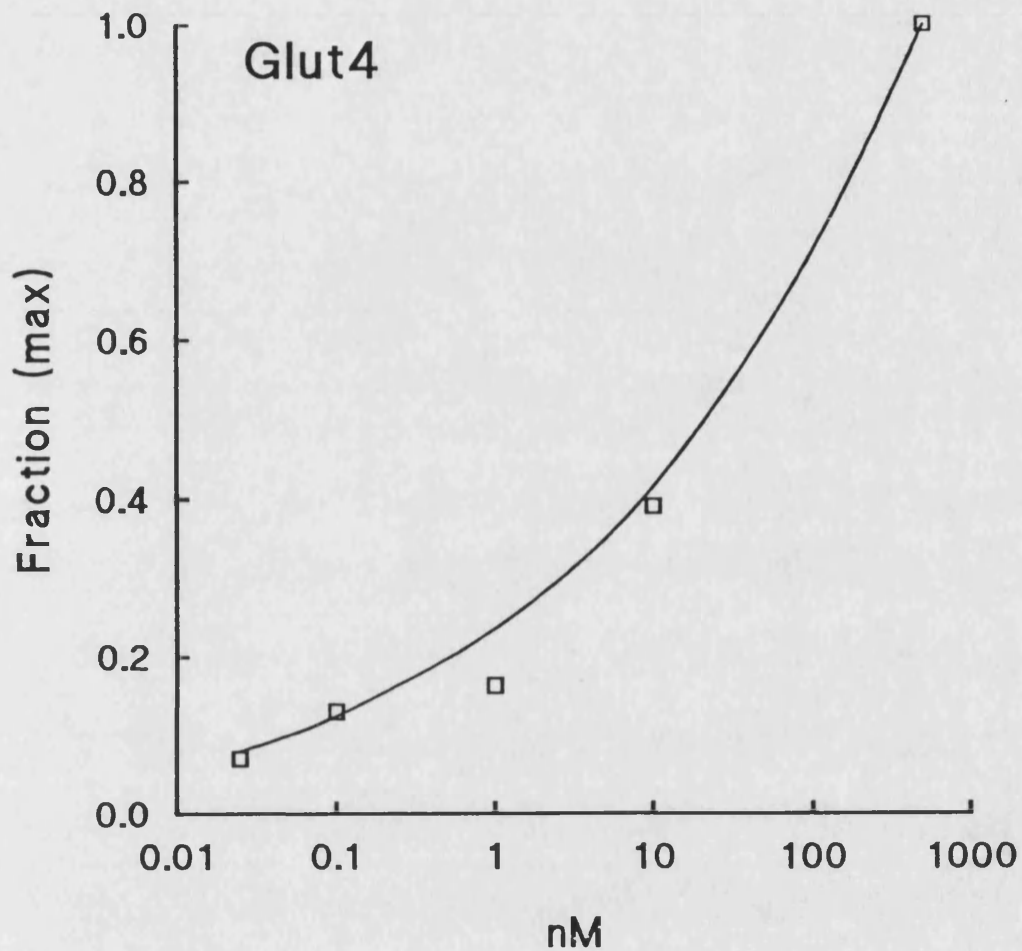


Fig.68 Dose response of translocation of GLUT4 at pH 6.5 by ATB-BMPA photolabelling in 3T3-L1 adipocytes.

3T3-L1 adipocytes were incubated with 0, 0.025, 0.1, 1, 10 and 500 nM of insulin in KRH buffer (pH 6.5) at 37°C for 30 min. The cells then were labelled with 100 μ Ci of ATB-[2-³H]-BMPA in 250 μ l of KRH buffer at 18°C. Following labelling the cells were washed four times in KRH buffer (pH 7.4) and solubilized in C₁₂E₉ detergent buffer. GLUT4 was then immunoprecipitated with anti-(C-terminal peptide) antibodies. The protein was then subjected to electrophoresis and the radioactivity was estimated by cutting out and counting the gel slices.

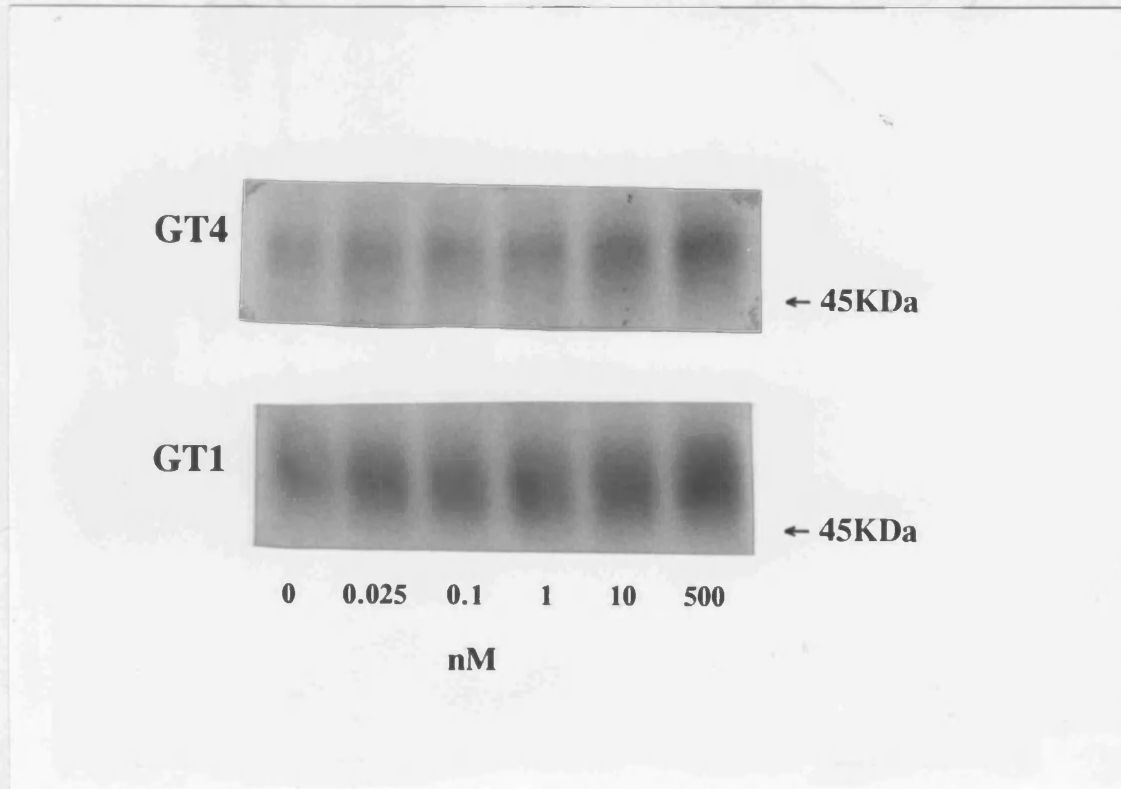


Fig.69 To test the dose response of translocation of GLUT1 and GLUT4 at pH 6.5 by Western blotting.

3T3-L1 adipocytes were incubated with 0, 0.025, 0.1, 1, 10 and 500 nM of insulin and KRH buffer (pH 6.5) at 37°C. The cells then were homogenized and purified plasma membrane (10 μ g) was subjected to SDS-PAGE. Proteins were transferred to nitrocellulose paper and incubated with a 1:500 dilution of anti-GLUT1 (a) and anti-GLUT4 (b) antibody. Blots were developed with 125 I labelled protein A and this photo was taken from x-ray films.

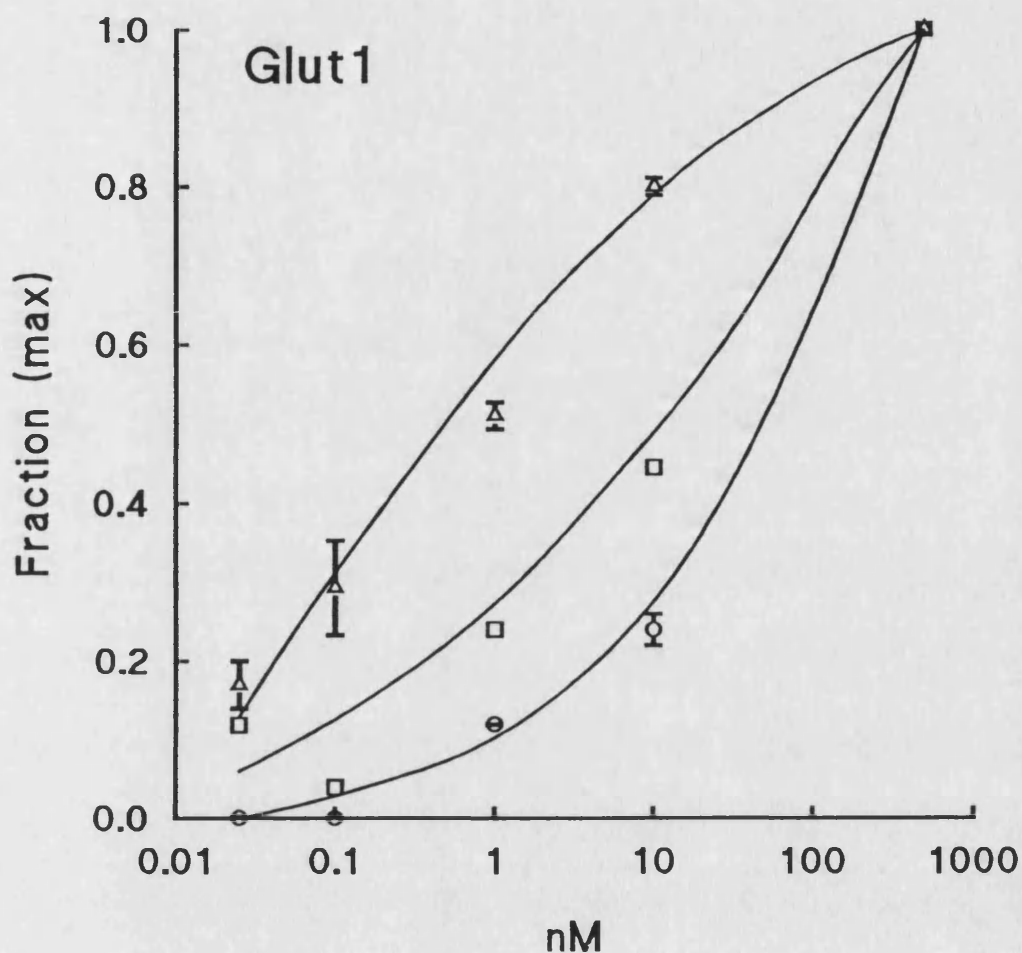


Fig.70 Comparison the dose response of translocation of GLUT1 and 2-deoxy-D-glucose transport activity at pH 6.5.

3T3-L1 adipocytes were incubated with 0, 0.025, 0.1, 1, 10 and 500 nM of insulin in KRH buffer (pH 6.5) at 37°C for 30 min. The fractions of 2-deoxy-D-glucose transport Fig.66 (○), the ATB-BMPA labelling Fig.67 (□) and immunoblotting Fig. 69 (Δ) of GLUT1 were compared.

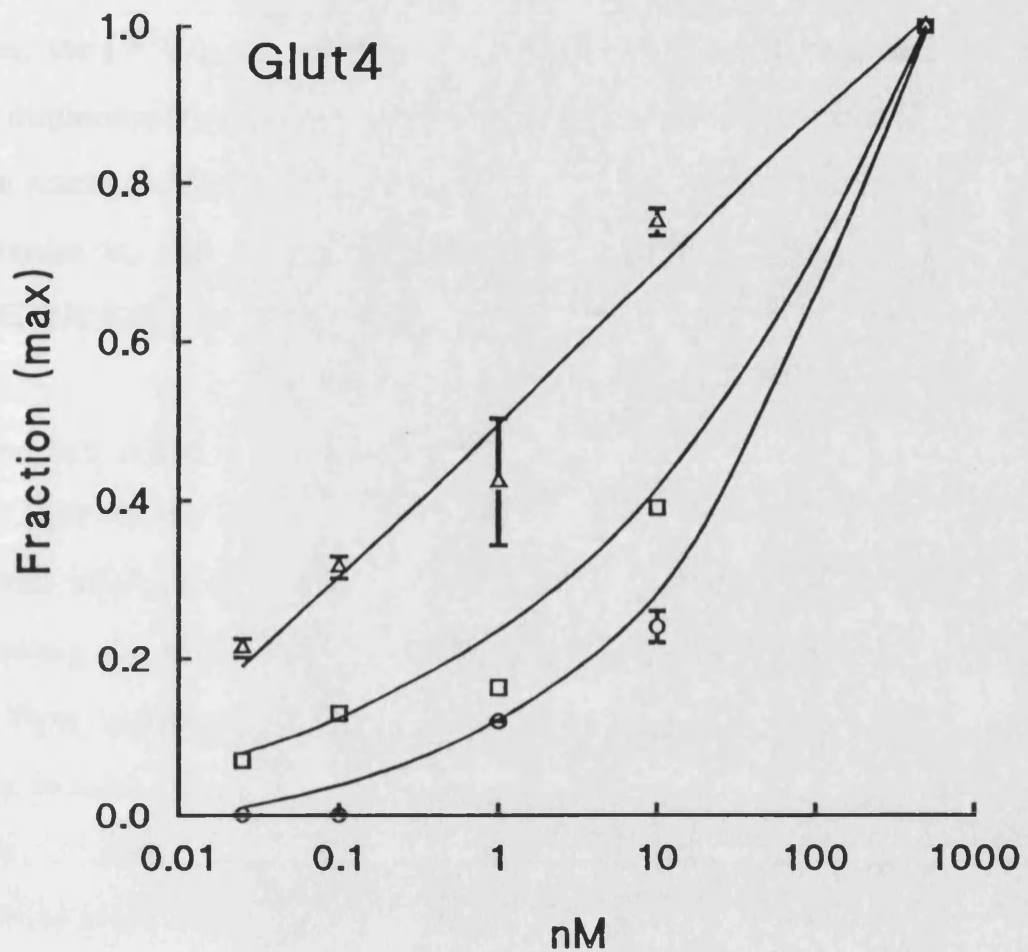


Fig.71 Comparison the dose response of translocation of GLUT4 and 2-deoxy-D-glucose transport activity at pH 6.5.

3T3-L1 adipocytes were incubated with 0, 0.025, 0.1, 1, 10 and 500 nM of insulin in KRH buffer (pH 6.5) at 37°C for 30 min. The fractions of 2-deoxy-D-glucose transport Fig.66 (○), the ATB-BMPA labelling Fig.68 (□) and immunoblotting Fig. 69 (Δ) of GLUT4 were compared.

To examine the effect of different pH on insulin binding at 3T3-L1 adipocytes, the [125 I]-insulin binding assay was performed at pH 6.5, pH 7.4, pH 8.0. The displacement curve of [125 I]-insulin binding at these three pH shown in Fig. 72. These results correspond well with the result that De Meyts and Van Putten. This result indicates that high pH (pH 8.0) increases the insulin binding to 3T3-adipocytes. At low pH (pH 6.5) a decrease insulin binding occurs.

The half effective dose of insulin binding at pH 7.4 and pH 8.0 are very similar. At pH 7.4 the half effective dose for insulin binding was 0.26 nM. At pH 8.0 the half effective dose for insulin binding was 0.39 nM. The K_d values for insulin binding and ED₅₀ values for glucose transport stimulation are summarized in Table 4. These results indicate that the high transport activity at pH 8.0 is not due the change on insulin binding. Possibly the high pH opens the vesicles in the cell surface which are occluded in the normal pH buffer. Further investigation will need to be done to improve our understanding of this finding.

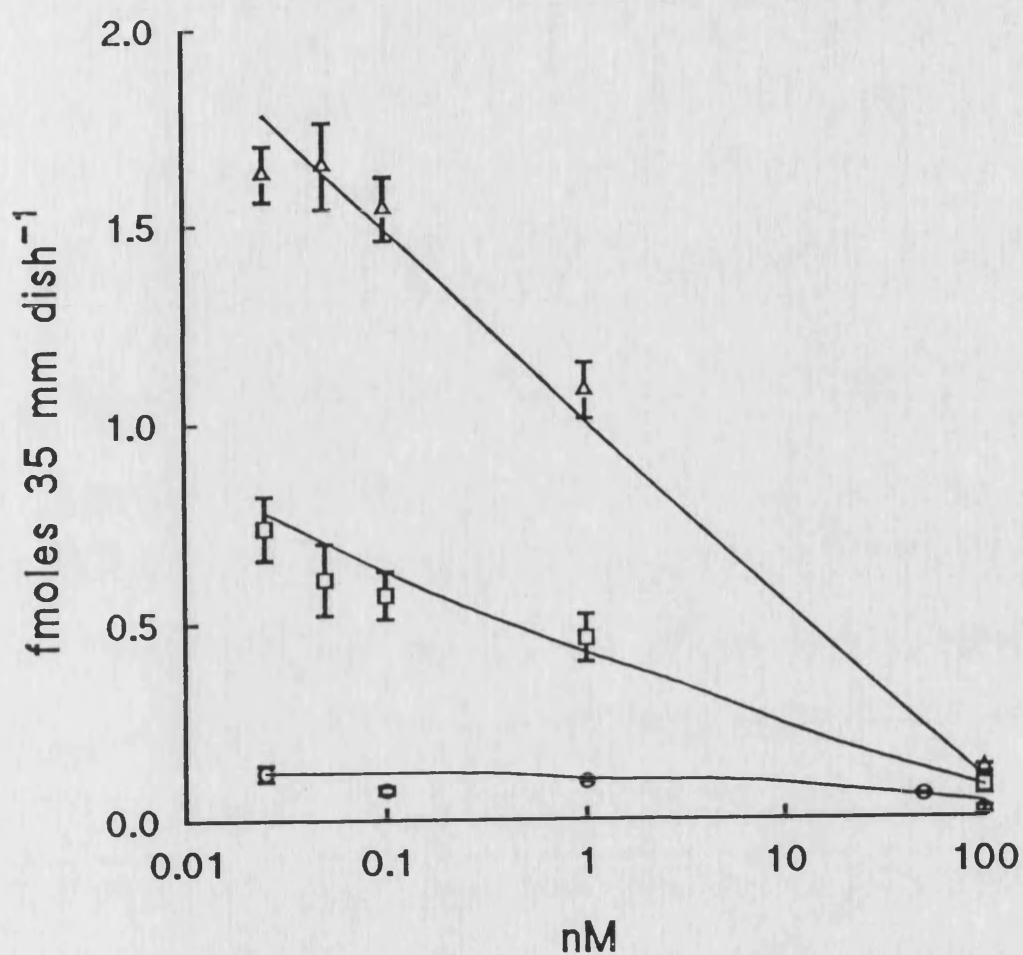


Fig. 72 Displacement curve of ^{125}I -insulin binding.

3T3-L1 adipocytes were incubated at pH 6.5 (○), pH 7.4 (□) and pH 8.0 (Δ) with 30 fmol ^{125}I -insulin and increasing amounts of unlabelled insulin for 3 hours at 20 °C. The results are from 4 determinations.

		pH7.4	pH8.0	pH6.5
2-deoxy-D-glucose transporter (ED ₅₀) nM		1.9	0.077	140.6
ATB-BMPA labelling (ED ₅₀) nM	Glut1	0.12	0.09	116.36
	Glut4	0.3	0.16	64.66
Western blotting (ED ₅₀) nM	Glut1	0.041	0.09	1.04
	Glut4	0.046	0.05	4.22
Insulin binding (K _d) nM		0.26	0.39	

Table 4 ED₅₀ for glucose transporter stimulation and K_d values for insulin binding at different pH

3T3-L1 adipocytes were incubated with 0, 0.025, 0.05, 0.1, 1 and 100 nM of insulin in KRH buffer (pH 7.4 and pH 8.0) and some cells were incubated with 0, 0.025, 0.1, 1, 10 and 500 nM of insulin in KRH buffer (pH 6.5) at 37°C for 30 min. The half effective dose of 2-deoxy-D-glucose transport, the ATB-BMPA labelling and immunoblotting at these pHs were compared. The K_d values for insulin binding at pH 7.4 and pH 8.0 were also compared.

4.0 DISCUSSION

4.1 BACKGROUND STUDIES

The transport of glucose in insulin-sensitive tissues is mediated by two transporter isoforms, GLUT1 and GLUT4. GLUT4 is the major isoform present in fat and muscle and its expression is restricted to insulin sensitive tissues (James *et al.*, 1989; Birnbaum, 1989; Charron *et al.*, 1989; Fukumoto *et al.*, 1989). GLUT1 is expressed in many cell types, including those that do not normally exhibit insulin-sensitive glucose transport (Mueckler *et al.*, 1985; Birnbaum *et al.*, 1986; Filer *et al.*, 1987; Fukumoto *et al.*, 1988).

It is well documented that insulin stimulates hexose transport in 3T3-L1 adipocytes rapidly and typically by 10-fold or more (Frost and Lane., 1985; Calderhead and Lienhard., 1988). Because of this large effect, this cell line has been used as a good model for investigations of the basis for insulin action on glucose transport.

It has been known that both GLUT1 and GLUT4 transporters are present in 3T3-L1 adipocytes. Unlike the rat adipocytes, the GLUT1 is a major transporter in 3T3-L1 cells. However, the increase in GLUT1 at the cell surface in response to insulin, which has been assessed by quantitative immunoelectron microscopy (Blok *et al.*, 1988), by labelling of surface GLUT1 with galactose oxidase and ^3H borohydride (Calderhead *et al.*, 1988), and by relative GLUT1 content of a plasma membrane fraction (Gould *et al.*, 1989), is only 2-3 fold; while the increase in GLUT4 is about 11 fold. The results presented in this thesis have shown that upon insulin stimulation, ATB-BMPA labelled GLUT1 was increased about 3-5 fold compared to basal, and GLUT4 was increased 15-20 fold. This indicated that GLUT4

is also a major isoform that responds to insulin stimulation of glucose transport on 3T3-L1 adipocytes. An increase in GLUT4 mRNA and protein has been shown to be associated with the differentiation of the adipocyte phenotype (Kaestner., *et al* 1989). It is the concentration of this novel glucose transporter in adipose cells which is lowered in streptozotocin-induced diabetes (Kahn *et al.*, 1989; Berger *et al.*, 1989). Both the mRNA and the intracellular pool of this glucose transporter are strikingly lowered, while the level of the GLUT1 transporter is unchanged. These studies show that the large stimulations by insulin of glucose transport in 3T3-L1 cell are clearly related to the presence of the GLUT4 isoform.

Clark and Holman (1990) have shown that the bis-D-mannose compound ATB-BMPA can photolabel the glucose transporter isoform GLUT1. In erythrocytes ATB-BMPA labels a single band of protein which when analysed by SDS-PAGE has an apparent molecular mass of 45-66 kDa. Holman *et al* (1990) reported this compound can also photolabel GLUT4. In adipocytes, the ATB-BMPA labels a \approx 55 kDa protein. It has been demonstrated that the label is specifically binding to a glucose transporter protein-GLUT1, by displacing ATB-BMPA labelling totally with 100 mM D-glucose (Clark and Holman, 1990). In adipocytes, the ATB-BMPA labelling of GLUT4, is also completely displaceable with D-glucose (Holman *et al.*, 1990). The label therefore specifically binds to these two glucose transporters.

The anti-GLUT1 antibody immunoprecipitates 70-80% of the ATB-BMPA photolabelled GLUT1 in intact erythrocytes (Clark and Holman, 1990). The anti-GLUT4 antibody immunoprecipitates 70-80% of the labelled transporter peak obtained in membranes which are isolated from insulin-treated adipose cells but which are not subjected to immunoprecipitation (Holman *et al.*, 1990). Although this comparison does not directly compare GLUT1 and GLUT4 in the same cell type, it does suggest that the antibodies probably immunoprecipitate GLUT1 and GLUT4 with similar efficiencies and that photolabelling with ATB-BMPA does not reduce the

precipitation efficiency.

Calderhead *et al.* (1990) have shown that when GLUT1 and GLUT4 were immunoprecipitated from 3T3-L1 adipocytes and then each immunoprecipitate was immunoblotted for both transporters, only GLUT1 was detected in the immunoprecipitate with antibodies against GLUT1 and only GLUT4 was detected in the immunoprecipitate with antibodies against GLUT4.

Palfreyman *et al.* (1992) have observed that the K_i for ATB-BMPA is $\approx 250 \mu\text{M}$ in acutely and chronically insulin-treated 3T3-L1 cells. These results are similar to those in which transport is inhibited by ATB-BMPA in erythrocytes. In those cells a GLUT1 $K_i \approx 250 \mu\text{M}$ has been reported (Clark and Holman, 1990). Transport inhibition by ATB-BMPA in rat adipocytes (where GLUT4 is the predominant isoform) has shown a GLUT4 $K_i \approx 250 \mu\text{M}$ (Holman *et al.*, 1990). The GLUT2 isoform in liver membranes also has a K_d for ATB-BMPA of about $200 \mu\text{M}$ (Jordan and Holman, 1992). Thus the binding of ATB-BMPA (a non-transported ligand) is approximately equal for all the mammalian isoforms tested (GLUT1, GLUT4 and GLUT2). This suggests that the ATB-BMPA binding site, in contrast to the cytochalasin B binding site, is conserved in all glucose-transporter isoforms. Recent studies indicate that, on irradiation, ATB-BMPA labels the exofacial region of the helix 8 and that helices 7, 8 and 9 are important in exofacial ligand binding (Davies *et al.*, unpublished work).

4.2 DEVELOPMENT OF AN INTRACELLULAR POOL OF GLUCOSE TRANSPORTERS IN 3T3-L1 CELLS

The sequestration of glucose transporters in an intracellular pool is likely to be a general mechanism by which cells regulate the supply of glucose to metabolic enzymes in line with the growth demands and cellular-metabolism requirements of

the cell. The phenomenon of intracellular transporter sequestration was first demonstrated in insulin-sensitive rat adipose cells by Cushman and Wardzala, (1980) and Suzuki and Kono, (1980) and has subsequently been found in other insulin responsive tissues such as brown adipose tissue (Slot *et al.*, 1991a), heart muscle (Watanabe *et al.*, 1984, Slot *et al.*, 1991b), diaphragm muscle (Wardzala and Jeanrenaud, 1983) and skeletal muscle (Klip *et al.*, 1987; Hirshman *et al.*, 1990; Klip *et al.*, 1990). In addition it has been shown that virus infection of BHK cells (Widnell *et al.*, 1990) leads to a redistribution of internalized GLUT1 transporters to the cell surface. Widnell *et al.*, 1990 have also shown that in BHK cells the sequestered GLUT1 transporters redistribute to the cell-surface in response to stress stimuli such as arsenite and heat shock. Haspel *et al.*, (1986) have shown that in fibroblasts GLUT1 redistribution can occur in response to glucose starvation. Although the cellular redistributions of glucose transporters can be followed by subcellular fractionation and separation of plasma membrane from the light microsome membranes (Slot *et al.*, 1991a,b; Smith *et al.*, 1991), this is not a technique that can be readily applied to cells and tissues that are difficult to successfully homogenize and fractionate such as skeletal muscle (Klip *et al.*, 1987) and cultured cells (Calderhead *et al.*, 1990).

Immunochemical techniques (Blok *et al.*, 1988; Slot *et al.*, 1991a,b; Smith *et al.*, 1991, Widnell *et al.*, 1990, Tordjman *et al.*, 1990) circumvent the need to obtain subcellular membrane fractions but these methods are not easily adaptable to investigations of the kinetics of transporter regulation.

As an alternative to these methods, impermeant photolabel ATB-BMPA has been used to measure both the cell-surface and total-cellular levels of transporters. The method, when applied to differentiated 3T3-L1 adipocytes, gives results which are consistent with those obtained by Gould *et al.*, (1986) who used Western blotting of isolated membrane fractions to determine that about half of the cell GLUT1 was at

the cell-surface in the insulin-stimulated state.

ATB-BMPA has been used to investigate at what stage during growth and differentiation of 3T3-L1 cells the transporter sequestration develops. Initially, it was assumed that the cellular mechanisms necessary for transporter sequestration was most likely to develop during the period of differentiation from fibroblasts to adipocytes. It was surprising to find that GLUT1 transporters were down-regulated from the cell surface as the cells reached confluence as fibroblasts. The sequestration mechanism seems capable of internalizing over 75% of the total GLUT1 transporter both in confluent fibroblasts and in differentiated adipocytes. At both the fibroblast and adipocyte stage insulin produced a redistribution of about half of the available GLUT1 to the cell surface. Additional sequestration capability may have also developed as additional GLUT1 transporters were synthesized during differentiation. Alternatively, there may have been spare capacity available in fibroblasts that could potentially sequester any new GLUT1 or GLUT4 that was introduced into fibroblasts or produced in subsequent differentiation.

Gould *et al.* (1989) have shown that in 3T3-L1 cells transfected with human GLUT1 $\approx 50\%$ of both the transfected and endogenous murine GLUT1 were sequestered in intracellular membranes and that both human GLUT1 and endogenous GLUT1 responded equally to insulin stimulation of translocation.

Joost *et al.* (1992) have shown that during growth of the fibroblasts to confluence, basal transport activity decreased to 20% of that in non-confluent cells. Corresponding with the reduction in transport activity, the abundance of GLUT1 in plasma membranes as normalized per cell decreased by 75% during growth of the cells to confluence. They suggested that this effect was mainly due to a reduction of total cellular GLUT1. In addition, the portion of GLUT1 located in intracellular vesicles (low-density microsomes) was moderately increased in confluent cells. The

reason for the difference between the results in this thesis and the results of Joost *et al* may be that they did not recover all the membrane protein after homogenization. Therefore it is an advantage to label permeabilized cells as membrane losses are minimized.

Other investigators have shown that there is either no change in the basal transport activity throughout differentiation (Kaestner, 1989) or that basal activity falls in the first few days after the initiation of differentiation (Weiland *et al.*, 1990; Harrison *et al.*, 1990). The results in this thesis show that basal activity can fall markedly if cells are maintained at full confluence for several days without the initiation of differentiation. Thus the studies cited above can be reconciled if there was a variable time after confluence was reached and before the differentiation regime was initiated. Thus if the initiation programme was started earlier than in these experiments the basal rate would have fallen during the first few days of differentiation. However, the results in this thesis suggest that the increase in transporter sequestration and the fall in the transport activity is not a direct consequence of the differentiation regime but develops because cells are in a growth arrested phase of the cell cycle.

The results from this thesis and those of other investigators (Kaestner *et al.*, 1989; Garcia de Herreros and Birnbaum 1989; Weiland *et al*, 1990), show that insulin-stimulated transport activity in adipocytes is much higher than in fibroblasts. Joost *et al*, (1992) have shown that in the differentiated adipocytes, insulin stimulated a 10-fold increase in glucose transport activity, the maximum levels approaching basal transport rates of non-confluent cells; both GLUT1 and GLUT4 were translocated in response to insulin.

The discrepancy between transport activity and labelled-transporter level when comparing fibroblasts with differentiated adipocytes in the basal state has also been

observed in this studies. In this thesis, the ratio of transport activity to GLUT1 labelling in fibroblasts can be calculated as $130 \text{ pmoles}/10^6 \text{ cells}/\text{min}$ divided by GLUT1 labelling of $970 \text{ dpm}/10^6 \text{ cells}$ or $0.044 \text{ pmoles}/10^6 \text{ cells}$ (the specific activity is $10 \text{ Ci}/\text{mmole}$). This intrinsic activity ratio is $41 \text{ pmoles}/10^6 \text{ cells}/\text{min}$ divided by GLUT1 labelling of $590 \text{ dpm}/10^6 \text{ cells}$ or $0.026 \text{ pmoles}/10^6 \text{ cells}$ in differentiated cells. Thus during the transition from preconfluent fibroblasts to differentiated adipocytes the intrinsic activity ratio falls from 2954 min^{-1} in fibroblasts to 1576 min^{-1} in adipocytes in the basal state. Any GLUT4 present at the surface of basal adipocytes would lower this ratio. These results suggest that the activity of GLUT1 and probably GLUT4 is suppressed by 40-50% and are consistent with estimates of the intrinsic activity of GLUT1 and GLUT4 previously reported for the basal state (Holman *et al.*, 1990; Kozka *et al.*, 1991; Clark *et al.*, 1991; Palfreyman *et al.*, 1992; present studies).

Several studies using the photolabel (as cited above) have shown an ≈ 2 -fold discrepancy between photolabelling and transport and have shown a lag between the appearance of transporters that can be photolabelled and the increase in transport activity following insulin stimulation of rat adipocytes (Clark *et al.*, 1991; Satoh *et al.*, 1991) and 3T3-L1 cells (present studies). These studies show that ATB-BMPA binds to transporters that are inactive in transport catalysis. These studies have suggested that it is this form of the transporter that may be associated with modifier proteins such as those involved in trafficking events in the normal translocation pathway. In addition, there is a further discrepancy between transporters that are detected by labelling compared with Western blotting, as in isoproterenol treated insulin-stimulated rat adipocytes (Vannucci *et al.*, 1992) and phenylarsine oxide-treated insulin-stimulated 3T3-L1 cells (present studies). This may be due to the formation of plasma membrane associated, but occluded, vesicles. These results suggest that the transport-inactive form at the plasma membrane is a relatively small fraction of the total plasma membrane pool, that these forms represent intermediates

in normal transporter trafficking and that translocation is the major mechanism by which glucose transport is stimulated in insulin-sensitive cells.

The experiments in which digitonin have been used suggest that the photolabel interacts with equal amounts of transporter in the basal and insulin-stimulated states and that this provides additional evidence, to that previously described (Calderhead *et al.*, 1990; Holman *et al.*, 1990), which suggests that basal and insulin-stimulated transporters do not have differing affinities for the photolabel. If an inhibitory protein were present in basal cells which produced a large increase in the proportion of transporters in a catalytically inactive state, then this association would be expected to reduce the apparent labelling of the total cellular transporter pool of basal cells. Thus these experiments in which cells are digitonin permeabilized also suggest that the proportion of transporters with suppressed activity is small and that the low surface-levels of transporters detected by labelling of cells in the basal state is due to transporter sequestration within the intracellular pool.

During the process of 3T3-L1 cell differentiation over 95% of the total cellular GLUT4 in the intracellular pool was sequestered. This is similar to the level of sequestration of GLUT4 seen in other insulin-responsive tissues (Slot *et al.*, 1991a,b). The greater sequestration of GLUT4 may be related to the targeting of this isoform to separate intracellular vesicles (Zorzano *et al.*, 1989), although Calderhead *et al.* (1990) have reported that GLUT1 and GLUT4 were detected in the same vesicles. It seems likely that the two isoforms leave the cell surface by the same endocytosis route as it has been shown that both isoforms are endocytosed with the same half-time when insulin is removed and the calculated rate constant k_{en} is similar. This has been observed in rat adipocytes (Clark *et al.*, 1991) and in 3T3-L1 cells (present studies). However, in insulin-stimulated 3T3-L1 cells which are treated with the vicinal dithiol inactivating reagent phenylarsine oxide, there may be some separation of the transporter vesicle processing as GLUT4 re-exocytosis appeared to

be blocked by this reagent but GLUT1 re-exocytosis was not. Cellular mechanisms for the separate localization and processing of GLUT4 must be very dependent on the GLUT4 protein structure as GLUT4 transfected into expression systems tends to become localized inside the cell rather than at the plasma membrane (Gould *et al.*, 1991).

The studies on the use of the photolabel in permeabilized 3T3-L1 cells described here have shown that transporter sequestration can occur before differentiation is initiated and that transporters produced in differentiation probably enter a pre-formed sequestration process.

4.3 DETERMINATION OF THE RATES OF APPEARANCE AND LOSS OF GLUCOSE TRANSPORTERS AT THE CELL SURFACE IN 3T3-L1 ADIPOCYTES

The acute activation of glucose transport into fat and muscle cells by insulin is probably the best-known biochemical action of this hormone, but until recently little was understood about its chemical basis.

Cushman and Wardzala (Cushman and Wardzala, 1980) and Suzuki and Kono (Suzuki and Kono, 1980) proposed in 1980 that glucose transporters, like receptors and other membrane proteins, were translocated from light-microsome vesicles to the plasma membrane of adipose cells in response to insulin.

Recently, two different but complementary approaches to investigating this membrane trafficking phenomenon have provided very strong support for their hypothesis. Slot *et al.* (1991b) have used antibodies specific for the insulin-regulatable glucose transporter (GLUT4) to immunolocalize this protein in brown adipose tissue from basal and insulin-treated rats. They showed under basal

conditions that 99% of the GLUT4 labelling was located within the cell. Labelling was predominantly in the trans-Golgi reticulum and tubulo-vesicular structures elsewhere in the cytoplasm. In insulin-stimulated cells about 40% of the GLUT4 labelling was at the cell surface. Upon insulin stimulation the GLUT4 located in the plasma membrane was increased by 40-fold.

The second approach that has provided strong supportive evidence for the translocation hypothesis has involved use of the bis-mannose photolabel-ATB-BMPA in trafficking kinetic experiments. ATB-BMPA can provide quantitative information on the abundance of glucose transporter isoforms at the plasma membrane (Clark *et al.*, 1990; Holman *et al.*, 1990; Calderhead *et al.*, 1990). This label is a good probe to examine the kinetic of the cellular trafficking, as it can selectively label transporters when they appear and are removed from the cell surface.

Satoh *et al.* (1991) have shown, in trafficking experiments using the ATB-BMPA photolabel, that transporters are recycled between plasma membrane and light-microsome pools. Fully insulin-stimulated cells were photolabelled with ATB-BMPA and then insulin was removed by collagenase treatment. Labelled transporters were shown to be transferred to the light-microsome membranes. Equilibration of cell-surface labelled transporters with the light-microsome pool also occurred when cells were maintained, after labelling, in the continuous presence of insulin. In the presence of insulin, the level of transporters in the light-microsomes reached a lower steady-state level than that which occurred following insulin removal. These experiments have thus provided direct evidence that transporters move between the plasma-membrane and light microsome pools. Furthermore, restimulation experiments have directly shown that internalized transporters are re-exocytosed to the plasma membrane. Insulin stimulation was shown to be due to an enhancement of exocytosis rather than due to an inhibition of the endocytosis of transporters (Clark *et al.*, 1991; Satoh, *et al.*, 1991).

Use of the ATB-BMPA photolabelling reagent has also allowed an assessment of the magnitude of translocation to be made in intact adipose cells. Insulin has been shown to increase cell-surface GLUT4 by 15-20-fold while GLUT1 is only increased by ≈ 5 -fold. The use of this in-situ labelling procedure has circumvented the need to use subcellular fractionation of cells which is considered to underestimate the magnitude of the translocation effect due to the cross-contamination of plasma membrane and light-microsome membrane fractions. (Holman *et al.*, 1990; Kozka *et al.*, 1991; Clark *et al.*, 1991).

The redistribution of the two transporters from the intracellular to the plasma membrane-containing fractions of the sucrose gradient in response to insulin provides further evidence for the translocation of each transporter. The fact that the insulin induced increase in translocation to the plasma membrane-containing fractions is considerably less (2-and 4-fold, respectively, for GLUT1 and GLUT4) than that found by the ATB-BMPA labelling method may be due to the contamination of these fractions with intracellular membrane containing the transporters (Calderhead *et al.*, 1990).

The photolabel ATB-BMPA has been used to compare the time-courses for appearance and loss of transporters in rat adipocytes with the time course for change in glucose transport activity. Clark *et al.* (1991) have found that the time course of GLUT4 and GLUT1 appearance at the cell surface showed no lag and a half time of about 2.3 min for both isoforms. The time course for insulin stimulation of glucose transport activity occurred with a slight lag period of 47 sec and a half time of 3.2 min. Thus at early times after insulin stimulation there was a discrepancy between transporter abundance and transport activity. The lag period in the stimulation of transport activity may represent the time required for about 2 fold stimulation of transport intrinsic activity. The decrease in transport activity after insulin removal occurred with a very high activation energy of 159kJ.mol. There was thus no

significant decrease in transport or loss of cell-surface transport over 60 min at 18°C. The decrease in transport activity occurred with a half time of 9-11 min at 37°C. The ATB-BMPA labelled experiment showed that the loss of GLUT4 and GLUT1 occurred with half time values of about 12 min. This study has shown that on insulin addition the arrival of GLUT1 and GLUT4 transporters at the cell-surface slightly precedes the increase in transport activity, but that the loss of these transporters from the cell-surface on insulin removal correlated well with transport. Results presented in this thesis show that these effects also occur in 3T3-L1 cells. At 27°C the half-time for the appearance of GLUT1 and GLUT4 at the cell surface were 5.7 and 5.4 min respectively and were slightly shorter than that for the observed stimulation of transport activity (half-time 8.6 min). These studies are consistent with the observations of Karnielli *et al.* (1981), who have shown that the appearance of cytochalasin B-binding sites in plasma membrane fractions isolated from insulin treated adipose cells preceded transport stimulation. In addition Gibbs *et al.* (1988) showed that the arrival of GLUT1 at the surface of 3T3-L1 cells preceded the stimulation of transport. This lag may occur because transporters are still associated with trafficking-proteins at early time points following insulin addition to the cells. Thus the translocation may precede the transport activation due to the requirement for a dissociation from these proteins.

When fully insulin stimulated cells were subjected to a low-pH washing procedure to remove insulin at 37°C, the cell-surface levels of GLUT1 and GLUT4 decreased, with half-time of 9.2 and 6.8 min respectively. These times correlated well with a decrease in 2-deoxy-D-glucose-transport activity that occurred during this washing procedure (half-time 6.5 min).

The loss of transporters from the cell-surface occurs with half-times which are very similar to the half-time for internalization of other membrane proteins and receptors such as the transferrin and the asialoglycoprotein receptors (Goldstein *et*

al., 1985; Stoorvogel *et al.*, 1987; Gibbs *et al.*, 1986) suggesting that this internalization step occurs by receptor mediated endocytosis (Lienhard, 1983). The high activation energy for reversal of transport stimulation and the almost complete cessation of glucose transporter internalization at 18°C (Clark *et al.*, 1991) are also consistent with this possibility.

The transporter immuno-localisation study of Slot *et al.* (1991b) have found that in the basal state GLUT4 is concentrated in tubulo-vesicular structures in the trans-Golgi region and elsewhere throughout the cytoplasm. Upon insulin treatment there is a marked shift in GLUT4 from these sites to the plasma membrane, such that the amount of GLUT4 at the cell-surface increases by at least 40-fold; moreover, GLUT4 is seen to enter the coated pit/coated vesicle/early endosome pathway typical for receptor-mediated endocytosis. These findings indicate that the translocation of GLUT4 is the major mechanism by which insulin stimulates glucose transport in brown adipocytes, and they provide evidence that this multi-spanning membrane protein can recycle by the same route as receptors.

The evidence for the localization of GLUT4 in coated pits and early endosomes is particularly interesting. This indicates that a transporter undergoes recycling by the pathway that has been well established for cell surface receptors. Unlike these receptors, which contain a single transmembrane segment per polypeptide chain, the glucose transporter has 12 putative membrane-spanning domains (Mueckler *et al.*, 1985; James *et al.*, 1990). This evidence that GLUT4 is continuously endocytosed in insulin-treated adipocytes points to a tentative conclusion concerning the locus of insulin action. GLUT4 could be effectively excluded from the membrane in the basal state by intracellular sequestration or by an efficient internalization process. Thus, the redistribution of GLUT4 to the cell-surface in response to insulin could be due either to an increased rate of exocytosis of the transporter or to decreased rate of its endocytosis.

The association of this transporter in clathrin-vesicles was increased by insulin treatment of the cells. Other trafficking-proteins that may be involved include small G-proteins. It is now known that these are intricately involved in many vesicle-trafficking events (Bourne *et al.*, 1991). Beckers and Balch (1989) have reported that Calcium and GTP are essential components in vesicular trafficking between the endoplasmic reticulum and Golgi apparatus. Transport was inhibited rapidly and irreversibly in the presence of micromolar concentrations of the nonhydrolyzable GTP analogue, GTP γ S. The transport block in the presence of GTP γ S was found to be distal to a post-endoplasmic reticulum, pre-Golgi compartment where proteins accumulate during incubation at 15°C. Transport was also completely inhibited in the absence of free Ca²⁺. A sharp peak defining optimal transport between the endoplasmic reticulum and the *cis*-Golgi was found to occur in the presence of 0.1 μ M free Ca²⁺. G-protein involvement in glucose transporter trafficking has been clearly implicated by the discovery of Baldini *et al* (Baldini *et al.*, 1991) that the non-hydrolysable GTP analogue γ -GTP stimulates translocation of GLUT4 from the light-microsome pool to the plasma membrane of rat adipocytes. The GTP itself is ineffective, thus, a GTP-binding protein might be involved in translocation of GLUT4 from the LDM to the plasma membrane. Many ras-like GTP-binding proteins are involved in intracellular vesicular traffic and /or cell growth.

Other proteins that are likely to be involved in the trafficking include adaptins. These have been implicated in the enhancement of receptor association with clathrin (Robinson, 1987) and their involvement in the trafficking of other membrane proteins is likely. A reasonable interpretation of some features of the trafficking kinetics of glucose transporters in 3T3-L1 cells that have been observed here is that a dissociation from trafficking-proteins occurs before the transporters can fully participate in transport.

4.4 EFFECT OF PHENYLARSINE OXIDE ON GLUT1 AND GLUT4 TRAFFICKING

The effects of PAO on the trafficking of membrane proteins have generally been reported to be due to inhibition of fluid-phase endocytosis by this reagent (Knutson, *et al.*, 1986; Wiley and Cunningham, 1982; Frost *et al.*, 1989). However, the resolution of an effect on endocytosis or exocytosis is difficult. It is possible for example that receptors are internalized and reappear at the surface but then fail to dissociate from the trafficking proteins because this process is blocked by PAO. Receptor abundance at the surface would remain high due to a single cycle of internalization and re-exocytosis and the whole cycling process would halt. The net result would be that endocytosis would appear to be inhibited. There is evidence against the possibility that a simple block of endocytosis occurs. PAO has been shown (Gould *et al.*, 1989) to reduce surface transferrin receptors as measured by transferrin binding to whole cells but to increase the level of plasma membrane associated receptors measured in an isolated membrane fraction. It was proposed (Gould *et al.*, 1989) that this effect may have occurred because recycled vesicles containing the receptors could not fuse with the plasma membrane but many remained associated with it during sub-cellular fractionation.

The GLUT1 contribution to transport is about one third of that of GLUT4 in fully insulin stimulated cells (Holman *et al.*, 1990; Calderhead *et al.*, 1990; Kozka *et al.*, 1991). Yet when the insulin stimulation was reversed with PAO the fall in transport followed the fall in GLUT4 and the remaining cell-surface GLUT1 appeared to make only a minimal contribution to transport. Thus GLUT1 may be internalized and recycled to the surface but many remain associated with trafficking-proteins which suppress its transport capability. This association with trafficking proteins may be similar to that which occurs in the lag-phase of insulin activation (Clark *et al.*, 1991; Satoh *et al.*, 1991; Gibbs, *et al.*, 1988; Karnielli *et al.*, 1981;

and the present study) and may account for the low contribution of cell-surface GLUT1 to the transport activity in basal cells (Calderhead *et al.*, 1990; Clancy and Czech, 1990).

Harrison *et al.* (1990) have proposed that GLUT1 activity is suppressed in transfected 3T3-L1 cells. Kozka, *et al* (1991) have shown that it is difficult to remove GLUT1 from the cell-surface following chronic-insulin treatment but that this cell-surface GLUT1 appears to have low transport capability. The location of transporters of suppressed activity may be in surface-attached vesicles. These may be intermediates in the insulin-stimulated trafficking pathway (Satoh *et al.*, 1991). If some of the surface-attached vesicles are surface-exposed then glucose transporters in these vesicles would be photolabelled but would possibly not be able to participate in transport if they were still associated with trafficking proteins.

If the effect of PAO is mainly due to an inhibition of exocytotic vesicle fusion with the plasma membrane and/or inhibition of transporter dissociation from trafficking-proteins then this inhibition could also account for the fall in cell-surface GLUT4 that is detectable with the ATB-BMPA photolabel. A proportion of the GLUT4 transporters which are removed from surface accessibility to the photolabel in PAO treated cells appear to fractionate with the plasma membrane. The percentage of transporters recovered in the light microsomes was similar to that obtained with insulin alone. This effect is being further investigated but it may be similar to that observed with transferrin receptors where a PAO-induced failure of recycled vesicles to fuse with the plasma membrane was proposed (Gould *et al.*, 1990). A similar effect was observed when insulin-stimulated rat adipocytes were treated by isoproterenol (Joost, H.G *et al.*, 1987).

4.5 COMPARISON OF GLUT1 AND GLUT4 SUBCELLULAR TRAFFICKING IN BASAL AND INSULIN-STIMULATED 3T3-L1 ADIPOCYTES

The studies on the steady-state distribution of GLUT1 and GLUT4 strongly support the recruitment hypothesis described by Cushman and Wardzala (Cushman and Wardzala, 1980) and Suzuki and Kono (Suzuki and Kono, 1980). An additional approach to studying insulin action on this system is to selectively tracer-tag plasma membrane localized transporters and then to follow the kinetics of label redistribution to the low-density microsomes.

Use of bis-hexoses with photoreactive substitutes (Clark *et al.*, 1991) has shown that GLUT4 constitutively recycles between the plasma membrane and the intracellular vesicle pool of rat adipose cells and in 3T3-L1 adipocytes (present studies). In the continuous presence of insulin the GLUT1 and GLUT4 isoforms recycle at similar rates and redistribute to the intracellular pool so that at equilibrium only approximately one-half of the labelled transporters remain in the plasma membrane. This is to be expected if all the cellular transporters are involved in the recycling process and is consistent with studies on the photolabelling of the cell-surface and total-cellular pools of glucose transporters in 3T3-L1 cells that approximately one-half of the total cellular pool of GLUT1 and GLUT4 transporters are located at the cell surface of insulin-stimulated cells.

In the basal state a much greater proportion of labelled GLUT4 transporters are lost from the plasma membrane. This is the result that would be expected if over 90% of the transporters were intracellularly localized. However, the half-time for removal of these labelled transporters in the basal state is somewhat slower than is observed in the insulin steady-state. These results contrast with those of Jhun *et al* (1992) who have reported that in basal rat adipose cells the half-time for tracer-

tagged GLUT4 equilibration is faster than that observed in insulin-stimulated cells. This discrepancy may be related to the need to rapidly process samples to determine the fraction of label removed from the plasma membrane. This is particularly important in the basal state where the fraction of the label removed from the plasma membrane is more extensive.

The data in this thesis show that the calculated endocytosis rate constants (*ken*) are similar for GLUT1 and GLUT4 and that these endocytosis rate constants are only $\approx 30\%$ slower in the insulin-stimulated compared with the basal state. These findings are consistent with observations on the rate of loss of cell-surface transporters from 3T3-L1 cells under conditions in which insulin was removed by a low pH buffer. In those experiments, the proportions of transporters remaining at the cell-surface can be estimated simply by labelling at different time points following insulin removal. The cell-surface levels of GLUT1 and GLUT4 decreased at a similar rate. The fractional loss of GLUT1 was slightly less than GLUT4 and suggested that this was due to a greater re-exocytosis of this isoform.

From this thesis, it has been shown quantitatively that insulin increases the rate constant (*kex*) for glucose transporter exocytosis. The exocytosis of the GLUT4 isoform is 8.6-fold faster in insulin-stimulated compared with basal cells. The basal exocytosis rate constant may be over-estimated because of some plasma-membrane contamination from label which transfers to the intracellular pool. However, the observed level of stimulation of GLUT4 exocytosis is almost sufficient to account for the ≈ 12 -15-fold stimulations of cell-surface appearance of GLUT4 previously observed using ATB-BMPA (Calderhead *et al.*, 1990; Holman *et al.*, 1990; Clark *et al.*, 1991; Kozka *et al.*, 1991). In turn, this level of recruitment of GLUT4 is almost sufficient to account for the increase in glucose transport activity in these cells (≈ 15 -20-fold). Insulin also stimulates GLUT1 exocytosis but only to ≈ 3 -fold above basal levels. Again, this level of stimulation of exocytosis accounts for the smaller, 3-5-

fold increases in cell-surface GLUT1 accessible to the photolabel.

The major difference between the trafficking of the GLUT1 and GLUT4 isoforms is the much slower exocytosis of GLUT4 in the basal state. However, in the presence of insulin, both isoforms are processed in the same way. This suggested that in basal cells intracellular processing steps remove GLUT4 from the normal endosome recycling pathway; possibly to a specialized compartment within the tubulo-vesicular system (Slot *et al.*, 1991). Insulin may then re-commit or re-target these transporters from the tubulo-vesicular system to the plasma membrane and thence to the early endosome system. Both intracellular transporter pools would then be in rapid equilibrium with each other in the insulin-stimulated state as the photolabel equilibration data shows that the cells entire complement of glucose transporters are involved in the recycling process both in 3T3-L1 cells (this study) and in rat adipose cell (Clark *et al.*, 1991).

The half-time for the initial stimulation of glucose transporter translocation by insulin is faster than the half-time for steady-state recycling of transporters and the half-time for loss of transporters when insulin is removed (Clark *et al.*, 1991; present studies). This may occur because, immediately following insulin addition, transporters are rapidly committed to the plasma membrane at a vesicle docking and fusion step and that once transporters are committed in this way they are then recycled at a slower rate through the early endosomes. The kinetic effects expected from this type of multiple-pool-trafficking system have been analyzed and have been shown to account for the observed disparity between the half-times for insulin stimulation of the initial translocation and the steady-state rates of transporter recycling (Holman, unpublished results).

4.6 DOSE RESPONSE OF INSULIN-STIMULATED TRANSLOCATION OF GLUT1 AND GLUT4 IN DIFFERENT pH BUFFERS

To better understand the differences in the intracellular distribution between GLUT1 and GLUT4, reported in this thesis, the dose response curves for insulin-stimulated translocation of these two glucose transporters has been studied.

The half effective dose of insulin for stimulation of 2-deoxy-D-glucose transport activity at pH 7.4 has been found to be 1.9 nM. This half effective dose corresponds well with the result that Piper *et al.* (1992) reported (1 nM). The dose responses of insulin-stimulated translocation of GLUT1 and GLUT4 (detected by Western blotting) have indicated that the half effective dose for stimulation of GLUT1 is 0.041 nM and GLUT4 is 0.046 nM. The half effective dose for stimulation of these two isoforms are not significantly different. These results are slightly different from those described by Piper *et al.* (1992). They found the half effective doses for stimulation of GLUT1 and GLUT4 (both detected by Western blotting) are both 1 nM. This difference may be due to the concentration range of insulin they used. The maximum concentration they used is 10 nM while results in this thesis show that this concentration does not give a maximum effect.

The half effective doses for stimulation of GLUT1 and GLUT4 as measured by Western blotting are lower than the half effective dose measured by ATB-BMPA labelling and by the transport assay. These findings are consistent with the hypothesis that there may be an occluded state in the plasma membrane. Some vesicles containing glucose transporters in the plasma membrane may not be opened and these transporters may not be detectable by the ATB-BMPA labelling and transport assay. Some vesicles may fused with plasma membrane but because the glucose transporter is still associated with trafficking protein, the glucose transporter can not participate in glucose transport. This may possibly explain the slightly higher half effective dose obtained from the transport assay compared with ATB-BMPA labelling assay.

Karnielli *et al.* (1981a) have postulated that there may be four plasma membrane intermediate states in the subcellular trafficking pathway. There is an occluded state that may be present in the plasma membrane. In this state, the membrane vesicles are not fused with the plasma membrane and therefore occlude the glucose transporter proteins from photolabelling and participating in glucose transport. Using ATB-BMPA to elucidate insulin-regulated GLUT4 subcellular trafficking kinetics in rat adipose cells, Satoh *et al.* (1993) have reported that those docking and fusion intermediate steps are critical sites of insulin action.

Alkaline pH stimulates glucose transport in rat adipocytes and the rat liver cell line (Sonne *et al.*, 1981; Toyoda *et al.*, 1986 and Ismail-Beigi *et al.*, 1990). The results from this thesis also show that the half effective dose for stimulation of 2-deoxy-D-glucose transport at pH 8.0 is lower than at pH 7.4. A very similar level of half effective dose of insulin is required to stimulate translocation as detected by Western blotting, ATB-BMPA labelling and 2-deoxy-D-glucose transport at pH 8.0. This indicates that an alkaline pH may have opened the occluded vesicles which have been postulated to be present at pH 7.4.

Sonne *et al.* (1981) have reported that, although the amount of tracer insulin bound at steady state at pH 7.8 was 6 times that at pH 6.8, the fractional degradation of receptor-bound iodinsulin remained the same.

The dose response of iodinsulin binding described in this thesis has shown that the half effective dose at different pH is not significantly different but that the maximum binding is reduced at low pH. This is consistent with the result that Sonne *et al.* (1981) have reported. This indicates that the differences in the half maximum dose of insulin required for stimulation of translocation as detected by Western blotting, ATB-BMPA labelling and transport assay are not due to an altered dose response for insulin binding. It may be that the alkaline pH opens vesicles which at

pH 7.4 are occluded.

To support the hypothesis that the alkaline pH may be opening occluded vesicles at the plasma membrane, more direct evidence needs to be obtained.

A technique of preparation of adipocytes plasma membrane vesicles has been reported by McKeel and Jarett (1970). This technique has been successfully used to measure the uptake of different concentration of D-glucose at rat adipocytes (Busza, Ph.D thesis 1983). A measurement of the 2-deoxy-D-glucose transport activity of these plasma membrane vesicles at different pH conditions will give more directly evidence to help us understand the effect of alkaline pH on glucose transport stimulation. The 2-deoxy-D-glucose transport activities in these vesicle preparations at pH 7.4 and pH 8.0 could be determined in future studies.

Sandvig *et al.* (1987) found that acidification of the cytosol of several cell types perturbed endocytosis of transferrin and epithelia growth factor by inhibiting invaginated coated pits from pinching off. Hansen *et al.* (1993) have shown that acidification of the cytosol leads to a significant decrease in surface area of both plasma membrane and trans Golgi network populations of clathrin-coated domains. Their findings also indicate that cytosol acidification prevents invaginated clathrin-coated domains from pinching off. Further studies are required to investigate the effect of pH 8.0 on internalization of GLUT1 and GLUT4 which may require clathrin association.

The effect of alkaline pH on the levels of these two glucose transporters may be due to either an effect on endocytosis or on exocytosis. The occluded vesicles may therefore be intermediates in endocytosis or exocytosis. Future studies should aim to give more information on the effect of pH 8.0 on glucose transporter trafficking.

REFERENCES

- Anderson, R.G.W., Goldstein, J.L. and Brown, M.S. (1970) *Nature* **270**, 695-699.
- Asano, T., Shibasaki, Y., Lin, J-L., Akanuma, Y., Takaku, F. and Oka, Y. (1989) *Nucleic Acids Res.* **260**, 8668-8676.
- Asano, T., Takata, K., Katagiri, H., Tsukuda, K., Lin, J.J., Ishihara, H., Inukai, K., Hirano, H., Yazaki, Y., and Oka, Y. (1992) *J. Biol. Chem.* **267**, 19636-19641
- Axelrod, J.D. and Pilch, P.F. (1983) *Biochemistry* **22**, 2221-2227.
- Backer, J.M., Schroeder, G.G., Cahill, D.A., Ullrich, A., Siddle, K. and White, M.F. (1991) *Biochemistry* **300**, 6366-6372.
- Backer, J.M., Schroeder, G.C., Kahn, C.R., Myers, M.G., Wilden, P.A., Cahill, D.A. and White, M.F. (1992) *J. Biol. Chem.* **267**, 1367-1374.
- Bader, M.F., Sontag, J.M., Thierse, D. and Aunis, D. (1989) *J. Biol. Chem.* **264**, 16426-16434.
- Bailly, E., McCaffrey, M., Touchot, N., Zahraoui, A., Goud, B. and Bornens, M. (1991) *Nature* **350**, 715-718.
- Baker, G.F. and Widdas, W.F. (1988) *J. Physiol. Lond.* **395**, 57-76.
- Balch, W.E. (1990) *Trends Biochem. Sci.* **15**, 473-477.
- Baldini, G., Hohman, R., Charron, M.J. & Lodish, H.F. (1991) *J. Biol. Chem.* **266**, 4037-4040
- Baldwin, S.A. and Lienhard, G.E. (1980) *Biochem. Biophys. Res. Commun.* **94**, 1401-1408.
- Basketter, D.A. and Widdas, W.F. (1978) *J. Physiol.* **278**, 389-401.
- Beckers, C.J.M., Block, M.R., Glick, B.S., Rothman, J.E. and Balch, W.E. (1989) *Nature* **339**, 397-398.
- Bell G.I., Kayano T., Buse J.B., Burant C.F., Takede J., Lin D., Fukumoto H. and Seino S. (1990) *Diabetes care* **13**, 198-208.
- Bernier, M., Laird, D. and Lane, M.D. (1987) *Proc. Natl. Acad. Sci. U.S.A.* **84**, 1844-1848.

- Birnbaum, M.J. (1989) *Cell* **57**, 305-315.
- Birnbaum, M.J. (1992) *International Review of Cytology*. **137A**, 239-298.
- Bourne, H.R. (1988) *Cell* **53**, 669-671.
- Bourne, H.R., Sanders, D.A., McCormick, F. (1990) *Nature* **348**, 125-132
- Bradford, M.M. (1976) *Anal. Biochem.* **72**, 248-254.
- Brown, M.S., Anderson, R.G.W, Basu, S.K. and Goldstein, J.L. (1982) *Cold Spring Harbour Symp. Quant. Biol.* **46**, 713-721.
- Brown, S.J., Gould, G.W., Davies, A., Baldwin, S.A., Lienhard, G.E. & Gibbs, E.M. (1988) *Biochim. Biophys. Acta.* **971**, 339-350
- Burant, C.F., Takeda, J., Takeda, J., Brot-Laroche, E., Bell, G.I. and Davidson, N.O. (1992) *J. Biol. Chem.* **267**, 14523-14526.
- Burgess, T.L. and Kelly, R.B. (1987) *Annu. Rev. Cell Biol.* **3**, 243-293.
- Calderhead, D.M., Kitagawa, K., Tanner, L.I., Holman, G.D. and Lienhard, G.E. (1990) *J. Biol. Chem.* **265**, 13800-13808
- Carpenter, G. (1987) *Ann. Rev. Biochem.* **56**, 881-914.
- Carpenter, C.L., Duckworth, B.C., Auger, K.R., Cohen, B., Schaffhausen, B.S. and Cantley, L.C. (1990) *J. Biol. Chem.* **265**, 19704-19711.
- Carruthers, A. (1990) *Physiol.Rev.* **70**, 1135-1176.
- Carter-Su, G., Pessin, J.E., Mora, R.E., Gitomer, W. and Czech, M.P. (1982) *J. Biol. Chem.* **257**, 5419-5425.
- Charron, M.J., Brosius, F.C., Alper, S.L., and Lodish, H.F. (1989) *Proc. Natl. Acad. Sci. U.S.A.* **86**, 2535-2539
- Chavrier, P., Parton, R.G., Hauri, H.P., Simons, K. and Zerial, M. (1990) *Cell (Cambridge, Mass.)* **62**, 317-329.
- Chen, W.S., Lazar, C.S., Lund, K.A., Welsh, J.B., Chang, C.-P., Waiton, G.M., Der, C.J., Wilet, H.S., Gill, G.N. and Rosenfeld, M.G. (1989) *Cell* **59**, 33-43.
- Ciechanover, A., Schwartz, A.L., Dauty-Varsat, A. and Lodish, H.F. (1983) *J. Biol. Chem.* **256**, 9681-9689.

III

- Clancy, B.M. & Czech, M.P. (1990) *J. Biol. Chem.* **265**, 12434-12443
- Clancy, B.M., Harrison, S.A., Buxton, J.M. and Czech, M.P. (1991) *J. Biol. Chem.* **266**, 10122-10130.
- Clark, A.E., and Holman, G.D. (1990) *Biochem. J.* **269**, 615-622
- Clark, A.E., Holman, G.D. & Kozka, I.J. (1991) *Biochem. J.* **278**, 235-241.
- Covera, S. and Czech, M.P. (1985) *Proc. Natl. Acad. Sci. U.S.A.* **82**, 7314-7318.
- Cuatrecasas, P. (1971) *J. Biol. Chem.* **246**, 7265-7264.
- Cushman, S.W., and Wardzala, L.T. (1980) *J. Biol. Chem.* **255**, 4758-4762
- Cutler, D.F. and Cramer, L.P. (1990) *J. Cell. Biol.* **110**, 721-730.
- Davis, C.G., Lehrmann, L.A., Russell, D.W., Anderson, R.G.W., Brown, M.S. and Goldstein, J.L. (1986) *Cell* **45**, 15-24.
- Davies, A., Meeran, K., Cairns, M.T. and Baldwin, S.A. (1987) *J. Biol. Chem.* **262**, 9347-9352.
- Davidson, N.O., Hausman, A.M.L., Ifkovits, C.A., Buse, J.B., Gould, G.W., Burant, C.F. and Bell, G.I. (1992) *Am. J. Physiol.* **262**, C795-C800.
- De Camilli, P. and Jahn, R. (1990) *Annu. Rev. Physiol.* **52**, 625-645.
- Deves, R. and Krupka, R.M. (1978) *Biochem. Biophys. Acta* **510**, 339-348.
- De Meyts, P., Bianco, A.R. and Roth, J. (1976) *J. Biol. Chem.* **251**, 1877-1888.
- Diaz, R., Mayoga, L.S., Weidman, P.J., Rothman, J.E. and Stahl, P.D. (1989) *Nature* **339**, 398-400.
- Douen, A.G. & Jones, M.N. (1988) *Biochem. Biophys. Acta* **968**, 109-118
- Ebina, Y., Ellis, L., Janagin, K., Edery, M., Graf, L., Clauser, E., Ou, J.-H., Mad#siarz, F., Kan, Y.W., Goldfine, I.D., Roth, R.A. and Ruther, W.J. (1985) *Cell* **40**, 747-758.
- Escobedo, J.A., Navankasattusas, S., Kavanaugh, W.M., Milfay, D., Fried, V.A. and Williams, L.T. (1991) *Cell* **65**, 75-82.
- Fan, J.Y., Carpentier, J., Gorden, P., Van Obberghen, E., Blackett, N.M., Grunfeld, C. and Orci, L. (1982) *Proc. Natl. Acad. Sci. U.S.A.* **79**, 7788-7791.

IV

Farese, R.V., Standaert, M.L., Barnes, D.E., Davis, J.S. and Pollet, R.J. (1985) *Endocrinology* **116**, 2650-2655.

Flier, J.S. and Kahn, B. B. (1990) *Diabetes Care*. **13**, 548-564.

Froehner, S.C., Davies, A., Baldwin, S.A. and Lienhard, G.E. (1988) *J. Neurocytol.* **17**, 173-178.

Frost, S.C., Lane, M.D. & Gibbs, E.M. (1989) *J. Cell. Physiol.* **141**, 467-474

Fukumoto, H., Seino, S., Imura, I., Seino, Y., Eddy, R.L., Fukushima, Y., Byers, M.G., Shows, T.B. and Bell, G.I. (1988) *Proc. Natl. Acad. Sci.* **85**, 5434-5438.

Fukumoto, H., Kayano, T., Buse, J.B., Edwards, Y., Pilch, P.F., Bell, G.I. & Seino, S. (1989) *J. Biol. Chem.* **264**, 7776-7779

Garcia de Herreros, A., and Birnbaum, M.J. (1989) *J. Biol. Chem* **264**, 19994-19999

Gavin, J.R., III, Gorden, P., Roth, J., Archer, J.A. and Bull, D.N. (1973) *J. Biol. Chem.* **248**, 2202-2207.

Gerhart, D.Z., Broderius, M.A., Borson, N.D. and Drewes, L.R. (1992) *Proc. Natl. Acad. Sci.* **89**, 733-737.

Gibbs, E.M., Lienhard, G.E., Appleman, J.R., Lane, M.D. & Frost, S.C. (1986) *J. Biol. Chem.* **261**, 3944-3951

Gibbs, E.M., Allard, W.J. & Lienhard, G.E. (1986) *J. Biol. Chem.* **261**, 16597-16603

Gibbs, E.M., Lienhard, G.E., & Gould, G.W. (1988) *Biochemistry* **27**, 6681-6685

Gibbs, E.M., Lienhard, G.E. and Mueckler, M. (1990) *J. Biol. Chem.* **264**, 2180-2184

Gibbs, E.M., Calderhead, D.M., Holman, G.D. and Gould, G.W. (1991) *Biochem. J.* **275**, 145-150.

Ginsberg, B.H., Kahn, C.R. and Roth, J. (1976) *Biochim. Biophys. Acta* **443**, 227-242.

Gorga, F.R and Lienhard, G.E. (1981) *Biochem.* **20**, 5108-5113.

Gorvel, J.P., Chavrier, P., Zerial, M. and Gruenberg, J. (1991) *Cell* **64**, 915-925.

Gould, G.W., Derechin, V., James, D.E., Tordjman, K., Ahern, S., Goldstein, J.L., Brown, M.S., Anderson, R.G.W., Russel, D.W. & Schneider, W.J. (1985) *Ann. Rev. Cell Biol.* **1**, 1-39

Gould, G.W. and Bell, G.I. (1990) *TIBS* **15**, 18-23.

Gould, G.W., Lienhard, G.E., Tanner, L.I. & Gibbs, E.M. (1989) *Arch. Biochem. Biophys.* **268**, 264-275

Gould, G.W., Thomas, H.M., Jess, T.J. and Bell, G.I. (1991) *Biochemistry* **30**, 5139-5145

Green, H. and Kehinde, O. (1974) *Cell* **1**, 113-116

Green, H. and Meuth, M. (1974) *Cell* **3**, 127-133.

Green, H. and Kehinde, O. (1975) *Cell* **5**, 19-27

Green, H. and Kehinde, O. (1976) *Cell* **7**, 105-113.

Griffiths, G. and Simons, K. (1986) *Science* **234**, 438-443.

Harrison, S.A., Buxton, J.M., Clancy, B.M. and Czech, M.P. (1990) *J. Biol. Chem.* **265**, 20106-20116

Gruenberg, J. and Howell, K.E. (1986) *EMBO J.* **5**, 3091-3101.

Harrison, S.A., Buxton, J.M. and Czech, M.P. (1991a) *Proc. Natl. Acad. Sci. U.S.A.* **88**, 7839-7843

Haney, P.M., Slot, J.W., Piper, R.C., James, D.E. and Mueckler, M. (1991) *J. Cell. Biol.* **114**, 689-699

Harrison, S.A., Buxton, J.M., Clancy, B.M. and Czech, M.P. (1991b) *J. Biol. Chem.* **266**, 19438-19449

Haspel, H.C., Wilk, E.W., Birnbaum, M.J., Cushman, S.W. and Rosen, O.M. (1986) *J. Biol. Chem.* **261**, 6778-6789

Haystead, T.A., Sim, A.T., Carling, D., Honnor, R.C., Tsukitani, Y., Cohen, P. and Hardie, D.G. (1989) *Nature* **337** 78-81.

Hirshman, M.F., Goodyear, L.J., Wardzala, L.J., Horton, E.D. and Horton, E.S. (1990) *J. Biol. Chem.* **265**, 987-991

Holman, G.D., Kozka, I.J., Clark, A.E., Flower, C.J., Saltis, J., Habberfield, A.D., Simpson, I.A., and Cushman, S.W. (1990) *J. Biol. Chem.* **265**, 18172-18179

- Holman, G.D., Parkar, B.A. and Midgley, P.J.W. (1986) *Biochem. Biophys. Acta* **855**, 115-126.
- Holman, G.D. and Rees, W.D. (1987) *Biochem. Biophys. Acta* **897**, 395-405.
- Holman, G.D., Karim, A.R. and Karim, B. (1988) *Biochim. Biophys. Acta* **946**, 75-84.
- Holman, G.D. and Rees, W.D. (1982) *Biochem. Biophys. Acta* **897**, 395-405.
- Hopkins, C.R., Gibson, A., Shipman, M. and Miller, K. (1990) *Nature* **346**, 335-339.
- Hudson, A.W., Ruiz, M., Birnbaum, M.J. (1992) *J. Cell. Biol.* **116**, 785-79714.
- James, D.E., Brown, R., Navarro, J. & Pilch, P.F. (1988) *Nature* **333**, 183-185
- Ismail-Beigi, F., Mercado, C.L. and Loeb, J.N. (1990) *Am. J. Physiol.* **258**, C327-C335.
- James, D.E., Strube, M.I., & Mueckler, M. (1989) *Nature* **338**, 83-87
- Jhun, B.H., Rampal, A.L., Liu, H., Lachaal, M., and Jung, C.Y. (1992) *J. Biol. Chem.* **267**, 17710-17715
- Joost, H.G., Weber, T.M., Cushman, S.W. and Simpson, I.A. (1986) *J. Biol. Chem.* **261**, 10033-10036.
- Joost, H.G., Weber, T.M., Cushman, S.W. & Simpson, I.A. (1987) *J. Biol. Chem.* **262**, 11261-11267
- Jung, C.Y. and Rampal, A.L. (1977) *J. Biol. Chem.* **252**, 5456-5463.
- Kaestner, K.H., Christy, R.J., McLenithan, J.C., Braiterman, L.T., Cornelius, P., Pekela, P.H. and Lane, D.M. (1989) *Proc. Natl. Acad. Sci U.S.A.* **86**, 3150-3154
- Kahn, B.B. and Flier, J.S. (1990) *Diabetes Care* **13**, 548-564.
- Karnielli, E., Zarnowski, M.J., Hissin, P.J., Simpson, I.A., Salans, L.B. & Cushman, S.W. (1981a) *J. Biol. Chem.* **256**, 4772-4777
- Karnielli, E., Hissin, P.J., Simpson, I.A., Salans, L.B. and Cushman, S.W. (1981b) *J. Clin. Invest.* **68**, 811-814.
- Kayano, T., Fukumoto, H., Eddy, R.L., Fan, Y-S., Byers, M.G., Shows, T.B. and Bell, G.I. (1988) *J. Biol. Chem.* **263**, 15245-15248.

VII

Kayano, T., Burant, C. F., Fukumoto, H., Gould, G.W., Fan, Y-s., Eddy, R.L., Byers, M. G., Shows, T. B., Seino, S. and Bell, G.I. (1990) *J. Biol. Chem.* **265**, 13276-13282.

Keller, K., Strube, M. and Mueckler, M. (1989) *J. Biol. Chem.* **264**, 18884-18889.

Kelly, K.L., Ruderman, N.B. and Chen, K.S. (1992) *J. Biol. Chem.* **267**, 3423-3428.

Kirchhausen, T. and Harrison, S.C. (1981) *Cell* **23**, 755-761.

Klip, A., Rampall, T., Young, D. and Holloszy, J.O. (1987) *FEBS. Lett.* **224**, 224-230

Klip, A. and Douen, A.G. (1989) *J. Membrane Biol.* **111**, 1-23.

Klip, A., Rampall, T., Bilan, P.J., Cartee, G.D., Gulve, E.A. and Holloszy, J.O. (1990) *Biochem. Biophys. Res. Comm.* **172**, 728-736

Knutson, V.P., Ronnett, G.V. & ane, M.D. (1986) *J. Biol. Chem.* **258**, 12139-12142

Kishimoto, A., Takai, Y., Mori, T., Kikkawa, U. and Nishizuka, Y. (1980) *J. Biol. Chem.* **255**, 2273-2276.

Koch, C.A., Anderson, D., Moran, M.F., Ellis, C. and Pawson, T. (1991) *Science* **252**, 668-674.

Kozka, I.J., Clark, A.E. and Holman, G.D. (1991) *J. Biol. Chem.* **266**, 11726-11731

Kuroda, M., Honnor, R.C., Cushman, S.W., Londos. C. and Simpson, I.A. (1987) *J. Biol. Chem.* **262**, 245-253.

Laemmili, U.K. (1970) *Nature* **227**, 680-685.

Lawrence, J.C.J., Hiken, J.F. and James, D.E. (1990a) *J. Biol. Chem.* **265**, 2324-2332.

Lienhard, G.E., Kin, H.K., Ransome, K.J., Gorga, J.C. (1982) *Biochem. Biophys. Res. Commun.* **105**, 1150-1156.

Lienhard, G.E. (1983) *Trends in Biol. Sci.* **8**, 125-127

Lienhard, G.E., Crabb, J.H., Ransome, K.J. (1984) *Biochem. Biophys. Acta* **769**, 404-410.

VIII

Lienhard, G.E., Slot, J.W., James, D.E. and Mueckler, M.M. (1992) *Sci. Am.* **266**, 86-91.

Ludvigsen, C., Jarett, L. and McDonald, J.M. (1980) *Endocrinology* **106**, 786-790.

Mackall, J.C., Student, A.K., Polakis, S.E. and Lane, M.D. (1976) *J. Biol. Chem.* **251**, 6462-6464.

Malhotra, V., Orci, L., Glick, B.S., Blok, M.R. and Rothman, J.E. (1988) *Cell* **54**, 221-227.

Marsh, M. and Helenius, A. (1980) *J. Mol. Biol.* **142**, 439-454.

Massague, J., Pilch, and Czech, M.P. (1980) *Proc. Natl. Acad. Sci. U.S.A.* **77**, 7137-7141.

Mayorga, L.S., Diaz, R. and Stahl, P.D. (1989) *Science* **244**, 1475-1477.

McClain, D.A., Maegawa, H., Freidenberg, G., Olefsky, J.M., Dull, T.J., Lee, J. and Ullrich, A. (1988) *J. Biol. Chem.* **263**, 8912-8917.

McKeel, D.W. and Jarett, L. (1970) *J. Cell. Biol.* **44**, 417-432.

Mehler, P.S., Sussman, A.L., Maman, A., Leitner, J.W. and Sussman, K.E. (1980) *J. Clin. Invest.* **66**, 1334-1338.

Midgley, P.J.W., Parkar, B.A. and Holman, G.D. (1985) *Biochem. Biophys. Acta* **812**, 33-41.

Mueckler, M., Caruso, C., Baldwin, S. A., Panico, M., Blench, I., Morris, H.R., Allard, W. J., Lienhard, G.E. and Lodish, H.F. (1985) *Science* **229**, 941-945.

Mueckler, M. (1990) *Diabetes* **39**, 6-11.

Mullins, R.E. and Langdon, R.G. (1980) *Biochem.* **19**, 1199-1205.

Nagamatsu, S., Kornhauser, J.M., Seino, S., Mayo, K.E., Steiner, D.E. and Bell, G.I. (1992) *J. Biol. Chem.* **267**, 467-472.

Naftalin, R.J., Smith, P.M. and Roselaar, S.E. (1985) *Biochim. Biophys. Acta* **820**, 235-249.

Navone, F., Jahn, R., Di, G.G., Stukenbrok, H., Greengard, P. and De, C.P. (1986) *J. Cell. Biol.* **103**, 2511-2527.

Oka, Y. and Czech, M.P. (1984) *J. Biol. Chem.* **259**, 8125-8133.

- Oka, Y., Rozek, L.M. and Czech, M.P. (1985) *J. Biol. Chem.* **260**, 9435-9442.
- Oka, Y. and Czech, M.P. (1986) *J. Biol. Chem.* **261**, 9090-9093.
- Oka, Y., Asano, T., Shibasaki, Y., Kanazawa, Y. and Takaku, F. (1988) *J. Biol. Chem.* **263**, 13432-13439.
- Okuno, Y. and Gliemann, J. (1986) *Biochim. Biophys. Acta* **862**, 329-334.
- Palfreyman, R.W., Clark, A.E., Denton, R.M., Holman, G.D. and Kozka, I.J. (1992) *Biochem. J.* **284**, 275-281
- Pearse, B.M.F. (1975) *J. Mol. Biol.* **97**, 93-98.
- Pearse, B.M.F. (1976) *Proc. Natl. Acad. Sci. U.S.A.* **73**, 1255-1259.
- Pearse, B.M.F. (1988) *EMBO J.* **7**, 3331-3336.
- Pearse, B.M.F. and Bretscher, M.S. (1981) *Ann. Rev. Biochem.* **50**, 85-101.
- Pedersen, O. and Beck-Nielsen, H. (1976) *Acta Endocrinol.* **83**, 556-564.
- Pessin, J.E. and Bell, G.I. (1992) *Annu. Rev. Physiol.* **54**, 911-930.
- Pilch, P.F. (1990) *Endocrinology* **126**, 3-5.
- Piper, R.C., Hess, L.J. and James, D.E. (1991) *Am. J. Physiol.* **260**, C570-C580.
- Piper, R.C., Tai, C., Slot, J.W., Hahn, C.S., Rice, C.M., Huang, H. and James, D.E. (1992) *J. Cell. Biol.* **117**, 729-743
- Pollard, H.B., Pazoles, C.J., Creutz, C.E., Zinder, O. (1979) *Int. Rev. Cytol.* **58**, 158-197.
- Posner, B.I., Josefsberg, Z. and Bergeron, J.J.M. (1978) *J. Biol. Chem.* **253**, 4067-4073.
- Reed, B.C. and Lane, M.D. (1980) *Adv. Enz. Regul.* **18**, 97--117.
- Reed, B.C., Glasted, K. and Miller, B. (1984) *J. Biol. Chem.* **259**, 8134-8143.
- Reed, B.C., Shade, D., Alperovich, F. and Vang, M. (1990) *Arch. Biochem. Biophys.* **279**, 261-274
- Reetz, A., Solimena, M., Matteoli, M., Folli, F., Takei, K. and De Camilli, P. (1991) *EMBO J.* **10**, 1275-1284.

- Robinson, M.S., Rhodes, J.A. and Albertini, D.F. (1983) *J. Cell. Phys.* **117**, 43-50.
- Robinson, L.J., Pang, S., Harris, D.A., Heuser, J. and James, D.E. (1992) *J. Cell. Biol.* **117**, 1181-1196
- Ronnett, G.V., Tennekoon, G., Knutson, V.P. and Lane, M.D. (1983) *J. Biol. Chem.* **258**, 283-290.
- Rosen, O.M., Smith, C.J., Fung, C. and Rubin, C.S. (1978) *J. Biol. Chem.* **253**, 7579-7583.
- Rothenberg, P.L., Lane, W.S., Karasik, A., Backer, J., White, M. and Kahn, C.R. (1991) *J. Biol. Chem.* **266**, 8302-8311.
- Rubin, C.S., Hirsch, A., Fung, C. and Rosen, O.M. (1978) *Biol. Chem.* **253**, 7570-7578.
- Russell, T.R. and Ho, R. (1976) *Proc Natl. Acad. Sci. U.S.A.* **73**, 4516-4520.
- Saltis, J., Habberfield, A.D., Egan, J.J., Londos, C., Simpson, I.A. and Cushman, S.W. (1991) *J. Biol. Chem.* **266**, 261-267.
- Satoh, S., Gonzalez-Mulero, O.M., Clark, A.E., Kozka, I.J., Holman, G.D. & Cushman, S.W. (1991) *Diabetes* **40**, (Supp 1) 85A
- Satoh, S., Nishimura, H., Clark, A.E., Kozka, I.J., Vannucci, S.J., Simpson, I.A., Cushman, S.W. and Holman, G.D. *submitted to J. Biol. Chem.*
- Schroer, D.W., Frost, S.C., Kohanski, R.A., Lane, M.D. and Lienhard, G.E. (1986) *Biochem. Biophys. Acta.* **885**, 317-326.
- Schurmann, A., Monden, I., Joost, H.G. and Keller, K. (1992) *Biochim. Biophys. Acta.* **1131**, 245-252
- Shibasaki, F., Homma, Y. and Takenawa, T. (1991) *J. Biol. Chem.* **266**, 8108-8114.
- Shoelson, S.E., Chatterjee, S., Chaudhuri, M., Lowenstein, E., Fischer, R., Drepps, A., Ullrich, A. and Schlessinger, J. (1992) *Proc. Natl. Acad. Sci. U.S.A.* **89**, 2027-2031.
- Silverstein, S.C., Steinman, R.M. and Cohn, Z.A. (1977) *Ann. Rev. Biochem.* **46**, 669-722.
- Simpson, I.A., Yver, D.R., Hissin, P.J., Wardzala, L.J., Karnieli, E., Salans, L.B. and Cushman, S.W. (1983) *Biochim. Biophys. Acta.* **855**, 115-126
- Simpson, I.A. & Cushman, S.W. (1986) *Ann. Rev. Biochem.* **55**, 1059-1089

- Skolnik, E.Y., Margolis, B., Mohammadi, M., Lowenstein, E., Fischer, R., Drepps, A., Ullrich, A. and Schlessinger, J. (1991) *Cell* **65**, 83-90.
- Slot, J.W., Gueze, H.J., Gigengack, S., James, D.E., and Lienhard, G.E. (1991a) *Proc. Natl. Acad. Sci. U.S.A.* **88**, 7815-7819
- Slot, J.W., Gueze, H.J., Gigengack, S., Lienhard, G.E. and James, D.E. (1991b) *J. Cell. Biol.* **113**, 123-135
- Smith, R.M., Charron, M.J., Shah, N., Lodish, H.F. and Jarrett, L. (1991) *Proc. Natl. Acad. Sci. U.S.A.* **88**, 6893-6897
- Sonne, O. and Gliemann, J. (1980) *J. Biol. Chem.* **255**, 7449-7454.
- Sonne, O., Gliemann, J. and Linde, S. (1981) *J. Biol. Chem.* **256**, 6250-6254.
- Sonne, O. (1988) *Physiol. Rev.* **68**, 1129-1196.
- Stoorvogel, W., Geuze, H.J., Strous, G.J. (1987) *J. Cell. Biol.* **104**, 1261-1268
- Stoschck, C.M. and Carpenter, G. (1984) *J. Cell. Biol.* **98**, 1048-1053.
- Stralfors, P. (1988) *Nature* **335**, 554-556.
- Sun, X.J., Rothenberg, P., Kahn, C.R., Backer, J.M., Araki, E., Wilden, P.A., Cahill, D.A., Goldstein, B.J. and White, M.F. (1991) *Nature* **352**, 73-77.
- Susuki, K. & Kono, T. (1980) *Proc. Natl. Acad. Sci. U.S.A.* **77**, 2542-2545
- Tanner, L.I. and Lienhard, G.E. (1987) *J. Biol. Chem.* **262**, 8975-8980.
- Tanner, L.I. and Lienhard, G.E. (1989) *J. Cell. Biol.* **108**, 1537-1545.
- Taylor, L.P. & Holman, G.D. (1981) *Biochim. Biophys. Acta* **642**, 325-335
- Thorens, B., Sarkar, H.K., Kaback, H.R. and Lodish, H.F. (1988) *Cell* **55**, 281-290.
- Todaro, G.J. and Green, H. (1963) *J. Cell Biol.* **17**, 229.
- Tordjman, K.M., Liengang, K.A. and Mueckler, M. (1990) *Biochem. J.* **271**, 201-207
- Toyoda, N., Robinson, F.W., Smith, M.M., Flanagan, J.E. and Kono, T. (1986) *J. Biol. Chem.* **261**, 2117-2122.

- Ullrich, A., Bell, J.R., Chen, E.Y., Herrera, R., Petruzzelli, L.M., Dull, T.J., Gray, A., Ciussens, L., Liao, Y.-C., Tsubokawa, M., Mason, A., Seeburg, P.H., Grunfield, C., Rosen, O.M. and Ramachandran, J. (1985) *Nature* **313**, 756-761.
- Unanue, E.R., Ungewickell, E. and Branton, D. (1981) *Cell* **26**, 439-446.
- Ungewickell, E. and Branton, D. (1982) *Trends Biochem. Sci.* **7**, 358-361.
- Vannucci, S.J., Nishimura, H., Satoh, S., Cushman, S.W., Holman, G.D. and Simpson, I.A. (1992) *Biochem. J.* **288**, 325-330.
- Van Putten, J.P.M., Wieringa, Tj. and Krans, H.M.J. (1985) *Diabetes*. **34**, 744-750.
- Vinten, J., Gliemann, J. & Osterlind, K. (1976) *J. Biol. Chem.* **251**, 794-800
- Virshup, D.M. and Bennett, V. (1988) *J. Cell. Biol.* **106**, 39-50.
- Vogt, B., Mushack, J., Seffer, E. and Haring, H.U. (1991) *Biochem. J.* **275**, 597-600.
- Waddell, I.D., Zomerschoe, A.G., Voice, M.W. and Burchell, A. (1992) *Biochem. J.* **286**, 173-177.
- Wardzala, L.J. and Jeanrenauld, B. (1981) *J. Biol. Chem.* **256**, 7090-7093.
- Wardzala, L.J. and Jeanrenauld, B. (1983) *Biochim. Biophys. Acta.* **730**, 49-56
- Watanabe, T., Smith, M.M., Robinson, F. W., and Kono, T. (1984) *J. Biol. Chem.* **259**, 13117-13122
- Weber, T.M. and Eichholz, A. (1985) *Biochim. Biphys. Acta* **812**, 503-511.
- Weiland, M., Schurmann, A., Schmidt, W.E. and Joost, H.G. (1990) *Biochem. J.* **270**, 331-336
- White, M.F., Stegmann, E.W., Dull, T.J., Ullrich, A. and Kahn, C.R. (1987) *J. Biol. Chem.* **262**, 9769-9777.
- White, M.F., Maron, R. and Kahn, C.R. (1985) *Nature* **318**, 183-186.
- White, M.F., Stegmann, E.W., Dull, T.J., Ullrich, A. and Kahn, C.R. (1987) *J. Biol. Chem.* **262**, 9769-9777.
- White, M.F., Livingston, J.N., Backer, J.M., Lauris, V., Dull, T.J., Ullrich, A. and Kahn, C.R. (1988) *Cell* **54**, 641-649.

- Whitesell, R.R. and Gliemann, J. (1979) *J. Biol. Chem.* **254**, 5276-5283.
- Wick, A.N., Drury, D.R., Nakada, H. and Wolfe, J.B. (1951) *J. Biol. Chem.* **224**, 963-969.
- Widdas, W.F. (1952) *J. Physiol. Lond.* **118**, 23-39.
- Widnell, C.C., Baldwin, S.A., Davies, A., Martin, S. and Pasternak, C.A. (1990) *FASEB. J.* **4**, 1634-1637
- Wilden, P.A., Siddle, K., Haring, E., Backer, J.M., White, M.F. and Kahn, C.R. (1992) *J. Biol. Chem.* **267**, 16660-16668.
- Wiley, H.S. & Cunningham, D.D. (1982) *J. Biol. Chem.* **257**, 4222-4229
- Williams, I.H. and Polakis, S.E. (1977) *Biochem. Biophys. Res. Commun.* **77**, 175-186.
- Woodman, P.G. and Warren, G. (1988) *Eur. J. Biochem.* **173**, 101-108.
- Wright, E.W., Turk, E., Zabel, B., Mundios, S. and Dyer, J. (1991) *J. Clin. Invest.* **88**, 1435-1440.
- Zaremba, S. and Keen, J.H. (1983) *J. Cell. Biol.* **97**, 1339-1347.
- Ziehm, D., Schurmann, A., Weiland, M and Joost, H.G. (1993) *Hormone and Metabolic Research* **25**, 71-76.
- Zorzano, A., Wilkinson, W., Kotiar, G., Thoidis, G., Wadzinski, B.E., Ruoho, A.E. and Pilch, P.F. (1989) *J. Biol. Chem.* **264**, 12358-12363.

Trafficking of glucose transporters in 3T3-L1 cells

Inhibition of trafficking by phenylarsine oxide implicates a slow dissociation of transporters from trafficking proteins

Jing YANG, Avril E. CLARK, Roger HARRISON, Izabela J. KOZKA and Geoffrey D. HOLMAN*

Department of Biochemistry, University of Bath, Claverton Down, Bath BA2 7AY, Avon, U.K.

We have compared the rates of insulin stimulation of cell-surface availability of glucose-transporter isoforms (GLUT1 and GLUT4) and the stimulation of 2-deoxy-D-glucose transport in 3T3-L1 cells. The levels of cell-surface transporters have been assessed by using the bismannose compound 2-*N*-[4-(1-azido-2,2,2-trifluoroethyl)benzoyl]-1,3-bis-(D-mannos-4-yloxy)propyl-2-amine (ATB-BMPA). At 27 °C the half-times for the appearance of GLUT1 and GLUT4 at the cell surface were 5.7 and 5.4 min respectively and were slightly shorter than that for the observed stimulation of transport activity ($t_{1/2}$ 8.6 min). This lag may be due to a slow dissociation of surface transporters from trafficking proteins responsible for translocation. When fully-insulin-stimulated cells were subjected to a low-pH washing procedure to remove insulin at 37 °C, the cell-surface levels of GLUT1 and GLUT4 decreased, with half-times of 9.2 and 6.8 min respectively. These times correlated well with decrease in 2-deoxy-D-glucose-transport activity that occurred during this washing procedure ($t_{1/2}$ 6.5 min). When fully-insulin-stimulated cells were treated with phenylarsine oxide (PAO), a similar decrease in transport activity occurred ($t_{1/2}$ 9.8 min). However, surface labelling showed that this corresponded with a decrease in GLUT4 only ($t_{1/2}$ 7.8 min). The cell-surface level of GLUT1 remained high throughout the PAO treatment. Light-microsome membranes were isolated from cells which had been cell-surface-labelled with ATB-BMPA. Internalization of both transporter isoforms to this pool occurred when cells were maintained in the presence of insulin for 60 min. In contrast with the surface-labelling results, we have shown that the transfer to the light-microsome pool of both transporters occurred in cells treated with insulin and PAO. These results suggest that both transporters are recycled by fluid-phase endocytosis and exocytosis. PAO may inhibit this recycling at a stage which involves the re-emergence of internalized transporters at the plasma membrane. The GLUT1 transporters that are recycled to the surface in insulin- and PAO-treated cells appear to have low transport activity. This may be because of a failure to dissociate fully from trafficking proteins at the cell surface. GLUT4 transporters appear to have a greater tendency to remain internalized if the normal mechanisms that commit transporters to the cell surface, such as dissociation from trafficking proteins, are uncoupled.

INTRODUCTION

The large insulin stimulations of glucose transport in adipose cells [1–3] and in 3T3-L1 cells [4] are now known to be due to the presence of the GLUT4 isoform of the glucose transporter. This isoform has been cloned and sequenced by five independent laboratories [5–9]. The study of the cellular-trafficking pathways of GLUT4 is of great importance in the understanding of the effect of insulin on the translocation of this isoform to the cell surface. A recent, very elegant, study by Slot *et al.* [10] has clearly shown that insulin produces a very large increase in GLUT4 in the plasma membrane of brown adipose tissue as detected by immunogold electron microscopy. The increase in plasma-membrane transporter was paralleled by a decrease in glucose transporter in a cytoplasmic pool associated with tubulo-vesicular structures. An alternative approach to studying glucose-transporter trafficking that we have developed is to use a cell-impermeant photoaffinity label. The photolabel, 2-*N*-[4-(1-azido-2,2,2-trifluoroethyl)benzoyl]-1,3-bis-(D-mannos-4-yloxy)-2-propylamine (ATB-BMPA), is a bis-D-mannose derivative substituted with an (azido)trifluoroethylbenzoyl group. This only labels those transporters that are present at the cell surface of intact cells [11–14]. However, photolabelling of glucose transporters in light-microsome membranes can occur if the reagent has access

to these, as it does in permeabilized cells (J. Yang, A. E. Clark, I. J. Kozka, S. W. Cushman & G. D. Holman, unpublished work) or in membrane fractions [16].

In experiments using the bismannose photolabel we have studied the kinetics of trafficking in rat adipocytes at 37 °C [16] and have found that GLUT1 and GLUT4 appeared rapidly on the cell surface with half-times of \approx 2 min, which were slightly shorter than that for the stimulation of glucose transport. The losses of cell-surface GLUT1 and GLUT4 occurred with half-times of \approx 12 min. These results suggested that the larger insulin stimulation of cell-surface availability of GLUT4 (\approx 15–20-fold) compared with GLUT1 (\approx 5-fold) was due to a lower rate of exocytosis of GLUT4 in the basal state. In addition to the cell-surface detection of transporters, Satoh *et al.* [17] have shown that the reagent can be used to monitor the internalization of transporters directly. Thus, after labelling, the cells can be maintained at 37 °C to allow cell processing to occur and then plasma membrane and light-microsome fractions can be isolated. By measuring transporter redistribution in this way we have obtained direct evidence that glucose transporters are recycled between the plasma membrane and the light microsomes, even in the continuous presence of insulin. In the presence of insulin the cell-surface level of transporters was shown to be constant, but photolabelled transporters were internalized and equilibrated

Abbreviations used: ATB-BMPA, 2-*N*-[4-(1-azido-2,2,2-trifluoroethyl)benzoyl]-1,3-bis-(D-mannos-4-yloxy)propyl-2-amine; PAO, phenylarsine oxide; DMEM, Dulbecco's modified Eagle medium; KRH, Krebs-Ringer/Hepes; GLUT1 and GLUT4, glucose-transporter isoforms 1 and 4; C₁₂E₉, nona(ethylene glycol) dodecyl ether; G-protein, guanine-nucleotide-binding protein.

* To whom correspondence should be sent.

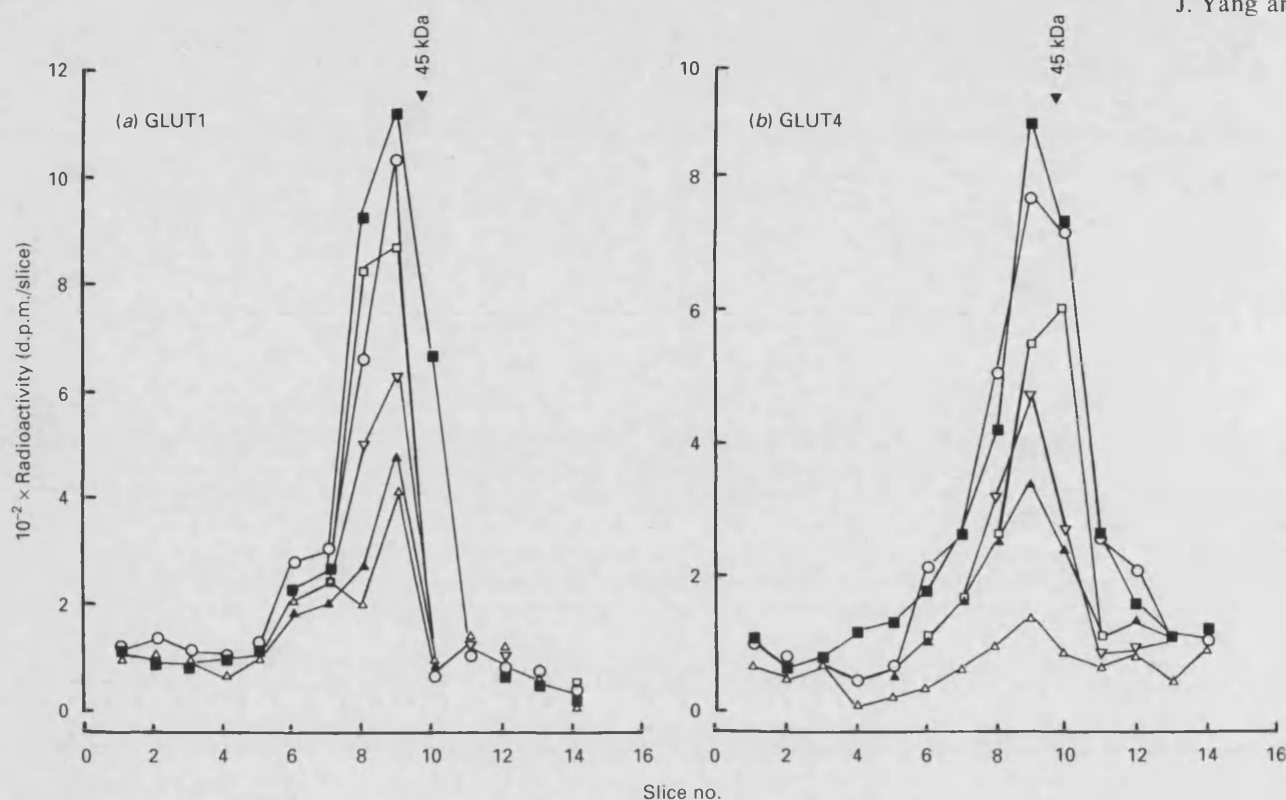


Fig. 1. Insulin stimulation of the cell-surface appearance of GLUT1 and GLUT4 in 3T3-L1 cells

3T3-L1 cells in 35 mm-diameter dishes were stimulated with 100 nM-insulin at 27 °C and then at zero time (△), 2.5 min (▲), 5 min (▽), 7.5 min (□), 12 min (○) and 30 min (■) the insulin was removed by washing twice in KRH buffer at 18 °C. The cells were then labelled at 18 °C with 100 µCi of ATB-BMPA in 250 µl of KRH buffer. After labelling the cells were washed four times in KRH buffer and then directly solubilized in C₁₂E₉ detergent buffer. GLUT1 (a) and GLUT4 (b) were then immunoprecipitated with anti-(C-terminal peptide) antibodies. The protein was then subjected to electrophoresis and the radioactivity was estimated by cutting out and counting the gel slices.

with the light-microsome pool. Studies on internalized ATB-BMPA-labelled GLUT4 have shown that insulin increases the rate of exocytosis of this isoform [17]. A similar conclusion was reached by Slot *et al.* [10] in their electron-microscopic study, which analysed the steady-state distribution of transporters in brown adipose tissue.

The kinetic studies suggest that some trafficking of GLUT1 and GLUT4 occurs via a common pathway, but that GLUT4 can be excluded from the common pathway in the absence of insulin and sequestered in a distinct vesicle pool. An approach to examining the possibly separate processing of the two transporters is to inhibit their trafficking. Phenylarsine oxide (PAO) is known to inhibit receptor endocytosis [18,19] and fluid-phase endocytosis in 3T3-L1 cells [20], but has been shown to inhibit the insulin stimulation of glucose transport in 3T3-L1 cells and in adipocytes [4,21] an exocytotic process [17]. Thus, in the study described here, we have kinetically monitored the insulin-stimulated translocation of GLUT1 and GLUT4 to the cell surface of 3T3-L1 cells and have, in addition, addressed the question of the site of action by PAO by monitoring the appearance and loss of these transporters in cells whose vesicle-processing pathways have been perturbed with this reagent.

MATERIALS AND METHODS

Materials

ATB-BMPA and ATB-[2-³H]BMPA (sp. radioactivity ≈ 10 Ci/mmol) were prepared as described [11]. 2-deoxy-D-[2,6-³H]glucose was from Amersham International. Dulbecco's modified Eagle medium (DMEM) was from Flow laboratories. Foetal-bovine serum was from Gibco. Monocomponent porcine insulin was a gift from Dr. Ronald Chance, Eli Lilly Corp.

Dexamethasone, isobutylmethylxanthine, Protein A-Sepharose and phenylarsine oxide were from Sigma. Nona(ethylene glycol) dodecyl ether (C₁₂E₉) was from Boehringer.

Cell culture

3T3-L1 fibroblasts were cultured in DMEM and differentiated to adipocytes by treatment with insulin, dexamethasone and isobutylmethylxanthine as described in [4,13]. Fully differentiated cells were washed with phosphate-buffered saline (154 mM-NaCl/12.5 mM-sodium phosphate, pH 7.4) and were then incubated for 2 h in serum-free medium containing 25 mM-D-glucose. This was followed by three washes in Krebs-Ringer/Hepes buffer (KRH buffer; 136 mM-NaCl/4.7 mM-KCl/1.25 mM-CaCl₂/1.25 mM-MgSO₄/10 mM-Hepes, pH 7.4) before use in experiments to determine 2-deoxy-D-glucose transport activity or cell-surface transporters.

Insulin stimulation experiments

Normally cell monolayers in 35 mm-diameter dishes were maintained at 37 °C with 100 nM porcine monocomponent insulin to produce fully stimulated cells. However, the half-time for stimulation of transport at 37 °C was found to be ≈ 3 min, which was considered to be too short a time for accurate comparisons with the time course of cell-surface photolabelling (*t*_{1/2} ≈ 2 min). In rat adipocytes we were able to measure the time course for stimulation at 37 °C because the stimulation of these cells could be blocked at short time points by the addition of KCN. We have found, however, that the stimulation of transport in 3T3-L1 cells was not blocked by KCN. Instead, to compare the time course for insulin stimulation of transport and cell-surface availability of transporters in these cells we stimulated at 27 °C and then washed the cells at 18 °C before measuring

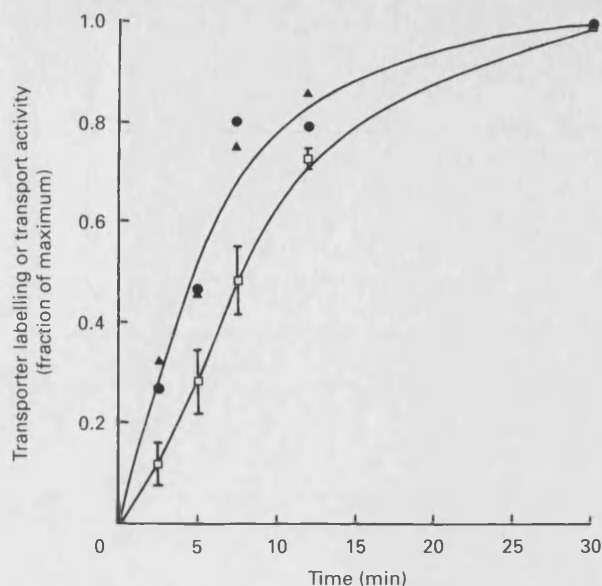


Fig. 2. Time course for insulin stimulation of cell-surface availability of glucose transporters and for stimulation of 2-deoxy-D-glucose transport

3T3-L1 cells were stimulated with 100 nM-insulin at 27 °C and then cell-surface GLUT1 (●), cell-surface GLUT4 (▲) and 2-deoxy-D-glucose transport activity (□) were determined at 18 °C. The immunoprecipitated transporters were subjected to electrophoresis and the total radioactivity associated with each transporter peak was determined. The levels of transporter labelling and transport activity at the indicated times were then calculated as a fraction of the maximum determined from the samples which were stimulated with insulin for 30 min. Two additional experiments showed the same result, and the average half-time for stimulation was calculated as described in the Materials and methods section.

transport and the amounts of photolabelled transporters. The uptake was measured by incubating the 35 mm dishes with 50 μ M-2-deoxy-D-glucose in 1 ml of KRH buffer for 1–5 min at 18 °C. We have found that no further insulin stimulation occurs once insulin is removed and the dishes are washed at 18 °C. The rates of stimulation were determined from semi-log plots of $-\ln(1-f)$ against time, where f is the fraction of the maximum stimulation. Normally the slope of such a plot gives the activation rate constant, but because a lag phase occurred before the transport activation, the $t_{1/2}$ values were calculated according to the equation:

$$t_{1/2} = (\ln 2 - a)/b$$

where a is the intercept on the $-\ln(1-f)$ axis and b is the slope.

Reversal of insulin stimulation

Cell monolayers were stimulated with 100 nM-insulin at 37 °C for 30 min. The insulin stimulation was then reversed by washing cell monolayers twice with a MES buffer (136 mM-NaCl/4.7 mM-KCl/1.25 mM MgSO_4 /1.25 mM- CaCl_2 /10 mM-MES, pH 6.0) and then maintaining them in this buffer at 37 °C. At the times indicated in the Figure legends the dishes were washed twice in KRH at 18 °C and then either used for 2-deoxy-D-glucose-uptake determinations (as described above) or in cell-surface photolabelling experiments.

ATB-BMPA photolabelling

Plates (35 mm diameter) of the 3T3-L1 cells were washed in KRH buffer and were irradiated at 18 °C for 1 min in the presence of 100 μ Ci of ATB-[2- ^3H]BMPA as described in [13,14]. The irradiated cells were washed four times in KRH buffer and

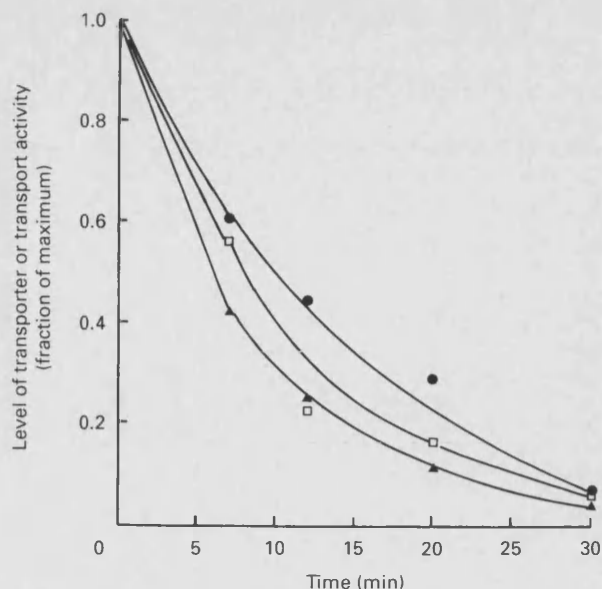


Fig. 3. Time course for the reversal of insulin stimulation

3T3-L1 cells in 35 mm-diameter dishes were stimulated with 100 nM-insulin for 30 min at 37 °C and then insulin was removed by washing twice with MES buffer and by maintaining the cells in this buffer for the indicated times. The cells were washed in KRH buffer at 18 °C and then photolabelled with 100 μ Ci of ATB-BMPA. After labelling, the levels of the GLUT1 (●) and GLUT4 (□) transporters were determined by immunoprecipitation and electrophoresis. Some cells were used for estimation of 2-deoxy-D-glucose transport activity (▲) as described in the Materials and methods section. The results shown are the means for two photolabelling experiments and for three experiments in the case of transport-activity determination.

solubilized in 1.5 ml of detergent buffer containing 2% C_{12}E_9 , 5 mM-sodium phosphate and 5 mM-EDTA, pH 7.2, and with the proteinase inhibitors antipain, aprotinin, pepstatin and leupeptin, each at 1 μ g/ml. After centrifugation at 20000 g_{max} for 20 min, the supernatant was carefully separated from unsolubilized pellet and the insoluble fat-cake and then subjected to immunoprecipitation to determine the amounts of photolabelled GLUT1 and GLUT4 transporter.

Cell fractionation

For each condition, two 35 mm dishes of fully-insulin-stimulated cells were photolabelled with 100 μ Ci each of ATB-[2- ^3H]BMPA. The labelling was carried out with the lids on the 35 mm dishes so that radiation damage to the cells was minimized. After four washes of the dishes in KRH to remove excess label, the cells were then incubated at 37 °C for a further 60 min with insulin or with insulin and 20 μ M-PAO. The cells from each dish were scraped into 0.5 ml for each dish of TES buffer (255 mM-sucrose/10 mM-Tris/HCl/0.5 mM-EDTA, pH 7.2). The pooled material from the two dishes were then homogenized at 900 rev./min in a 2 ml tight-fitting Teflon homogenizer (clearance \approx 0.15 mm) with ten complete strokes. The homogenate was then centrifuged at 20000 g_{max} for 20 min. The pellet, containing the crude plasma-membrane fraction, was dissolved in 0.5 ml of 6%- C_{12}E_9 detergent buffer and diluted with 1 ml of 5 mM-sodium phosphate buffer. The 20000 g_{max} supernatant from above, containing the crude light-microsome fraction, was mixed with 0.5 ml of 6%- C_{12}E_9 detergent buffer. Both detergent-solubilized samples were kept at 0–4 °C for 30 min and then re-centrifuged at 20000 g_{max} for 20 min. The supernatants were then subjected to immunoprecipitation with anti-GLUT1 and anti-GLUT4 antibodies. In some experiments cells were

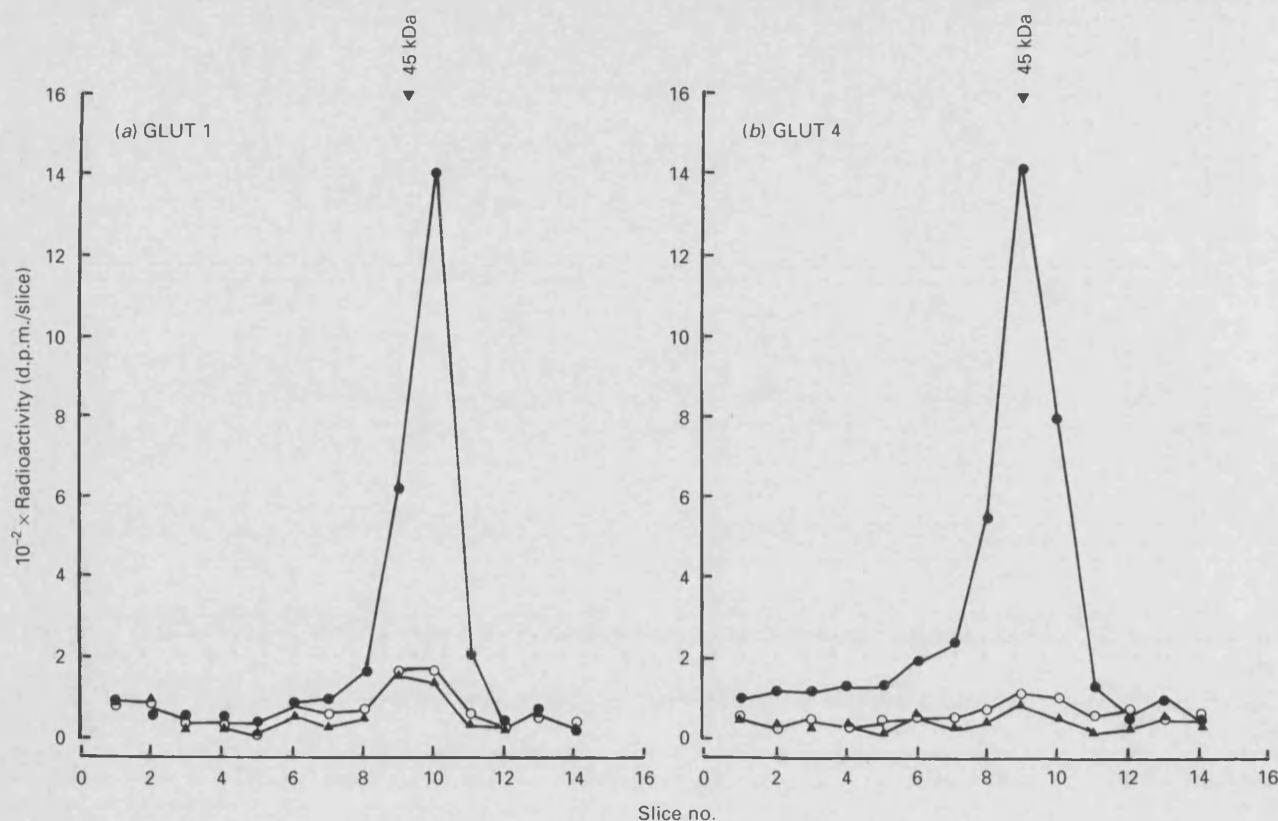


Fig. 4. Comparison of the effects of PAO and insulin on the cell-surface photolabelling of GLUT1 and GLUT4

3T3-L1 cells in 35 mm-diameter dishes were maintained either with no additions (\circ), with 100 nM-insulin (\bullet) or with 10 μM -PAO (\blacktriangle) for 30 min at 37 $^{\circ}\text{C}$. The cells were then labelled with 150 μCi of ATB-BMPA. After labelling, GLUT1 (a) and GLUT4 (b) were immunoprecipitated with anti-(C-terminal peptide) antibodies. The protein was then subjected to electrophoresis and the radioactivity was estimated by cutting out and counting gel slices.

homogenized in a KCl buffer (150 mM-KCl/2 mM-MgCl₂/20 mM-Hepes, pH 7.4) and a 16000 g_{max} plasma-membrane and supernatant fraction were isolated as described in [22]. The results obtained were the same as those obtained using the Tes buffer.

Immunoprecipitation and electrophoresis

The detergent-solubilized samples, either from solubilized cells or from crude plasma-membrane or crude light-microsome fractions prepared as described above, were subjected to sequential immunoprecipitation with 30 μl of Protein A-Sepharose coupled with 100 μl of anti-GLUT1 or 50 μl of anti-GLUT4 antiserum. These antisera were raised against C-terminal peptides as described in [12,16]. After incubation for 2 h at 0–4 $^{\circ}\text{C}$ and washing of the immunoprecipitates three times with 1.0% and once in 0.1% C₁₂E₉ detergent buffer, the labelled glucose transporters were released from the antibody complexes with 10% (w/v) SDS/6 M-urea/10% (v/v)-mercaptoethanol electrophoresis sample buffer and subjected to electrophoresis on 10% (w/v)-acrylamide gels. The radioactivity on the gel was extracted from gel slices and estimated by liquid-scintillation counting. The radioactivity in transporter peaks was corrected for background radioactivity which was based on the average radioactivity of the slices on either side of the peak [13].

RESULTS

Insulin stimulation of glucose transport and the availability of cell-surface transporters

The insulin stimulation of the cell-surface availability of

glucose transporters was found to be very rapid at 37 $^{\circ}\text{C}$ ($t_{\frac{1}{2}} \approx 2$ min). This was considered to be too rapid for comparison with the stimulation of 2-deoxy-D-glucose transport activity at this temperature ($t_{\frac{1}{2}} \approx 3$ min). Instead, we followed the approach of Gibbs *et al.* [23], who studied the time course for insulin stimulation at 27 $^{\circ}\text{C}$. At 27 $^{\circ}\text{C}$ the increase in cell-surface GLUT1 and GLUT4 occurred in parallel. Fig. 1 shows that a large increase above basal levels ($\approx 45\%$ of maximum) in cell-surface labelling of these two isoforms occurred with only 5 min of stimulation by 100 nM-insulin. The cell-surface levels of both isoforms then rose progressively and reached a maximum level of stimulation in ≈ 12 min. The cell-surface GLUT1 increases with $t_{\frac{1}{2}}$ of 5.7 ± 1.5 min (two experiments), which was similar to the rate of increase in cell-surface GLUT4 ($t_{\frac{1}{2}}$ 5.4 ± 0.7 min; two experiments). In Fig. 2 the time course for this stimulation of the cell-surface availability of transporters is shown to slightly precede the time course for insulin stimulation of 2-deoxy-D-glucose transport activity ($t_{\frac{1}{2}}$ 8.6 ± 1.5 min; three experiments).

Reversal of insulin action on glucose transport and loss of cell-surface glucose transporters

We examined the time course for the loss of cell-surface glucose transporters and compared this with the decrease in 2-deoxy-D-glucose transport activity (Fig. 3). The cells were fully stimulated by treatment with 100 nM-insulin for 30 min at 37 $^{\circ}\text{C}$, and then the insulin was removed by washing and incubation with MES buffer at pH 6.0 for the indicated times. This procedure was developed by Gibbs *et al.* [24], who showed that this low-pH buffer resulted in insulin dissociation and a consequent decrease in transport activity. The rate of loss of 2-deoxy-D-glucose-

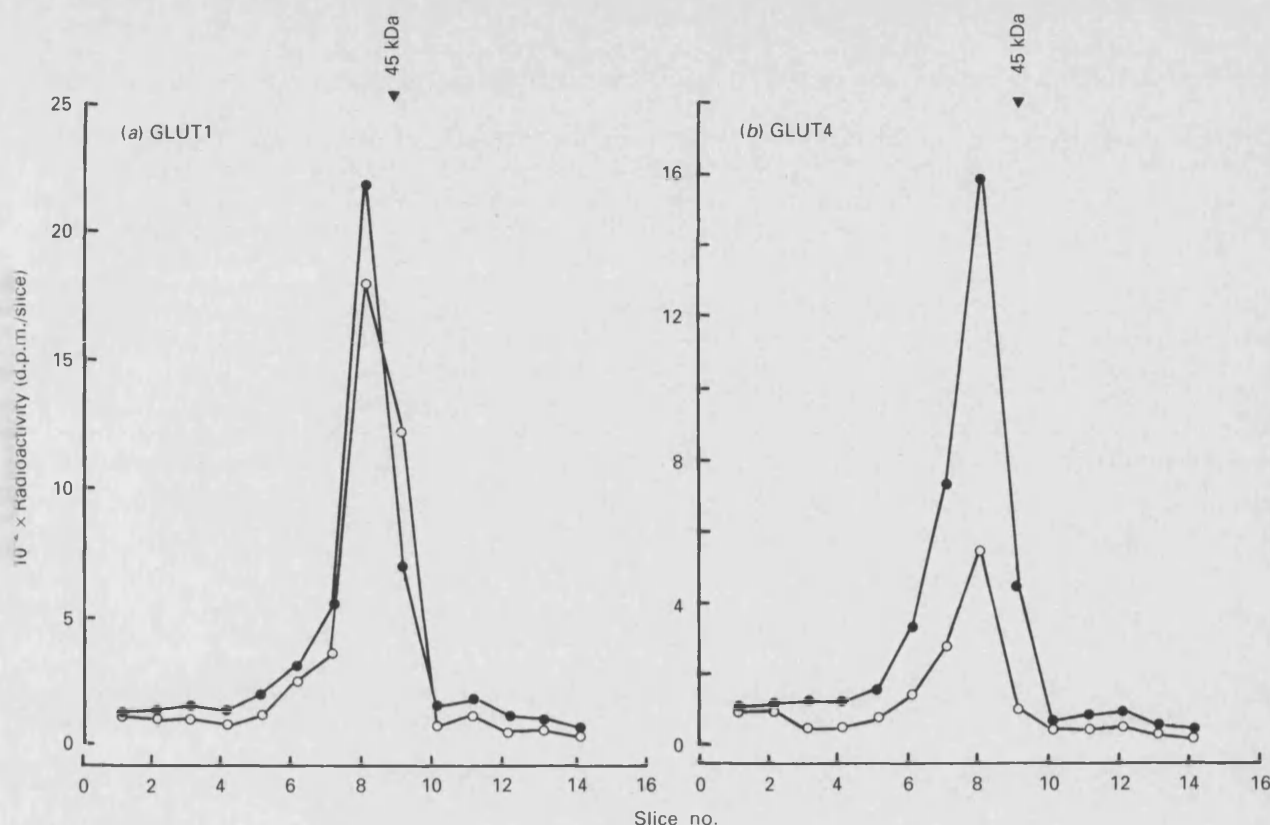


Fig. 5. Comparison of the effect of PAO on the availability of GLUT1 and GLUT4 in insulin-treated 3T3-L1 cells

3T3-L1 cells in 35 mm-diameter dishes were fully stimulated by treatment with 100 nM-insulin for 30 min at 37 °C. The cells were then maintained at 37 °C for a further 60 min in the presence (○) and the absence (●) of 20 μ M-PAO. The cells were then photolabelled with 100 μ Ci of ATB-BMPA and then the GLUT1 (a) and GLUT4 (b) were immunoprecipitated with anti-(C-terminal peptide) antibodies. The protein was then subjected to electrophoresis and the radioactivity was estimated by cutting out and counting gel slices.

transport activity that we have observed (Fig. 3) agrees with their results. The calculated half-time for the decrease in 2-deoxy-D-glucose-transport activity was 6.5 ± 0.4 min (three experiments). This correlates well with loss of cell-surface GLUT1 ($t_{1/2}$ 9.2 ± 0.8 min; two experiments) and GLUT4 ($t_{1/2}$ 6.8 ± 1.7 min; two experiments). The decrease in cell-surface GLUT4 was slightly more extensive than for GLUT1, possibly reflecting the greater tendency of GLUT1 to be re-exocytosed in the absence of insulin.

Effect of PAO on glucose-transporter trafficking

A number of effects of PAO on the glucose-transport activity in basal 3T3-L1 cells have been noted. Frost & Lane [4] reported that PAO decreased the insulin stimulation of transport activity, but had no effect on the transport activity of basal cells. However, Gould *et al.* [25] reported that, at low concentrations of PAO (< 20 μ M), a stimulation of the basal rate of transport occurred. Surprisingly, at concentrations of PAO where a transport stimulation was noted they found a decrease in cell-surface transporters (as detected by cell-surface labelling with NaB³H₄ of galactose oxidase-treated cells) and a rise in plasma-membrane-associated GLUT1 as detected by Western blotting. We therefore examined the effect of 5–10 μ M-PAO on basal transport activity and found a \approx 1.5-fold increase in 2-deoxy-D-glucose transport. As shown in Fig. 4, 10 μ M-PAO gave no detectable rise in either the concentration of GLUT1 or GLUT4. It is clear from this Figure, however, that any effect of PAO on basal levels of transporters is very small in comparison with the stimulatory effect of insulin.

Treatment of fully-insulin-stimulated 3T3-L1 cells with 20 μ M-PAO for 60 min markedly decreased the cell-surface level of the

GLUT4 isoform (Fig. 5b). However, the level of the GLUT1 isoform was only slightly decreased (Fig. 5a). The time course for the PAO-induced loss of cell-surface transporters is compared with the decrease in 2-deoxy-D-glucose-transport activity in Fig. 6. The loss of transport activity and GLUT4 occurred with half-times of 9.8 ± 1.6 and 7.8 ± 0.8 min respectively (two experiments), which were similar to the half-time for the decrease in transport activity that occurred when insulin was removed by the low-pH-washing procedure (Fig. 3). In contrast with this, the level of cell-surface GLUT1 remained high during the PAO treatment. During the PAO treatment the half-time for the decrease in cell-surface GLUT1 was greater than 60 min and was much longer than the half-time for the loss of GLUT1 that occurred when insulin was removed by the low-pH-washing procedure and which was only \approx 9 min. To confirm that the decrease in GLUT4 was due to a redistribution of these transporters within the cell and not to an irreversible inhibition of transport [21], we have measured the binding of ATB-BMPA to the transporters in cells which had been permeabilized by treatment with 0.025% digitonin. Figs. 7(a) and 7(b) show that the total concentration of available GLUT4 was only slightly decreased (by \approx 30%). This slight decrease may have occurred because the efficiency of labelling transporters present inside the cell may have been slightly less than for surface labelling. We also confirmed that neither GLUT1 nor GLUT4 was lost from the cell by Western-blotting crude membrane fractions obtained from cells treated with insulin and then 20 μ M-PAO (J. Yang, A. E. Clark, R. Harrison, I. J. Kozka & G. D. Holman, unpublished work). The more striking effect of PAO treatment was to decrease just the GLUT4 at the cell surface. In the cells treated

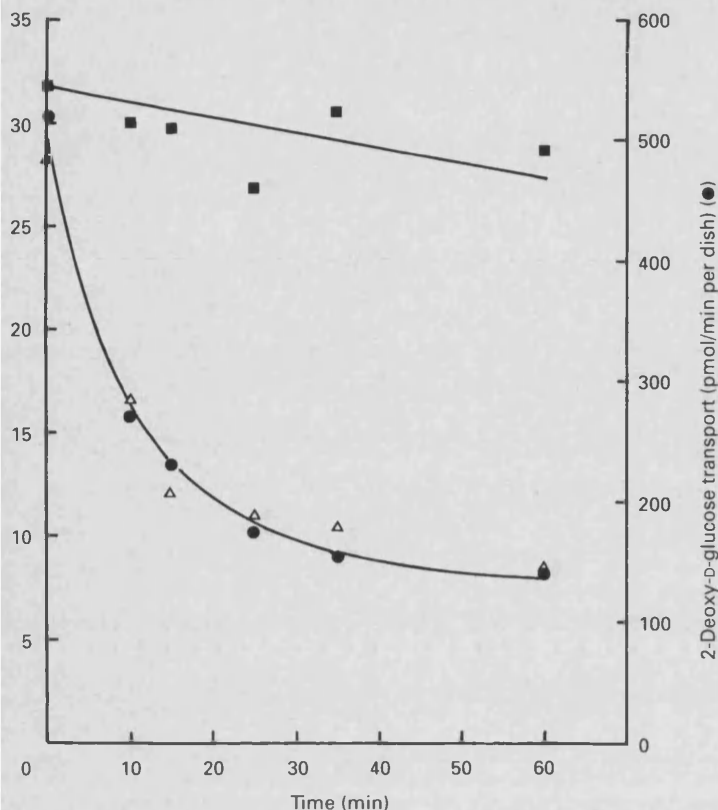


Fig. 6. Time course for the PAO-induced loss of cell-surface transporters and transport activity

PAO treatment of fully-insulin-stimulated 3T3-L1 cells was carried out as described in Fig. 5. The total radioactivity associated with photolabelled GLUT1 (■) and GLUT4 (△) was compared with the loss of 2-deoxy-D-glucose transport activity (●). The results are the means for two photolabelling experiments and, in the case of the transport-activity measurements, three experiments.

with insulin alone, $\approx 60\%$ of the available transporter was at the cell surface. In the cells treated with PAO, $\approx 20\%$ of the available transporters were at the surface (two experiments). In addition we have found, by measuring ATB-BMPA photolabelling in permeabilized cells, that the total available GLUT1 concentration was only slightly decreased after PAO treatment. Approx. 60% of the available GLUT1 transporters were at the surface both in the presence and in the absence of PAO.

A possible interpretation of this differential effect on GLUT1 and GLUT4 cell-surface availability is that, in the presence of PAO, both transporters are removed from the cell surface at the same rate, but their recycling is differentially perturbed. Thus both GLUT1 and GLUT4 could be endocytosed even in the presence of PAO, but inhibition of GLUT4, but not GLUT1, re-emergence and re-exposure to the photolabel at the cell surface could then have resulted in the observed decrease in its detected surface concentration.

To examine the possibility that both transporters were internalized in the presence of PAO, we labelled the cell-surface transporters in fully-insulin-stimulated cells with ATB-BMPA and then treated them with PAO and insulin for a further 60 min. We then homogenized the cells and separated a crude plasma membrane fraction from the light-microsome fraction. After 60 min in the continuous presence of insulin, the light-microsome level of photolabelled GLUT1 and GLUT4 was increased above that observed at zero time. This indicates that internalization of

transporters occurred even in the continuous presence of insulin (Table 1). The percentages of photolabelled transporter found in the light-microsome fraction are consistent with the results of Calderhead *et al.* [13], who determined by Western blotting that $\approx 50\%$ of the total recovered GLUT1 and GLUT4 were present in the light-microsome pool of basal cells and that this was decreased to $\approx 25\%$ in insulin-treated cells. The light-microsome association of GLUT1 was slightly less than that which occurred for the GLUT4 isoform. This probably reflects the greater tendency of GLUT1 to be re-exocytosed under these conditions.

Table 1 also shows that the internalization of GLUT1 and GLUT4 also occurred in cells treated with PAO. However, in PAO-treated cells the additional GLUT4, above that found with insulin alone, which was lost from the cell surface was not recovered in the light microsomes, but partitioned with the plasma-membrane fraction during homogenization. The total recovered photolabel was unaltered by the PAO treatment. Western blotting confirmed that neither GLUT4 nor GLUT1 internalization to the light-microsome fraction was increased by the PAO treatment compared with insulin alone (J. Yang, A. E. Clark, R. Harrison, I. Kozka & G. D. Holman, unpublished work). Fig. 8 shows that $\approx 35\%$ of GLUT4 transporters that were photolabelled in the insulin-stimulated state were transferred to the light-microsome fraction after 60 min. This proportion was not altered by the PAO treatment.

DISCUSSION

Cushman & Wardzala [26] and Suzuki & Kono [27] proposed in 1980 that glucose transporters, like receptors and other membrane proteins, were translocated from light-microsome vesicles to the plasma membrane of adipose cells in response to insulin. Recently two different, but complementary, approaches to investigating this membrane-trafficking phenomenon have provided very strong support for their hypothesis. Slot *et al.* [10] have shown that, in brown adipose tissue, immunodetectable GLUT4 was localized to a cytosolic-vesicle pool with very low transporter levels in the plasma membrane of basal cells. Upon insulin stimulation, the GLUT4 located in the plasma membrane was increased 40-fold. The second approach that has provided strong supportive evidence for the translocation hypothesis has involved use of the bis-D-mannose photolabel ATB-BMPA in trafficking kinetic experiments [16,17]. Satoh *et al.* [17] have shown, in trafficking experiments using the ATB-BMPA photolabel, that transporters are recycled between plasma-membrane and light-microsome pools. Fully-insulin-stimulated cells were photolabelled with ATB-BMPA and then insulin was removed by a collagenase treatment. Labelled transporters were shown to be transferred to the light-microsome membranes. Equilibration of cell-surface-labelled transporters with the light-microsome pool also occurred when cells were maintained, after labelling, in the continuous presence of insulin. In the presence of insulin, the level of transporters in the light microsomes reached a lower steady-state level than that which was reached after insulin removal. These experiments have thus provided direct evidence that transporters move between the plasma-membrane and light-microsome pools. Furthermore, re-stimulation experiments have directly shown that internalized transporters are re-exocytosed to the plasma membrane. Insulin stimulation was shown to be due to an enhancement of exocytosis rather than due to an inhibition of the endocytosis of transporters [16,17].

Use of the ATB-BMPA photolabelling reagent has also allowed an assessment of the magnitude of translocation to be made in intact adipose cells. Insulin has been shown to increase cell-surface GLUT4 15–20-fold, whereas GLUT1 is only increased ≈ 5 -fold. The use of this 'in situ' labelling procedure

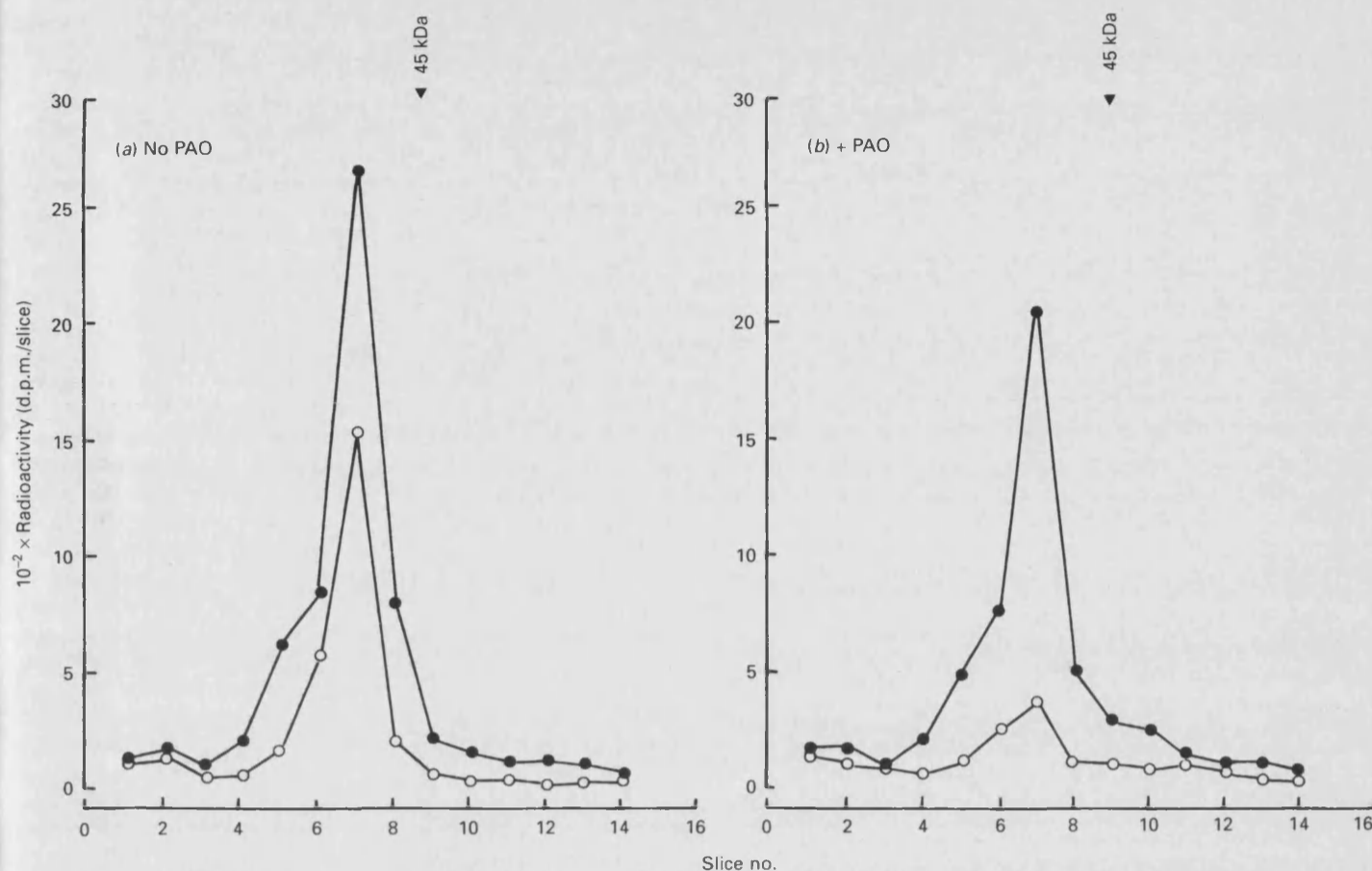


Fig. 7. Experiment to determine whether the PAO-induced decrease in cell-surface GLUT4 is due to a redistribution to the cell interior

3T3-L1 cells in 35 mm-diameter dishes were fully stimulated by treatment with 100 nM-insulin for 30 min at 37 °C. The cells were then maintained at this temperature for a further 50 min in the absence (a) or in the presence (b) of 20 μ M-PAO. The cells were then either photolabelled directly with 100 μ Ci of ATB-BMPA (○) or were permeabilized in the presence of 100 μ Ci of ATB-BMPA by treatment with 0.025 % digitonin for 8 min at 18 °C and then irradiated (●). GLUT4 was then immunoprecipitated with anti-(C-terminal peptide) antibody. The protein was then subjected to electrophoresis and the radioactivity was estimated by cutting out and counting gel slices.

Table 1. Internalization of glucose transporters in 3T3-L1 cells

Fully-insulin-stimulated 3T3-L1 cells were photolabelled with ATB-BMPA and then either homogenized immediately (0 min) or maintained at 37 °C with insulin (60 min) or insulin + 20 μ M-PAO (60 min) before homogenization. Crude plasma-membrane and light-microsome fractions were prepared and solubilized in $C_{12}E_8$ detergent buffer. GLUT1 and GLUT4 were then immunoprecipitated and subjected to electrophoresis. The radioactivity in the transporter peaks was estimated, and the results are expressed as a percentage of radioactivity recovered in the light-microsome fraction compared with the sum of the radioactivity recovered in the plasma-membrane and the light-microsome fractions.

Addition	Time (min)	Expt.	Percentage of radioactivity in light-microsome fraction			
			Transporter ...			
			GLUT1		GLUT4	
			Individual results	Mean \pm S.E.M.	Individual results	Mean \pm S.E.M.
Insulin	0	1	13.7	11.0 \pm 0.5	17.1	14.0 \pm 0.8
		2	9.8		10.9	
		3	13.1		14.4	
		4	11.0		13.2	
Insulin	60	1	38.1	27.9 \pm 4.5	39.0	35.6 \pm 5.3
		2	29.8		31.1	
		3	27.5		42.0	
		4	16.2		18.2	
Insulin + PAO	60	1	21.9	23.2 \pm 1.8	33.3	32.0 \pm 1.2
		2	29.3		35.4	
		3	20.6		29.8	
		4	20.9		29.5	

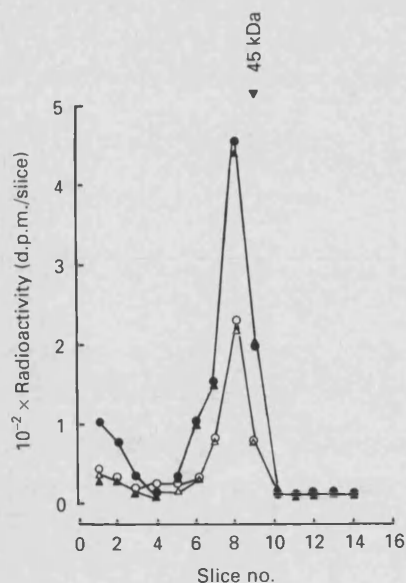


Fig. 8. Redistribution of photolabelled GLUT4 to subcellular membrane fractions of 3T3-L1 cells

3T3-L1 cells in 35 mm-diameter dishes were fully insulin-stimulated by treatment with 100 nM-insulin for 30 min at 37 °C. They were then photolabelled with 100 μ Ci of ATB-BMPA and then maintained with (circles) and without (triangles) 20 μ M-PAO for a further 60 min. Crude plasma membrane (closed symbols) and light-microsome membranes (open symbols) were prepared from two dishes for each condition. These fractions were solubilized in $C_{12}E_9$ detergent buffer. GLUT4 was then immunoprecipitated with anti-(C-terminal peptide) antibody and subjected to electrophoresis; radioactivity was estimated by cutting out and counting gel slices.

has circumvented the need to subject the cells to subcellular fractionation, a procedure that is considered to underestimate the magnitude of the translocation effect, owing to the cross-contamination of plasma-membrane and light-microsome fractions. The photolabel has been used to compare the time courses for appearance and loss of transporters in rat adipocytes with the time course for a change in glucose-transport activity [16]. This study has shown that, on insulin addition, the arrival of GLUT1 and GLUT4 transporters at the cell surface slightly precedes the increase in transport activity, but that the loss of these transporters from the cell surface on insulin removal correlated well with transport. We have confirmed here that these effects also occur in 3T3-L1 cells. The loss of transporters from the cell surface occurs with half-times that are very similar to that for the internalization of other membrane proteins and receptors [28–30], suggesting that this internalization step occurs by fluid-phase endocytosis [31]. The high activation energy for reversal of transport stimulation and the almost complete cessation of glucose-transporter internalization at 18 °C [16] are also consistent with this possibility.

Now that the essential predictions of the translocation hypothesis have been confirmed, questions concerning the mechanistic details of the trafficking pathways can be addressed. The transporter-immunolocalization study of Slot *et al.* [10] has provided evidence that the GLUT4-trafficking pathway involves clathrin-coated vesicles. The association of this transporter in clathrin vesicles was increased by insulin treatment of the cells. Other trafficking proteins that may be involved include small guanine-nucleotide-binding proteins (G-proteins). It is now known that these are intricately involved in many vesicle-trafficking events [32]. G-protein involvement in glucose-transporter trafficking has been clearly implicated by the discovery by

Baldini *et al.* [33] that the non-hydrolysable GTP analogue guanosine 5'-[γ -thio]triphosphate stimulates translocation of GLUT4 from the light-microsome pool to the plasma membrane of rat adipocytes. Other proteins that are likely to be involved in the trafficking include adaptins. These have been implicated in the enhancement of receptor association with clathrin [34], and their involvement in the trafficking of other membrane proteins is likely. A reasonable interpretation of some features of the trafficking kinetics of glucose transporters in 3T3-L1 cells that we have observed here is that a dissociation from trafficking proteins occurs before the transporters can fully participate in transport.

The observed lag between transporter appearance at the cell surface and the full stimulation of transport [16,17,23,35; the present study] may occur because transporters are still associated with trafficking proteins at early time points after the addition of insulin to the cells. Thus translocation may precede transport activation, owing to the requirement for a dissociation from these proteins. The effects of PAO on the trafficking of membrane proteins have generally been reported to be due to inhibition of fluid-phase endocytosis by this reagent [18–20]. However, the resolution of an effect on endocytosis or exocytosis is difficult. It is possible, for example, that receptors are internalized and reappear at the surface, but then fail to dissociate from the trafficking proteins because this process is blocked by PAO. Receptor abundance at the surface would remain high, owing to a single cycle of internalization and re-exocytosis, and the whole cycling process would halt. The net result would be that endocytosis would appear to be inhibited. There is evidence against the possibility that a simple block of endocytosis occurs. PAO has been shown [25] to decrease surface transferrin receptors, as measured by transferrin binding to whole cells, but to increase the level of plasma-membrane-associated receptors measured in an isolated membrane fraction. It was proposed [25] that this effect may have occurred because recycled vesicles containing the receptors could not fuse with the plasma membrane, but remained associated with it, during subcellular fractionation. An alternative explanation is that vesicles do fuse with the plasma membrane, but that the receptors are associated with trafficking proteins and therefore not fully available for ligand binding. These two proposals are not mutually exclusive, and a combination of both these effects may occur.

We have shown here that PAO has distinct effects on the trafficking of GLUT1 and GLUT4. The abundance of GLUT1 at the cell surface remained high when fully-insulin-stimulated cells were treated with PAO. However, the surface level of GLUT4 decreased with a time course for redistribution similar to that which occurred after insulin removal by washing in a low-pH buffer. This suggests they were internalized by the fluid-phase-endocytosis route. In contrast with the above results (which were obtained from surface labelling, which was carried out after PAO treatment) we have shown that, when photolabelling was carried out in fully-insulin-stimulated cells and cells were subsequently treated with PAO, then both GLUT1 and GLUT4 were internalized to the light-microsome pool.

An additional observation concerning the transport activity of GLUT1 in PAO-treated cells also suggests that, although the GLUT1 surface-level is constant, recycling of this isoform may have occurred. We have calculated that the GLUT1 contribution to transport is about one-third of that of GLUT4 in fully-insulin-stimulated cells [R. W. Palfreyman, A. E. Clark, R. M. Denton, G. D. Holman & I. J. Kozka, unpublished work]. Yet when the insulin stimulation was reversed with PAO, the fall in transport paralleled the decrease in GLUT4 and the remaining cell-surface GLUT1 appeared to make only a minimal contribution to transport. Thus GLUT1 may be internalized and recycled to the surface, but remain associated with trafficking proteins, which

suppress its transport capability. This association with trafficking proteins may be similar to that which occurs in the lag phase of insulin activation [16,17,23,35; the present study] and may account for the low contribution of cell-surface GLUT1 to the transport activity in basal cells [13,37]. Harrison *et al.* [38] have proposed that GLUT1 activity is suppressed in transfected 3T3-L1 cells. We have shown [14] that it is difficult to remove GLUT1 from the cell surface after a chronic insulin treatment, but that this cell-surface GLUT1 appears to have low transport capability. The location of transporters of suppressed activity may be in surface-attached vesicles. These may be early intermediates in the insulin-stimulated trafficking pathway [17]. If some of the surface-attached vesicles are surface-exposed, then glucose transporters in these vesicles would be photolabelled, but would possibly not be able to participate in transport if they were still associated with trafficking proteins.

If the effect of PAO is mainly due to an inhibition of exocytotic vesicle fusion with the plasma membrane and/or inhibition of transporter dissociation from trafficking proteins, then this inhibition could also account for the decrease in cell-surface GLUT4 that is detectable with the ATB-BMPA photolabel. GLUT4 transporter vesicles may have a greater tendency to remain internalized and not fully surface-exposed if the normal mechanisms that commit transporters to the cell surface, such as dissociation from trafficking proteins, are uncoupled. A proportion of the GLUT4 transporters which are removed from surface accessibility to the photolabel in PAO-treated cells appear to be fractionated with the plasma membrane. The percentage of transporters recovered in the light microsomes was similar to that obtained with insulin alone. The effect requires further investigation, but it may be similar to that observed with transferrin receptors, where a PAO-induced failure of recycled vesicles to fuse with the plasma membrane was proposed [25]. A similar effect was observed when insulin-stimulated rat adipocytes were treated with isoproterenol [39].

The greater tendency of GLUT4 to remain internalized also accounts for the low levels of this isoform at the cell surface of basal cells [12,13,40].

In conclusion, we have shown, by measuring trafficking kinetics of glucose-transporter isoforms in 3T3-L1 cells, that there is a lag between transporter appearance and participation in transport. We have provided evidence that the GLUT1 and GLUT4 isoforms are recycled even in the presence of insulin. In addition, we have shown that GLUT1 and GLUT4 exhibit different trafficking properties when processing is perturbed with PAO. The above properties of translocation indicate an involvement of a slow dissociation from trafficking proteins during recycling. This proposal implicates an involvement of unspecified trafficking proteins, and further resolution of the proposed mechanism will depend on the identification and characterization of these proteins.

We are grateful to the Medical Research Council and the British Diabetic Association for financial support. We also thank Dr. S. W. Cushman for helpful advice throughout the study.

REFERENCES

1. Vinten, J., Gliemann, J. & Osterlind, K. (1976) *J. Biol. Chem.* **251**, 794–800
2. Simpson, I. A. & Cushman, S. W. (1986) *Annu. Rev. Biochem.* **55**, 1059–1089

3. Taylor, L. P. & Holman, G. D. (1981) *Biochim. Biophys. Acta* **642**, 325–335
4. Frost, S. C. & Lane, M. D. (1985) *J. Biol. Chem.* **260**, 2646–2652
5. James, D. E., Strube, M. I. & Mueckler, M. (1989) *Nature (London)* **338**, 83–87
6. Birnbaum, M. J. (1989) *Cell (Cambridge, Mass.)* **57**, 305–315
7. Charron, M. J., Brosius, F. C., Alper, S. L. & Lodish, H. F. (1989) *Proc. Natl. Acad. Sci. U.S.A.* **86**, 2535–2539
8. Kaestner, K. H., Christy, R. J., McLenithan, J. C., Briterman, L. T., Cornelius, P., Pekela, P. H. & Lane, M. D. (1989) *Proc. Natl. Acad. Sci. U.S.A.* **86**, 3150–3154
9. Fukumoto, H., Kayano, T., Buse, J. B., Edwards, Y., Pilch, P. F., Bell, G. I. & Seino, S. (1989) *J. Biol. Chem.* **264**, 7776–7779
10. Slot, J. W., Gueuze, H. J., Gigengack, S., Lienhard, G. E. & James, D. E. (1991) *J. Cell. Biol.* **113**, 123–135
11. Clark, A. E. & Holman, G. D. (1990) *Biochem. J.* **269**, 615–622
12. Holman, G. D., Kozka, I. J., Clark, A. E., Flower, C. J., Saltis, J., Habberfield, A. D., Simpson, I. A. & Cushman, S. W. (1990) *J. Biol. Chem.* **265**, 18172–18179
13. Calderhead, D. M., Kitagawa, K., Tanner, L. I., Holman, G. D. & Lienhard, G. E. (1990) *J. Biol. Chem.* **265**, 13800–13808
14. Kozka, I. J., Clark, A. E. & Holman, G. D. (1991) *J. Biol. Chem.*, in the press
15. Reference deleted
16. Clark, A. E., Holman, G. D. & Kozka, I. J. (1991) *Biochem. J.* **278**, 235–241
17. Satoh, S., Gonzalez-Mulero, O. M., Clark, A. E., Kozka, I. J., Holman, G. D. & Cushman, S. W. (1991) *Diabetes* **40**, (Suppl. 1), 85A
18. Knutson, V. P., Ronnett, G. V. & Lane, M. D. (1986) *J. Biol. Chem.* **258**, 12139–12142
19. Wiley, H. S. & Cunningham, D. D. (1982) *J. Biol. Chem.* **257**, 4222–4229
20. Frost, S. C., Lane, M. D. & Gibbs, E. M. (1989) *J. Cell. Physiol.* **141**, 467–474
21. Douen, A. G. & Jones, M. N. (1988) *Biochim. Biophys. Acta* **968**, 109–118
22. Brown, S. J., Gould, G. W., Davies, A., Baldwin, S. A., Lienhard, G. E. & Gibbs, E. M. (1988) *Biochim. Biophys. Acta* **971**, 339–350
23. Gibbs, E. M., Lienhard, G. E. & Gould, G. W. (1988) *Biochemistry* **27**, 6681–6685
24. Gibbs, E. M., Allard, W. J. & Lienhard, G. E. (1986) *J. Biol. Chem.* **261**, 16597–16603
25. Gould, G. W., Lienhard, G. E., Tanner, L. I. & Gibbs, E. M. (1989) *Arch. Biochem. Biophys.* **268**, 264–275
26. Cushman, S. W. & Wardzala, L. J. (1980) *J. Biol. Chem.* **255**, 4758–4762
27. Suzuki, K. & Kono, T. (1980) *Proc. Natl. Acad. Sci. U.S.A.* **77**, 2542–2545
28. Goldstein, J. L., Brown, M. S., Anderson, R. G. W., Russel, D. W. & Schneider, W. J. (1985) *Annu. Rev. Cell Biol.* **1**, 1–39
29. Stoorvogel, W., Geuze, H. J. & Strous, G. J. (1987) *J. Cell. Biol.* **104**, 1261–1268
30. Gibbs, E. M., Lienhard, G. E., Appleman, J. R., Lane, M. D. & Frost, S. C. (1986) *J. Biol. Chem.* **261**, 3944–3951
31. Lienhard, G. E. (1983) *Trends Biol. Sci.* **8**, 125–127
32. Bourne, H. R., Sanders, D. A. & McCormick, F. (1990) *Nature (London)* **348**, 125–132
33. Baldini, G., Hohman, R., Charron, M. J. & Lodish, H. F. (1991) *J. Biol. Chem.* **266**, 4037–4040
34. Robinson, M. (1987) *J. Cell. Biol.* **104**, 887–895
35. Karnielli, E., Karnowski, M. J., Hissin, P. J., Simpson, I. A., Salans, L. B. & Cushman, S. W. (1981) *J. Biol. Chem.* **256**, 4772–4777
36. Reference deleted
37. Clancy, B. M. & Czech, M. P. (1990) *J. Biol. Chem.* **265**, 12434–12443
38. Harrison, S. A., Buxton, J. M., Clancy, B. M. & Czech, M. P. (1990) *J. Biol. Chem.* **265**, 20106–20116
39. Joost, H. G., Weber, T. M., Cushman, S. W. & Simpson, I. A. (1987) *J. Biol. Chem.* **262**, 11261–11267
40. James, D. E., Brown, R., Navarro, J. & Pilch, P. F. (1988) *Nature (London)* **333**, 183–185

Development of an Intracellular Pool of Glucose Transporters in 3T3-L1 Cells*

(Received for publication, December 30, 1991)

Jing Yang, Avril E. Clark, Izabela J. Kozka, Samuel W. Cushman†, and Geoffrey D. Holman

From the Department of Biochemistry, the University of Bath, Claverton Down, Bath BA2 7AY United Kingdom and the
†Experimental Diabetes, Metabolism and Nutrition Section, Diabetes Branch, National Institutes of Diabetes and Digestive and
Kidney Disease, National Institutes of Health, Bethesda, Maryland 20892

The membrane-impermeant bis-mannose photolabel 2-*N*-4-(1-*azi*-2,2,2-trifluoroethyl)benzoyl-1,3-bis-(*D*-mannos-4-yloxy)-2-propylamine (ATB-BMPA) has been used to study the development of an intracellular pool of glucose transporters in 3T3-L1 cells. The subcellular distributions of the transporter isoforms GLUT1 and GLUT4 were determined by comparing the labeling obtained in cells in which the impermeant reagent only had access to the cell surface and the labeling obtained in digitonin-permeabilized cells. ATB-BMPA labeling showed that only GLUT1 was present in preconfluent fibroblasts and that most of the transporters were distributed to the cell surface. In preconfluent fibroblasts, the 2-deoxy-*D*-glucose transport activity was ≈ 5 times higher than in confluent fibroblasts. ATB-BMPA labeling showed that the decrease in transport as cells reached confluence was associated with a decrease in the proportion of GLUT1 distributed to the cell surface. The sequestration of these transporters was associated with the development of an insulin-responsive transport activity which increased by ≈ 2.5 -fold compared with unstimulated confluent cells. ATB-BMPA labeling showed that insulin stimulation resulted in an ≈ 2 -fold increase in surface GLUT1 so that about one-half of the available transporters became recruited to the cell surface. Measurements of the changes in the distribution of both GLUT1 and GLUT4 throughout the differentiation of confluent fibroblasts into adipocytes showed that both transporters were sequestered in parallel. Basal levels of transport and photolabeling remained low throughout the differentiation period when the total pool of transporters (GLUT1 plus GLUT4) was increased by ≈ 5 -fold. These results suggest that the sequestration process was present before new transporters were synthesized. Thus, the sequestration mechanism develops in confluent growth-arrested fibroblasts although the capacity to sequester additional transporters may increase as differentiation proceeds.

3T3-L1 cells have been used for studying insulin action on glucose transport because these cells can be differentiated to produce a reserve of internal glucose transporters which can be translocated to the cell surface in response to insulin. When the cells are grown as fibroblasts, they produce only

the glucose transporter isoform GLUT1 (Kaestner *et al.*, 1989; Garcia de Herreros and Birnbaum, 1989; Tordjman *et al.*, 1990; Harrison *et al.*, 1990; Reed *et al.*, 1990; Weiland *et al.*, 1990). The fibroblasts are induced to differentiate using isobutylmethylxanthine, dexamethasone, and insulin (Green and Kehinde, 1975; Frost and Lane, 1985). During the course of this differentiation, the cells produce the acutely insulin-responsive isoform GLUT4 (Kaestner *et al.*, 1989; Garcia de Herreros and Birnbaum, 1989; Tordjman *et al.*, 1990; Weiland *et al.*, 1990). It is known from these studies that both GLUT1 and GLUT4 mRNA and total cellular protein rise in concentration over 8 days, and, at 8–11 days after initiation of differentiation, the concentrations of these transporters within the cells reach a maximum.

To examine the proportion of newly synthesized transporters which become available at the cell surface, we have extended the use of our bis-mannose photolabel to measure both cell surface and the total cellular pool of transporters. We have previously used this photolabel to measure the cell surface availability of insulin-stimulated adipose cells (Holman *et al.*, 1990; Clark *et al.*, 1991) and differentiated 3T3-L1 cells (Calderhead *et al.*, 1990; Kozka *et al.*, 1991). We show here that permeabilization of 3T3-L1 cells with digitonin allows the normally impermeant photolabel access to those transporters that are sequestered within the cell. We have therefore compared the labeling at the cell surface and the labeling of the total cellular transporter pool both before differentiation, when the 3T3-L1 cells are confluent fibroblasts, and during the subsequent period of the differentiation regime. The results suggest that mechanisms for sequestration of transporters develop before new transporters are synthesized in the course of differentiation.

The method for examining the distribution of glucose transporters that we have developed here should be a useful addition to the range of techniques that are available for studying transporter processing. The technique has the advantage that it does not depend upon homogenization and separation of membrane fractions and should be useful in studying systems where homogenization procedures are technically very difficult. In addition, it may be useful in investigations of expression systems where transporter cDNA or mRNA are introduced and in which the proportion of the expressed protein that reaches the cell surface needs to be determined.

EXPERIMENTAL PROCEDURES

Materials—ATB-BMPA¹ and ATB-[2-³H]BMPA (specific activity ≈ 10 Ci/mmol) were prepared as described (Clark and Holman, 1990).

¹ The abbreviations used are: ATB-BMPA, 2-*N*-4-(1-*azi*-2,2,2-trifluoroethyl)benzoyl-1,3-bis-(*D*-mannos-4-yloxy)-2-propylamine; Hepes, 4-(2-hydroxyethyl)-1-piperazineethanesulfonic acid; C₁₂E₉, nonaethyleneglycol dodecyl ether; DMEM, Dulbecco's modified Eagle's medium.

* This work was supported by the Medical Research Council of the United Kingdom and the British Diabetic Association. The costs of publication of this article were defrayed in part by the payment of page charges. This article must therefore be hereby marked "advertisement" in accordance with 18 U.S.C. Section 1734 solely to indicate this fact.

2-deoxy-[2,6- ^3H]D-glucose was from Amersham International. DMEM was from Flow Laboratories. Fetal bovine serum was from Gibco Laboratories. Monocomponent porcine insulin was a gift from Dr. Ronald Chance, Eli Lilly Laboratories. Dexamethasone, isobutylmethylxanthine, and protein A-Sepharose were from Sigma. Non-aethyleneglycol dodecyl ether (C_{12}E_9) was from Boehringer.

Cell Culture—3T3-L1 fibroblasts were seeded at a density of $\approx 0.03 \times 10^6$ cells per 35-mm dish and cultured in DMEM with 10% newborn calf serum. Fibroblasts were differentiated to adipocytes in DMEM and 10% fetal bovine serum by treatment with insulin, dexamethasone, and isobutylmethylxanthine as described by Frost and Lane, 1975. Fully differentiated cells were washed with phosphate-buffered saline (154 mM NaCl, 12.5 mM sodium phosphate, pH 7.4) and were then incubated for 2 h in serum-free medium containing 25 mM D-glucose. This was followed by three washes in Krebs-Ringer-Hepes buffer (KRH buffer, 136 mM NaCl, 4.7 mM KCl, 1.25 mM CaCl_2 , 1.25 mM MgSO_4 , 10 mM Hepes, pH 7.4) before use in experiments to determine 2-deoxy-D-glucose transport activity or cell surface transporters. Cell numbers were determined by counting, in a cytometer, the trypan blue excluding cells harvested from trypsin treatment of the cell monolayers.

Transport Activity—Cells in 35-mm dishes were maintained at 37 °C either in the absence or presence of 100 nM porcine monocomponent insulin for 30 min. The cells were then incubated with 50 μM 2-deoxy-D-[2,6- ^3H]glucose in 1 ml of KRH buffer at 37 °C for 5 min. Cells were then rapidly washed three times in KRH buffer at 0–4 °C, and the radioactivity was extracted into 1 ml of 0.1 M NaOH.

ATB-BMPA Photolabeling—Cells in 35-mm dishes were maintained at 37 °C either in the absence or the presence of 100 nM insulin for 30 min. The dishes were washed in KRH buffer and were irradiated for 1 min in a Rayonet photochemical reactor in the presence of 100 μCi of ATB-[2- ^3H]BMPA in 250 μl of KRH buffer at 18 °C as described by Kozka *et al.*, 1991. To measure labeling of the total cellular transporter pool, cells were permeabilized by treatment with 0.025% (w/v) digitonin for 8 min at 18 °C in the presence of 100 μCi of ATB-[2- ^3H]BMPA. The digitonin used (Sigma D1407 and suitable for use in aqueous solutions) was 50% pure, and an allowance for this was made in preparing the digitonin solution. The irradiated cells were washed four times in KRH buffer and solubilized in 1.5 ml of detergent buffer containing 2% C_{12}E_9 , 5 mM sodium phosphate, 5 mM EDTA, pH 7.2 and with the proteinase inhibitors antipain, aprotinin, pepstatin, and leupeptin, each at 1 $\mu\text{g}/\text{ml}$ and maintained at ≈ 18 °C for 15 min. We have found that fibroblasts tended to detach from the dishes when labeled in the presence of digitonin. Therefore, in the case of photolabeled fibroblasts, the washing of irradiated cells was omitted and cells were immediately solubilized in C_{12}E_9 detergent buffer. Following centrifugation of the solubilized cell material at $20,000 \times g_{\text{max}}$ for 20 min, the supernatant was carefully separated from unsolubilized pellet and the insoluble fat-cake and then subjected to immunoprecipitation to determine the amounts of photolabeled GLUT1 and GLUT4 transporter.

Immunoprecipitation and Electrophoresis—The detergent-solubilized samples were subjected to sequential immunoprecipitation with 30 μl of protein A-Sepharose coupled with 100 μl of anti-GLUT1 or 50 μl of anti-GLUT4 antiserum. These antisera were raised against C-terminal peptides as described by Clark and Holman, 1990, and Holman *et al.*, 1990. After incubation for 2 h at 0–4 °C and washing of the immunoprecipitates three times with 1.0% and once in 0.1% C_{12}E_9 detergent buffer, the labeled glucose transporters were released from the antibody complexes with 10% SDS, 6 M urea, 10% mercaptoethanol electrophoresis sample buffer and subjected to electrophoresis on 10% acrylamide gels. The radioactivity on the gel was determined by cutting and counting gel slices. The radioactivity in transporter peaks was corrected for a background which was based on the average radioactivity of slices on either side of the peak (Calderhead *et al.*, 1990).

RESULTS

We have examined the rate of 2-deoxy-D-glucose transport in fibroblasts at stages from initial seeding of dishes to the development of a confluent cell monolayer which occurs at about Day 5 after seeding (Fig. 1). One day after initial seeding of the dishes, the transport rate was 0.13 nmol/ 10^6 cells/min (with 0.026×10^6 cells/35-mm dish). This gradually fell over 7 days to 0.025 nmol/ 10^6 cells/min (with 0.3×10^6 cells/35-mm dish) and stayed at this low level for at least another 6

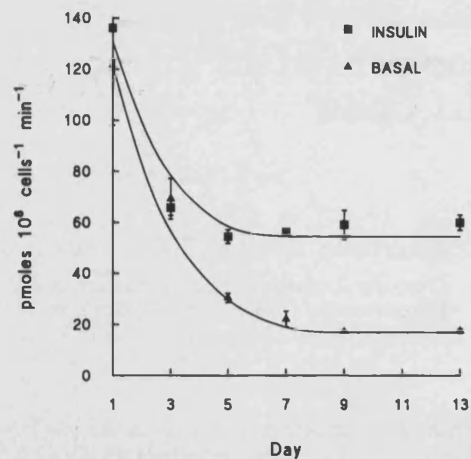


FIG. 1. 2-Deoxy-D-glucose transport activity in 3T3-L1 fibroblasts. Cells were seeded at a density of $\approx 0.03 \times 10^6$ cells per 35-mm dish and maintained in culture in DMEM with 10% newborn calf serum for up to 13 days. On the indicated days, the cells were incubated in the presence of serum-free medium for 2 h and then maintained at 37 °C for 30 min in either the absence (\blacktriangle) or presence (\blacksquare) of 100 nM insulin in 1 ml of KRH buffer. The transport of 50 μM 2-deoxy-D-[2,6- ^3H]glucose was then measured, and cell number was determined. Results are mean and S.E. from four independent determinations.

days. We have also examined the stage at which the transport rate in fibroblasts becomes insulin-responsive. From about 7 days after seeding, the 2-deoxy-D-glucose transport rate was increased by acute insulin stimulation to ≈ 2.5 times the basal level. However, even in the presence of insulin, the transport rate (0.06 nmol/ 10^6 cells/min) was approximately one-half the rate which was observed in preconfluent fibroblasts.

In order to determine the subcellular distribution of transporters, we have measured the cell surface availability of transporters with our impermeant photolabel ATB-BMPA and compared this with labeling that was obtained in digitonin-permeabilized cells. Fig. 2 shows the subcellular distribution of GLUT1 in confluent cells. No GLUT4 was detected in the fibroblasts. There was an ≈ 4 -fold increase in labeling in permeabilized cells compared with untreated cells. Insulin only increased the cell surface labeling by ≈ 2 -fold and did not increase the total pool of cellular GLUT1. The data from three experiments are shown in Fig. 3. This figure also shows that in preconfluent cells there is no significant increase in labeling in the presence of digitonin indicating that most of the cell transporters were at the cell surface.

Together with the transport data in Fig. 1, the labeling data show that in preconfluent 3T3-L1 fibroblasts the high transport rate is associated with the presence of most of the transporters at the cell surface. As the cells reach confluence, transporters are sequestered from the cell surface, and an intracellular reserve pool of transporters develops. Associated with this sequestration is a fall in the transport activity which can then be partially restored by acute insulin treatment which redistributes approximately one-half of the available transporters to the cell surface.

The technique for comparing cell surface and total cellular transporters has also been used to examine the distribution of the acutely insulin-sensitive isoform GLUT4 in differentiated 3T3-L1 adipocytes. Fig. 4 shows an SDS-polyacrylamide gel of ATB-BMPA-labeled and immunoprecipitated GLUT4. As shown in previous studies by Calderhead *et al.* (1990), Kozka *et al.* (1991), and Yang *et al.* (1992), there was very little GLUT4 at the cell surface in the basal state. Upon insulin stimulation, the GLUT4 labeling increased by ≈ 12 -fold in this experiment. However, as is the case with GLUT1

in confluent fibroblasts, only about one-half of the total available transporters were returned to the cell surface upon insulin treatment. In the digitonin-permeabilized cells, there

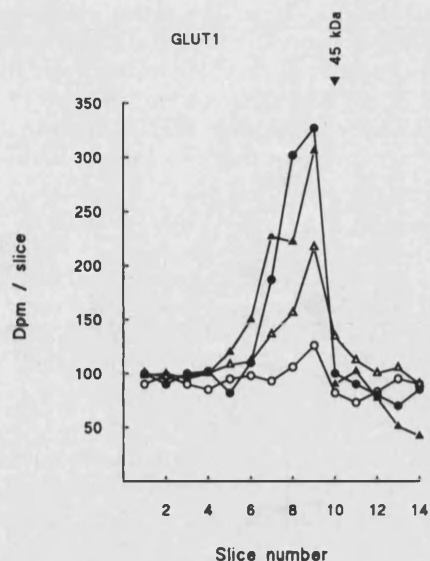


FIG. 2. ATB-BMPA labeling of cell surface and total cellular pools of GLUT1 in confluent 3T3-L1 fibroblasts. Cells were maintained in culture for 11 days in DMEM with 10% newborn calf serum and then incubated in serum-free medium for 2 h. Cells were then maintained at 37 °C for 30 min either in the absence (circles) or in the presence (triangles) of 100 nM insulin in 1 ml of KRH buffer. Cells were then labeled with 100 μ Ci of ATB-[2- 3 H]BMPA in 250 μ l of KRH buffer at 18 °C either without (open symbols) or with (closed symbols) of 0.025% digitonin. Labeled cells were immediately solubilized in $C_{12}E_9$ detergent buffer, and the labeled proteins were subjected to immunoprecipitation with GLUT1 C-terminal peptide antibody and then analyzed by electrophoresis.

was only a slight difference between the amount of GLUT4 labeled in the basal compared with the insulin-treated condition. The small difference observed in this experiment and others (Fig. 5) was possibly due to a difference in efficiency of labeling of the intracellular pool compared with the cell surface GLUT4. This small difference was not observed in all experiments, and, over seven experiments, the mean was only slightly lower than that observed with insulin-treated cells. However, Fig. 5 also shows that the S.E. was larger for the labeling of the total cellular pool of both GLUT1 and GLUT4 in the basal cells. The greater variability of labeling of the intracellular pool (which constitutes a greater proportion of the total in the basal state) was probably a consequence of variations between cell batches in the susceptibility to digitonin permeabilization or the efficiency with which the uv light could penetrate to intracellular sites of transporter localization. Fig. 5 also shows that in the insulin-stimulated state approximately half of the total of both GLUT1 and GLUT4 was recruited to the plasma membrane. However, as previously shown by Calderhead *et al.* (1990) and Yang *et al.* (1992), the GLUT4 has a greater tendency to be internalized in the absence of insulin, and the cell surface labeling of GLUT4 is about one-third of the GLUT1 level in this basal state.

We next examined the time course for changes in the glucose transport activity and subcellular transporter distribution during the transition from confluent fibroblasts to fully differentiated adipocytes (Fig. 6). This figure shows that the basal level of 2-deoxy-D-glucose transport remained low throughout the differentiation period. The transport rate in basal cells was ≈ 8 pmol/dish/min in confluent fibroblasts (with 0.3×10^6 cells/dish) increased to ≈ 25 pmol/dish/min in fully differentiated cells where the cell number had also in-

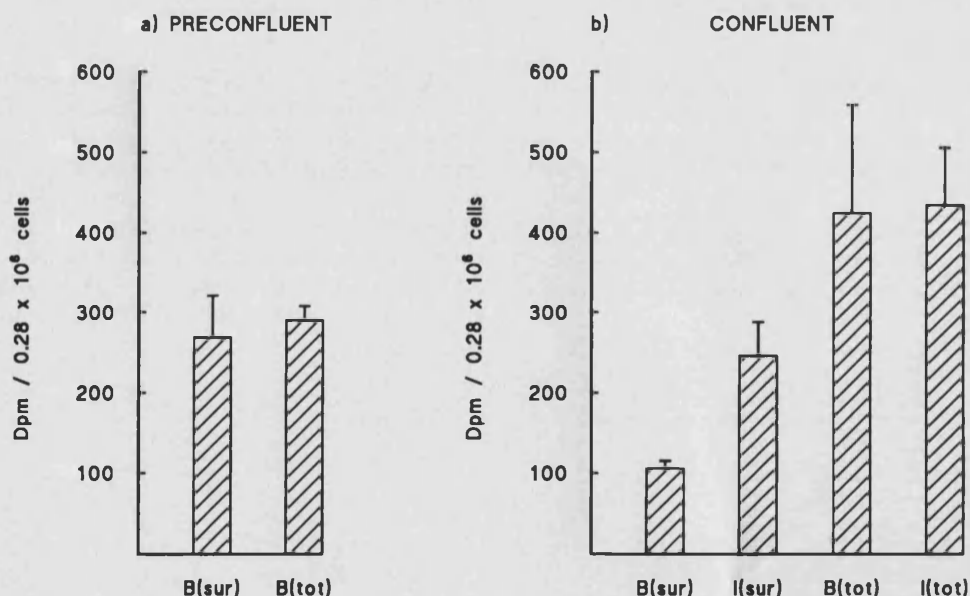


FIG. 3. Comparison of GLUT1 cellular distribution in preconfluent and confluent 3T3-L1 fibroblasts. In *a*, 3T3-L1 fibroblasts were harvested and plated into two 35-mm dishes to give a total of 0.28×10^6 subconfluent cells after 1 day in culture. Cells in each dish were incubated in serum-free medium for 2 h and then labeled with 100 μ Ci of ATB-[2- 3 H]BMPA in 250 μ l of KRH buffer at 18 °C either in the absence, *B(sur)*, or presence, *B(tot)*, of 0.025% digitonin. Labeled cells from the two dishes were then immediately solubilized in $C_{12}E_9$ detergent buffer, and labeled proteins were subjected to immunoprecipitation with GLUT1 C-terminal peptide antiserum followed by electrophoresis. Results are the mean and S.E. from four experiments. In *b*, 3T3-L1 fibroblasts were maintained in culture for 11 days and at confluence reached a density of 0.28×10^6 cells/35-mm dish. The cells were incubated for 2 h in serum-free medium and then maintained at 37 °C for 30 min either without (*B*) or with (*I*) 100 nM insulin in 1 ml of KRH buffer. Cells were then labeled with 100 μ Ci of ATB-[2- 3 H]BMPA in 250 μ l of KRH buffer at 18 °C either in the absence (*sur*) or presence (*tot*) of 0.025% digitonin, and GLUT1 immunoprecipitated as described in the Fig. 2 legend. Results are the mean and S.E. of three experiments.

creased to 0.6×10^6 cells/dish. During the differentiation, the amount of protein per 35-mm dish increased enormously from 88 μ g/dish to 1.1 mg/dish. The insulin-stimulated rate of transport was approximately double the basal rate for about 4 days after the initiation of differentiation. By 6 days, there was a very marked increase in the insulin-stimulated rate of transport to reach by 11 days, a rate which was ≈ 20 times the basal rate.

Fig. 7a shows the distribution of GLUT1 throughout this differentiation period. During the first 4 days, the cells behaved in a manner similar to that observed in confluent fibroblasts. The basal level of labeling was approximately 2.5-

fold lower than the insulin-stimulated level. The total cellular levels were approximately double the level found at the cell surface in the insulin-stimulated state. Between 6 and 11 days, there was a marked rise in the total cellular GLUT1. The cell surface GLUT1 in the basal cells rose slightly throughout this period, and this may have been a consequence of the increased cellular level of this transporter. The GLUT4 was produced in parallel with the rise in GLUT1 (Fig. 7b). Thus, there was little detectable GLUT4 over the first 2 days of differentiation and then this rose steeply between days 6 and 11.

In contrast with the rise in the basal level of labeled GLUT1, labeling showed that the GLUT4 that was newly synthesized was very effectively sequestered inside the cell. The basal GLUT4 labeling remained consistently low from days 4–11 after the initiation of differentiation while the total cellular GLUT4 rose by >10 -fold over this period.

DISCUSSION

The sequestration of glucose transporters in an intracellular pool is likely to be a general mechanism by which cells regulate the supply of glucose to metabolic enzymes in line with the growth demands and cellular metabolism requirements of the cell. The phenomenon of intracellular transporter sequestration was first demonstrated in insulin-sensitive rat adipose cells by Cushman and Wardzala (1980) and Suzuki and Kono (1980) and has subsequently been found in other insulin-responsive tissues such as brown adipose tissue (Slot *et al.*, 1991a), heart muscle (Watanabe *et al.*, 1984; Slot *et al.*, 1991b), diaphragm muscle (Wardzala and Jeanrenaud, 1983), and skeletal muscle (Klip *et al.*, 1987; Hirshman *et al.*, 1990; Klip *et al.*, 1990). In addition, it has been shown that virus infection of BHK cells (Widnell *et al.*, 1990) leads to a redistribution of internalized GLUT1 transporters to the cell surface. Widnell *et al.* (1990) have also shown that in BHK cells the sequestered GLUT1 transporters redistribute to the cell surface in response to stress stimuli such as arsenite and heat shock. Haspel *et al.*, 1986 have shown that in fibroblasts GLUT1 redistribution can occur in response to glucose starvation. Although the cellular redistributions of glucose transporters can be followed by subcellular fractionation and separation of plasma membrane from the light microsome membranes, this is not a technique that can be applied readily to cells and tissues that are difficult to successfully homogenize and fractionate such as skeletal muscle (Klip *et al.*, 1987) and cultured cells (Calderhead *et al.*, 1990). Immunochemical tech-

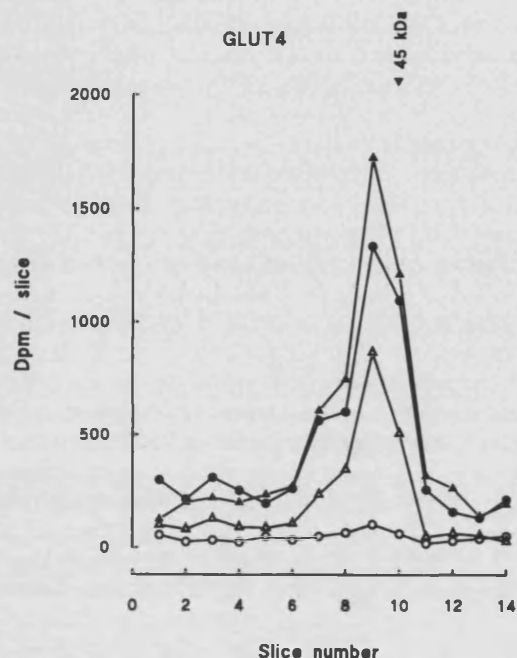


FIG. 4. ATB-BMPA labeling of cell surface and total cellular pools of GLUT4 in 3T3-L1 adipocytes. Fully differentiated 3T3-L1 adipocytes in 35-mm dishes were incubated in serum-free medium for 2 h and were then maintained at 37 °C for 30 min either in the absence (circles) or presence (triangles) of 100 nM insulin in 1 ml of KRH buffer. Cells were then labeled with 100 μ Ci of ATB-[2- 3 H]BMPA in 250 μ l of KRH buffer at 18 °C either without (open symbols) or with (closed symbols) 0.025% digitonin. Cells were then washed twice in KRH buffer and then solubilized in $C_{12}E_9$ detergent buffer, and the labeled proteins were subjected to immunoprecipitation with GLUT4 C-terminal peptide antiserum and then analyzed by electrophoresis.

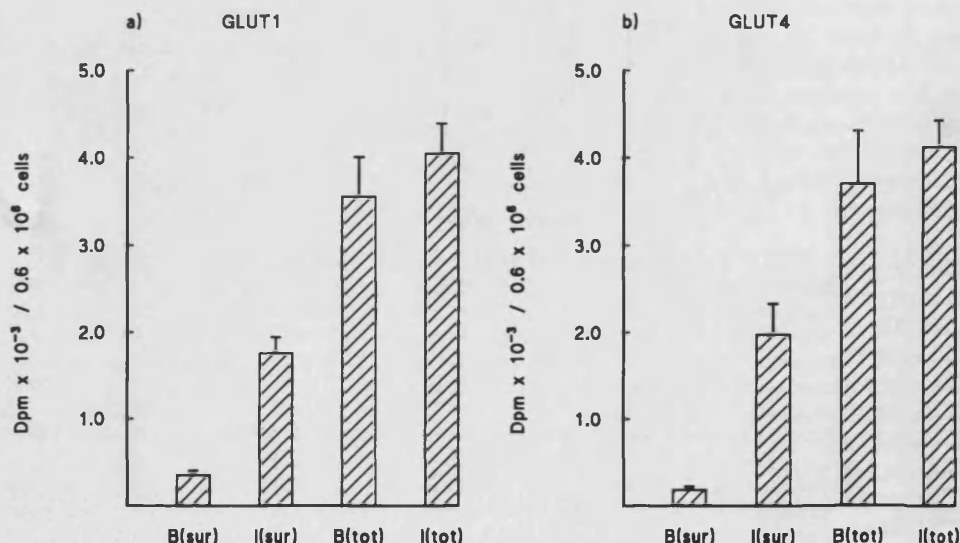


FIG. 5. GLUT1 and GLUT4 cellular distribution in 3T3-L1 adipocytes. Cells were fully differentiated in 35-mm dishes and then subjected to the labeling procedure described in the Fig. 4 legend. The total disintegrations/min under the gel peaks were calculated for GLUT1 (a) and GLUT4 (b) either without or with 0.025% digitonin to obtain cell surface (sur) or total cellular (tot) levels of labeling for basal cells (B) or cells treated with 100 nM insulin (I). The results are the mean and S.E. from seven experiments.

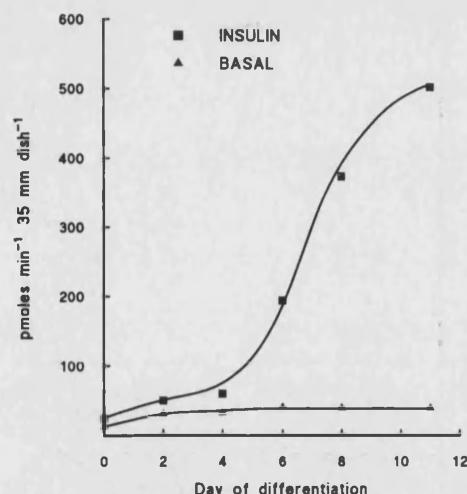


FIG. 6. Time course for differentiation of highly insulin-responsive glucose transport in 3T3-L1 cells. Confluent 3T3-L1 cells in 35-mm dishes were treated with dexamethasone, isobutylmethylxanthine, and insulin in DMEM with 10% fetal bovine serum to initiate differentiation. On the indicated days, cells were incubated in serum-free medium for 2 h and then maintained at 37 °C for 30 min in the absence (\blacktriangle) or presence (\blacksquare) of 100 nM insulin in 1 ml of KRH buffer. This was followed by determination of the rate of uptake of 50 μ M 2-deoxy-D-[2,6- 3 H]glucose. Results are the mean of two experiments.

niques (Blok *et al.*, 1988; Slot *et al.*, 1991a, 1991b; Smith *et al.*, 1991; Widnell *et al.*, 1990; Tordjman *et al.*, 1990) circumvent the need to obtain subcellular membrane fractions, but these methods are not easily adaptable to investigations of the kinetics of transporter regulation.

As an alternative to these methods, we have extended the use of our impermeant photolabel ATB-BMPA to measure both the cell surface and total cellular levels of transporters. We have shown here that the method when applied to differentiated 3T3-L1 adipocytes gives results which are consistent with those obtained by Gould *et al.* (1989a) who used Western blotting of isolated membrane fractions to determine that about one-half of the cell GLUT1 was at the cell surface in the insulin-stimulated state. The new method has also been used successfully to measure the distribution of GLUT1 in BHK cells² and in CHO cells transfected with the GLUT1 gene.³

Here we have extended the use of this method to investigate at what stage during growth and differentiation of 3T3-L1 cells the transporter sequestration develops. We initially assumed that the cellular mechanisms necessary for transporter sequestration were most likely to develop during the period of differentiation from fibroblasts to adipocytes. We were surprised to find that GLUT1 transporters were down-regulated from the cell surface as the cells reached confluence as fibroblasts. The sequestration mechanisms seem capable of internalizing over 75% of the total GLUT1 transporter both in confluent fibroblasts and in differentiated adipocytes. At both these stages, insulin produced a redistribution of about one-half of the available GLUT1 to the cell surface. Additional sequestration capability may have also developed as additional GLUT1 transporters were synthesized during differentiation. Alternatively, there may have been spare capacity available in fibroblasts that could potentially sequester any new GLUT1 or GLUT4 that was introduced into fibro-

blasts or produced in subsequent differentiation. Gould *et al.* (1989b) have shown that 3T3-L1 cells transfected with human GLUT1, that \approx 50% of both the transfected and endogenous murine GLUT1 were sequestered in intracellular membranes, and that both human GLUT1 and endogenous GLUT1 responded equally to insulin stimulation of translocation.

Other investigators have shown that there is either no change in the basal transport activity throughout differentiation (Kaestner *et al.*, 1989) or that basal activity falls in the first few days after the initiation of differentiation (Weiland *et al.*, 1990; Harrison *et al.*, 1990). Our results show that basal activity can fall markedly if cells are maintained at full confluence for several days without the initiation of differentiation. Thus, the studies cited above can be reconciled if there is a variable time after confluence was reached and before the differentiation regime was initiated. Thus, if the initiation program was started earlier than in our experiments, the basal rate would have fallen during the first few days of differentiation. However, our results suggest that the increase in transporter sequestration and the fall in the transport activity is not a direct consequence of the differentiation regime but develops because cells are in a growth-arrested phase of the cell cycle.

Harrison *et al.* (1990, 1991a, 1991b) and Clancy *et al.* (1991) have recently described evidence that the intrinsic activity of glucose transporters in 3T3-L1 cells and particularly that of GLUT1 is suppressed during differentiation. Their evidence is based on an apparent higher insulin-stimulated glucose transport activity in fibroblasts where GLUT1 is present, compared with differentiated 3T3-L1 cells where both GLUT1 and GLUT4 are present. Our results, and those of other investigators (Kaestner *et al.*, 1989; Garcia de Herreros and Birnbaum, 1989; Weiland *et al.*, 1990), show, however, that insulin-stimulated transport activity in adipocytes is much higher than in fibroblasts. In addition, however, Harrison *et al.* (1990, 1991a, 1991b) argue that as the binding of their exofacial GLUT1 antibody, the δ -antibody, is increased 2.6-fold in adipocytes in the basal state compared with fibroblasts while the transport activity is reduced by \approx 2.5-fold, the GLUT1 intrinsic activity is suppressed by 90%. They suggest that inactivation is due to interaction with an inhibitory protein (Harrison *et al.*, 1991b; Clancy *et al.*, 1991). Our results also show a discrepancy between transport activity and labeled transporter level in comparing fibroblasts with differentiated adipocytes in the basal state but suggest that the discrepancy is smaller than the 90% (10-fold) discrepancy calculated by Harrison *et al.*, 1990. The ratio of transport activity to GLUT1 labeling in fibroblasts can be calculated as 130 pmol/10⁶ cells/min divided by GLUT1 labeling of 970 dpm/10⁶ cells or 0.044 pmol/10⁶ cells (the specific activity is 10 Ci/mmol). This intrinsic activity ratio is 41 pmol/10⁶ cells/min divided by GLUT1 labeling of 590 dpm/10⁶ cells or 0.026 pmol/10⁶ cells in differentiated cells. Thus, during the transition from preconfluent fibroblasts to differentiated adipocytes, the intrinsic activity ratio falls from 2954 min⁻¹ in fibroblasts to 1576 min⁻¹ in adipocytes in the basal state. Any GLUT4 present at the surface of basal adipocytes would lower this ratio. Thus these results suggest that the activity of GLUT1 and probably GLUT4 is suppressed by 40–50% or by 1.5–2-fold and are consistent with estimates of the intrinsic activity of GLUT1 and GLUT4 previously reported for the basal state (Holman *et al.*, 1990; Kozka *et al.*, 1991; Clark *et al.*, 1991; Palfreyman *et al.*, 1992).

Harrison *et al.* (1991b) have suggested that the exofacial probe that we have used may react only with transporters that are catalytically active. They suggest that in basal cells

² C. A. Pasternak, I. J. Kozka, A. E. Clark, and G. D. Holman, unpublished results.

³ A. E. Clark, M. Hashiramoto, T. Kadowaki, G. D. Holman, and M. Kasuga, unpublished results.

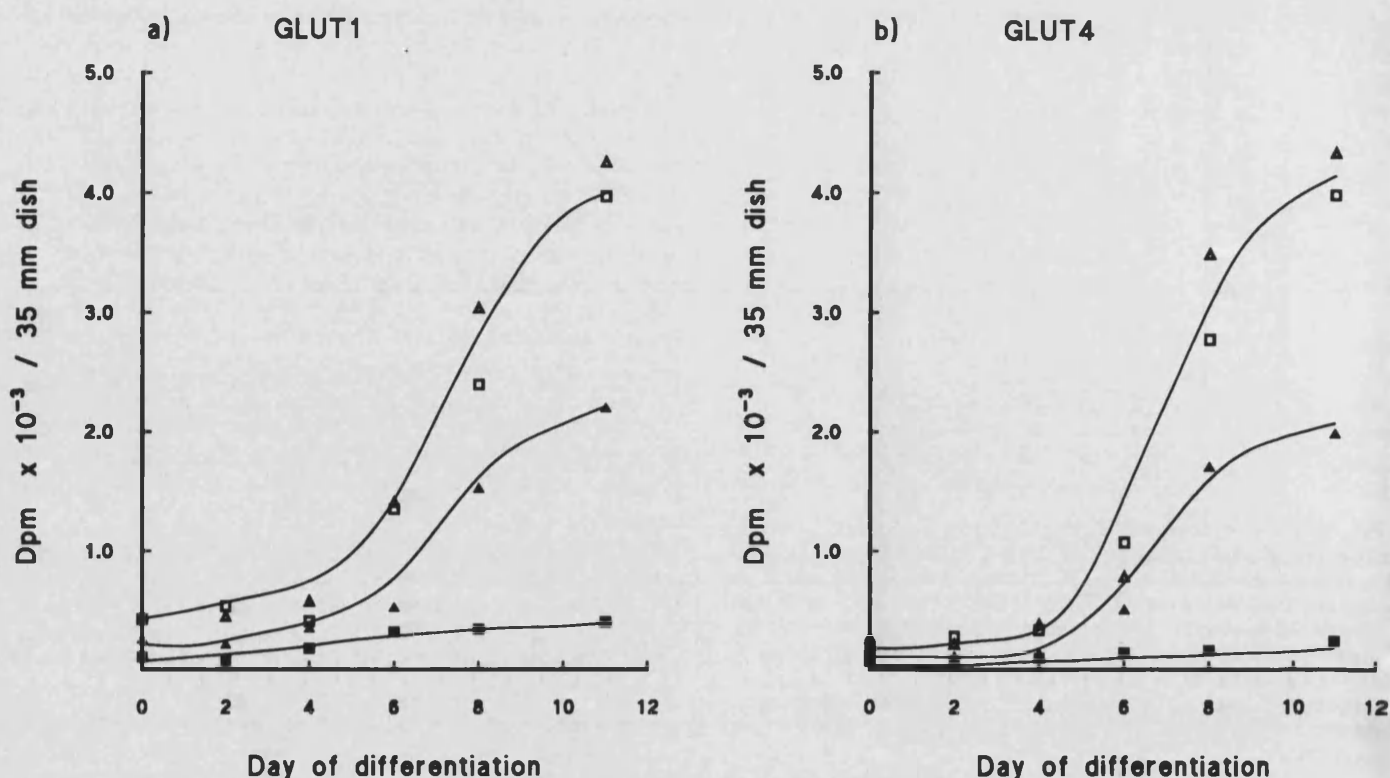


FIG. 7. Time course for the increase in cell surface and total cellular pools of GLUT1 and GLUT4 in 3T3-L1 cells. Cells in 35-mm dishes were treated with dexamethasone, isobutylmethylxanthine, and insulin in DMEM with 10% fetal bovine serum to initiate differentiation. On the indicated days, cells were incubated in serum-free medium for 2 h and were then maintained at 37 °C for 30 min either in the absence (squares) or presence (triangles) of 100 nM insulin in 1 ml of KRH buffer. In GLUT1 (a) and GLUT4 (b), distribution was determined by labeling with 100 μ Ci (closed symbols) or total cellular levels in cells permeabilized with 0.025% digitonin (open symbols). Cells were washed twice in KRH buffer and then solubilized in $C_{12}E_9$ detergent buffer except Day 0 cells which were immediately solubilized in detergent buffer. The isoforms were then immunoprecipitated with anti-C-terminal peptide antibodies and analyzed by electrophoresis to obtain the total disintegrations/min under the gel peaks. Results are the mean from two experiments.

a pool of transporters exists which has suppressed activity due to an inactivating modifier protein. However, several studies using the photolabel (as cited above) have shown an ≈ 2 -fold discrepancy between photolabeling and transport and have shown a lag between the appearance of transporters that can be photolabeled and the increase in transport activity following insulin stimulation of rat adipose cells (Clark *et al.*, 1991; Satoh *et al.*, 1991) and 3T3-L1 cells (Yang *et al.*, 1992). These studies show that ATB-BMPA binds to transporters that are inactive in transport catalysis. We have suggested that it is this form of the transporter that may be associated with modifier proteins such as those involved in trafficking events in the normal translocation pathway (Yang *et al.*, 1992). In addition we have suggested that where there is a further discrepancy between transporters that are detected by labeling compared with Western blotting, as in isoproterenol-treated insulin-stimulated rat adipocytes⁴ and phenylarsine oxide-treated insulin-stimulated 3T3-L1 cells (Yang *et al.*, 1992), that this is due to the formation of plasma membrane-associated but occluded vesicles. Thus, we, to some extent concur, with the hypothesis described by Harrison *et al.* (1990, 1991a, 1991b), but suggest that the transport-inactive form at the plasma membrane is a relatively small fraction of the total plasma membrane pool, that these forms represent intermediates in normal transporter trafficking and that translocation is the major mechanism by which glucose transport is stimulated in insulin-sensitive cells.

Our experiments in which we have used digitonin suggest that the photolabel interacts with equal amounts of transporter in the basal and insulin-stimulated states and that this provides additional evidence, to that previously described (Calderhead *et al.*, 1990; Holman *et al.*, 1990), which suggests that basal and insulin-stimulated transporters do not have differing affinities for the photolabel. If an inhibitory protein were present in basal cells which produced a large increase in the proportion of transporters in a catalytically inactive state, then this association would be expected to reduce the apparent labeling of the total cellular transporter pool of basal cells. Thus, these experiments in which cells are digitonin-permeabilized also suggest that the proportion of transporters with suppressed activity is small and that the low surface levels of transporters detected by labeling of cells in the basal state is due to transporter sequestration within the intracellular pool.

During the process of 3T3-L1 cell differentiation, over 95% of the total cellular GLUT4 in the intracellular pool was sequestered. This is similar to the level of sequestration of GLUT4 seen in other insulin-responsive tissues (Slat *et al.*, 1991a, 1991b). The greater sequestration of GLUT4 may be related to the targeting of this isoform to separate intracellular vesicles (Zorzano *et al.*, 1989), although Calderhead *et al.*, 1990, have reported that GLUT1 and GLUT4 were detected in the same vesicles. It seems likely that the two isoforms leave the cell surface by the same endocytosis route as we have shown that both isoforms are endocytosed with the same half-time when insulin is removed. This has been observed in rat adipocytes (Clark *et al.*, 1991) and in 3T3-L1 cells (Yang

⁴ S. J. Vannucci, H. Nishimura, S. Satoh, S. W. Cushman, G. D. Holman, and I. A. Simpson, unpublished results.

et al., 1992). However, we have observed that, in insulin-stimulated 3T3-L1 cells which are treated with the vicinal dithiol inactivating reagent phenylarsine oxide, there may be some separation of the transporter vesicle processing as GLUT4 re-exocytosis appeared to be blocked by this reagent, but GLUT1 re-exocytosis was not (Yang *et al.*, 1992). Cellular mechanisms for the separate localization and processing of GLUT4 must be very dependent on the GLUT4 protein structure as GLUT4 transfected into expression systems tends to become localized inside the cell rather than at the plasma membrane (Gould *et al.*, 1991).

The studies on the use of the photolabel in permeabilized 3T3-L1 cells that we have described here have shown that transporter sequestration can occur before differentiation is initiated and that transporters produced in differentiation probably enter a preformed sequestration process. Further studies will be required to determine whether growth arrest alone is sufficient to induce transporter sequestration or whether cell confluence and cell-cell contact phenomena result in morphological changes in the cell membrane system responsible for down-regulation of transporters and transport activity.

Acknowledgment—We thank Professor H. G. Joost for sending us a copy of his manuscript (Weiland *et al.*, 1990) prior to publication.

REFERENCES

- Blok, J., Gibbs, E. M., Lienhard, G. E., Slot, J. W., and Geuze, H. J. (1988) *J. Cell Biol.* **106**, 69–76
- Calderhead, D. M., Kitagawa, W., Tanner, L. I., Holman, G. D., and Lienhard, G. E. (1990) *J. Biol. Chem.* **265**, 13800–13808
- Clark, A. E., and Holman, G. D. (1990) *Biochem. J.* **269**, 615–622
- Clark, A. E., Kozka, I. J., and Holman, G. D. (1991) *Biochem. J.* **278**, 235–241
- Clancy, B. M., Harrison, S. A., Buxton, J. M., and Czech, M. P. (1991) *J. Biol. Chem.* **266**, 10122–10130
- Cushman, S. W., and Wardzala, L. J. (1980) *J. Biol. Chem.* **255**, 4758–4762
- Frost, S. C., and Lane, M. D. (1985) *J. Biol. Chem.* **260**, 2646–2652
- Garcia de Herreros, A., and Birnbaum, M. J. (1989) *J. Biol. Chem.* **264**, 19994–19999
- Gould, G. W., Lienhard, G. E., Tanner, L. I., and Gibbs, E. M. (1989a) *Arch. Biochem. Biophys.* **268**, 264–275
- Gould, G. W., Derechin, V., James, D. E., Tordjman, K., Ahern, S., Gibbs, E. M., Lienhard, G. E., and Mueckler, M. (1989b) *J. Biol. Chem.* **264**, 2180–2184
- Gould, G. W., Thomas, H. M., Jess, T. T., and Bell, G. I. (1991) *Biochemistry* **30**, 5139–5145
- Green, H., and Kehinde, O. (1975) *Cell* **5**, 19–27
- Harrison, S. A., Buxton, J. M., Clancy, B. M., and Czech, M. P. (1990) *J. Biol. Chem.* **265**, 20106–20116
- Harrison, S. A., Buxton, J. M., and Czech, M. P. (1991a) *Proc. Natl. Acad. Sci. U. S. A.* **88**, 7839–7843
- Harrison, S. A., Buxton, J. M., Clancy, B. M., and Czech, M. P. (1991b) *J. Biol. Chem.* **266**, 19438–19449
- Haspel, H. C., Wilk, E. W., Birnbaum, M. J., Cushman, S. W., and Rosen, O. M. (1986) *J. Biol. Chem.* **261**, 6778–6789
- Hirshman, M. F., Goodyear, L. J., Wardzala, L. J., Horton, E. D., and Horton, E. S. (1990) *J. Biol. Chem.* **265**, 987–991
- Holman, G. D., Kozka, I. J., Clark, A. E., Flower, C. J., Saltis, J., Habberfield, A. D., Simpson, I. A., and Cushman, S. W. (1990) *J. Biol. Chem.* **265**, 18172–18179
- Kaestner, K. H., Christy, R. J., McLenithan, J. C., Braiterman, L. T., Cornelius, P., Pekela, P. H., and Lane, D. M. (1989) *Proc. Natl. Acad. Sci. U. S. A.* **86**, 3150–3154
- Klip, A., Rampall, T., Young, D., and Holloszy, J. O. (1987) *FEBS. Lett.* **224**, 224–230
- Klip, A., Rampall, T., Bilan, P. J., Cartee, G. D., Gulve, E. A., and Holloszy, J. O. (1990) *Biochem. Biophys. Res. Commun.* **172**, 728–736
- Kozka, I. J., Clark, A. E., and Holman, G. D. (1991) *J. Biol. Chem.* **266**, 11726–11731
- Palfreyman, R. W., Clark, A. E., Denton, R. M., Holman, G. D., and Kozka, I. J. (1992) *Biochem. J.*, in press
- Reed, B. C., Shade, D., Alperovich, F., and Vang, M. (1990) *Arch. Biochem. Biophys.* **279**, 261–274
- Satoh, S., Gonzalez-Mulero, O. M., Clark, A. E., Kozka, I. J., Holman, G. D., and Cushman, S. W. (1991) *Diabetes* **40** (Suppl. 1), 85A
- Simpson, I. A., Yver, D. R., Hissin, P. J., Wardzala, L. J., Karnieli, E., Salans, L. B., and Cushman, S. W. (1983) *Biochim. Biophys. Acta* **763**, 393–407
- Slot, J. W., Geuze, H., Gigengack, S., Lienhard, G. E., and James, E. (1991a) *J. Cell Biol.* **113**, 123–135
- Slot, J. W., Geuze, H., Gigengack, S., James, D. E., and Lienhard, G. E. (1991b) *Proc. Natl. Acad. Sci. U. S. A.* **88**, 7815–7819
- Smith, R. M., Charron, M. J., Shah, N., Lodish, H. F., and Jarett, L. (1991) *Proc. Natl. Acad. Sci. U. S. A.* **88**, 6893–6897
- Suzuki, K., and Kono, T. (1980) *Proc. Natl. Acad. Sci. U. S. A.* **77**, 2542–2545
- Tordjman, K. M., Liengang, K. A., and Mueckler, M. (1990) *Biochem. J.* **271**, 201–207
- Wardzala, L. J., and Jeanrenaud, B. (1983) *Biochim. Biophys. Acta* **730**, 49–56
- Watanabe, T., Smith, M. M., Robinson, F. W., and Kono, T. (1984) *J. Biol. Chem.* **259**, 13117–13122
- Weiland, M., Schurmann, A., Schmidt, W. E., and Joost, H. G. (1990) *Biochem. J.* **270**, 331–336
- Widnell, C. C., Baldwin, S. A., Davies, A., Martin, S., and Pasternak, C. A. (1990) *FASEB J.* **4**, 1634–1637
- Yang, J., Clark, A. E., Harrison, R., Kozka, I. J., and Holman, G. D. (1992) *Biochem. J.* **281**, 809–817
- Zorzano, A., Wilkinson, W., Kotiar, G., Thodis, G., Wadzinski, B. E., Ruoho, A. E., and Pilch, P. F. (1989) *J. Biol. Chem.* **264**, 12358–12363

Fetal bovine serum was from Gibco Laboratories. Dexamethasone, isobutylmethylxanthine, and protein A-Sepharose were from Sigma. Nonaethyleneglycol dodecyl ether ($C_{12}E_9$) was from Boehringer. Monocomponent porcine insulin was a gift from Dr. Ronald Chance, Eli Lilly Laboratories. Polyclonal antisera were raised against the C-terminal peptides of GLUT4 (CSTELEYGPDEND) and GLUT1 (CGEELFHPLGADSQV) as described (22, 23).

Cell Culture—3T3-L1 fibroblasts were differentiated to adipocytes as described (20). Fully differentiated cells were washed with phosphate-buffered saline (154 mM NaCl, 12.5 mM sodium phosphate, pH 7.4) and were then incubated for 2 h in serum-free medium containing 25 mM D-glucose. This was followed by three washes in Krebs-Ringer-Hepes buffer (KRH buffer, 136 mM NaCl, 4.7 mM KCl, 1.25 mM $CaCl_2$, 1.25 mM $MgSO_4$, 10 mM Hepes, pH 7.4).

ATB-BMPA Photolabeling—Cells in 35-mm dishes were maintained at 37 °C either in the absence or the presence of 100 nM insulin in 1 ml of KRH buffer for 30 min. The buffer was removed and replaced by 350 μ l of KRH buffer, either with or without insulin respectively, containing 250 μ Ci (insulin samples) or 500 μ Ci (basal samples) of ATB-[2- 3 H]BMPA at 18 °C. The dishes were placed between two 2-mm glass plates and were irradiated for 1 min in a Rayonet photochemical reactor equipped with eight 300-nm bulbs and eight 350-nm bulbs. The irradiated cells were then either washed rapidly and immediately homogenized in Tris-EDTA-sucrose (TES buffer, 10 mM Tris-HCl, 0.5 mM EDTA, 255 mM sucrose at 18 °C) or were maintained at 37 °C in 1 ml of KRH buffer containing 10 mM D-glucose for the times indicated in the figure legends before washing and homogenization. For each time point the combined material from two 35-mm dishes was pooled.

Immunoprecipitation and Electrophoresis—The 3T3-L1 cells were vigorously homogenized to ensure all cell material was broken. This was carried out in 2 ml of TES buffer, using a tightly fitting Teflon homogenizer operating at 1500 rpm and with 15 full strokes. Samples were then centrifuged at $12,500 \times g_{max}$ for 20 min. The crude plasma membrane and post-plasma membrane supernatants were then solubilized in 1.5 ml of detergent buffer containing 2% $C_{12}E_9$, 5 mM sodium phosphate, pH 7.2, and with the proteinase inhibitors antipain, aprotinin, pepstatin, and leupeptin, each at 1 μ g/ml (24). Any non-solubilized material was then removed by centrifugation at $20,000 \times g_{max}$ for 20 min. Antisera (50 μ l of anti-GLUT4 and 100 μ l of anti-GLUT1) were premixed with 30 μ l of swollen protein A-Sepharose, washed in phosphate-buffered saline, and then mixed with the solubilized membranes for 2 h at 0–4 °C. The immunoprecipitates were washed four times (insulin) or five times (basal) in 0.1% then once in 0.01% $C_{12}E_9$ detergent buffer. The extent of washing of the immunoprecipitates was more extensive than previously reported (24) because of the low counts recovered in basal cells. The labeled glucose transporters were released from the antibody complexes with 10% SDS, 6 M urea, 10% mercaptoethanol and subjected to electrophoresis on 10% acrylamide gels. The radioactivity in gel slices was extracted with hydrogen peroxide as described (24). For the insulin-treated samples the background was determined by estimating the radioactivity of slices on either side of the transporter peak. The background radioactivity in basal samples was determined by immunoprecipitating with preimmune serum and then running this material on the same gel as the other basal samples. The preimmune serum did not produce a peak of radioactivity but allowed a correction of background from slices, which exactly corresponded to the position of the transporter peak.

Estimation of Rate Constants—The glucose transporter levels as determined from electrophoresis (above) were used to calculate the fractional loss of plasma membrane label. These data were then fitted to an integrated rate equation, describing transporter recycling, by least squares analysis (weighted for relative error) using Fig P software (Biosoft).

RESULTS

We have used the impermeant glucose transporter photolabel, ATB-BMPA, to tracer-tag cell surface GLUT4 and GLUT1 in 3T3-L1 cells. We have then followed the removal of these transporters from the plasma membrane of cells maintained in either basal or insulin-stimulated states. The maintenance of a steady state of non-labeled transporter distribution was confirmed by comparing the amounts of immunodetectable GLUT4 and GLUT1 at the initial labeling time and following an additional 40 min of incubation at

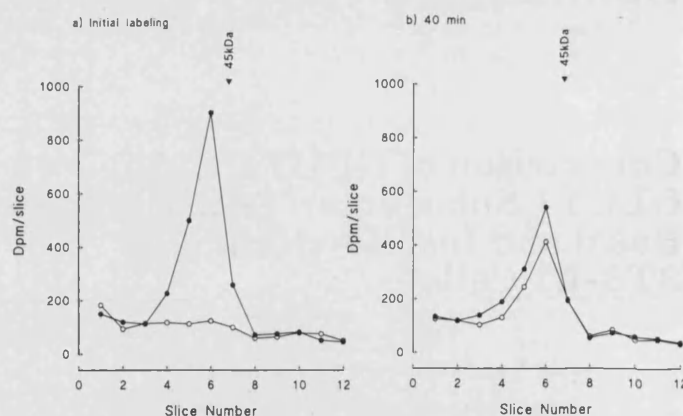


FIG. 1. Equilibration of tracer-tagged GLUT4 with the intracellular membrane pool in 3T3-L1 cells. Confluent 3T3-L1 cells (two 35-mm dishes) were stimulated for 30 min with 100 nM insulin and then labeled with 250 μ Ci of ATB-[2- 3 H]BMPA. Following labeling, the dishes were either homogenized immediately (a) or were maintained at 37 °C in the continuous presence of insulin for another 40 min and then homogenized (b). GLUT4 was immunoprecipitated from either the plasma membrane (●) or the post plasma membrane supernatant (low density microsomes) (○) and then analyzed by electrophoresis.

37 °C.³ Fig. 1a shows an SDS-polyacrylamide gel electrophoresis profile obtained by labeling and immunoprecipitating GLUT4 in insulin-treated 3T3-L1 cells. The label recovered in the post-plasma membrane fraction of cells that were homogenized immediately was very low. This suggests that tracer-tagged GLUT4 was not significantly transferred to the low density microsomes during the processing period. Our results contrast with those of Jhun *et al.* (17), who have reported that in rat adipose cells approximately one-third of the labeled GLUT4 was recovered in the post plasma membrane fraction in samples which were processed immediately after labeling.

Following 40 min of incubation of the cells at 37 °C, the label in the plasma membrane was reduced to approximately one-half its initial value. The label that was lost from the plasma membrane was recovered in the low density microsome fraction (Fig. 1b). We have not routinely analyzed the material transferred to the low density microsome fraction because of the need to simultaneously process multiple immunoprecipitated samples obtained for estimating GLUT4 and GLUT1 in the plasma membrane. Previous studies have demonstrated that constitutive turnover of transporters occurs (23, 24)¹ and that label which is lost from the plasma membrane is recovered in the low density microsome fraction.

In basal cells the labeling of GLUT4 and GLUT1 was low (Fig. 2, a and b), and following 40 min of incubation of the labeled cells at 37 °C, the level of tracer-tagged transporters in the plasma membrane were reduced toward background levels.

We have used least squares curve fitting to directly estimate exocytosis and endocytosis rate constants from time courses of loss of tracer-tagged GLUT4 and GLUT1 from the plasma membrane (Fig. 3, a and b). For analytical purposes the rate of loss of label from the plasma membrane is assumed to be dependent on just two rate constants; one describing the exocytosis (k_{ex}) and one the endocytosis (k_{en}). The rate of loss of labeled transporters is then given by Equation 1, where L_p is the fraction of the label in the plasma membrane.

$$\frac{dL_p}{dt} = k_{ex}(1 - L_p) - k_{en} \cdot L_p \quad (\text{Eq. 1})$$

³ J. Yang and G. D. Holman, unpublished results.

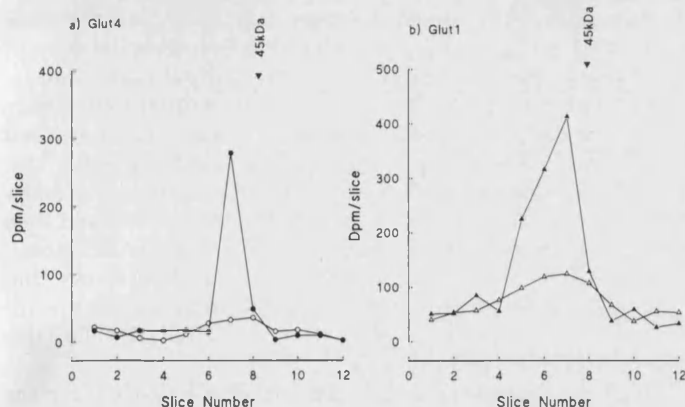


FIG. 2. Equilibration of tracer-tagged GLUT4 and GLUT1 in basal 3T3-L1 cells. Confluent 3T3-L1 cells (two 35-mm dishes) were labeled in the basal state with 500 μ Ci of ATB-[2- 3 H]BMPA. Following labeling the dishes were either homogenized immediately (\bullet , \blacktriangle) or were maintained at 37 $^{\circ}$ C for another 40 min and then homogenized (\circ , \triangle). GLUT4 (a) and GLUT1 (b) were then immunoprecipitated from the plasma membrane fractions and analyzed by electrophoresis.

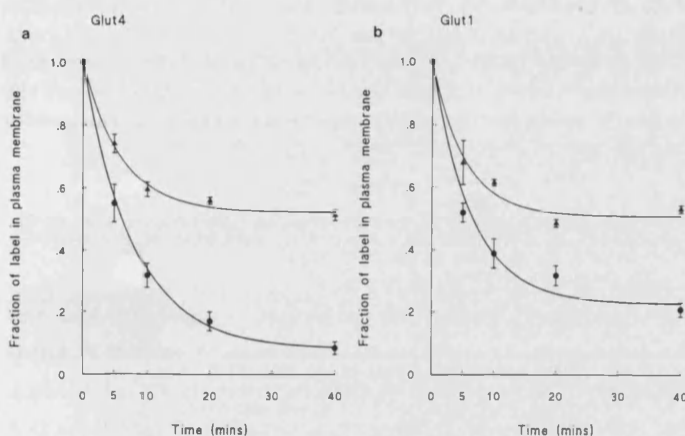


FIG. 3. Time courses for equilibration of tracer-tagged GLUT4 and GLUT1 in 3T3-L1 cells. Confluent 3T3-L1 cells were labeled either in the basal (\bullet) or insulin-stimulated (\blacktriangle) states and were then maintained in these steady states for the indicated times before homogenization to obtain the plasma membrane fraction. GLUT4 (a) and GLUT1 (b) were then immunoprecipitated and analyzed by electrophoresis. The lines through the data were derived from least squares fitting to Equation 2. (see "Results"). The results are the mean \pm S.E. from three separate experiments, except in the case of GLUT4 in basal cells, where the data are from four experiments.

Integration of Equation 1 with $L_p = 1.0$ at $t = 0$ gives Equation 2.

$$L_p = \frac{k_{ex} + k_{en} \exp(-t(k_{ex} + k_{en}))}{(k_{ex} + k_{en})} \quad (\text{Eq. 2})$$

In the experiments described here we have used this equation to analyze the redistribution of label under steady-state conditions, but Equation 2 is equally applicable to an analysis of label equilibration under non-steady-state conditions. All that is required is that the total pool of transporters be conserved. It is only necessary to consider the concentration of unlabeled transporters if there are saturation steps in the flux pathway, as would be the case if one were analyzing equilibrium exchange by a carrier protein.

In the continuous presence of insulin both tracer-tagged GLUT4 and GLUT1 were rapidly removed from the plasma membrane. The values of k_{ex} and k_{en} derived from the mean results of three separate experiments are shown in Table I.

TABLE I

Kinetic parameters for glucose transporter trafficking in 3T3-L1 cells

Kinetic parameters were calculated from the mean data shown in Fig. 3. These data were from three separate experiments (Insulin) and three separate experiments (Basal) except in the case of GLUT4 in basal cells where the results were from four separate experiments. The data were fitted to Equation 2 using least squares analysis (weighted for relative error).

	k_{ex} min^{-1}	k_{en} min^{-1}	$t_{1/2}$ min
Basal			
GLUT4	0.010 ± 0.001	0.116 ± 0.006	5.6 ± 0.3
GLUT1	0.035 ± 0.009	0.121 ± 0.020	4.4 ± 0.6
Insulin			
GLUT4	0.086 ± 0.011	0.080 ± 0.007	4.2 ± 0.3
GLUT1	0.096 ± 0.023	0.093 ± 0.017	3.7 ± 0.6

The estimated rate constants were similar for both GLUT1 and GLUT4. In addition, the end points of the equilibration of the tracer-tagged transporters were not significantly different. At 40 min the levels of tracer-tagged GLUT4 and GLUT1 remaining in the plasma membrane were $51.1 \pm 1.7\%$ ($n = 3$) and $53 \pm 1.2\%$ ($n = 3$), respectively, of the initial values. The maintenance of the insulin steady-state in which approximately one-half of the total transporter pool is at the surface (24) thus occurs because the exocytosis of transporters (dependent on k_{ex}) matches an equal rate of endocytosis (dependent on k_{en}).

In the basal state tracer-tagged GLUT4 was more extensively removed from the plasma membrane than in the insulin-stimulated state. At 40 min the fraction of the tracer-tagged GLUT4 remaining in the plasma membrane was only $8.4 \pm 2.0\%$ ($n = 4$) of the initial value. By contrast, the fraction of the tracer-tagged GLUT1 remaining in the plasma membrane was $20.8 \pm 1.3\%$ ($n = 3$) of the initial value. Analysis of the time course of tracer-tagged GLUT4 and GLUT1 redistribution (Table I) showed that the endocytosis rate constants were only $\approx 30\%$ slower in the insulin-stimulated compared with the basal state. However, the GLUT4 and GLUT1 exocytosis rate constants were 8.6 and 3 times higher, respectively, in the insulin-stimulated compared with the basal state (Table I).

Although we have used curve fitting to directly obtain the rate constants k_{ex} and k_{en} , the half-time for label equilibration can also be easily calculated from least squares curve fitting using Equation 2. The half-time is only dependent on the exponential term, as shown by the following equation.

$$t_{1/2} = \ln 2 / (k_{ex} + k_{en}) \quad (\text{Eq. 3})$$

The values for the half-times for equilibration of tracer-tagged transporter were therefore calculated from summing the rate constants k_{ex} and k_{en} as in Equation 3 and are shown in Table I. The half-times for GLUT4 and GLUT1 equilibration in basal cells were 5.6 and 4.4 min, respectively. These values are similar to, but slightly faster than, the half-times (6.5 min) for the decrease in glucose transport activity in 3T3-L1 cells following removal of insulin (24). The calculated half-times for loss of tracer-tagged transporters in the continuous presence of insulin were slightly faster than in its absence because of the greater contribution of the re-exocytosis, the k_{ex} term in Equation 3, to the equilibration rate.

DISCUSSION

Use of bis-hexoses with photoreactive substituents (17, 23)¹ has shown that GLUT4 constitutively recycles between the plasma membrane and the intracellular vesicle pool of rat adipose cells, and we have also demonstrated this phenome-

non in 3T3-L1 cells (Ref. 24 and this study). In the continuous presence of insulin, the GLUT4 and GLUT1 isoforms recycle at a similar rates and redistribute to the intracellular pool so that at equilibrium only approximately one-half of the labeled transporters remain in the plasma membrane. This is to be expected if all the cellular transporters are involved in the recycling process and is consistent with our previous studies on the photolabeling of the cell-surface and total-cellular pools of glucose transporters in 3T3-L1 cells, where we showed that approximately one-half of the total cellular pool of GLUT4 and GLUT1 transporters is located at the cell surface of insulin-stimulated cells.

In the basal state a much greater proportion of labeled GLUT4 transporters are lost from the plasma membrane. This is the result that would be expected if over 90% of the transporters were intracellularly localized. However, the half-time for removal of these labeled transporters in the basal state is somewhat slower than is observed in the insulin steady-state. These results contrast with those of Jhun *et al.* (17), who have reported that in basal rat adipose cells the half-time for tracer-tagged GLUT4 equilibration is faster than that observed in insulin-stimulated cells. This discrepancy may be related to the need to rapidly process samples to determine the fraction of label removed from the plasma membrane. This is particularly important in the basal state, where the fraction of the label removed from the plasma membrane is more extensive.

Our data show that the calculated endocytosis rate constants (k_{en}) are similar for GLUT4 and GLUT1 and that these endocytosis rate constants are only $\approx 30\%$ slower in the insulin-stimulated compared with the basal state. These findings are consistent with our previous observations on the rate of loss of cell-surface transporters from 3T3-L1 cells under conditions in which insulin was removed by a low pH buffer. In those experiments we simply estimated the proportions of transporters remaining at the cell surface by labeling at different time points following insulin removal. We observed that cell-surface levels of GLUT4 and GLUT1 decreased at a similar rate. We observed that the fractional loss of GLUT1 was slightly less than GLUT4 and suggested that this was due to a greater re-exocytosis of this isoform (24).

We have now shown quantitatively that insulin increases the rate constant (k_{ex}) for glucose transporter exocytosis. The exocytosis of the GLUT4 isoform is 8.6-fold faster in insulin-stimulated cells compared with basal cells. The basal exocytosis rate constant may be overestimated because of some plasma-membrane contamination from label, which transfers to the intracellular pool. However, the observed level of stimulation of GLUT4 exocytosis is almost sufficient to account for the ≈ 12 – 15 -fold stimulations of cell-surface appearance of GLUT4 previously observed using ATB-BMPA (20, 21, 24). In turn, this level of recruitment of GLUT4 is almost sufficient to account for the increase in glucose transport activity in these cells (≈ 15 – 20 -fold). Insulin also stimulates GLUT1 exocytosis but only to ≈ 3 -fold above basal levels. Again, this level of stimulation of exocytosis accounts for the smaller, 3–5-fold increases in cell-surface GLUT1 accessible to the photolabel that we have observed in our previous studies.

The major difference between the trafficking of the GLUT4 and GLUT1 isoforms is the much slower exocytosis of GLUT4 in the basal state. However, in the presence of insulin, both

isoforms are processed in the same way. Our data therefore supports the suggestion that in basal cells intracellular processing steps remove GLUT4 from the normal endosome recycling pathway, possibly to a specialized compartment within the tubulo-vesicular system (7). Insulin may then re-commit or re-target these transporters from the tubulo-vesicular system to the plasma membrane and thence to the early endosome system. Both intracellular transporter pools would then be in rapid equilibrium with each other in the insulin-stimulated state, as our photolabel equilibration data shows that the cells entire complement of glucose transporters are involved in the recycling process both in 3T3-L1 cells (this study) and in rat adipose cells.¹

We have consistently observed that the half-time for the initial stimulation of glucose transporter translocation by insulin is faster than the half-time for steady-state recycling of transporters and the half-time for loss of transporters when insulin is removed (18, 24).¹ We have suggested that this may occur because, immediately following insulin addition, transporters are rapidly committed to the plasma membrane at a vesicle docking and fusion step and that, once transporters are committed in this way, they are then recycled at a slower rate within the early endosomes. The kinetic effects expected from this type of multiple pool-trafficking system have been analyzed and have been shown to account for the observed disparity between the half-times for insulin stimulation of the initial translocation and the steady-state rates of transporter recycling.³

REFERENCES

- James, D. E., Strube, M. I., and Mueckler, M. (1989) *Nature* **338**, 83–87
- Charron, M. J., Brosius, F. C., Alper, S. L., and Lodish, H. F. (1989) *Proc. Natl. Acad. Sci. U. S. A.* **86**, 2535–2539
- Birnbaum, M. J. (1989) *Cell* **57**, 305–315
- Kaestner, K. H., Christy, R. J., McLenithan, J. C., Braiterman, L. T., Cornelius, P., Pekela, P. H., and Lane, M. D. (1989) *Proc. Natl. Acad. Sci. U. S. A.* **86**, 3150–3154
- Fukumoto, H., Kayano, T., Buse, J. B., Edwards, Y., Pilch, P. F., Bell, G. I., and Seino, S. (1989) *J. Biol. Chem.* **264**, 7776–7779
- Smith, R. M., Charron, M. J., Shah, N., Lodish, H. F., and Jarrett, L. (1991) *Proc. Natl. Acad. Sci. U. S. A.* **88**, 6893–6897
- Slot, J. W., Gueze, H. J., Gigengack, S., Lienhard, G. E., and James, D. E. (1991) *J. Cell Biol.* **113**, 123–135
- Klip, A., Rampall, T., Bilan, P. J., Cartee, G. D., Gulve, E. A., and Holloszy, J. O. (1990) *Biochim. Biophys. Res. Commun.* **172**, 728–736
- Slot, J. W., Gueze, H. J., Gigengack, S., James, D. E., and Lienhard, G. E. (1991) *Proc. Natl. Acad. Sci. U. S. A.* **88**, 7815–7819
- Haney, P. M., Slot, J. W., Piper, R. C., James, D. E., and Mueckler, M. (1991) *J. Cell Biol.* **114**, 689–699
- Hudson, A. W., Ruiz, M., and Birnbaum, M. J. (1992) *J. Cell Biol.* **116**, 785–797
- Gould, G. W., Thomas, H. M., Jess, T. J., and Bell, G. I. (1991) *Biochemistry* **30**, 5139–5145
- Asano, T., Takata, K., Katagiri, H., Tsukuda, K., Lin, J. J., Ishihara, H., Inukai, K., Hirano, H., Yazaki, Y., and Oka, Y. (1992) *J. Biol. Chem.* **267**, 19636–19641
- Schurmann, A., Monden, I., Joost, H. G., and Keller, K. (1992) *Biochim. Biophys. Acta* **1131**, 245–252
- Piper, R. C., Tai, C., Slot, J. W., Hahn, C. S., Rice, C. M., Huang, H., and James, D. E. (1992) *J. Cell Biol.* **117**, 729–743
- Robinson, L. J., Pang, S., Harris, D. A., Heuser, J., and James, D. E. (1992) *J. Cell Biol.* **117**, 1181–1196
- Jhun, B. H., Rampal, A. L., Liu, H., Lachal, M., and Jung, C. Y. (1992) *J. Biol. Chem.* **267**, 17710–17715
- Clark, A. E., Holman, G. D., and Kozka, I. J. (1991) *Biochem. J.* **278**, 235–241
- Karnieli, E., Zarnowski, M. J., Hissin, P. J., Simpson, I. A., Salans, L. B., and Cushman, S. W. (1981) *J. Biol. Chem.* **256**, 4772–4777
- Calderhead, D. M., Kitagawa, K., Tanner, L. I., Holman, G. D., and Lienhard, G. E. (1990) *J. Biol. Chem.* **265**, 13800–13808
- Palfreyman, R. W., Clark, A. E., Denton, R. M., Holman, G. D., and Kozka, I. J. (1992) *Biochem. J.* **284**, 275–281
- Holman, G. D., Kozka, I. J., Clark, A. E., Flower, C. J., Saltis, J., Habberfield, A. D., Simpson, I. A., and Cushman, S. W. (1990) *J. Biol. Chem.* **265**, 18172–18179
- Holman, G. D., Karim, A. R., and Karim, B. (1988) *Biochim. Biophys. Acta* **946**, 75–84
- Yang, J., Clark, A. E., Harrison, R., Kozka, I. A., and Holman, G. D. (1992) *Biochem. J.* **281**, 809–817